Isolation and functional characterization of Arabidopsis powdery mildew effector proteins

Inaugural-Dissertation

zur

Erlangung des Doktorgrades

der Mathematisch-Naturwissenschaftlichen Fakultät

der Universität zu Köln

vorgelegt von

Ralf Weßling

aus Rheine

Köln, Juni 2013

Die vorliegende Arbeit wurde am Max-Planck-Institut für Pflanzenzüchtungsforschung in Köln in der Abteilung für Pflanze-Mikroben Interaktionen (Direktor: Prof. Dr. Paul Schulze-Lefert) angefertigt.

Berichterstatter:	Prof. Dr. Paul Schulze-Lefert
	Prof. Dr. Martin Hülskamp
	Dr. Frank Takken
Prüfungsvorsitzender:	Prof. Dr. Ulf-Ingo Flügge
Tag der Disputation:	7.12.2012

Für Lisa und Oskar,

meine kleine Familie

Publications

Spanu P. D., Abbott J. C., Amselem J., Burgis T. A., Soanes D. M., Stüber K., Ver Loren van Themaat E., Brown J. K. M., Butcher S. A., Gurr S. J., Lebrun M.-H., Ridout C. J., Schulze-Lefert P., Talbot N. J., Ahmadinejad N., Ametz C., Barton G. R., Benjdia M., Bidzinski P., Bindschedler L. V., Both M., Brewer M. T., Cadle-Davidson L., Cadle-Davidson M. M., Collemare J., Cramer R., Lopez-Ruiz F., Frenkel O., Godfrey D., Harriman J., Hoede C., King B. C., Klages S., Kleemann J., Knoll D., Koti P. S., Kreplak J., Lu X., Maekawa T., Mahanil S., Micali C., Milgroom M. G., Montana G., Noir S., O'Connell R. J., Oberhaensli S., Parlange F., Pedersen C., Quesneville H., Reinhardt R., Rott M., Sacristán S., Schmidt S. M., Schön M., Skamnioti P., Sommer H., Stephens A., Takahara H., Thordal-Christensen H., Vigouroux M., **Weßling R.**, Wicker T., and Panstruga R. 2010. Genome expansion and gene loss in powdery mildew fungi reveal functional tradeoffs in extreme parasitism. **Science** 330: 1543-1546

Weßling R., Schmidt S. M., Micali C. O., Knaust F. Reinhardt R., Neumann U., Ver Loren van Themaat E., and Panstruga, R. 2012. Transcriptome analysis of enriched *Golovinomyces orontii* haustoria by deep 454 pyrosequencing. **Fungal Genetics and Biology** 49: 470-482.

Weßling, R. and Panstruga, R. 2012. Rapid quantification of plant-powdery mildew interactions by qPCR and conidiospore counts. **Plant Methods** 8: 35.

Table of Contents

Abbreviations

ABA	abscisic acid
AC	average coverage
ACC	1-aminocyclopropane-1-carboxylic acid
AI-1	Arabidopsis interactome version 1
APC	Anaphase-promoting complex
Arabidopsis	*Arabidopsis thaliana*
Avr	Avirulence
Bgh	*Blumeria graminis* f.sp. *hordei*
BiFC	bimolecular fluorescence complementation
BAK1	brassinosteroid receptor 1 (BRI1)–associated kinase
Bgh	*Blumeria graminis* f.sp. *hordei*
BIK1	*Botrytis*-induced kinase 1
BR	Brassinosteroid
CC	coiled-coil domain
Cf	*Cladosporium fulvum*
cfu	colony forming unit
Ch	*Colletotrichum higgansianum*
CLSM	confocal laser scanning microscopy
CUL	cullin
CRLs	cullin RING ligases
CSEP	candidate secreted protein
CSN	COP9 signalosome
C-terminal	carboxy terminal
Da	Dalton
DMSO	dimethylsulfoxide
DNA	deoxyribonucleic acid
dpi	days post inoculation
DRMIP-HESP	developmentally regulated MAPK interacting protein-haustorially expressed protein domain
eds	enhanced disease susceptibility
edr	enhanced disease resistance
EDTA	Na_2-ethylenediamine tetraacetic acid
EDV	effector detector vector
EF-Tu	elongation factor Tu
EFR	EF-Tu receptor
ER	endoplasmic reticulum
EST	expressed sequence tag
ET	ethylene
ETI	effector-triggered immunity
FDR	false discovery rate
FLS2	flagellin sensing 2
f.sp.	formae specialis
GA	gibberellic acid
GABA	γ-aminobutyric acid
GO	gene ontology
Hpa	*Hyaloperonospora arabidopsidis*
hpi	hours post inoculation
HR	hypersensitive response
JA	jasmonic acid
JAZ	jasmonate-ZIM domain containing protein
LRR	leucine-rich repeat
MAMP	microbe-associated molecular pattern
MAP	mitogen-activated protein
MES	2-(*N*-morpholino)ethanesulfonic acid

NLP	necrosis and ethylene-inducing proteins (NEP1)-like proteins
mM	millimolar
µM	micromolar
MFS	major facilitator superfamily
MTI	MAMP-triggered immunity
MVB	multi-vesicular body
Nb	*Nicotiana benthamiana*
NB	nucleotide binding site
N-terminal	amino terminal
OEC	*G. orontii* effector candidate
ORF	open reading frame
o/n	overnight
PCR	polymerase chain reaction
Pi	*Phytophthora infestans*
PPIN-1	plant pathogen interactome version 1
PR	pathogenesis-related protein
PRA	prenylated rab acceptor
PRR	pattern-recognition receptor
Pst	*Pseudomonas syringae* pv *tomato* DC3000
Psy	*Pseudomonas syringae* (several pathovars)
pv.	pathovar
PVC	prevacuolar compartment
qPCR	quantitative real time PCR
qRT-PCR	quantitative reverse transcription PCR
R	resistance
RIN4	RPM1 interacting protein 4
RNA	ribonucleic acid
rpm	revolutions per minute
RT	room temperature
RING	really interesting new gene
RLK	receptor-like kinase
RLP	receptor-like protein
ROS	reactive oxygen species
RT	room temperature
SA	salicylic acid
SAG101	senescence-associated gene 101
SCF	S-phase kinase-associated protein (SKP), CUL1, really interesting new gene (RING) box 1 (Rbx1), F-box protein complex
SDS-PAGE	sodium dodecyl sulfate (SDS) polyacrylamide gel electrophoresis
SNAP	synaptosomal-associated protein
SNARE	soluble N-ethylmaleimide sensitive factor attachment protein receptor
TAL	transcription-activator like
TCP	*teosinte branched*1, cycloidea (CYC), proliferating cell factor (PCF)
TF	transcription factor
TIR	Toll-interleukin1 receptor
TM	transmembrane
T3SS	Type III secretion system
T-DNA	transfer DNA
VAMP	vesicle-associated membrane protein
YFP	yellow fluorescent protein
Y2H	yeast two-hybrid
°C	degrees Celsius

Summary

Plants are resistant to the majority of potential pathogenic microbes. Adapted pathogens can however overcome plant defense and induce susceptibility. The molecular processes underlying this adaptation are only partially understood. Obligate biotrophic pathogens, which require a living host for growth and reproduction, establish especially intimate relationships with their plant hosts. A crucial aspect of this lifestyle is the formation of a specialized infection structure termed the haustorium. Haustoria are believed to represent pivotal sites of nutrient uptake and deliver effectors, proteins that manipulate the host cell during infection to promote susceptibility. While the effector arsenal of pathogenic bacteria has been investigated intensively, the repertoires and host targets of fungal effectors are currently underexplored. The work presented here thus aims at characterizing virulence mechanisms employed by the obligate biotrophic Ascomycete *Golovinomyces orontii,* the causal agent of the powdery mildew disease in *Arabidopsis thaliana* (hereafter Arabidopsis). To this end, the haustorial transcriptome of *G. orontii* was obtained by pyrosequencing of a cDNA library generated from isolated haustorial complexes. Transcripts coding for gene products with roles in protein turnover, detoxification of reactive oxygen species and fungal pathogenesis were abundant, while surprisingly transcripts encoding presumptive nutrient transporters were not highly represented in the haustorial cDNA library.

A substantial proportion (~38%) of transcripts encoding predicted secreted proteins comprised effector candidates. These candidates were cloned and found to frequently suppress induced plant cell death. A subset of effectors enhanced bacterial virulence and could suppress callose deposition, indicating a role in defense suppression. Transcript profiling of these effectors suggested their sequential delivery during pathogenesis. Furthermore, subcellular localization revealed diverse target compartments in the host. In a complementing approach, a large-scale yeast 2-hybrid (Y2H) assay was performed on the 84 cloned effector candidates and revealed convergence onto 61 potential host targets. These targets were enriched in transcription factors and components involved in development and cellular trafficking. Bimolecular fluorescence complementation assays confirmed the interaction of selected effectors with their host interactors. Finally, the Y2H targets of effectors were used to construct an integrated protein-protein interaction network of Arabidopsis and the three adapted pathogens *Pseudomonas syringae* (*Psy*), *Hyaloperonospora arabidopsidis* (*Hpa*) and *G. orontii*. This network revealed pathogen-specific as well as nine common host targets. These common targets are highly connected in the Arabidopsis cellular network. After the development of suitable quantitative methods, the important role of these common targets in the Arabidopsis immune response was validated by screening respective T-DNA insertion lines. In sum, my work supports the hypothesis that pytopathogenic microbes target hubs in the host cellular network to promote susceptibility. The effector targets identified will therefore form the basis of subsequent effector research in *G. orontii*.

Zusammenfassung

Pflanzen sind immun gegen den Großteil potentieller Schädlinge. Angepasste Schädlinge können die pflanzlichen Verteidigungsmechanismen allerdings überwinden und so die Pflanze für eine Infektion empfänglich machen. Die molekularen Prozesse, die dieser Anpassung zugrundeliegen sind nur teilweise verstanden. Obligat biotrophe Schädlinge, welche auf einen lebenden Wirt für Wachstum und Vermehrung angewiesen sind, etablieren eine besonders enge Beziehung mit ihrem pflanzlichen Wirt. Ein kritischer Aspekt dieser Lebensform ist die Bildung einer spezialisierten Infektionsstruktur, des Haustoriums. Das Haustorium ist entscheidend für sowohl die Nahrungsaufnahme als auch die Sekretion von Effektoren, kleinen Proteinen die die Wirtszelle manipulieren und so empfänglich für eine Besiedlung machen. Während die Effektorarsenale von Bakterien bereits intensiv erforscht wurden, sind die Effektoren von pilzlichen Schädlingen sowie ihre Zielproteine in der Wirtszelle noch weitgehend unbekannt. Die hier präsentierte Arbeit zielt deshalb auf das Verständnis der Virulenzmechansimen des obligat biotrophen Schlauchpilzes (Ascomycet) *Golovinomyces orontii*, des Erregers des Mehltaus auf *Arabidopsis thaliana* (folgend Arabidosis). Dazu wurde das haustorielle Transkriptom von *G. orontii* durch die Pyro-Sequenzierung einer cDNA-Bibliothek aus isolierten haustoriellen Komplexen charakterisiert. Viele Transkripte kodierten für Proteine mit Funktionen in der Proteinumsetzung, der Entgiftung von reaktiven Sauerstoffspezies und pilzlicher Pathogenese. Überraschenderweise konnten nur wenige Transkripte für mögliche Nährstofftransporter identifiziert werden.

Ein substanzieller Anteil (38%) der Transkripte für vorhergesagte sekretierte Proteine kodiert für Effektorkandidaten. Diese Kandidaten wurden kloniert und konnten häufig induzierten pflanzlichen Zelltod unterdrücken. Eine Untergruppe der Effektorkandidaten erhöhte die Virulenz von Bakterien und verringerte teilweise die Ablagerung von Callose. Zusammengenommen weist dies auf eine Rolle in der Unterdrückung der pflanzlichen Verteidigungsmechanismen hin. Die Analyse der Transkriptprofile dieser Kandidaten deutete auf eine sequentielle Produktion während der Infektion hin. Außerdem zeigten Lokalisationstudien unterschiedliche subzelluläre Zielkompartimente der einzelnen Effektorkandidaten. In einer komplementären Herangehensweise wurde eine großmaßstäbliche Hefe-Zwei-Hybird (Y2H) Analyse der 84 klonierten Effektorkandidaten durchgeführt. Dieser Ansatz enthüllte die Konvergenz der Kandidaten auf 61 potentielle Zielproteine des Wirtes.

In diesen Zielproteinen sind Transkriptionsfaktoren sowie Komponenten aus der Pflanzenentwicklung und dem zellulären Transport überrepräsentiert. Versuche über die bimolekulare Fluoreseszens-komplementation bestätigten die Interaktion von ausgewählten Effektoren mit den jeweiligen Wirtsproteinen. Schließlich wurden die Y2H-Interaktoren der Effektorkandidaten zur Konstuktion eines integrierten Protein-Protein Interaktions-Netzwerks von Arabidopsis und den drei adaptieren Schädlingen *Pseudomonas syringae* (*Psy*),

Hyaloperonospora arabidopsidis (*Hpa*) und *G. orontii* genutzt. Dieses Netzwerk enthüllte sowohl Schädling-spezifische als auch gemeinsame Zielproteine im Wirt. Die gemeinsamen Zielproteine sind hochvernetzt im zellulären Netzwerk von Arabidopsis. Nach der Entwicklung geeigneter quantitativer Methoden konnte eine Rolle dieser Proteine in der Immunantwort von Arabidopsis durch die Analyse von entsprechenden T-DNA-Insertionsmutanten bestätigt werden. Die hier präsentierte Arbeit unterstüzt die Hypothese das mikrobielle Pflanzenschädlinge hochvernetzte Proteine in der Pflanze angreifen um ihre Anfälligkeit zu erhöhen. Die identifizierten Effektoren und Zielproteine werden daher die Grundlage für eine weitere Erforschung des Arabidopsis-Mehltaus bilden.

1 Introduction

1.1 Plant immunity

Plants are sessile organism and have to continuously adapt to a changing environment. They are continuously exposed to pathogens with various infection strategies and feeding habits, including viruses, bacteria, fungi, nematodes and insects. The world is however still a green place as plants, similarly to invertebrates and vertebrates, possess an innate immune system that detects and wards off potential pathogens. Accordingly, plants are resistant against the vast majority of pathogenic microbes, a phenomenon termed non-host resistance. In comparison to vertebrates however, plants do not have an adaptive immune system with dedicated mobile immune cells but rather rely on the ability of each cell to defend against invaders (Ausubel, 2005). Plant innate immunity involves both preformed barriers and a multitude of responsive processes triggered by the recognition of potential pathogens, orchestrated by transcriptional reprogramming and executed by defense responses such as cell wall reinforcement and the delivery of anti-microbial compounds (Jones and Dangl, 2006; Thordal-Christensen, 2003). The immune response can be broadly divided into two distinct but overlapping layers: microbe-associated molecular pattern (MAMP)- and effector-triggered immunity (MTI and ETI, Jones and Dangl, 2006). Adapted pathogens are able to overcome plant innate immunity to cause disease.

1.1.1 Non-host resistance and MAMP-triggered immunity – two sides of the same coin

Plants are resistant to the majority of potential pathogens; they are non-hosts for these pathogens. This is due to the multilayered defense system of plants and specific requirements of the pathogens. In general, pathogens require certain cues to initiate pathogenesis, including surface topologies and cuticular waxes (Thordal-Christensen, 2003). Subsequently, successful pathogens need to overcome preformed plant defenses like secondary metabolites or the rigid cell wall (Mysore and Ryu, 2004). In the first responsive layer of defense, plants, analogous to animals, recognize MAMPs, conserved and indispensable microbial signatures such as bacterial flagellin, the elongation factor Tu (EF-Tu), fungal chitin and many more (Boller and Felix, 2009). These cellular components create a “non-self” signal that is perceived by the plant. The active epitopes of MAMPs are recognized by membrane-resident pattern-recognition receptors (PRRs) of the receptor-like kinase (RLK) and receptor-like protein (RLP) type (Boller and Felix, 2009). These PRRs are distinguished by their domain structure. RLKs such as flagellin sensing 2 (FLS2) and the EF-Tu receptor (EFR) contain an extracellular leucine-rich repeat (LRR) domain, a short transmembrane (TM) domain and an intracellular kinase domain (Gómez-Gómez and Boller, 2000; Zipfel et al., 2006). RLPs such as chitin elicitor receptor kinase 1 (CERK1), by contrast harbor an extracellular LysM domain, a TM domain and a short cytoplasmic domain without kinase function (Miya et al., 2007; Wan et al., 2008). The receptor proteins can be either

restricted to specific plant families or widely conserved, as shown for *EFR*, which is specific to the Brassicaceae and *FLS2*, which has also been found in tobacco, tomato and rice (Hann and Rathjen, 2007; Kunze et al., 2004; Robatzek et al., 2007; Takai et al., 2008). Transfer of *EFR* to tobacco and tomato generates responsiveness to elf18, the active epitope of EF-Tu, and enhanced resistance to bacteria, indicating that the downstream signaling components of the receptor are conserved (Lacombe et al., 2010). The transfer of *EFR* shifts the recipient plant towards a non-host state, further underlining the role of PRRs in non-host resistance.

The recognition of MAMPs by FLS2 and EFR, but not CERK1, triggers their association with brassinosteroid receptor 1–associated kinase (BAK) 1, phosphorylation of both partners and the subsequent activation of plant responses (Chinchilla et al., 2007). This is a key step in receptor activation, as *bak1* mutants are strongly impaired in downstream signaling events (Chinchilla et al., 2007). CERK1 functions independent of BAK1 but also associates with Botrytis-induced kinase (BIK) 1, a cytoplasmic kinase with a key role in the relay of receptor signals (Lu et al., 2010; Zhang et al., 2010). Subsequent to receptor complex activation, a stereotypical signaling cascade is activated that is mostly independent of the MAMP applied. There is a marked Ca^{2+}-influx, an oxidative burst occurs and MAP (mitogen-activated protein) kinases are activated (Boller and Felix, 2009). Subsequently, the phytohormone ethylene (ET) is produced and transcriptional reprogramming occurs (Zipfel et al., 2006; Zipfel et al., 2004). Even later, callose deposits appear and seedling growth is inhibited, indicating the reallocation of energy to the defense response (Gómez-Gómez and Boller, 2000; Gómez-Gómez et al., 1999). MAMP-triggered responses limit development and growth of both adapted and non-adapted pathogens and thus significantly contribute to plant immunity (Miya et al., 2007; Wan et al., 2008; Zipfel et al., 2006; Zipfel et al., 2004). It has to be noted that MAMPs, by definition, are also contained in commensal and beneficial microorganisms. The plant thus has to discriminate between neutral or beneficial and pathogenic microbes, as defense induction against the former would be detrimental for the plant. Specificity is probably achieved through the integration of MAMP and danger-associated molecular pattern (DAMP) perception. DAMPs are plant-derived signals released by pathogen activities such as cell wall degradation, sucrose degradation and cell permeabilization and comprise oligogalacturonides, extracellular sugars, or endogenous elicitor peptides (Doares et al., 1995; Herbers et al., 1996; Huffaker et al., 2006). Perception of these DAMPs by membrane-resident RLKs initiates a signaling cascade that is integrated with MAMP-signaling to promote defense response induction (Brutus et al., 2010; Krol et al., 2010; Yamaguchi et al., 2010; Yamaguchi et al., 2006).

But what are the executers of MTI? This question leads back to the genetic dissection of non-host resistance, especially to the characterization of components involved in the interaction of *Arabidopsis thaliana* with the non-adapted powdery mildew pathogen of barley, *Blumeria graminis* f.sp. *hordei* (*Bgh*). In this patho-system, non-host resistance at the pre-penetration stage is conferred by two parallel pathways. The first pathway leads to vesicle-mediated secretion of

unknown defense compounds and involves soluble *N*-ethylmaleimide sensitive factor attachment protein receptor (SNARE)-complex formation by the membrane-resident syntaxin PEN1/SYP121, the synaptosomal-associated protein (SNAP) 33 and the endomembrane-resident vesicle-associated membrane proteins (VAMPs) 721 and 722 (Collins et al., 2003; Kwon et al., 2008). The second pathway generates active glucosinolates for antifungal defense. It involves the biosynthesis of 4-methoxyindol-3-ylmethylglucosinolate by CYP81F2, a P450 monooxygenase, and subsequent activation by the peroxisomal β-glycosyl hydrolase PEN2 (Bednarek et al., 2009; Clay et al., 2009; Lipka et al., 2005). The active compound is then presumably secreted by PEN3, a pleiotropic drug resistance/ATP-binding cassette transporter (Stein et al., 2006). Both pathways limit the colonization by adapted as well as non-adapted pathogens and are thus also involved in MTI (Bednarek et al., 2009; Hiruma et al., 2010; Kwon et al., 2008; Stein et al., 2006). CYP81F2, PEN2 and PEN3 are required for MAMP-induced callose deposition and PEN1, VAMP722 and PEN3 accumulate in callosic haustorial encasements of the adapted powdery mildew fungus *G. orontii*, clearly demonstrating their role in MTI (Clay et al., 2009; Meyer et al., 2009). Components of the two pathways are transcriptionally induced after challenge with *G. orontii* and part of a transcriptional regulon conserved in both Arabidopsis and barley, showing that an ancient transcriptional program controls their expression (Chandran et al., 2010; Humphry et al., 2010). Additional inducible defense components comprise the phytoalexin camalexin, which is involved in resistance to both adapted and non-adapted necrotrophic pathogens and the pathogenesis-related (PR) proteins, which include chitinases and glucanases (Schlaeppi et al., 2010; Stotz et al., 2011; Thomma et al., 1999b; van Loon et al., 2006). The induction of defense responses is costly for the plant and therefore needs to be tailored towards invading microbes. One mechanism allowing a specific defense response is the production of different plant hormones and the cross-talk of their signaling modules.

1.1.2 Plant hormones – integrators of multiple defense responses

MAMP and DAMP perception induces the generation of several defense-related hormones, most prominently salicylic acid (SA), jasmonic acid (JA) and ET (Pieterse et al., 2009; Tsuda and Katagiri, 2010). These hormonal pathways act mostly antagonistically, with SA controlling defense against biotrophic and JA/ET synergistically controlling the defense response against necrotrophic pathogens (Glazebrook, 2005). However, all three pathways contribute positively to MTI and are probably needed to amplify the defense signal (Tsuda et al., 2009).

Induction of SA production requires the defense regulator enhanced disease susceptibility (EDS) 1 and its interaction partner phytoalexin deficient (PAD) 4, both of which also regulate SA-independent responses (Falk et al., 1999; Feys et al., 2001; Zhou et al., 1998). EDS1 also interacts with and signals through senescence-associated gene (SAG) 101, putatively forming a ternary complex with PAD4 (Feys et al., 2005; Zhu et al., 2011). All three proteins are also involved in basal immune responses, and define a third layer of post-invasive resistance against

Bgh (Lipka et al., 2005). The *pen2 pad4 sag101* triple mutant renders Arabidopsis a host for *Bgh*, as the fungus can in rare cases complete its life cycle on these plants (Lipka et al., 2005).

SA is produced predominantly through a chloroplast-localized pathway from chorismate by the isochorismate synthase ICS1/SID2 (Wildermuth et al., 2001). The mode of SA perception has long remained elusive, but two recent publications argue for either NPR1 (nonexpressor of pathogenesis-related genes 1) or its paralogs NPR3 and NPR4 as SA receptors (Fu et al., 2012; Wu et al., 2012). Previously, NPR1 has been characterized as the key signal transducer downstream of SA production, as loss of NPR1 impairs both local and systemic resistance to pathogens (Cao et al., 1994; Mou et al., 2003). In the non-induced state, NPR1 oligomers are localized in the cytoplasm. Upon SA-induced redox changes the monomers are liberated, enter the nucleus and initiate signaling through TGA transcription factors (TFs) (Mou et al., 2003; Tada et al., 2008). This leads to the activation of downstream responses such as *PR* gene expression, the establishment of systemic acquired resistance in non-challenged leaves and contributes to the hypersensitive response (HR), a localized plant cell death (Durrant and Dong, 2004). Constitutive signaling is prevented by constant proteasome-dependent degradation of NPR1 in the nucleus (Spoel et al., 2009). The cytosolic pool of NPR1 is important for the repression of JA signaling (Spoel et al., 2003).

JA is a lipid-derived compound originating from α-linolenic acid that is produced by several enzymatic reactions in both the chloroplast and peroxisomes (Wasternack, 2007). It is perceived through a receptor complex containing the ubiquitin-conjugating E3 ligase SCF^{COI1} (S-phase kinase-associated protein, cullin (CUL) 1, really interesting new gene (RING) box 1 (Rbx1), F-box protein) (Pauwels and Goossens, 2011). COI1 is an F-box protein and thus functions as the eponymous substrate adaptor of the complex (Xie et al., 1998). It interacts with several Jasmonate-ZIM domain containing (JAZ) proteins that repress JA signaling by binding to the JA-responsive TF MYC2 and recruiting the corepressor TOPLESS (Pauwels et al., 2010). Binding of JA-isoleucine, the bioactive JA conjugate, to the SCF^{COI1}-JAZ coreceptor complex induces ubiquitination of JAZ proteins by SCF^{COI1} and subsequent degradation of the JAZs (Chini et al., 2007; Sheard et al., 2010; Thines et al., 2007; Yan et al., 2007). This allows the induction of JA-responsive genes by the TF MYC2. In addition to its role in the defense response, JA also influences several developmental processes, as exemplified by the male sterility phenotype of the *coi1* mutant (Pauwels and Goossens, 2011; Wasternack, 2007; Xie et al., 1998).

Similar to JA, ET is a versatile hormone involved in defense responses as well as plant development. The production of ET from its precursor S-adenosylmethionine via 1-aminocyclopropane-1-carboxylic acid (ACC) synthase and ACC oxidase is rapidly induced by MAMP perception (Boller and Felix, 2009; Wang et al., 2002). Five membrane-bound ET receptors have been described which constitutively repress ET signaling (Wang et al., 2002). Upon ET perception these receptors are inactivated, leading to derepression of the pathway and activation of gene expression through EIN2 and the TFs EIN3 and EIL3 (Shan et al., 2012). JA

and ET predominantly act synergistically. This synergism is in large parts controlled by the two TFs ERF1 and ORA59 (Lorenzo et al., 2003; Pré et al., 2008). JA- and JA/ET-induced genes can thus be separated by the requirement of either MYC2 or ERF1 and ORA59 for their induction (Lorenzo et al., 2004).

The outcome of hormone signaling is governed by a large network of crosstalk. In addition to the archetypical JA-SA antagonism, many interactions of different hormone branches have been described. They include, but are not limited to, synergism of ET and SA signaling, antagonism between abscisic acid (ABA), JA/ET and SA responses, antagonism between SA and auxin signaling, a role of gibberellic acid (GA) signaling in SA-JA crosstalk and antagonism between cytokinins and SA and auxin (Anderson et al., 2004; Leon-Reyes et al., 2009; Naseem et al., 2012; Navarro et al., 2008; Wang et al., 2007; Yasuda et al., 2008). The complexity of hormonal crosstalk is essential for integrating both immune and developmental signals and generating an appropriate response. The use of proteasome mediated degradation is another common theme in these hormone signaling pathways. Constitutive repression of ET signaling is mediated through the constant degradation of EIN2 and EIN3 through $SCF^{ETP1/2}$ and $SCF^{EBF1/2}$, respectively (Guo and Ecker, 2003; Potuschak et al., 2003; Qiao et al., 2009). Additionally, SCF^{COI1}, SCF^{TIR1} and SCF^{GID2} perceive the plant hormones JA, auxin and GA, respectively (Santner and Estelle, 2009). Finally, the potential perception of SA by an E3 ligase complex containing CUL3, NPR3 and/or NPR4 also provides a link to SA signaling (Fu et al., 2012). Despite the complexity and redundancy of plant innate immunity, adapted pathogens have found ways to disturb or abuse the plant defense response and cause disease. One such mechanism is the production of the phytotoxin coronatine, a structural analog of JA-Isoleucine, by the hemibiotrophic bacterium *Pseudomonas syringae* pv. *tomato* DC3000 (*Pst*) (Weiler et al., 1994; Yan et al., 2009). Coronatine activates JA-signaling and induces susceptibility owing to the suppression of SA-induced responses by hormonal crosstalk (Brooks et al., 2005; Uppalapati et al., 2007).

1.1.3 Adapted pathogens have evolved to cause disease

Arabidopsis can be colonized by many microbial pathogens, including bacteria and the filamentous oomycetes and fungi. Their lifestyle ranges from necrotrophy, where nutrients are obtained by lysis of the host, to obligate biotrophic pathogens that can only grow and reproduce on the living host (O'Connell and Panstruga, 2006). Obligate biotrophy has evolved in unrelated pathogens several times independently, indicating that this life-style provides a selective advantage (Kemen and Jones, 2012; O'Connell and Panstruga, 2006). Accordingly, obligate biotrophy is associated with specific genomic adaptations, including increased genome size mediated by the expansion of transposable elements, reduced sets of lytic enzymes and enzymes for the production of secondary metabolites and the loss of some biosynthetic pathways (Kemen and Jones, 2012; Schmidt and Panstruga, 2011). Obligate biotrophic pathogens use a characteristic feeding organ, the haustorium to establish an intimate relationship with their host

and facilitate the uptake of carbohydrates, amino acids and possibly water from the host (Gil and Gay, 1977; Hahn and Mendgen, 1997; Voegele and Mendgen, 2003). Nutrient uptake is thought to be driven by a proton gradient across the membrane that is generated by fungal H^+-ATPases (O'Connell and Panstruga, 2006). Haustoria remain separated from the host cell by the extrahaustorial matrix, the battleground of the host-pathogen interaction, and the extrahaustorial membrane (EHM), a derivative of the plant plasma membrane whose composition is modified remarkably (Koh et al., 2005; Meyer et al., 2009; Micali et al., 2011). Arabidopsis can be colonized by several obligate biotrophs, including the oomycetes downy mildew *Hyaloperonospora arabidopsidis* (*Hpa*) and white rust *Albugo* species as well as powdery mildew fungi (Kemen and Jones, 2012). The haustoria of obligate biotrophic pathogens have been shown to secrete effectors, small proteins that undermine the host immune system and reprogram the host cell for compatibility (Kemen et al., 2005; Sohn et al., 2007; Stergiopoulos and de Wit, 2009). These effectors can in turn be recognized by the plant, triggering ETI.

1.2 Effectors of microbial pathogens

1.2.1 Effectors as avirulence determinants

It has long been recognized that plants are resistant to specific isolates of adapted pathogens. A conceptual framework for these observations was first provided by the gene-for-gene concept, which stated that isolate-specific resistance requires complementary Avirulence (*Avr*) and resistance (*R*) genes in host and pathogen, respectively (Flor, 1971). Interactions of plants and adapted pathogens can thus be classified as compatible (*R* or *Avr* gene absent) or incompatible (*R* and *Avr* gene present). The cloning and analysis of several *Avr/R* gene combinations has elucidated the molecular mechanisms underlying the gene-for-gene concept and shown that *Avr* genes encode effectors, thus coining the term ETI (Dangl and Jones, 2001; Jones and Dangl, 2006; Van Der Biezen and Jones, 1998). *R* genes predominantly encode cytoplasmic proteins with a modular structure. They contain a central nucleotide-binding (NB) domain, a C-terminal LRR domain and one of two possible N-terminal domains (Takken and Tameling, 2009). The N-terminal coiled-coil (CC) or Toll/Interleukin-1 receptor (TIR) domains form the signaling hubs of the proteins. The LRR domain generates the recognition specificity of R proteins by either binding to Avr proteins (direct recognition) or by monitoring effector-induced modifications of host proteins (guardees). This "guard" model has provided a valuable extension of the gene-for-gene concept (Dangl and Jones, 2001; Van Der Biezen and Jones, 1998). One of the best studied guardees is the plasma membrane-resident RPM1 interacting protein 4 (RIN4). It is targeted by at least four independent effectors (AvrRpm1, AvrB, AvrRpt2 and HopF2) and guarded by two distinct CC-NB-LRR proteins, RPM1 and RPS2, which recognize its phosphorylation or cleavage, respectively (Kim et al., 2005a; Kim et al., 2005b; Mackey et al., 2002; Wilton et al., 2010). The guard model has recently been modified to also encompass decoys, non-functional proteins that mimic effector targets solely to trigger R protein mediated resistance (van der Hoorn and Kamoun, 2008). It is

important to note that in contrast to non-host resistance, which acts at the species level, *R* gene-mediated resistance is cultivar-specific.

The signaling cascades downstream of R protein activation are only poorly understood. TIR-NB-LRRs and CC-NB-LRRs activate at least partially distinct signaling modules, as illustrated by the differential requirement of EDS1 or NDR1 (non-race specific resistance 1), respectively, for the activation of downstream responses (Aarts et al., 1998). The most frequent executor of ETI is the HR, but resistance and HR can also be uncoupled (Bendahmane et al., 1999; Clough et al., 2000; Heidrich et al., 2011). Notably, ETI can also be characterized as an enhanced and prolonged MTI response (Tsuda and Katagiri, 2010). There is a significant overlap of transcriptional changes induced by MTI and ETI and both MTI and ETI trigger reactive oxygen species (ROS) production and MAP kinase activation (Navarro et al., 2004; Torres et al., 2006; Underwood et al., 2007). In ETI, the kinase activation is however more extensive and ROS production is biphasic with a second prolonged ROS burst probably triggered by effector recognition (Torres et al., 2006; Underwood et al., 2007). Hormonal responses are also involved in MTI and ETI alike, playing synergistic and compensatory roles in the former and latter, respectively (Tsuda et al., 2009). In addition, the separation of MAMPs from effectors and PRRs from R proteins is sometimes difficult (Thomma et al., 2011). The rice Xa21 and tomato Cf-2 R proteins are transmembrane proteins with an extracellular LRR domain and thus resemble PRRs. They do however specifically recognize the bacterial effector protein Ax21 and modifications of the tomato cysteine protease Rcr3, respectively (Lee et al., 2009; Rooney et al., 2005). Notably, the recognized epitope of Ax21 was mapped to a 17 amino acid sulfated peptide that is conserved in all *Xanthomonas* species, thus resembling a MAMP (Lee et al., 2009).

1.2.2 Effectors as virulence factors

Effectors can be defined as “all pathogen proteins and small molecules that alter host-cell structure and function” (Hogenhout et al., 2009). These compounds are predominantly proteins and can be divided into apoplastic and intracellular effectors, based on their localization. They have been extensively characterized in bacterial pathogens (Feng and Zhou, 2012). Pathogenic bacteria use a syringe-like structure, the Type III secretion system (T3SS), to insert effectors into the plant cell (Jin and He, 2001). The *Pst* genome contains 28 well expressed effectors and the function of many of these has been elucidated (Cunnac et al., 2009; Feng and Zhou, 2012). Collectively, effectors interfere with many events of MTI but have varying contributions to susceptibility (Cunnac et al., 2011). Many bacterial effectors target PRR complexes at the plasma membrane and interfere with subsequent MAP kinase signaling cascades (Cheng et al., 2011; Cui et al., 2010; Feng et al., 2012; Gimenez-Ibanez et al., 2009; Göhre et al., 2008; Wang et al., 2010; Zhang et al., 2010; Zhang et al., 2007). Additional functions include the modification of RNA metabolism and the interference with vesicle trafficking and secretion (Bartetzko et al., 2009; Fu et al., 2007; Nomura et al., 2006). Effectors of *Xanthomonas* can also abuse the host

transcriptional machinery by acting as TFs that induce susceptibility genes (Kay et al., 2007; Römer et al., 2007). These TAL (transcription activator-like) effectors recognize specific DNA elements through their central repeat domain (Boch et al., 2009; Moscou and Bogdanove, 2009). The susceptibility genes induced include two SWEET-type sugar exporters, suggesting that effectors also affect pathogen nutrition (Chen et al., 2010). In response, plants have evolved atypical *R* genes which are transcriptionally induced by TAL effectors and induce a cell death response, thus complying with the gene-for-gene model (Gu et al., 2005; Römer et al., 2007).

In comparison to bacteria, the effector functions of filamentous pathogens are far less understood. Cloned Avr effector proteins have been found to be secreted via the classical vesicle trafficking pathway and bioinformatic predictions of unknown secreted proteins has thus been used to define candidate effector sets (Saunders et al., 2012; Schmidt and Panstruga, 2011). These analyses revealed large (>200) effector candidate sets, complicating the selection of appropriate candidates (Schmidt and Panstruga, 2011). Most information is currently available on the function of apoplastic effectors. These can roughly be divided into cell wall degrading enzymes, toxins, protease inhibitors and effectors preventing chitin degradation or signaling (de Jonge et al., 2011). Cell-wall degrading enzymes are more prevalent in the genomes of necrotrophic and hemibiotrophic relative to biotrophic pathogens, as biotrophic pathogens do not lyse their host cells for nutrient acquisition (Schmidt and Panstruga, 2011). Toxins are also associated with hemibiotrophic and necrotrophic pathogens. A good example are the necrosis and ethylene-inducing proteins (NEP1)-like proteins (NLPs), that are present in genomes of pathogenic fungi, oomycetes and even bacteria and induce membrane permeabilization (Ottmann et al., 2009). NLPs are also present in the genomes of biotrophic pathogens, but these orthologs do not induce necrosis (Cabral et al., 2012). Protease inhibitors are effectors of many pathogens and have even evolved independently to target the same protease. This is evident for the cysteine protease Rcr3 of tomato, which is inhibited by effectors of *Cladosporium fulvum* (*Cf)*, *Phytophthora infestans* (*Pi*) and the nematode *Globodera rostochiensis* (Lozano-Torres et al., 2012; Song et al., 2009). Interestingly, Rcr3 is guarded by the atypical LRR transmembrane R protein Cf-2 (Dixon et al., 2000; Rooney et al., 2005). Finally, *Cf* Avr4 protects the fungus from plant chitinases and *Cf* Ecp6 scavenges chitin in the apoplast, thereby preventing chitin-triggered responses (de Jonge et al., 2010; van den Burg et al., 2006). Orthologs of Ecp6 have been detected in many other fungal species, indicating the chitin scavenging is a common virulence mechanism (Bolton et al., 2008).

For cytoplasmic effectors, most progress has recently been made in oomycete pathogens. Protein sequence comparison of several oomycete Avr effectors allowed the delineation of the common RXLR-(D)EER motif (short RXLR), which was subsequently shown to be involved in effector uptake (Dou et al., 2008; Rehmany et al., 2005; Whisson et al., 2007). Subsequently, the LXLFLAK motif was shown to mediate uptake in another group of oomycete intracellular effectors, the Crinkler proteins (CRNs) (Haas et al., 2009; Schornack et al., 2010). The RXLR and

LXLFLAK motives allow rapid bioinformatic searches for effector candidates in the genomes and/or transcriptomes of oomycete species, which can be subjected to subsequent biological analysis (Vleeshouwers et al., 2008; Wang et al., 2011). These screens have uncovered several previously uncloned *Avr* effectors and corresponding *R* genes, clearly demonstrating the power of the approach (Goritschnig et al., 2012; Vleeshouwers et al., 2008). Large-scale approaches have also revealed MTI suppression functions and subcellular localization of both *Hpa* and *P. sojae* effector candidates (Caillaud et al., 2012; Fabro et al., 2011; Wang et al., 2011). Recently, the functions of AvrBlb-2, which inhibits the secretion of an immune protease, and CRN8, a functional serine/threonine RD kinase have also been determined (Bozkurt et al., 2011; van Damme et al., 2012). Additionally, the first described intracellular host target of a filamentous pathogen effector, the E3 ubiquitin ligase CMPG1 was identified by analysis of the *Pi* effector Avr3a (Bos et al., 2010). A common theme of both oomycete and fungal effectors is the suppression of plant cell death, which has been frequently reported (Dou et al., 2008; Kleemann et al., 2012; Wang et al., 2011). Recently, a large-scale yeast two-hybrid (Y2H) screen of effectors from *Hpa* and several *Pseudomonas syringae* (Psy) pathovars has recently revealed many potential host targets (Mukhtar et al., 2011). The authors showed that these unrelated pathogens target overlapping sets of proteins, suggesting that effectors show convergent evolution for the inhibition of key defense targets.

The functional analysis of fungal cytoplasmic effectors is currently lacking behind. Although the uptake of effectors into host cells has been described, the uptake signal remains enigmatic (Kemen et al., 2005; Khang et al., 2010). Additionally, the frequent cloning of Avr proteins has not led to the definition of effector functions or their role in virulence (de Jonge et al., 2011; Stergiopoulos and de Wit, 2009). Cloned effect have however been utilized to define the spatiotemporal organization of effector delivery (Khang et al., 2010; Kleemann et al., 2012). Research on the maize smut fungus *Ustilago maydis* has revealed Pep1, an effector necessary for cell to cell movement of the pathogen and Cmu1, a secreted chorismate mutase that probably interferes with SA production and also moves to neighboring cells (Djamei et al., 2011; Doehlemann et al., 2009). Recently, Pep1 was shown to inhibit a host peroxidase, thus preventing a localized oxidative burst (Hemetsberger et al., 2012). The xylem-colonizing fungus *Fusarium oxysporum* f.sp. *lycopersici* secretes Avr1, which is recognized by the intracellular R protein I-1 and interferes with resistance triggered by I-2 and I-3 (Houterman et al., 2008). The exact mechanism of this inference remains to be determined. The effector functions of obligate biotrophic fungal pathogens have so far not been elucidated. Several Avr proteins of rust fungi have been cloned, but remain to be characterized functionally (Catanzariti et al., 2006; Stergiopoulos and de Wit, 2009). In powdery mildew fungi, attempts to clone *Avr* genes have been mostly unsuccessful. These pathogens cause extensive yield losses worldwide, and effector proteins might provide important insights into their virulence mechanisms.

1.3 *G. orontii* and the powdery mildew infection of Arabidopsis

Powdery mildew fungi are widespread pathogens infecting more than 10,000 plant species, including many agronomically relevant crops (Takamatsu, 2004). They are obligate biotrophic parasites and are thus dependent on a living host to complete their life cycle. In recent years Arabidopsis has been used to achieve great progress in the dissection of the interaction of powdery mildews with their host (Consonni et al., 2006; Shen et al., 2007). Arabidopsis can be colonized by four powdery mildew fungi: *Erysiphe cruciferarum*, *Golovinomyces cichoracearum*, *Golovinomyces orontii* and *Oidium neolycopersici*, (see Micali et al. (2008) for review). Until recently research in this field was primarily focussed on the plant side of the interaction. Accordingly, several Arabidopsis mutants with both enhanced and reduced susceptibility to powdery mildew have been characterized (Consonni et al., 2006; Dewdney et al., 2000; Vogel and Somerville, 2000; Vogel et al., 2002; Xiao et al., 2001).

Most powdery mildew fungi grow epiphytically, completing their life cycle on the leaf surface. After landing of a conidiospore on the leaf a germ tube emerges, which subsequently differentiates an appressorium at the site where the fungal sporeling attempts to break through the host cuticle and cell wall. Following successful penetration, the haustorium invaginates the plant plasma membrane and matures into a lobe-shaped structure. Subsequently, secondary hyphae emerge from the spore, spread epiphytically and secondary haustoria are inserted into neighbouring host cells. Around seven days post inoculation (dpi) abundant epiphytic conidiation is apparent, generating the characteristic white powdery mildew pustules (Micali et al., 2008). While the interaction of *Bgh* with barley follows the gene-for-gene concept and up to 85 *R* genes with different specificities against powdery mildew isolates have been characterized in barley, no canonical powdery mildew *R* genes have been found in Arabidopsis yet (Joergensen, 1994; Micali et al., 2008). *G. orontii* infections of Arabidopsis have only been reported in 1998 and the fungus first coevolved with the plant family Asteraceae before experiencing frequent host jumps (Matsuda and Takamatsu, 2003; Plotnikova et al., 1998). Arabidopsis might thus not have coevolved with *G. orontii* long enough to select for canonical *R* genes. Broad-spectrum resistance to powdery mildew pathogens has however been observed. Loss of function mutations in the *mildew resistance locus O* (*MLO*) gene render barley plants resistant to all powdery mildew isolates (Büschges et al., 1997). Similarly, the combined loss of the orthologous *MLO2*, *MLO6* and *MLO12* genes generates broad-spectrum powdery mildew resistance in Arabidopsis (Consonni et al., 2006). Additionally, the RPW8 locus that encodes the non-canonical TM-CC R proteins RPW8.1 and RPW8.2 confers resistance to several powdery mildew species in a wide range of Arabidopsis accessions (Göllner et al., 2008; Xiao et al., 2001). Similar to canonical R proteins of the TIR type, the RPW8 proteins require EDS1 and additional SA signaling components to induce HR (Xiao et al., 2005). Strikingly, RPW8.2 localizes to the EHM and increases the formation of callosic haustorial encasements as well as localized defense responses (Micali et al., 2011; Wang et al., 2009).

Previously, transcriptomic studies of the barley pathogen, *Bgh*, have been used to reveal the timing and stage-specificity of fungal gene expression, indicating the co-regulation of large gene sets during infection (Both et al., 2005a; Both et al., 2005b). To understand the basis of biotrophy, it is crucial to also characterize the set of haustorially expressed genes. In rust fungi, for instance, these studies provided first indications for the potential importance of haustorially-expressed sugar and amino acid transporters during fungal pathogenesis (Hahn and Mendgen, 1997; Jakupovic et al., 2006). In addition, many effector genes have been discovered by transcriptomic studies of haustoria (Catanzariti et al., 2006; Hahn and Mendgen, 1997). The initial genome analysis of *Bg*h revealed 248 candidate effectors, of which very few could also be identified in the genomes of the pea powdery mildew pathogen, *Erysiphe pisi* and *G. orontii* (Spanu et al., 2010). The effector repertoire of *G. orontii* has not been explored. This pathogen and its effectors can serve as a model system for dicot-infecting powdery mildew fungi, which are the vast majority of powdery mildews species described to date (Glawe, 2008; Takamatsu, 2004). Recently, a protocol for the efficient preparation of powdery mildew haustoria from Arabidopsis has been developed, allowing the in depth transcriptomic analysis of these important infection structures (Micali et al., 2011).

1.3.1 Quantification of powdery mildew infection

Currently, the quantification of powdery mildew infection on plants is based on three major methods that all have certain limitations: macroscopic categorization and microscopy-based penetration and conidiophore counts (Consonni et al., 2006; Reuber et al., 1998; Vogel and Somerville, 2000). For crude categorization, disease symptoms can be scored by eye at late stages of pathogenesis (7-14 dpi) and ratings assigned based on the severity of disease symptoms (Humphry et al., 2010; Reuber et al., 1998). While this method is quick and suitable for high throughput, it is prone to subjectivity, relies on equal inoculation densities and can only reveal strong differences in colonization that are readily visible to the naked eye. Assessment of host cell entry by penetration counts is a quantitative way to measure powdery mildew infection, but this method is limited to differences in susceptibility that are already manifested at early stages of infection (Consonni et al., 2010; Consonni et al., 2006). In addition, it requires time-consuming staining and mounting steps of multiple microscopic samples and the subsequent assessment of hundreds of interaction sites. Finally, conidiophore counts have been used to characterize small mutant sets in detail (Consonni et al., 2006; Reuber et al., 1998; Vogel and Somerville, 2000). This method requires tight control of inoculation density to ensure the presence of single fungal colonies, and, similar to penetration counts, necessitates tedious staining and mounting of multiple microscopic samples. In addition, hyper-susceptibility of genotypes can sometimes not be resolved by this technique (Reuber et al., 1998). Based on their microscopic nature involving staining of specimens, the latter two methods are unsuitable for the analysis of large sample contingents such as mutant collections or segregating populations. A microscopy-based quantification method for the analysis of intermediate stages (fungal colonies)

has also been developed, but either requires tedious manual micro-photographic time series or expensive automated microscopy systems (Göllner et al., 2008; Seiffert and Schweizer, 2005; Baum et al., 2011). Additional methods are thus needed to facilitate large-scale quantitative analysis of mutant populations.

1.4 Thesis aims

Effectors are important pathogenicity agents of plant pathogens. They suppress the plant innate immune system to induce susceptibility of the host. While increasing knowledge has been gained on the function of bacterial effectors, the contributions of effectors from filamentous pathogens to virulence are still mostly enigmatic. This is especially true for effectors of the powdery mildew fungi, important pathogens of both monocot and dicot plants. The effector repertoire of *Bgh* has only been defined by bioinformatic analysis, and information on the effector arsenal of dicot infecting powdery mildews is lacking completely.

The aim of this thesis was therefore to (I) characterize a transcriptome library of isolated *G. orontii* haustoria, (II) predict and clone effector candidates from this library and (III) analyze these effector candidates functionally.

The haustorial library was queried for gene ontology (GO) annotations and enrichment of GO terms. Additionally, the highest expressed transcripts and those encoding secreted proteins or transmembrane proteins were analyzed in detail. Finally, the library was used as a starting point for the prediction of *G. orontii* effector proteins. To explore the functions of effector candidates, these were analyzed for their ability to suppress induced cell death and enhance bacterial virulence. Additionally, the subcellular localization and temporal expression patterns of selected candidates were explored. In a complementary approach, all candidate effectors were subjected to a large scale Y2H screen. The interactors of the effectors were used to construct an integrated protein-protein interaction network of Arabidopsis and the three adapted pathogens *Pst*, *Hpa* and *G. orontii*. This network revealed common host targets whose involvement in the Arabidopsis immune response was examined by screens of respective T-DNA insertion lines. Finally, selected Y2H interactions were to be confirmed by bimolecular fluorescence complementation. The development of suitable assays for the medium to high-throughput quantitative analysis of powdery mildew susceptibility completes this work.

2 Results

2.1 Rapid quantification of plant-powdery mildew interactions by qPCR and conidiospore counts

At the beginning of my thesis I realized that the current protocols available for the quantification of powdery mildew infections were not sufficient for the medium to large-scale screenings I had to conduct. In addition, the recent advances in the field of powdery mildew research clearly necessitate the development of such protocols for the validation of -omics approaches (Hückelhoven and Panstruga, 2011). At the time, the quantification of powdery mildew infection on plants was based on three major methods that all had certain limitations: macroscopic categorization and microscopy-based penetration and conidiophore counts (Consonni et al., 2006; Reuber et al., 1998; Vogel and Somerville, 2000). I thus aimed at developing two complementary methods with superior performance relative to present methods. I focused on a quantitative real time PCR (qPCR)-based and a spore count-based method as these procedures have been successfully applied to other plant-pathogenic microorganisms before (Brouwer et al., 2003; Feys et al., 2005; Gachon and Saindrenan, 2004; Silvar et al., 2005; Stuttmann et al., 2011). Yet, to the best of my knowledge, these methods have not been adapted to the quantification of powdery mildew pathogenesis.

2.1.1 The powdery mildew infection on seedlings

First, a cytological analysis of the *G. orontii* infection on wild type (ecotype Col-0) seedlings was conducted (Figure 1). The use of seedlings allowed a more rapid screening of phenotypes (2-3 week old instead of 4-5 week old plants) and produced an averaging effect due to the use of many individuals (up to a hundred in the case of spore counts) per genotype and biological replicate. The susceptibility of a genotype can vary based on environmental conditions like pot humidity and averaging across pots can help to control this effect. A settling tower was used as this method allows a uniform and controlled inoculation and can be used efficiently for larger amounts of genotypes (Adam et al., 1999; Humphry et al., 2010; Reuber et al., 1998). Inoculation densities were kept low (~750 spores/cm^2) to discern single powdery mildew colonies on the leaves.

The life cycle of *G. orontii* can be separated into several distinct stages, but so far its timing has not been characterized on Arabidopsis seedlings. At 1 day post inoculation (dpi) most primary haustoria had been formed and growth of secondary hyphae began (

Figure **1**). Hyphal development continued slowly until 2 dpi and increased rapidly after the formation of secondary haustoria at 3 dpi. The Col-0 ecotype is highly susceptible to *G. orontii* and conidiophores therefore sometimes already formed at 4 dpi. Subsequently, the number of

conidiophores increased and numerous growing chains of conidiospores were observed at 5 and 6 dpi. The observations of the infection process on seedlings were in line with previous reports on *G. orontii* infections of 4-5 week old Arabidopsis plants (Micali et al., 2008; Plotnikova et al., 1998). The use of seedlings therefore faithfully reflected the timing of the natural infection process on mature plants.

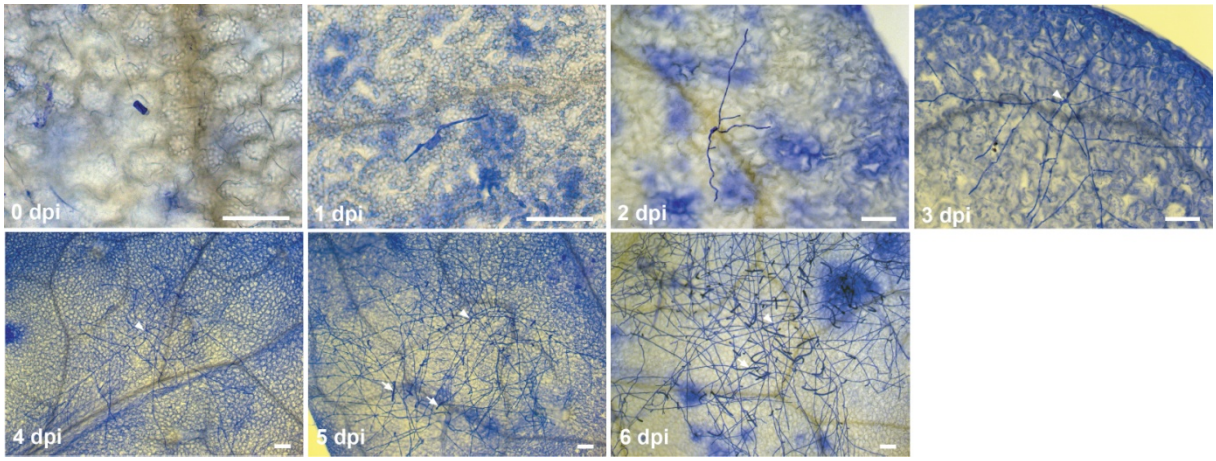

Figure 1: Powdery mildew disease progression on Arabidopsis seedlings. Microscopic images of powdery mildew disease progression on Col-0 plants. Samples were harvested at the indicated time points and stained with Coomassie Brilliant Blue. Arrows indicate conidiospore chains and arrowheads point to the initial spore. Images are representative of three independent experiments. Scale bar is 50 µm.

2.1.2 qPCR-based quantification of *G. orontii* infection

Methods on the basis of qPCR have been developed for biomass quantification of many plant-pathogenic microorganisms (Brouwer et al., 2003; Gachon and Saindrenan, 2004; Silvar et al., 2005). For this procedure, the quantitative extraction of pure genomic DNA as well as the efficient and specific amplification of target sequences is key. Therefore a phenolic extraction technique for genomic DNA isolation was used that was previously found to allow quantitative DNA isolation from both fungal and bacterial plant pathogens (Brouwer et al., 2003). The protocol was modified by introducing a disruption step of frozen material, as direct disruption of fresh seedlings was inefficient in my hands. Subsequently a series of qPCR primers from arbitrarily chosen genes was designed to amplify either *G. orontii* or Arabidopsis genomic sequences and tested for amplification efficiency. For efficient primer pairs the annealing temperatures and primer concentrations were optimized to obtain most specific PCR results. Primer dimers were not detected for any of the primer pairs by either melting curve analysis or agarose gel electrophoresis. Subsequently, a 5-fold dilution series of genomic DNA from heavily infected Col-0 tissue (harvested at ~14 dpi) was performed to generate a standard curve for primer efficiency calculation across the dynamic range (Supplemental Figure 1A). All tested primer pairs were found to have high amplification efficiencies of 90 to 100% (Supplemental Table 1). For the *G. orontii* primer pairs, marginal background amplification of unspecific products was detected on an uninfected Col-0 control sample (Supplemental Figure 1 B). The unspecific amplification did not affect the procedure since it was associated with Ct values (>35) that were outside the range used in the subsequent experiments (ca. 25-35). The amplification of *G. orontii*-derived amplicons

relative to products obtained from Arabidopsis genomic DNA was used for the quantification of fungal biomass. This measure controls for variation in both sample harvesting and the efficiency of DNA isolation.

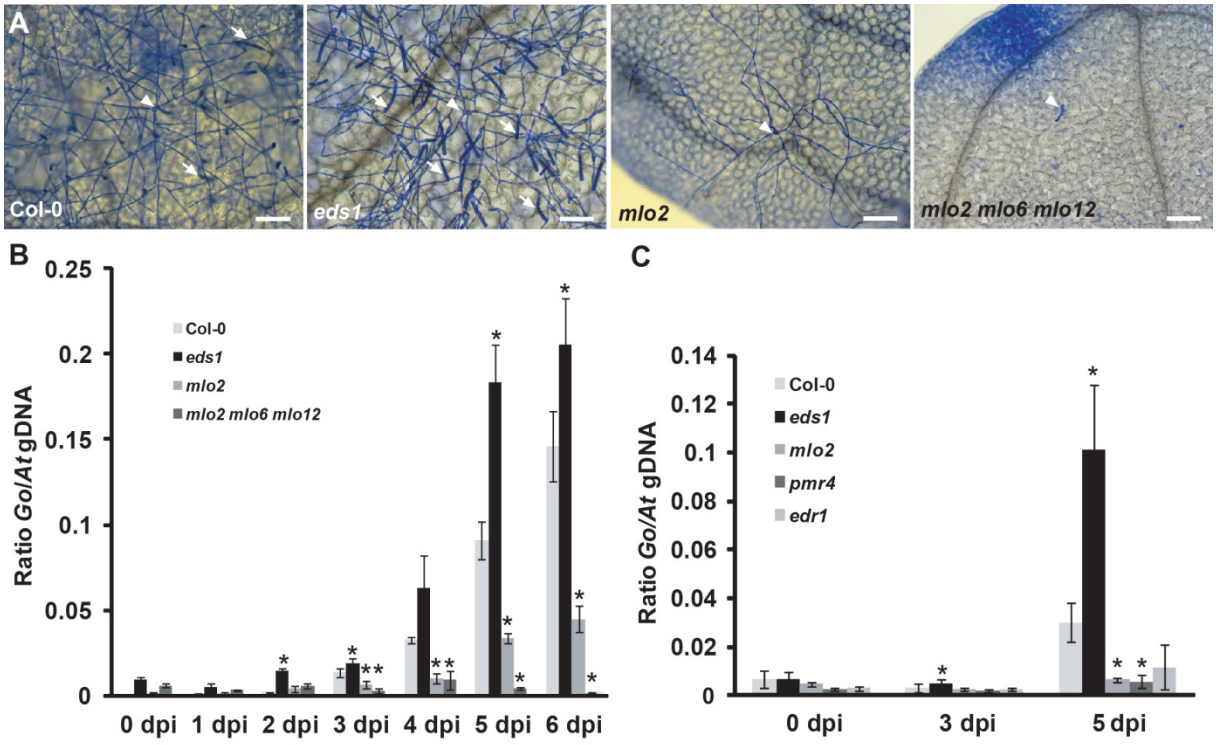

Figure 2: Time series analysis of powdery mildew infection by qPCR. (**A**) *G. orontii*-infected leaves were harvested at 5 dpi from Col-0 wild type and indicated mutant plants and stained with Coomassie Brilliant Blue. Arrows indicate conidiospore chains and arrowheads point to the initial spore. Images are representative of three independent experiments. (**B**) qPCR analysis of a time series of powdery mildew infection on Col-0 wild type, *eds1*, *mlo2* and *mlo2 mlo6 mlo2* plants. Ratios of *G. orontii* to Arabidopsis gDNA were determined by qPCR with primers R189/R192 and R193/R194, respectively. Bars represent the mean ± standard deviation of three technical replicates from a DNA sample of ten pooled seedlings grown in five different pots (two seedlings/pot used). (**C**) qPCR analysis of powdery mildew infection on Arabidopsis mutants that show powdery mildew-induced cell death. Representative time points of infection on Col-0 wild type, *eds1*, *mlo2, pmr4* and *edr1* plants were used. Ratios of *G. orontii* to Arabidopsis gDNA were determined by qPCR with primers R189/R192 and R193/R194, respectively. Bars represent the mean ± standard deviation of three DNA samples (each derived from ten pooled seedlings grown in five different pots) with three technical replicates each. Asterisks indicate statistically significant differences to Col-0 in two-tailed Student's t-test ($p<0,05$). Data shown are representative of three independent experiments. Scale bar is 50 µm.

To determine the dynamic range of our qPCR assay an infection time series of Col-0 wild type, *eds1*, *mlo2* and *mlo2 mlo6 mlo12* triple mutant plants was utilized (Figure 2A). Col-0 plants are very susceptible to *G. orontii* as penetration rates of up to 90% are typically observed (Consonni et al., 2006). The *eds1* mutant is compromised in both salicylic acid-dependent and -independent defense signaling pathways and thus hyper-susceptible to *G. orontii* infection (Bartsch et al., 2006; Dewdney et al., 2000). Mutations in particular *Mildew Resistance Locus O (MLO)* genes confer quantitative and additive penetration resistance to *G. orontii*, with penetration rates of ~40% in *mlo2* single mutants and ~1% in the *mlo2 mlo6 mlo12* triple mutant (Consonni et al., 2010; Consonni et al., 2006). Using primers R189/R192 (At3G21215) and R193/R194 (GoPMA1; Supplemental Table 1) in the qPCR analysis, relative *G. orontii* DNA abundance increased slightly until 2 dpi in the wild type and subsequently increased strongly, which reflects the microscopic observations (Figure 2 A). Differences between genotypes became first detectable at 3 dpi and increased until 5 dpi. For the hyper-susceptible mutant *eds1*, we repeatedly detected a saturation effect at 6 dpi (Figure 2B). The *mlo2 mlo6 mlo12* plants show complete resistance to

G. orontii penetration and therefore allow no hyphal expansion. Differences between ratios in the time course of this genotype are therefore probably due to small differences in inoculation densities as well as DNA degradation in dead and dying spores. This also leads to a dilution effect at later (4-6 dpi) time points of infection. At 5 dpi, approximate 5:2:1 ratios of relative *G. orontii* abundance of *eds1* to wild type to *mlo2* were repeatedly obtained (Figure 2B). Similar results were obtained with primer pairs R243/R244 and R263/R264 (data not shown). Also, from 3-5 dpi, the method can be used to resolve kinetics of powdery mildew pathogenesis.

Powdery mildew infection is often associated with host cell death, in particular exemplified as the final consequence of resistance (*R*) gene-mediated fungal growth arrest (Panstruga and Schulze-Lefert, 2002). Owing to a potential shift in the ratios of plant to fungal genomic DNA, host cell death responses may interfere with the qPCR-based quantification of powdery mildew pathogenesis. To assess this possibility, the qPCR time course was repeated at representative time points including two Arabidopsis mutants that exhibit powdery mildew-triggered cell death responses. Since no canonical (isolate-specific) cell death-associated *R* gene response has been described for the Arabidopsis-powdery mildew patho-systems (Micali et al., 2008) two induced mutants (*edr1* (*enhanced disease resistance1*) and *pmr4* (*powdery mildew resistant4*)) in the Col-0 genetic background were used. These mutants exhibit local powdery mildew-induced host cell death at the post penetration stage (Frye and Innes, 1998; Nishimura et al., 2003). The occurrence of confined powdery mildew-triggered cell death around fungal infection sites in the conditions used was confirmed by Trypan Blue staining (data not shown). Results from the qPCR assay indicate that the *pmr4* mutant supports similar fungal biomass as the *mlo2* mutant, while fungal biomass seems to be higher (intermediate between Col-0 and *mlo2*/*pmr4*) in case of the *edr1* mutant (Figure 2C).

2.1.3 Spore counts of *G. orontii*

Spore formation is a widely used surrogate to determine susceptibility of Arabidopsis to another obligate biotrophic pathogen, the oomycete *Hpa* (Feys et al., 2005; Stuttmann et al., 2011). This technique was therefore adopted for quantification of the reproductive success of *G. orontii*. First macroscopically visible powdery mildew symptoms were usually observed on *eds1* plants at 5 dpi and wild type plants at 6 dpi as previously described (Plotnikova et al., 1998). No macroscopic symptoms were detected on *mlo2* or *mlo2 mlo6 mlo12* mutant plants (Consonni et al., 2010; Consonni et al., 2006). The Col-0 ecotype is already very susceptible to *G. orontii* infection and from 7 dpi onwards no clear differences to eds*1* could be macroscopically detected anymore. Therefore, spore abundance was quantified at 6 dpi. After harvesting by centrifugation (see Materials and Methods for details), conidia were counted using a haemocytometer (Figure 3A and B). *G. orontii* conidiospores could clearly be detected as approximately 35 µm long and 18 µm wide ellipsoid structures that were easily distinguishable from contaminating particles. Size and appearance of spores matched earlier reports on *G. orontii* (Micali et al., 2008; Plotnikova et al.,

1998). As expected, no conidia were detected in any isolation from *mlo2 mlo6 mlo12* plants. On *mlo2* plants, significantly reduced numbers (10%-15%) of spores relative to the wild type were observed (Figure 3C).

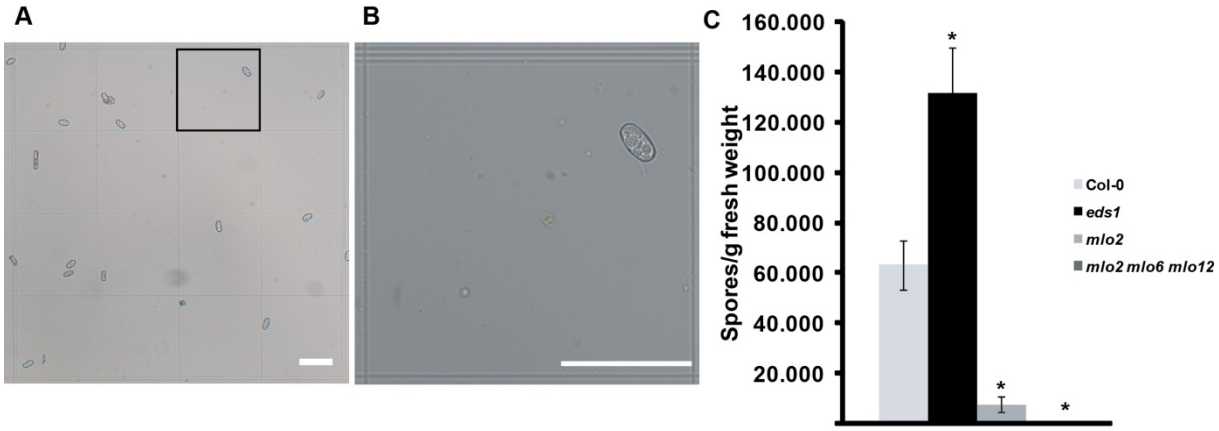

Figure 3: Analysis of powdery mildew infection by spore counts. (**A+B**) Brightfield images of isolated spores in the haemocytometer. (B) is a close-up of the indicated area in (A). (**C**) Spore counts of indicated genotypes at 6 dpi normalized to seedling fresh weight. Bars represent the mean ± standard deviation of three samples (500 mg of seedlings each) from one experiment counting eight fields/sample. Asterisks indicate statistically significant differences to Col-0 in two-tailed Student's t-test ($p<0,05$). Scale bars in (A+B) are 100 µm. Experiments were repeated twice with similar results.

From *eds1* plants we could repeatedly isolate twice the amount of conidiospores relative to the wild type (Figure 3C), although infection phenotypes were difficult to distinguish macroscopically at 6 dpi. The absolute number of isolated conidia varied from 50.000-90.000 spores/g fresh weight for the wild type across three repeated experiments, probably due to differences in the quality of the inoculum and/or inoculation density. The assay has a high dynamic range of four to five orders of magnitude (0 to about 120.000 spores/g fresh weight) and thus can also reveal even small differences in susceptibility between genotypes (see Figure 14 below).

2.2 Transcriptome analysis of enriched *G. orontii* haustoria

The haustorium is the fungal structure with closest contact to the host. It is believed to be the main site of both nutrient uptake and effector delivery by obligate biotrophic pathogens (Panstruga and Dodds, 2009). The haustorial transcriptome is amenable for expression analysis and has been used to unravel important aspects of host-pathogen interactions (Both et al., 2005a; Both et al., 2005b; Catanzariti et al., 2006; Duplessis et al., 2011b). I thus also used a transcriptomics approach to characterize the gene expression of *G. orontii* in more detail. Previously, *G. orontii* haustoria had been isolated by Percoll centrifugation in our lab and a non-normalized cDNA library had been generated from this material (Micali et al., 2011). In the following, I will present data that was obtained from the analysis of this library.

2.2.1 Sequencing and EST analysis of a haustorial cDNA library

The library was sequenced by 454 pyrosequencing technology, yielding 881,000 sequence reads and a total of 306 million base pairs (see Materials and Methods for details). All reads were mapped to the genomes of *G. orontii* (Spanu et al., 2010) and the *A. thaliana* TAIR9 assembly (Swarbreck et al., 2008). Eighty five percent of the reads mapped to the draft genome assembly of *G. orontii*, 6% to Arabidopsis and 10% could not be unambiguously assigned. Thus, although the haustorial centrifugation sample contained a considerable amount of contaminating chloroplasts, plastid RNA was mostly excluded by reverse transcription with oligo-dT primers. The 10% of unassigned sequences hint at a considerable amount of uncovered gene space in the present *G. orontii* draft assembly, although these reads may also correspond to contaminations of various origin. After removal of all unassigned sequences and stringent quality filtering, 679,000 reads (mean read length 346 bp±114 bp) were used for the final assembly into 20,259 contigs (see Materials and Methods for details). Many of the EST contigs obtained had comparably low sequence coverage (Figure 4A). To reduce sample complexity and increase reliability of the assembled transcripts, only contigs with ≥5-fold average coverage (AC) (7,077 contigs; mean AC 26±57, range from 5- to 1,436-fold; Figure 4A) were used for the final analysis. Open reading frames (ORFs) were predicted on these contigs using BestORF. Derived conceptual proteins were then annotated by Blast2GO (Conesa et al., 2005) using default parameters. It was found that 3,247 (45.9%) proteins lack any detectable homologs in the NCBI non-redundant (nr) database. Of the remaining proteins, 728 (10.3%) were annotated as retrotransposons, 824 (11.6%) had homologs in other species but no functional annotation, and 2,278 (32.2%) could be functionally annotated. To further reduce the number of non-annotated sequences, BLASTx searches of the assembled transcript sequences against the NCBInr database were also performed. This increased the number of sequences with BLAST hits by 14.7% to 3,725 but did not increase the overall number of annotated sequences, indicating no significant annotations associated with these BLAST hits.

The difference in average size of predicted proteins with (177±91 amino acids, corresponding ESTs 855±372 bp) and without recognizable homologs (58±45 amino acids, corresponding ESTs 353±265 bp) indicated that predicted proteins lacking BLAST hits are typically small and originate from small EST contigs. This finding suggests that they either encode genuine small peptides and/or represent truncated or misassembled transcripts. Additionally, non-canonical ORFs might have been inaccurately predicted by BestORF.

2.2.2 Functional classification indicates high protein turn-over in haustoria

For visualization, all predicted proteins with a "biological process" assignment (1,678) were annotated using the GOSlim terms generated from the *Candida albicans* genome. The majority of annotated sequences represented elements associated with gene expression and protein metabolism (translation, RNA metabolism, protein catabolism, transcription, protein modification, protein folding) (Figure 4B). The disproportionate representation of components involved in both protein synthesis and degradation suggests extensive protein turnover in haustorial complexes. Indeed, 44 of the 100 transcripts with the highest AC (AC >210; Supplemental Table 2) are involved in "translation". These chiefly encoded ribosomal subunits. Moreover, transcripts encoding proteins with functions in protein modification (5), protein catabolism (3) and protein folding (2) were among the Top100 expressed genes. Thus, more than 50% of the 100 most highly expressed genes were devoted to protein turnover.

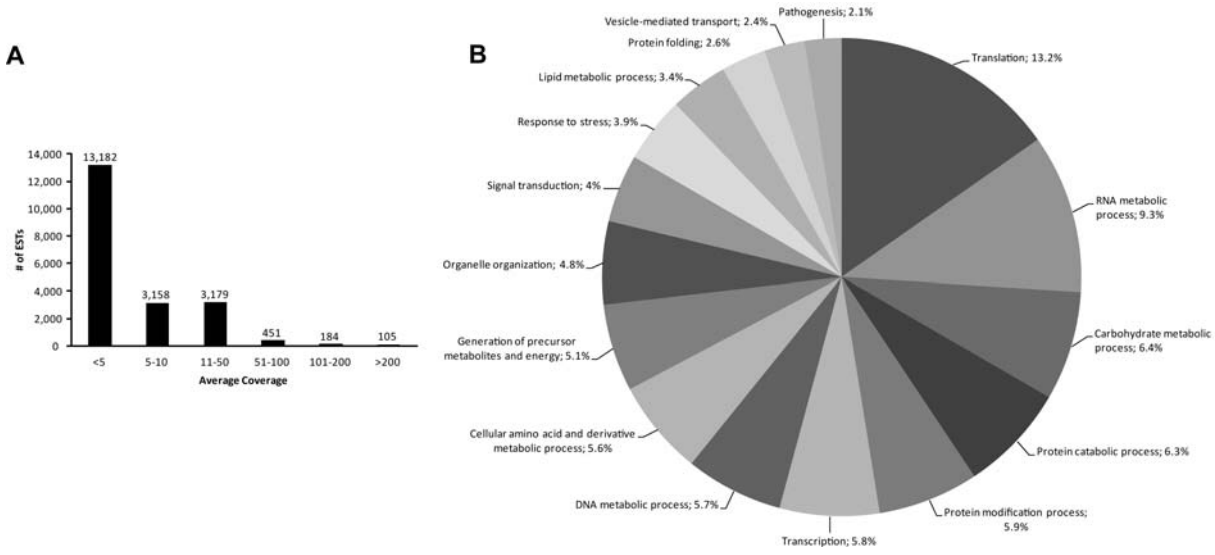

Figure 4: Quantitative analysis of the haustorial EST library. (A) Frequency distribution of sequences from the haustorial transcript library. EST contigs were classified according to their average coverage. All 20,259 contigs were included in the analysis. (B) Multilevel pie chart representing the functional annotation of predicted proteins. The diagram displays the relative abundance of *Candida albicans* GOSlim categories among the 1,678 annotated predicted proteins. Only categories with more than 35 members were included. Individual proteins may be represented in more than one category.

Transcripts encoding proteins of primary metabolism (carbohydrate, DNA, amino acid and lipid metabolism as well as energy production) were also well represented in the library. However, they were on average not as highly covered as transcripts encoding elements of protein turnover, as exemplified by the lack of transcripts related to carbohydrate metabolic proteins in the Top100

represented transcripts (Supplemental Table 2). Smaller subsets of proteins were also involved in signal transduction, the response to stress, vesicle-mediated transport and pathogenesis.

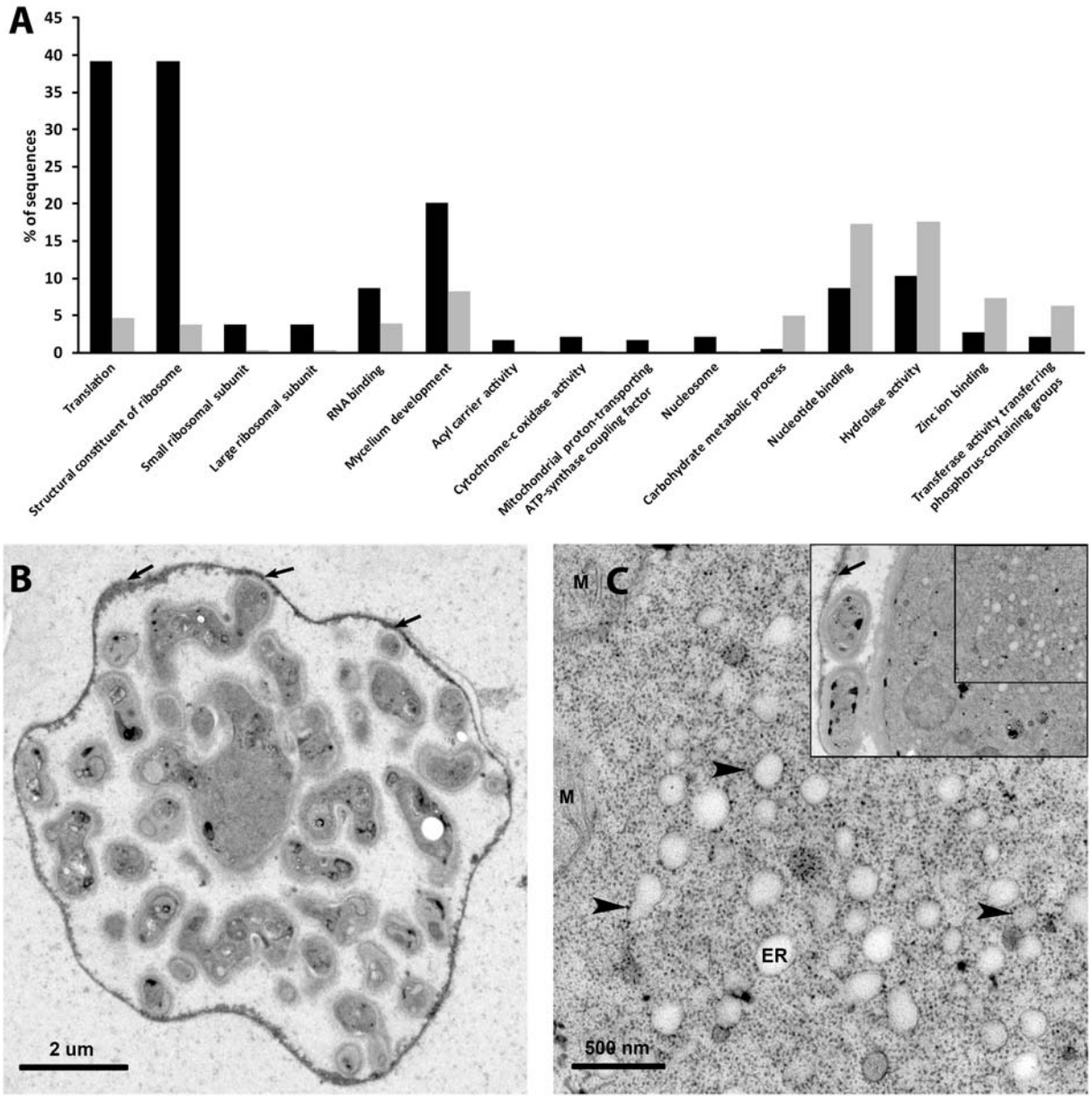

Figure 5: Haustoria show indications of high protein synthesis. (**A**) Enrichment analysis of GO categories in highly expressed genes. Sequences were divided into two groups, >100 AC (black bars) and 100>AC>5 (grey bars). A Fisher's exact test was performed to find significantly enriched (FDR<0,05) GO categories. (**B**) Ultrastructure of an isolated *G. orontii* haustorium displaying multiple lobes surrounded by an intact EHM (arrows). Isolated haustoria were processed by high-pressure freezing and freeze-substitution in osmium tetroxide/acetone (see Micali et al. 2011 for details). (**C**) Detail of an isolated haustorium showing abundant cytoplasmic ribosomes and a network of rough endoplasmic reticulum (ER). Notice the ribosomes tethered at the surface of the reticulum (arrowheads). M, mitochondrion. ER, endoplasmic reticulum. B and C are courtesy of Ulla Neumann.

To analyze the functions of the most highly expressed genes (AC >100) an enrichment analysis against the remaining sequences (100> AC >5) was performed. To this end, all annotated sequences of the two groups were compared by a Fisher's exact test to discover GO terms that were significantly (false discovery rate (FDR) <0,05) over- or underrepresented. Among the highly expressed genes, transcripts coding for proteins involved in translation and RNA binding were the most clearly overrepresented ones (Figure 5A), which is in line with their dominance in the

Top100 expressed genes (Supplemental Table 2). This finding was consistent with a large quantity of both cytoplasmic and endoplasmic reticulum-tethered ribosomes in isolated haustoria (Figure 5C and D) and further underlined the role of the haustorium as a prominent site of protein production. In addition, nuclear-encoded elements of the respiratory chain were also overrepresented. This was supported by the fact that 24% of the Top50 transcripts coding for transmembrane proteins constituted subunits of the mitochondrial respiratory chain (Supplemental Table 3) and further corroborated by the marked prevalence of mitochondria in the haustorial cytoplasm (Figure 5C and D and (Micali et al., 2011). The transcript abundance of riboflavin kinase (GoEST_c729; AC ~283), the key enzyme in flavin mononucleotide biosynthesis, further underlined this finding. Flavin mononucleotide is a mandatory cofactor of the NADH dehydrogenases of the respiratory chain. Interestingly, elements of carbohydrate metabolism were more abundant among the less represented transcripts. In general, basic metabolic activities (nucleotide binding, hydrolase activity, transferase activity transferring phosphorus containing groups) were underrepresented in the highly expressed genes, indicating low expression during this phase of pathogenesis.

2.2.3 ROS-detoxifying enzyme transcripts are abundant in *G. orontii* haustoria

Phytopathogens have to cope with different plant defense responses, one of the first being the generation of ROS (Hückelhoven and Kogel, 2003). The barley powdery mildew pathogen *Bgh* secretes a catalase during early pathogenesis, possibly to relieve oxidative stress at the infection site (Zhang et al., 2004). Therefore, the expression of protective proteins and ROS scavenging enzymes in the haustorial EST library was determined in detail. Among the Top100 expressed genes, two genes coding for proteins involved in the protection against ROS, thioredoxin H (GoEST_c612; AC ~284) and a thiol-specific antioxidant protein (TSA)/alkyl hydroperoxide peroxidase C (AhpC) family protein (GoEST_c351; AC ~467; Supplemental Table 2) were identified. Additional prominently expressed genes coding for ROS scavenging enzymes comprised genes encoding a Mn-type superoxide dismutase (GoEST_c417; AC ~204), a mannitol dehydrogenase (GoEST_c207; AC ~124), a gluthathione peroxidase (GoEST_c200; AC ~116) and a putative Fe-type superoxide dismutase (GoEST_c95; AC ~114). The fungus also expressed a gene coding for a secreted Cu/Zn-type superoxide dismutase (GoEST_c1259), although at lower levels (AC ~30; Supplemental Table 4).

2.2.4 Low abundance of nutrient transporter transcripts in haustoria

Haustoria are believed to be the key structures for nutrient uptake during fungal infection (Hahn and Mendgen, 1997; Voegele and Mendgen, 2003). Therefore, the transcript abundance of presumptive nutrient transporters was studied. Unexpectedly, a gene coding for a predicted phosphate transporter (GoEST_c38; AC ~216) (Supplemental Table 3) was the only gene of this category among the Top50 expressed genes encoding transmembrane proteins. Hence, a

detailed BLAST survey of putative transporters was conducted and revealed 39 annotated transporters expressed above 5-fold AC (Supplemental Table 5). Additionally, a targeted search for homologs of known fungal carbohydrate and amino acid transporter genes was performed to exclude the possibility that transcripts encoding *G. orontii* nutrient transporters were missed owing to fragmented cDNAs and/or inappropriate annotation. Query sequences were derived from the *Saccharomyces cereviseae* genome as well as Wahl et al., (2010). Using this diverse query set no additional highly expressed transporter sequences were uncovered. The annotated transporters mostly comprised Major Facilitator Superfamily (MFS) transporters and included nine putative sugar transporters (AC ~8-26), six predicted amino acid transporters (AC ~5-49) and eight drug efflux carriers (AC ~9-60). An additional phosphate transporter was also detected, although at low transcript level (AC ~6). Drug efflux and multidrug transporters displayed the highest transcript abundance, indicating a high demand for the export of antifungal compounds that are most likely produced by the plant during infection. In addition, a homolog of a putative *Bgh* glucose transporter gene, *GLTRN1* (GoEST_c22345), was expressed at very low levels (AC ~2). The gene coding for a homolog of the *Bgh* plasma membrane ATPase 1 (PMA1), a protein believed to generate the H^+ gradient required for nutrient uptake, was however expressed at a similar level as the MFS transporters (AC ~16). Among the higher expressed amino acid transporter genes in the library were two genes encoding transporters for γ-aminobutyric acid (GABA), a compound that has been implicated as a nitrogen source during infection of tomato by *Cladosporium fulvum* (Solomon and Oliver, 2002).

3.7 Pathogenesis-related transcripts are abundant in the haustorial cDNA library

Next, genes encoding homologs of proteins known or predicted to be involved in fungal pathogenesis were analyzed. Generally, the expression of these genes was comparatively low and they mostly coded for components of signal transduction (Supplemental Table 6). However, several pathogenesis genes with higher transcript abundance were also discovered (Supplemental Table 2). One of them (GoEST_c886; AC ~264) encodes a homolog of *Colletotrichum gloeosporioides* CAP20, a protein involved in host cell penetration (Hwang et al., 1995). Two genes encoding secreted proteins were also annotated as being involved in pathogenesis. One of them (GoEST_c231, AC ~224) encodes a homolog of *M. grisea* EMP1, an extracellular matrix protein required for appressorium formation and pathogenicity (Ahn et al., 2004). Similarly to EMP1, it contains a GPI-anchor signal predicted by PredGPI (http://gpcr.biocomp.unibo.it/predgpi/). The other gene (GoEST_c5330, AC ~16) encodes a homolog of Egh16H1 from *Bgh*, a member of a family of predicted extracellular proteins (Grell et al., 2003). The EMP1 homolog contains a so-called DRMIP-HESP (developmentally regulated MAPK interacting protein-haustorially expressed protein) domain, which has also been found in a haustorially secreted protein of the flax rust fungus, *Melampsora lini* (Catanzariti et al., 2006). This domain is also present in another secreted protein, an “extracellular serine-threonine rich protein” (GoEST_c4284; AC ~17). In addition, two genes encoding extracellular cell wall

modifying enzymes were detected: a protein with homology to a chitinase (GoEST_c1140) and a beta-glucanosyltransferase (GoEST_c4743; AC ~29).

2.2.5 qRT-PCR analysis of haustorial transcripts

To assess the temporal expression pattern of *G. orontii* transcripts eleven genes of different function were chosen for analysis by quantitative reverse transcription PCR (qRT-PCR). Among these were five genes encoding proteins involved in nutrient uptake (a phosphate transporter, a GABA permease, GoGLTRN1, GoPMA1 and a MFS maltose permease), three unknown secreted proteins (GoEST_c2903, GoEST_2438, GoEST_c253) as well as the secreted SOD (GoEST_1259), the CAP20 homolog (GoEST_c886) and a conserved hypothetical protein (GoEST_c501) with marked transcript abundance in the library (AC ~664). The qRT-PCR analysis was performed on cDNA from both infected leaves (ecotype Col-0) covered with epiphytic fungal mycelium as well as infected leaves from which the epiphytic mycelium was manually removed by cellulose acetate peeling. For most genes, transcript profiles from both materials were similar (see below for exceptions). Therefore, I focused on the samples devoid of mycelium, as these were more likely to recapitulate transcript abundance in isolated haustoria.

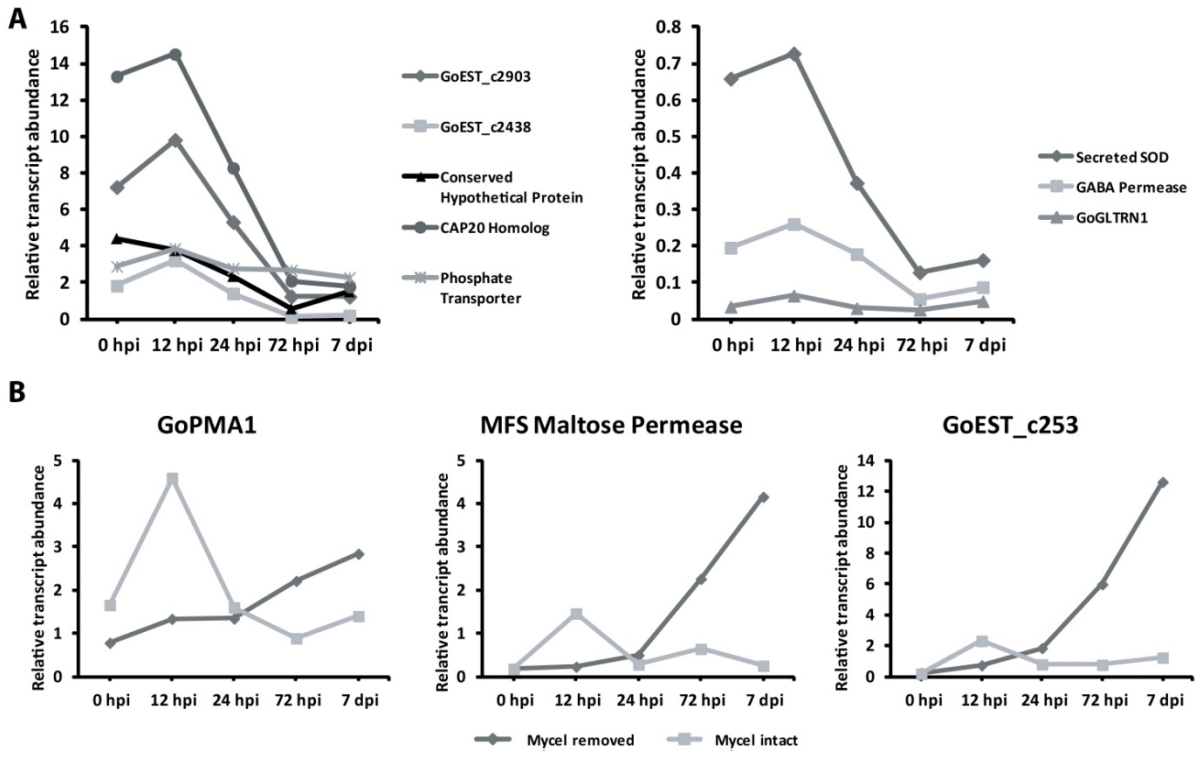

Figure 6: Transcriptional profiling of selected *G. orontii* genes in a time-course experiment. Eleven genes from different Gene Ontology categories were selected for qRT-PCR analysis. (A) qRT-PCR was performed on cDNA from Col-0 total leaf material with epiphytic mycelium removed at 24 hpi and later time points by cellulose acetate peeling. (B) Comparison of transcript profiles from native (epiphytic mycelium present) and cellulose acetate-peeled leaves (epiphytic mycelium removed). The experiment was repeated once with Col-0 and once with *NahG* transgenic plants with similar results. Transcript abundance was normalized to *G. orontii* β-tubulin.

Unexpectedly, many transcripts that were highly abundant in the cDNA library did not display high transcript levels in haustoria (peeled leaf samples) at 24 hpi or any later time point (72 hpi and 7 dpi; Figure 6A) when assayed by qRT-PCR. Instead, they showed rather reduced transcript

abundance at later stages of fungal development and highest transcript levels were typically observed at 12 hpi, just prior to host cell penetration and haustorium formation (Figure 6A). Using qRT-PCR the low expression levels of *SOD* and *GLTRN1* could however be confirmed (Figure 6A). The haustorial preparation used for RNA extraction and cDNA library construction was derived from *NahG* transgenic plants. The possibility that the difference in transcript abundance between the haustorial cDNA library and the qRT-PCR analysis of peeled leaf samples may originate from the plant source used was therefore also considered. To test for this possibility, one of the three replicates of the peeled leaf samples was derived from *NahG* plants. No marked difference in transcript patterns and/or abundance were observed between the two plant lines (Col-0 and *NahG* transgenics), indicating that the plant genotype does not account for the observed discrepancy between transcript abundance in the haustorial cDNA library and qRT-PCR data.

For three of the eleven transcripts tested by qRT-PCR (two coding for transporters and one for an effector candidate), a clear difference between the samples containing the epiphytic mycelium and the peeled leaf samples was detected (Figure 6B). These genes showed an increase in transcript levels at later time points (72 hpi and 3 dpi) in the peeled leaf samples, whereas they exhibited rather constant expression in the samples containing the epiphytic mycelium. In the case of these three genes the increase in transcript abundance was probably masked by the elevated expression of the reference gene, *β-tubulin*, in the mycelium-containing samples.

2.3 Functional characterization of *G. orontii* effector candidates

Microbial plant pathogens secrete a diverse set of effector molecules to manipulate the host during infection (Feng and Zhou, 2012; Stergiopoulos and de Wit, 2009). They manipulate a multitude of host processes to suppress host immunity and prepare the plant for colonization. While the effector arsenal of phytopathogenic bacteria has been characterized extensively, the effector repertoire of filamentous phytopathogens is comparatively unexplored. This is especially true for powdery mildew fungi, where research has mainly focused on bioinformatic analysis of effector proteins of the barley powdery mildew *Bgh* (Godfrey et al., 2010; Spanu et al., 2010). The functions of *Bgh* effector proteins are however only beginning to become elucidated (Schmidt, 2010; Zhang et al., 2012). Currently, information on the effector arsenal of dicot infecting powdery mildews, which are important agricultural pathogens, is completely lacking. The major aim of this thesis was therefore to both predict and functionally characterize the effector arsenal of *G. orontii*, a powdery mildew fungus of the model dicot *Arabidopsis thaliana*.

2.3.1 *G. orontii* effector prediction and cloning

Many effector genes have been discovered by transcriptomic studies of haustoria (Catanzariti et al., 2006; Hahn and Mendgen, 1997). I thus decided to employ the haustorial library (see 2.2) for effector prediction. Effectors typically carry a canonical amino (N)-terminal secretion signal and show little or no sequence-relatedness to proteins from distantly related species. These characteristics were used to implement a bioinformatic prediction pipeline (Figure 7A). Only contigs with ≥2 AC were fed into the pipeline. SignalP3.0 and TMHMM were used to identify proteins that possess a canonical secretion signal but lack any transmembrane domain(s) outside the signal peptide region. Subsequently, a size cut-off of 60 amino acids, the smallest size of known *Avr* effectors (Stergiopoulos and de Wit, 2009), was applied. A total of 250 of putatively secreted proteins were discovered, 105 of which did not have homology to proteins in the NCBInr database outside the mildews and were therefore considered as *G. orontii* effector candidates (OECs). Subsequently, the identified OECs were used for iterative BLAST searches ($e<10^{-5}$) against the haustorial library to detect paralogous effectors. The candidate secreted proteins (CSEPs) identified in *Bgh* were used as additional queries in this analysis (Spanu et al., 2010). In total, 115 OECs were identified. Nineteen of these genes represent 38% of the Top50 genes coding for secreted proteins (Supplemental Table 3). The OECs are considerably shorter (mean length 105 amino acids) than annotated secreted proteins (mean length 166 amino acids) and only eight contain a protein domain detectable by InterProScan (Supplemental Table 7). Three of these proteins had structural homology to microbial ribonucleases, a feature that has recently been noted for many *Bgh* CSEPs (Pedersen et al., unpublished results).

Many effector proteins have been found to be cysteine-rich. The presence of multiple cysteine residues is supposed to stabilize effectors in the apoplast via the formation of disulfide bridges. I thus inspected the cysteine content of the OECs. The average cysteine content was 2.8 per 100

amino acids but varied tremendously from 0 to almost 11 cysteine residues per 100 amino acids (Supplemental Table 7). A high frequency of cysteine residues has been associated (although not exclusively) with apoplastic effectors (Stergiopoulos and de Wit, 2009). A subset of the OECs might therefore act in the apoplast. For subsequent assays, a cytoplasmic activity of OECs was however assumed. Previously, the so called Y/W/FxC amino acid motif had been found to be associated with haustorially expressed powdery mildew and rust effectors, but no function could be attributed to it (Godfrey et al., 2010). This motif was also found in 27 OECs by manual inspection (Supplemental Table 7). The YxC motif occurred 13 and the FxC motif 16 times, respectively. OECs with the WxC motif were not detected. Recently, several effectors with nuclear localization have been described (Caillaud et al., 2012; Kleemann et al., 2012; Schornack et al., 2010). The OECs were thus also scanned for the presence of a canonical nuclear localization signal (NLS) by NLStradamus and NucPred (Nguyen Ba et al., 2009; Brameier et al., 2007). Signatures of NLS were detected for OEC10, OEC40 and OEC125, which form a cluster of phylogenetically closely related proteins (Figure 7 and Supplemental Table 7), as well as OEC56.

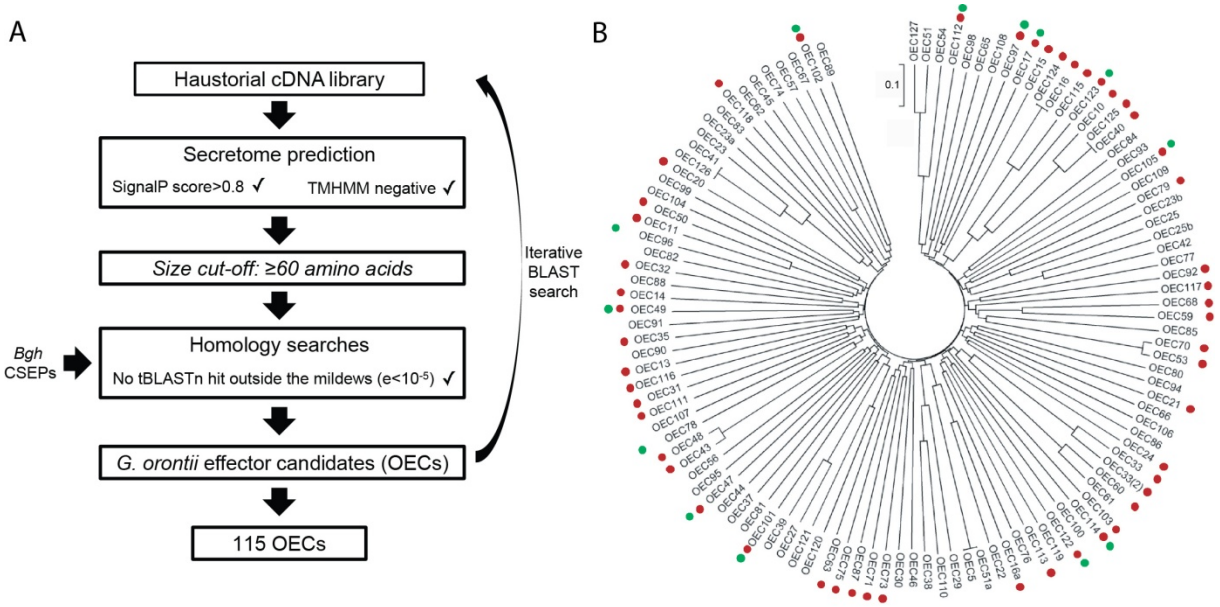

Figure 7: Bioinformatic prediction and phylogenetic analysis of *G. orontii* effector candidates. (**A**) Schematic overview of the prediction pipeline used to derive the OECs. (**B**) Circular dendogram showing the phylogeny of the OECs. A multiple sequence alignment of the OECs was created by ClustalW and imported into MEGA4. The phylogeny was computed using the Neighbor-joining algorithm and a p-distance model for amino acid substitutions. OECs with homologs (tBLASTn, e<10-^{5}) in *E. pisi* or *Bgh* are indicated in red and green, respectively.

Subsequently, the phylogenetic organization of the OECs was explored. The predicted protein sequences were aligned by ClustalW (http://www.ebi.ac.uk/Tools/msa/clustalw2/) and the alignment was used for the computation of phylogeny with MEGA4 (Tamura et al., 2007). The *Bgh*, CSEPs are organized into several larger and smaller protein families (Spanu et al., 2010) and I thus expected to observe a similar pattern for *G. orontii*. Surprisingly, only few larger families of OECs were identified (Figure 7B) and most OECs were found to have no close paralogs. My analysis was however solely based on the haustorial cDNA library as the genome of *G. orontii* was too fragmented for a reliable identification of paralogs.

During the effector prediction process, homologies of OECs to *Bgh* ESTs or genomic contigs had been noted. Therefore, the conservation of the OECs in the two related powdery mildews *Bgh* and *E. pisi* was explored (Figure 7B and Supplemental Table 7). *G. orontii* is more closely related to *E. pisi* than *Bgh* (Spanu et al., 2010) and this is also reflected in the number of detected homologs: 50 OECs were homologous to *E. pisi* genes while homologs to *Bgh* were only detected for 13 OECs. To confirm these results, a BLASTp survey against an extended set of 491 *Bgh* CSEPs (Pedersen et al., unpublished results) was conducted and 16 OECs were found to have homologies to these CSEPs (Supplemental Table 7). This finding supports the previous analysis, as the differences in numbers can be explained through improved ORF predictions in the manually curated CSEPs relative to the raw genome surveyed by tBLASTn.

Subsequently, the OECs were cloned without the signal peptide into Gateway®-compatible vector systems in two successive rounds. First, attB-site containing primers were used which allowed the cloning of only 32 OECs. This set was used for most of the assays described in the following paragraphs. Later, TOPO®-TA cloning with corresponding shorter primers was employed which extended the number of cloned OECs to 84.

2.3.2 Most effector candidates suppress induced cell death

Obligate biotrophic pathogens like the powdery mildews can only thrive on living host cells. The induction of localized programmed cell death is therefore a common and effective response of plants to these pathogens (Ellis et al., 2007; Panstruga and Schulze-Lefert, 2002). Previously, effectors of different filamentous pathogens have been found to suppress host cell death and this possibility was therefore also explored for the OECs (Bos et al., 2006; Kleemann et al., 2012; Oh et al., 2009). To address this, transient coexpression assays of the OECs with the two necrosis-inducing peptides NLP1 from *Colletotrichum higginsianum* (Kleemann et al., 2012) and INF1 from *Phytophthora infestans* (Kamoun et al., 1997) were performed. Briefly, Agrobacteria containing a vector for OEC expression and Agrobacteria containing a vector with one of the two necrosis-inducing peptides were co-infiltrated in one leaf of *Nicotiana benthamiana* and macroscopic cell death symptoms assessed at 7 dpi. These two proteins have different modes of action and might thus allow the discrimination of cell death pathways targeted (Kanneganti et al., 2006). As controls, a second co-infiltration was performed on the same leaf in which the necrosis-inducing peptide was replaced with Yellow Fluorescent Protein (YFP) and OECs were also infiltrated alone. Co-infiltration sites of *Ch*NLP1 and YFP consistently displayed confluent necrosis at 7dpi (Figure 8A and B), while necrosis induced by *Pi*INF1 was more patchy and less consistent (Figure 8C) and thus more difficult to score reproducibly. Inhibition of ChNLP1-induced necrosis was also much clearer relative to *Pi*NF1 (Figure 8A and C) and led to the absence of visible necrosis on the leaf after Trypan Blue staining (Figure 8B). Inhibition of cell death triggered by either inducer by YFP was never observed.

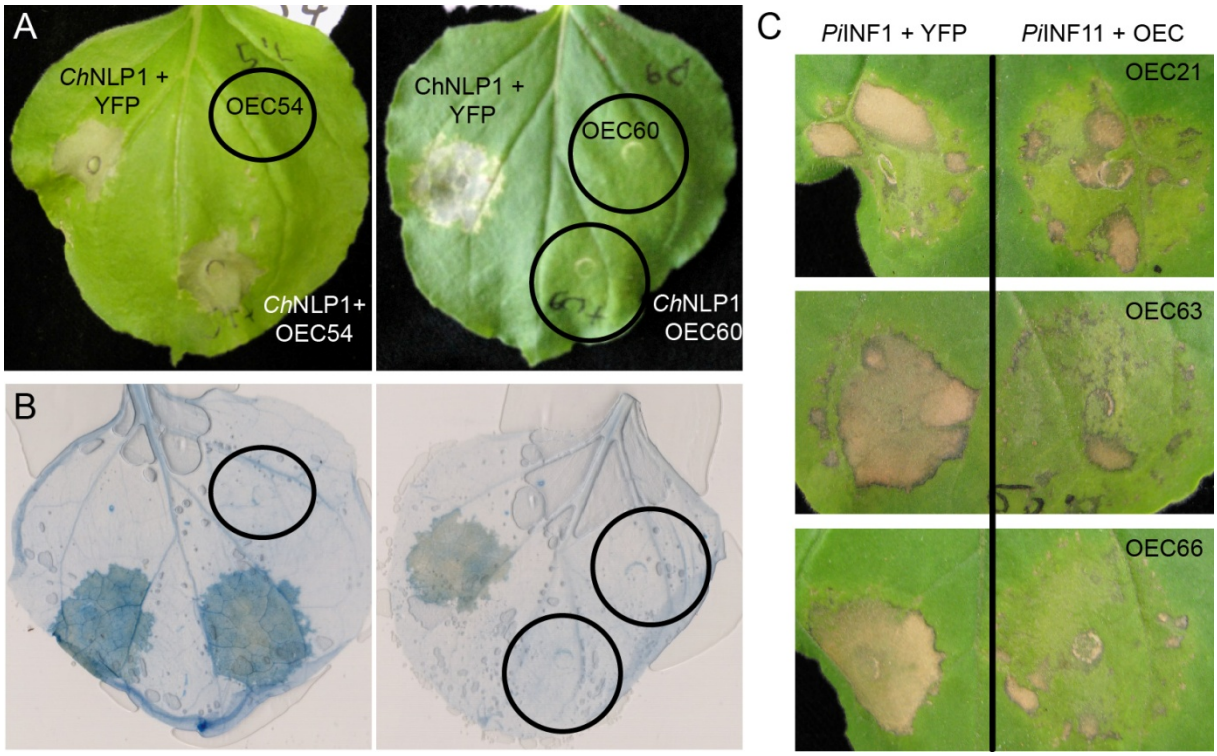

Figure 8: OECs suppress induced plant cell death. Agrobacteria containing vectors for either OEC or YFP expression were mixed with those carrying cell death inducer vectors. Mixtures or OECs alone were infiltrated into opposite sides of *N. benthamiana* leaves for comparison. Macroscopic symptoms on three leaves from three different plants were documented per OEC at 7 dpi. (**A, B**) Examples of *Ch*NLP1-infiltrated leaves showing lack of and successful cell death suppression. (**B**) Cell death on leaves shown in A was visualized by Trypan Blue staining. (**C**) Examples of leaves infiltrated with *Pi*NF1 at 7dpi. OEC63 and 66 were the only OECs inhibiting *Pi*NF1-induced cell death. The experiment was repeated twice (**A**+**B**) or once (**C**) with similar results.

All 32 OECs cloned at the time were surveyed and the inhibition of *Ch*NLP1-triggered cell death was observed for 72% of the tested OECs (Table 1). At the moment, it cannot be excluded that this effect is due to the interference with *Ch*NLP1 expression in the co-infiltration assay, as an epitope-tagged version of *Ch*NLP1 was non-functional in my hands. In contrast to *Ch*NLP1, cell death triggered by *Pi*NF1, was only suppressed by OEC63 and OEC66. These effectors also suppressed *Ch*NLP1-triggered necrosis (Figure 8C and Table 1). The prevalent interference of OECs with *Ch*NLP1-triggered cell death signaling might therefore be elicitor-specific.

The suppression of R protein-triggered HR has also been described for few selected effectors and was thus tested for the OECs (Houterman et al., 2008; Kelley et al., 2010; Macho et al., 2010). The combination of the *Pi* effector *Avr3a* and the potato *R3a* resistance gene was used for transient infiltrations in *N. benthamiana* (Armstrong et al., 2005; Huang et al., 2005). Agrobacteria containing OECs and *Avr3a* were co-infiltrated one day after the infiltration of an *R3a*- delivering Agrobacterium strain. None of the OECs could suppress cell death in this assay (Luigi Faino, personal communication).

Table 1: OECs suppress induced plant cell death. Summary of three (two for INF1) independent co-infiltration experiments. For categorizations see Figure 8 (+++= Figure 8A, left panel; ++= Figure 8C, OEC63/66; ---= Figure 8A, right panel)

	Inhibition of cell death induced by	
OEC	*Ch*NLP1	*Pi*INF1
OEC10	---	---
OEC11	+++	---
OEC14	---	---
OEC15	+++	---
OEC16	+++	---
OEC21	---	---
OEC24	---	---
OEC25	---	---
OEC27	+++	---
OEC28	+++	---
OEC31	---	---
OEC37	+++	---
OEC39	+++	---
OEC41	+++	---
OEC42	+++	---
OEC45	+++	---
OEC48	+++	---
OEC50	+++	---
OEC51	---	---
OEC54	---	---
OEC55	+++	---
OEC56	+++	---
OEC57	+++	---
OEC60	+++	---
OEC61	+++	---
OEC63	+++	++
OEC65	+++	---
OEC66	+++	++
OEC67	---	---
OEC68	+++	---
OEC70	+++	---
OEC71	+++	---

2.3.3 **Bacterial delivery of selected effectors interferes with host immunity**

Besides the suppression of host cell death, many effectors target additional components of MTI to promote infection. In powdery mildews and other obligate biotrophic pathogens, it is however difficult to assess the contribution of single effectors to pathogenicity, as methods for targeted gene disruption or overexpression are not yet available. The delivery of fungal or oomycete effectors to the plant cell cytoplasm by genetically engineered bacteria is one way to circumvent this problem. The so called effector detector vector system (EDV) exploits this possibility. It comprises a fusion protein of amino acids 1-136 of *Pst* AvrRPS4, a T3SS based effector, and the effector of interest (Fabro et al., 2011; Sohn et al., 2007). A luciferase-expressing *Pst* strain is then employed for fusion protein delivery via the T3SS and bioluminescence-based bacterial growth assessment. The domain of AvrRPS4 used still contains an *in planta* proteolytic cleavage signal which leads to the liberation of the effector of interest in the plant cytoplasm (Sohn et al., 2007). Suppression of MTI by single effectors leads to enhanced growth of bacteria. This assay has successfully been applied to both fungal and oomycete effectors (Fabro et al., 2011; Kleemann et al., 2012; Sohn et al., 2007) and was thus also employed in this study. In brief, OECs and YFP as a control were subcloned into pEDV and transferred to *Pst* carrying the Luciferase operon (*Pst* LUC). No differences in growth of pEDV-OECs relative to the YFP control were observed. Luciferase activity was also not different between strains (data not shown). The secretion of AvrRPS4-OEC/YFP fusion proteins was confirmed by an *in vitro* secretion assay

(Supplemental Figure 2). For three of the OECs (OEC27, OEC51 and OEC54) no secretion could be detected. These were therefore excluded from the subsequent analysis.

In a primary screen, three replicates of plants were spray-inoculated with *Pst* LUC pEDV strains and bioluminescence assessed on four leaf discs per replicate and genotype at 3 dpi. No OECs were found to reduce bacterial growth on Col-0, indicating the absence of effectors with Avirulence activity in our set, which was expected due to the apparent lack of *R* gene triggered immunity towards powdery mildew fungi in Arabidopsis (Micali et al., 2008). The assay had high intrinsic variability and I therefore decided to score only significantly increased bacterial bioluminescence of more than 10-fold compared to the YFP control. Using these criteria, 14 constructs that produced increased bioluminescence in three of four repeated experiments were selected for in depth analysis by bacterial titer measurements. Plants were again spray-inoculated and bacteria isolated and quantified at 0 and 3 dpi. No differences in the initial bacterial titer were detected. The *eds1* mutant was used to confirm the virulence activity of the YFP negative control, which was able to grow to high titers in this mutant. Six effectors (OEC25, 48, 60, 61, 63 and 65) were found to allow >10fold significantly increased growth of transgenic bacteria in repeated experiments and were thus short-listed for subsequent screens. OEC56, an effector with confirmed nuclear localization (see Figure 10A below) was also included in this list.

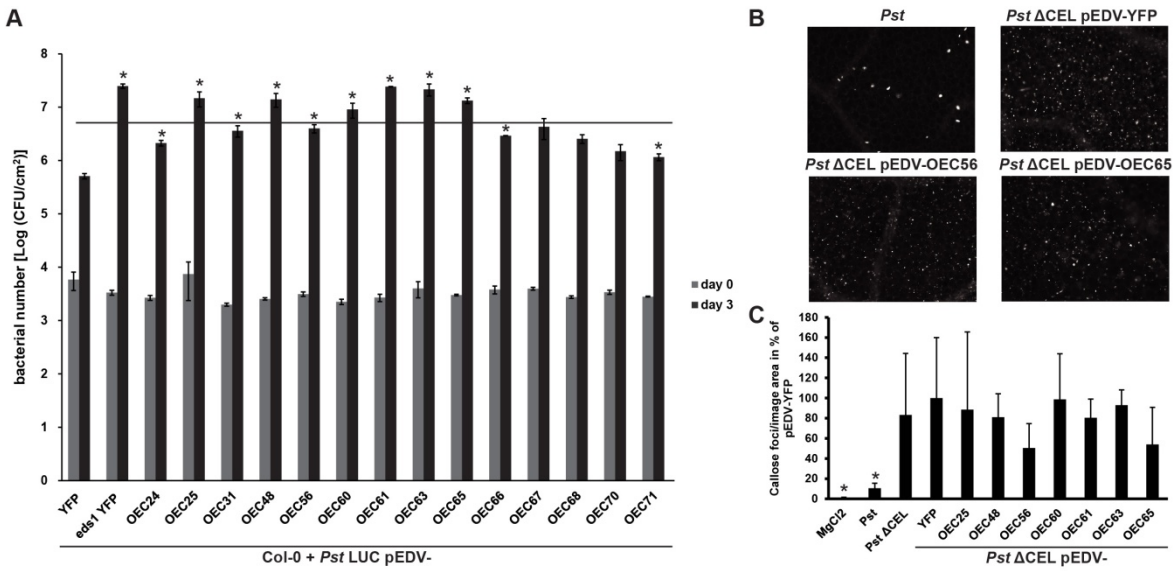

Figure 9: OECs delivered by bacteria promote virulence aft and suppress callose deposition. (**A**) Five week old Col-0 plants were spray-infected with OD_{600nm} 0,05 of *Pst* LUC strains delivering the indicated OECs in pEDV. Bacteria were isolated from triplicate samples at day 0 and day 3. The *eds1* mutant was used as a positive control. Bars are average of three biological replicates ± SE. Significant differences to Col-0 ($p<0,05$ in Student´s t-test) are indicated by *. Only OECs with >10-fold differences to the YFP control (above horizontal bar) were considered for subsequent analysis. The experiment was repeated thrice with similar results. (**B**+**C**) Col-0 plants were infiltrated with OD_{600nm} 0,2 of indicated *Pst* strains or $MgCl_2$. Leaf samples were taken at 14 h after infiltration and callose stained with aniline blue. (**B**) Exemplary images from indicated infiltrations. (**C**) Quantitative analysis of callose foci/ image area for indicated strains. Two images per leaf were taken from 20 infiltrated leaves per strain and callose foci were counted using ImageJ. Bars represent the average of three independent experiments; data was normalized to *Pst* ΔCEL pEDV-YFP for each experiment. Significant differences to *Pst* ΔCEL pEDV-YFP ($p<0,05$ in Student´s t-test) are indicated by an asterisk *.

The increased growth of OEC-delivering, but already virulent bacteria pointed towards a role of powdery mildew effectors in the suppression of MTI. The MAMP-triggered deposition of callose at the cell wall is a prominent MTI output that is suppressed by virulent *Pst* strains (DebRoy et al.,

2004; Gómez-Gómez et al., 1999). A mutant strain of *Pst* that lacks the conserved effector locus (CEL), which contains the effectors AvrE and HopM1, can however no longer suppress callose deposition (DebRoy et al., 2004). This strain can therefore be used for EDV-based screens of callose suppression (Sohn et al., 2007). Short-listed pEDV-OEC clones (Figure 9A) were monitored for suppression of callose deposition by introduction into *Pst* ΔCEL and infiltration into Col-0. The assay was functional as exemplified by the significant differences between the number of callose deposits induced by $MgCl_2$, the positive control *Pst* and the negative control *Pst* ΔCEL mutant (Figure 8B and C). OEC56 and OEC65 were found to reduce the amount of callose foci by 50% and 46% on average, respectively, but these results were not statistically significant due to the high variability of the assay. No callose suppression was observed for the remaining OECs. This experiment has to be repeated additional times to allow clear conclusions.

2.3.4 Effectors show differential localization and expression patterns

The subcellular localization of effectors in the plant cell can give important clues on their targets and function (Bartetzko et al., 2009; Caillaud et al., 2012). Ideally, the delivery to and subcellular localization in the plant cell is studied by expressing genes encoding effector – fluorophore fusion proteins from the native promoter (Doehlemann et al., 2009; Khang et al., 2010; Mosquera et al., 2009). These approaches are however often hampered by insufficient protein amounts transferred to the plant cell. For powdery mildew fungi and other obligate biotrophic pathogens that are not amendable to transformation, this approach is completely unfeasible. The subcellular localization of OECs was therefore investigated by transient overexpression in *N. benthamiana,* a system that has been widely adopted for localization screens (Caillaud et al., 2012; Schornack et al., 2010). Citrine, a less photosensitive version of yellow fluorescent protein (YFP) was used as a fluorophore for OEC fusion proteins (Griesbeck et al., 2001). Agrobacteria carrying vectors with genes coding for OEC-Citrine fusion proteins were co-infiltrated with constructs carrying the p19 silencing suppressor in *N. benthamiana* leaves (Voinnet et al., 2003). Samples were investigated at 3 dpi by confocal laser scanning microscopy (CLSM).

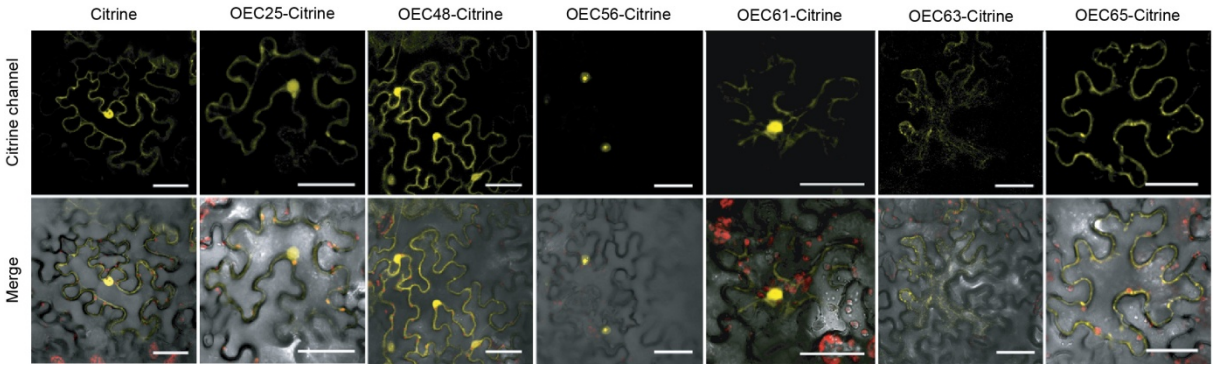

Figure 10: Subcellular localization of OECs. Agrobacteria containing vectors with genes encoding OEC-Citrine fusion proteins or Citrine alone were infiltrated into *N. benthamiana* leaves. CLSM images of indicated constructs in *N. benthamiana* epidermal cells were taken at three days after infiltration from at least two leaves and three cells/leaf. Representative images are shown. Merged image is an overlay of the Citrine, brightfield and chloroplast channels. Scale bar is 50 µm.

As expected, Citrine alone was localized to the nucleus and cytoplasm. OEC25-, OEC48- and OEC61-Citrine fusions localized to both the cytoplasm and the nucleus, with predominant nuclear localization for OEC61-Citrine (Figure 10A). OEC56-Citrine, an effector with a predicted NLS (Supplemental Table 7), displayed exclusive nuclear localization. No cytoplasmic signal could be detected even after signal saturation in the nucleus. This localization could also be confirmed by bombardment of the OEC-Citrine construct into detached Arabidopsis leaves (

Supplemental Figure **3**B). The predicted nuclear localization of OEC10, another effector with a predicted NLS could not be confirmed in Arabidopsis (

Supplemental Figure **3**B). This effector was therefore not investigated further. OEC63 was found to localize to a network-like structure indicative of the ER. This still awaits confirmation by co-localization experiments with ER marker proteins. OEC65 was detected in the cytosol and was excluded from the nucleus, although the fusion protein was clearly below the size exclusion limit of the nucleus (Wang and Brattain, 2007). Additional foci of OEC65-Citrine accumulation were also observed. The expression of OEC60-Citrine was never detected and this effector thus excluded from subsequent analyses. Generally, the expression of fusion proteins was greatly reduced relative to Citrine alone. Due to the low expression of fusion constructs, protein abundance could not be visualized by Western Blotting with anti-GFP antibodies (data not shown). Overall, the tested OECs localize to several distinct or overlapping subcellular compartments.

The original material used for the generation of the EST library comprised an enriched preparation of haustorial complexes that were isolated from infected Arabidopsis plants at fout to six dpi. At this stage of pathogenesis, fungal mycelia were fully developed and conidiophores emerged, but the colonies contained mixtures of juvenile and mature haustoria. The temporal patterns of effector production could therefore not be resolved, although this information is useful for subsequent functional analysis (Kleemann et al., 2012; Wang et al., 2011).

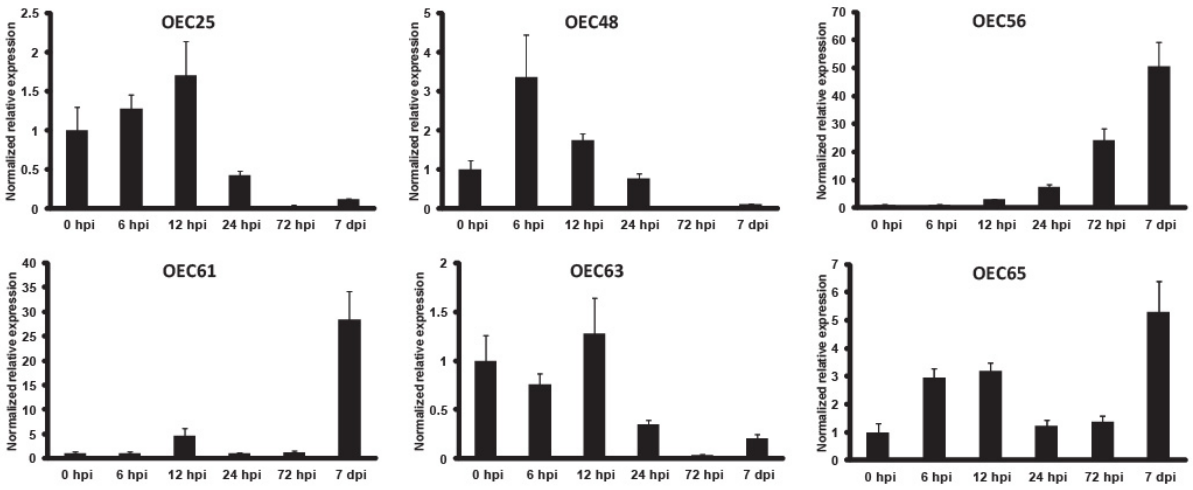

Figure 11: Analysis of OEC expression by qRT-PCR during infection. The qRT-PCR was performed on cDNA from Col-0 total leaf material with epiphytic mycelium removed at 24 hpi and later time points by cellulose acetate peeling. Transcript

abundance was quantified relative to *G. orontii* β-tubulin and normalized to the 0 hpi time-point. The experiment was repeated once with similar results.

To cope with this limitation, a qRT-PCR analysis of effector transcript abundance was conducted as a time-course experiment throughout fungal pathogenesis (Figure 10B). I previously found that qRT-PCR on infected leaves containing epiphytic fungal structures can underestimate the relative transcript abundance of genes in haustoria (2.2.5). At 24 hpi and later, the epiphytic mycelium was therefore removed to analyze the haustorial expression of effectors only. Unexpectedly, OEC25, OEC48 and OEC63 were predominantly expressed at the early stages of infection (0-24 hpi), with expression peaking as early as six hpi (OEC48) and twelve hpi (OEC25 and 63). This is before the appearance of first haustoria at approximately 14 hpi (Micali et al., 2008), suggesting that these effectors potentially prepare the host cell for the accommodation of the haustorium. OEC56 and OEC61 transcripts were strongly induced at late stages of infection and accumulated 51- and 38-fold relative to the 0 hpi time point at 7 dpi, respectively. Early and late acting effectors could therefore clearly be distinguished by qRT-PCR analysis. OEC65, by contrast, was expressed to similar levels throughout the infection process.

2.3.5 Systematic Y2H reveals effector host targets and convergence onto hubs of the host cellular network.

Effectors exert their function through the interaction with and manipulation of host proteins (Bozkurt et al., 2012; Feng and Zhou, 2012). The characterization of effector targets has therefore revealed several previously uncharacterized players in the host immune system (Fu et al., 2007; Mackey et al., 2002; Nomura et al., 2006). I was also interested in putative host targets of the OECs. Recently, a systematic Y2H screen has revealed host targets of a large set of effectors from different *Pseudomonas syringae* pathovars *(Psy)* and *Hpa* isolates in Arabidopsis (Mukhtar et al., 2011). To identify OEC host targets and complement the existing data with an additional unrelated pathogen of Arabidopsis, the set of 84 cloned OECs was also screened using an extended prey library and the same experimental pipeline. The library used was comprised of Space 1, which included the AtORFeome2.0 (8583 ORFs) (Arabidopsis Interactome Mapping Consortium, 2011; Yamada et al., 2003) and selected Arabidopsis immune proteins (415 ORFs) (Mukhtar et al., 2011), and Space2 (3396 ORFs, see Supplemental Table 9), which was not included in the previous screens. Binary protein-protein interactions between the OECs and these proteins were mapped in a high-throughput Y2H pipeline as described (Dreze et al., 2010). Briefly, OECs were first transferred into Y2H vectors in AD-OEC and DB-OEC configuration, transformed into yeast and screened for autoactivation of reporters. Fifteen OECs were identified as autoactivators in the DB-OEC orientation (OEC11, OEC29, OEC31, OEC33 OEC42, OEC59, OEC61, OEC76, OEC99, OEC105, OEC112, OEC116, OEC118, OEC25c, OEC47), leaving a total of 69 effectors for the DB screen. No autoactivators were detected in the AD-OEC orientation. First, each DB-OEC yeast strain was tested for possible interactions against mini-libraries of 192 AD-*At* yeast strains and pools of all AD-OECs were screened against the DB-*At* library. This first step was completed twice to increase sampling depth. In total, 1370

primary positive interactions were obtained, 1052 in DB-OEC and 318 in AD-OEC orientation. These were then tested again in a second round of screening and 830 interactions were confirmed. While the confirmation rate was 73% for DB-OEC clones, it was only 24% for AD-OEC clones. Individual interactors were then identified by insert sequencing revealing 313 distinct interactions. Finally, interactions were confirmed by four independent pairwise matings of individual clones. Only pairs whose phenotype could be confirmed in at least three of four experiments and did not show any signs of autoactivation were considered as final Y2H interactions. This was successful for 132 interactions (42%) of 47 effectors with 61 Arabidopsis proteins (Figure 12 and Supplemental Table 10), all of them in the DB-OEC orientation. The reason for the lack of confirmed AD-OEC interactions is unknown, but similar observations were also made with effectors of *Hpa* and *Pst* (Pascal Braun, personal communication). The Y2H pipeline used here is identical to the one used for generating AI-1 (Arabidopsis Interactome Mapping Consortium, 2011). The screening sensitivity (the coverage of all possible interactions in the tested space – 16%) and precision (proportion of true biophysical interactions – 80%) of AI-1 can thus also be applied to the current screen. These parameters indicate that a high-quality interactome was obtained.

While the average number of interactors per effector was 2.8, both effectors with many interactions (e.g. OEC78: 17 interactors, OEC45: 15 interactors) and single interactions were identified. Similar observations were made for Arabidopsis effector targets. The average number of interacting OECs per Arabidopsis protein was 2.2, while several proteins with many or single hits were detected. The TF *teosinte branched*1, cycloidea (CYC), proliferating cell factor (PCF) (TCP) 14, a member of a large family of transcriptional regulators believed to mainly function in plant development (Martín-Trillo and Cubas, 2010), was targeted by 23 distinct OECs. This was the highest number detected in the screen. Interestingly, three other TCPs (TCP13, TCP15, TCP20) were also targeted multiple times by OECs. The highly homologous COP9 signalosome subunits 5a (CSN5a) and CSN5b also interacted with nine and ten OECs in the screen, respectively. These proteins are involved in the regulation of many processes by controlling the neddlyation status of E3 ubiquitin ligases (Gusmaroli et al., 2007). To investigate the proportion of defense-related proteins among effector targets, literature-curated protein categorization were imported (Mukhtar et al., 2011). Similar to observations made for *Psy* and *Hpa* effectors (Mukhtar et al., 2011), OECs mostly did not interact with Arabidopsis defense proteins directly (Figure 12A). Only three immune-related proteins (Fibrillin, PRA1.F2 and PRA1.F3) were directly targeted by effectors. Interactors of primary OEC targets were however frequently interacting with components of the host immune system, indicating an indirect manipulation of the host. Four different effectors (OEC25, OEC45, OEC63 and OEC125) were for instance directly interacting with two interactors of the immune system component RIN4 which is guarded by RPM1 and RPS2 (Kim et al., 2005b; Mackey et al., 2002). Similarly, 15 of the direct effector targets also interact with NB-LRR proteins. Both NB-LRR and RLK proteins were however only screened as

truncated versions, interactions with additional domains of these proteins can therefore not be excluded.

To address the overall functional properties of primary host targets, a GO analysis was performed. The distribution of GO terms in the Y2H library was included for comparison, as this library already included significant bias. Effector targets were clearly enriched for protein involved in transcription, developmental processes and transport, proteins with binding and transcription factor activities as well as nuclear and ER-resident proteins (Figure 12B). In addition, effector targets were underrepresented among proteins with transferase activity. For a complete set of GO annotations see Supplemental Figure 4.

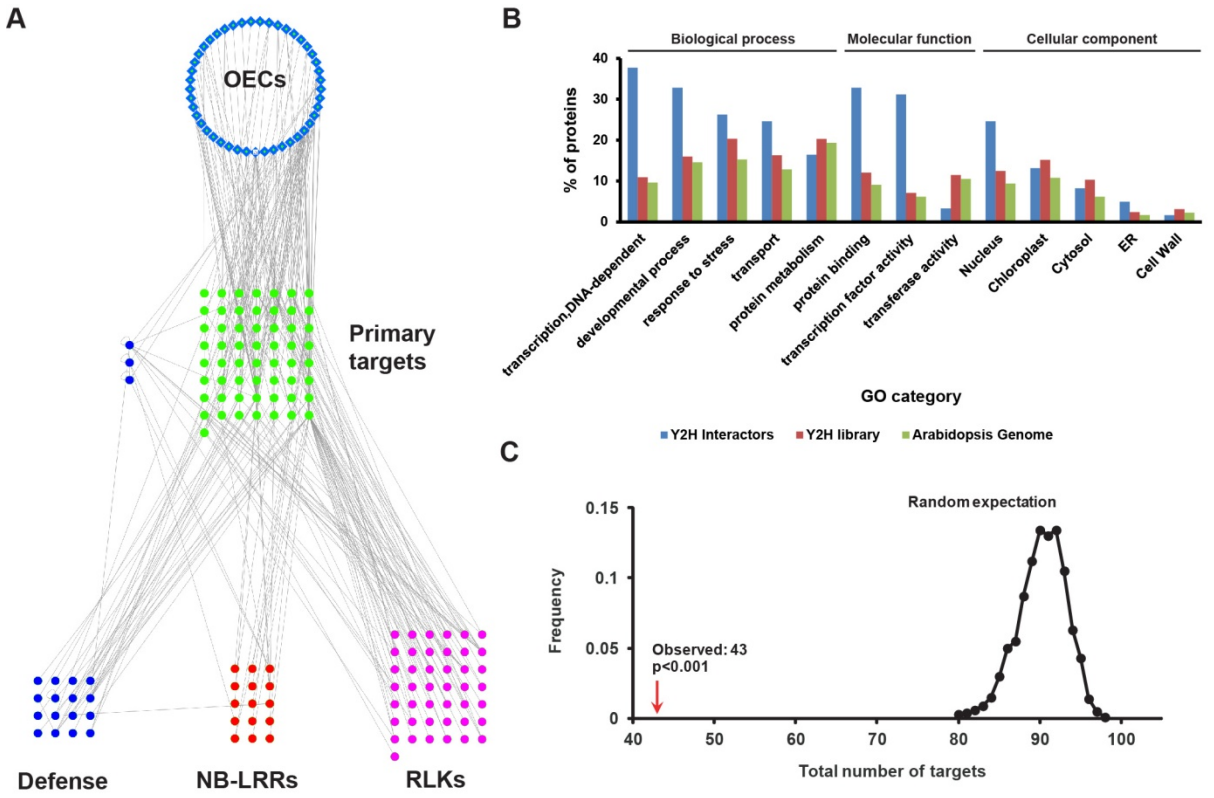

Figure 12: A large scale Y2H screen of OECs reveals convergence onto putative virulence targets. (**A**) Network visualization of the OEC interactome in three layers: OECs, their direct (primary) targets and annotated interactors of primary targets. Arabidopsis proteins and OECs (nodes) are represented by circles and diamonds respectively. They are color coded as follows: OECs (light blue), Arabidopsis proteins (green) including literature-curated defense proteins (blue), N-terminal domains of NB-LRR immune receptors (red) and cytoplasmic domains of LRR-containing receptor-like kinases (RLKs - pink). Y2H interactions are indicated by grey bars (edges). Literature-curated annotations are derived from Mukthar et al., 2011. The graph was prepared in Cytoscape. (**B**) Gene Ontology distribution among OEC interactors (blue), Y2H library proteins (red) and the TAIR10 Arabidopsis proteome (green). The GO terms and distributions were retrieved from TAIR. Individual proteins may be represented in more than one category. (**C**) Convergence of OECs on a limited set of target proteins. To estimate the probability of a specific number of distinct effector targets, the experimentally determined number of interactions of OECs within AI-1 were counted. The same number of interactions was then drawn from AI-1 at random 1000 times. In this AI-1 matrix, proteins were represented according to their degree (a protein with degree 20 was represented 20 times). Subsequently, the number of different effector targets per simulation was calculated and summarized in a Monte-Carlo-Ranking. For visualization, the frequency of a certain number was displayed. The red arrow at 43 represents the experimentally determined number of OEC targets in Space 1. Simulations were performed by Christine Gläßer, Institute for Bioinformatics and Systems Biology at the Helmholtz Center Munich, Germany.

The plant immune system consists of a multilayered, complex network and the previous analysis of *Psy* and *Hpa* effector targets indicated the convergence of effectors on a limited set of host proteins within this network (Jones and Dangl, 2006; Mukhtar et al., 2011). This possibility was

therefore also explored for the OECs. For the analysis, only effector targets within AI-1 were considered. It is important to note that the list used for simulations contained the degree information of AI-1, excluding the possibility of error introduction due to the negligence of the network degree distribution. By repeated simulation, the average number of effector targets in AI-1 expected at random was found to be 91. The observed number of OEC interactors, in contrast, was 43, showing a clear convergence of OECs onto specific host proteins (p<0,001, Figure 12C). The 61 putative virulence targets of *G. orontii* effectors identified will be the basis for future research on effectors of this fungus.

2.3.6 Unrelated phytopathogens target overlapping sets of host proteins

The oomycete *Hpa*, the bacterium *Psy* and the ascomycete fungus *G. orontii* are plant pathogens from three different kingdoms of life and have evolved the ability to colonize plant hosts independently of each other (Richards et al., 2006). Their effectors, however, are converging onto a subset of the Arabidopsis cellular network (Figure 12C). This prompted us to examine the overlap of effector protein targets for these three, unrelated pathogens. Published interactions of *Psy* and *Hpa* effectors (Mukhtar et al., 2011), the Arabidopsis interactome (Arabidopsis Interactome Mapping Consortium, 2011) and Space 1 interactors of the OECs were integrated into a plant-pathogen interaction network (Figure 13).

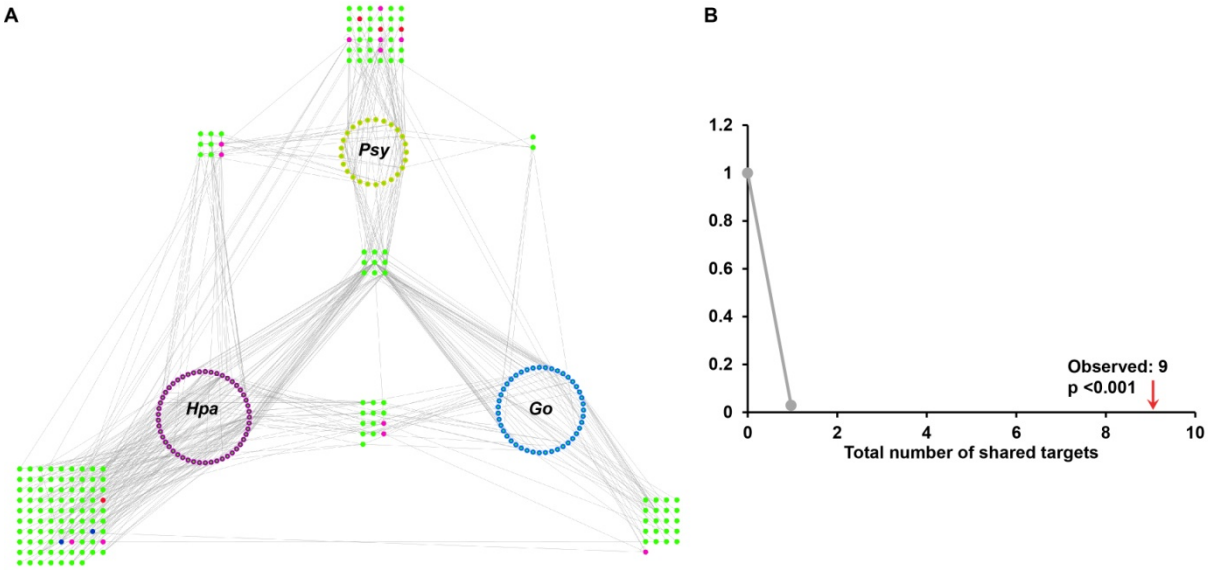

Figure 13: Effectors of unrelated phytopathogens converge onto common host proteins. (**A**) Visualization of the combined protein-protein interaction network of effectors of *G. orontii (Go)*, the oomycete *Hpa* and the bacterial pathogen *Psy* and their targets. Data for *Hpa* and *Psy* is derived from Mukthar et al., 2011. Color codings are as in Figure 12. Edges (grey) represent protein-protein interactions. (**B**) Effectors converge onto common host targets. First, random samples of targets were created for each pathogen according to the observed total number of targets. Then, random samples were chosen and the common targets were calculated. This was done 1000 times. Subsequently, the total number of shared targets was summarized in a Monte-Carlo-Ranking. The red arrow at 9 represents the experimentally determined number of common effector targets of the three pathogens. Only Space 1 targets of OECs were included in the analyses. The graph in A was generated by Pascal Braun, Department of Systems Biology, Technical University Munich. Simulations in B were performed by Christine Gläßer, Institute for Bioinformatics and Systems Biology at the Helmholtz Center Munich, Germany.

In this network, 185 direct effector targets were observed. In general, effectors were found to mostly target pathogen-specific host proteins. In the case of *G. orontii*, 21 host targets were

targeted exclusively and two and 13 targets were shared with *Psy* or *Hpa*, respectively. While nine common interactors of *Psy* and *Hpa* effectors were also detected, a trend towards overlapping host targets of the two filamentous obligate biotrophic pathogens (*Hpa* and *G. orontii*) could be observed. Nine host proteins were targeted by effectors of all three pathogens tested (Figure 13 and Table 2). This overlap is clearly significant (p<0,001), as repeated random simulations expect an average overlap of almost zero (Figure 13B). Again, TCP14 and CSN5a stick out in this analysis, as they interacted with a total of 52 and 32 effectors, respectively. Interestingly, TCP14 preferentially interacted with *Hpa* (25) and *G. orontii* effectors (23). Two additional TCP TFs, TCP13 and TCP15, are also targets of the three unrelated pathogens, suggesting an important role of these TFs for plant immunity. TCP20 was not included in Space 1, therefore no interactions with *Hpa* or *Psy* effectors could be determined. TCP13 and TCP14 also interact in Y2H and have WRKY36, a member of the immune related WRKY TF family, as a common interactor, thus suggesting the existence of a transcriptional complex involving these and other TFs (Arabidopsis Interactome Mapping Consortium, 2011). JAZ3 was also targeted by effectors from multiple pathogens. This protein is part of a family involved in the transcriptional repression of JA-signaling (Chini et al., 2007; Thines et al., 2007), which is mostly involved in the response to necrotrophic pathogens (Glazebrook, 2005). When activated, JA-signaling can however induce resistance to powdery mildew infection (Zimmerli et al., 2004).

The Arabidopsis interactome is organized similarly to a scale-free network and shares its most important property: It is resistant to perturbation by random removal of proteins (nodes) from the network, but sensitive to the removal of hubs (highly connected proteins), which can easily destabilize the network (Albert et al., 2000; Mukhtar et al., 2011). Therefore, the occurrence of hubs among effector targets was investigated. The modification of hubs by effectors would be a highly efficient method for host manipulation. Hubs were previously defined as proteins with a degree (number of interactions) ≥50 in AI-1. Five hubs were targeted by *G. orontii* effectors, and four of the previously defined 15 hubs in AI-1 (Mukhtar et al., 2011) were targeted by effectors from all three pathogens (Table 2). These include CSN5a, TCP14, TCP13 and the Anaphase promoting complex (APC) subunit 8.

Table 2: Arabidopsis proteins targeted by *Hpa*, *Psy* and *G. orontii*.

AGI identifier	Gene name	Degree in AI-1[a]	Hubs50 in AI-1[a]	Number of targeting effectors from		
				Psy[b]	*Hpa*[b]	*G. orontii*
AT1G22920	CSN5a	135	x	12	11	9
AT3G47620	TCP14	102	x	4	25	23
AT3G02150	TCP13	74	x	2	1	3
AT3G48150	Anapahase promoting complex (APC) 8	67	x	4	5	1
AT1G69690	TCP15	40		2	4	4
AT4G17680	SBP (S-ribonuclease binding protein) family protein	39		4	1	1
AT5G24660	response to low sulfur (LSU) 2	37		2	1	1
AT4G02590	unfertilized embryo sac (UNE) 12	24		1	2	1
AT3G17860	Jasmonate-ZIM-domain protein (JAZ) 3	23		3	1	1

a: derived from Arabidopsis Interactome Mapping Consortium 2011
b: derived from Mukthar et al.,2011

2.3.7 **Effector targets function in immunity towards *G. orontii***

To functionally validate the involvement of OEC targets in the immune response to *G. orontii*, the infection phenotypes of insertion mutants in respective loci was examined. Homozygous mutants could be obtained for 38 of the 61 targeted loci (Supplemental Table 11). At first, the phenotype of loci also targeted by *Hpa* effectors was examined, as homozygous insertion lines for these genes could be provided by collaborators. I used the spore count assay I developed (see 2.1.3) to assess the contribution of single knock-out lines to immunity against *G. orontii* (Figure 14A). Of the 15 lines tested in the first screen, seven were found to display significant changes in reproductive success of *G. orontii*. A mutant of *CSN5a* was clearly more resistant to the fungus. This mutant corresponds to *csn5a*-2 (Gusmaroli et al., 2007) and is therefore only a partial loss-of-function mutant. It does however show dwarfism and the lack of trichomes on the leaf, similar to the complete knock out *csn5a*-1 (Gusmaroli et al., 2007). A pleiotropic effect of reduced CSN5a levels in the cell might therefore explain the phenotype observed. No developmental phenotype was detected for any other mutant line, but several mutants with an enhanced disease susceptibility (eds) phenotype were observed. Interestingly, this effect was most striking for the *TCP* genes, as insertion lines of *TCP14*, *TCP13* and *TCP15* allowed enhanced reproduction of the fungus. TCP20 (AT3G27010) was also targeted by six effectors and displayed a slight, but not significant, eds phenotype (Figure 14B). For *tcp14*, the eds effect was as strong as for the positive control *eds1*, a mutant compromised in both salicylic acid-dependent and -independent defense signaling pathways (Bartsch et al., 2006). The similar phenotypes of these related, interacting TFs indicate a role of a TCP transcriptional complex in restricting *G. orontii* growth. Interestingly, similar observations were made with *Hpa* (Petra Epple, personal communication). Insertion mutants of *APC8* and a gene coding for a SBP family protein also allowed enhanced growth of *G. orontii*. In summary, insertion mutants in genes coding for six of the nine proteins targeted by all three pathogens had immunity phenotypes and five of these allowed enhanced colonization by the fungus (Figure 14A). Pathogen effectors thus converge onto proteins with important functions in immunity. The mode of action of these effectors however remains unclear.

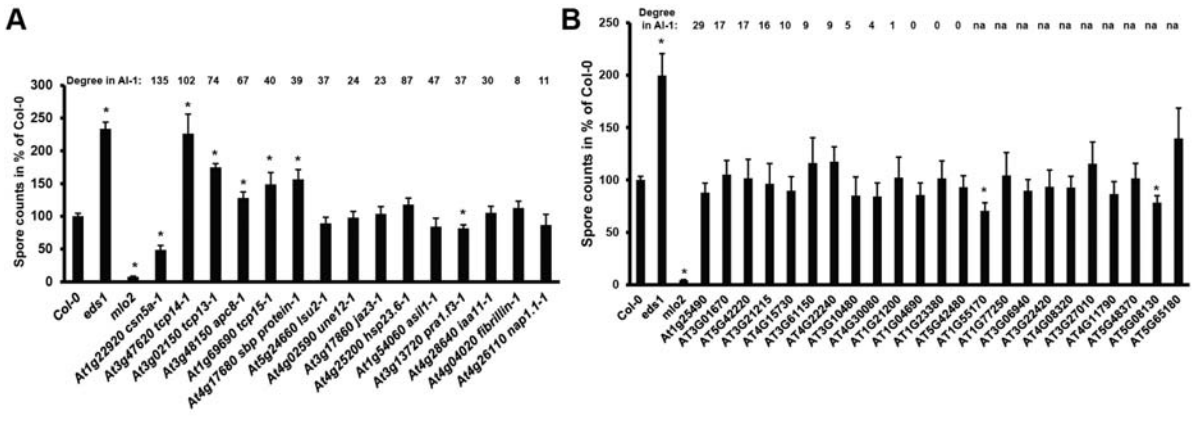

Figure 14: A subset of OEC target genes is involved in the plant immune response. Spore counts of indicated genotypes at 7 dpi normalized to seedling fresh weight. (**A, B**) Spore numbers per seedling fresh weight were determined from three replicates per genotype and experiment, normalized to the average of Col-0 within each experiment and subsequently

integrated. Bars represent the mean of three experiments (A) and four experiments (B) ± SE. The degree of proteins from indicated loci in AI-1 are indicated above (na: not available, Space 2 protein). Asterisks indicate statistically significant differences to Col-0 in two-tailed Student's t-test (p<0,05).

For another protein targeted by OECs, PRA1.F3, an enhanced resistance phenotype was observed and could also be verified by a second insertion mutant (Supplemental Figure 5). This protein is a member of a larger protein family in Arabidopsis, of which two closely related members, PRA1.F1 and PRA1.F2, were also targeted by the same, bacterial virulence enhancing effector, OEC65 (Supplemental Table 10). Insertion lines for these genes could not be obtained. PRA1 proteins are involved in vesicle trafficking by regulating the insertion of small GTPases into the membrane, which in turn regulate vesicle trafficking and fusion events (Alvim Kamei et al., 2008). Vesicle-mediated trafficking of defense compounds is an important component of plant immunity, and interfering with this process might render the plant more susceptible to pathogens (Collins et al., 2003; Kwon et al., 2008). For the insertion mutants of PRA1.F3, we observed an opposite effect. This indicates two possible scenarios. The protein might either be required to negatively regulate defense responses or be a susceptibility factor for powdery mildew infection. At the moment we cannot discriminate between these possibilities.

For proteins only targeted by effectors of *G. orontii*, the effects of gene disruption were less severe. Insertion lines of only two genes, an unknown gene (At1G55170) and *BIM1* (At5G08130), a TF involved in brassinosteroid (BR) signaling, displayed significantly reduced susceptibility (Figure 14B). For this second set of lines, the variation from experiment to experiment was generally larger, most probably due to strong fluctuations in the quality of the inoculum available.

It is important to note that for all nine insertion lines with powdery mildew phenotypes, the degree of the corresponding protein in AI-1 is ≥37 or unknown, while the average degree across AI-1 is 2.2 (Arabidopsis Interactome Mapping Consortium, 2011). Gene disruption of mitochondrial heat shock protein 23.6, a hub targeted by *G. orontii* and *Hpa*, had no effect. Overall, this clearly illustrates that removal of highly connected proteins indeed destabilizes the cellular interaction network. Moreover, four of these nine mutants are hubs in AI-1, suggesting that *G. orontii* has evolved effectors that specifically target hubs to promote susceptibility.

2.3.8 Bimolecular fluorescence complementation (BiFC) confirms Y2H interactions

Finally, I wanted to confirm the interactions of OECs with their Arabidopsis targets by an orthogonal assay. I focused on six of the seven shortlisted effectors (OEC25, OEC56, OEC60, OEC61, OEC63, OEC65), as most complementary information was available for these at the time. For OEC48, no interactors could be obtained. Eleven of the 14 effector targets could be cloned and used for bimolecular fluorescence complementation assays (BiFC) in *N. benthamiana* (Walter et al., 2004). A clone of *CSN5a* was kindly provided by the lab of Jane Parker (MPIPZ Cologne). To reduce the detection of false positive BiFC signals owing to strong p35S-based overexpression, a p*At*UBQ10-based vector system was used which was previously shown to

result in 20-fold lower expression levels compared to p35S (Grefen et al., 2010). The well described interaction of EDS1 and SAG101 (Feys et al., 2005) was used as a positive control, while Y2H-negative OEC-Arabidopsis protein combinations were used as negative controls. These combinations faithfully produced nuclear or no BiFC signal, respectively (Figure 15). BiFC signals could be detected in four of the twelve OEC-target combinations tested with C-terminal fluorophore fusions. OEC56 was confirmed to interact with the Nucleosome assembly protein (NAP) 1.1. Members of this protein family are well described chaperones of the histone subunits H2A and H2B in yeast and humans (Park and Luger, 2006). In Arabidopsis, four isoforms (NAP1.1-4) have been identified and found to bind H2A *in vitro* (Liu et al., 2009b). NAP1.2 and NAP1.3 were also included in the Y2H library. While they did interact with NAP1.1, no interaction with OEC56 was detected, indicating a preferential binding of OEC56 to NAP1.1. All isoforms are primarily localized to the cytoplasm (Liu et al., 2009b). The BiFC signal of NAP1.1 and OEC56 is also localized to the cytoplasm and clearly excluded from the nucleus (Figure 15). OEC56-Citrine was however almost exclusively detected in the nucleus (Figure 10).

In addition, the interaction of OEC65 with PRA1.F1, PRA1.F2 and PRA1.F3 was confirmed by BiFC. The F subclade of this protein family contains a fourth member, PRA1.F4, which is sequence-divergent from the other three PRA1s and was previously shown not to interact with these in Y2H (Alvim Kamei et al., 2008). This protein and several other PRA1 proteins were included in the Y2H library but not found to interact with OEC65, indicating specificity of the interaction between OEC56 and PRA1.F1, PRA1.F2 and PRA1.F3. The BiFC signal for all three PRA1.F proteins was mostly localized to punctuate spots in the cell periphery, indicating localization in the secretory pathway of the cell.

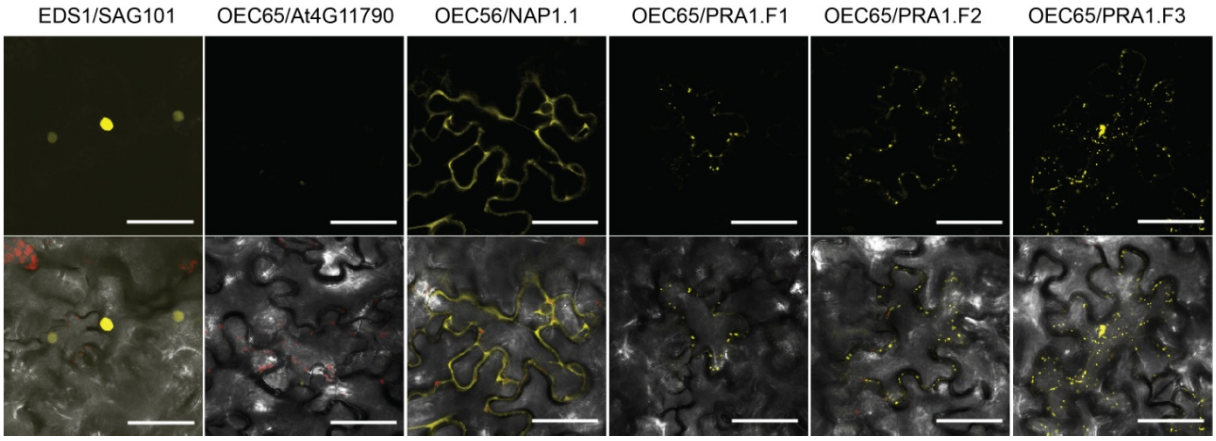

Figure 15: Bimolecular fluorescence complementation (BiFC) confirms Y2H interactions. Agrobacteria carrying *At*-nYFP or OEC-cYFP constructs were co-infiltrated into *N. benthamiana* leaves using a pAtUBQ10-based promoter system and a tightly controlled infiltration protocol. Three leaves/infiltration were checked at 3 dpi by CLSM. EDS1/SAG101 and OEC65/At4G11790 were used as positive and negative controls, respectively. Representative images are shown. The experiment was repeated twice with similar results. Scale bar is 50µm.

Overall, four of the twelve interactions tested by C-terminal fusions in BiFC could be confirmed. This is in the range of 20-35% sensitivity observed for systematic reconfirmations of Y2H data by orthogonal assays (Braun et al., 2009). Additional interactions might be confirmed by N-terminal BiFC experiments or other assays. While the set of interactions tested was very small, the

recovery rate of 30% indicates a high quality of our interactome, as expected from the analysis of AI-1, which was generated via the same experimental pipeline (Arabidopsis Interactome Mapping Consortium, 2011).

3 Discussion

3.1 Quantification of powdery mildew infections by qPCR and spore counts

In recent years the dicotyledonous model plant *A. thaliana* has been used to achieve great progress in the dissection of the interaction of powdery mildews with their host (Consonni et al., 2006; Shen et al., 2007). Easily usable medium- to high-throughput assays for the quantification of the powdery mildew infection are however currently lacking. I thus adopted a qPCR-based and a spore count-based method to the requirements of powdery mildew research and validated these assays on a set of hyper-susceptible and resistant mutant genotypes.

3.1.1 qPCR-based quantification of *G. orontii* biomass

Methods based on qPCR have been widely used for the quantification of phytopathogen biomass (Brouwer et al., 2003; Gachon and Saindrenan, 2004; Silvar et al., 2005). Surveying biomass instead of disease symptoms is often critical, as pathogen growth and macroscopic symptom development are not always correlated (Consonni et al., 2006; Thomma et al., 1999a; Thomma et al., 1999c) and symptoms often appear late in the infection cycle. This was also observed for the mutant set used in this study, as macroscopic disease symptoms did not appear on *mlo2*, *mlo2 mlo6 mlo12*, *edr1* and *pmr4* mutants, although they allowed different extents of hyphal proliferation (Figure 2 and (Consonni et al., 2006; Frye and Innes, 1998; Vogel and Somerville, 2000). The qPCR data correlate well with the microscopic analysis of the genotypes at 5 dpi (Figure 2). At this time, *eds1* plants display enhanced hyphal growth and more conidiation than the wild type. The *mlo* mutants show either strongly reduced (*mlo2*) or no hyphal growth (*mlo2 mlo6 mlo12*). Previous reports on the *mlo* mutants used penetration as well as conidiophore counts to assess differences in susceptibility among mutants and the wild type (Consonni et al., 2010; Consonni et al., 2006). While *mlo2* and *mlo2 mlo6 mlo12* plants differed considerably in penetration resistance, conidiophore counts were similar (both close to zero). The qPCR-based quantification of fungal biomass at 5 dpi therefore accurately reflects the impaired fungal development on enhanced disease resistance (edr) mutants. The method does, however, not reproducibly resolve differences in penetration rates at early time points, e.g. at 1 or 2 dpi (Figure 2B). In the *eds1* mutant, penetration rates are indistinguishable from wild type and hyper-susceptibility only becomes evident at later stages of infection (Dewdney et al., 2000; Töller, 2010). The qPCR assay can detect the hyper-susceptibility phenotype of this mutant already at 3 dpi, demonstrating the power of the method. Overall, 5 dpi is most suitable for the qPCR-based comparative quantification of *G. orontii* infection. At this time point differences in fungal biomass between genotypes are most pronounced and saturation effects are not yet noticeable. In other plant patho-systems, colonization differences could be detected at earlier time points. For *Phytophthora capsici* and *Botrytis cinerea*, differences in colonization could already be discerned as early as 1 dpi (Gachon and Saindrenan, 2004; Silvar et al., 2005). Disease progression was

however also faster in these systems, as maximum pathogen DNA was already detected at 3 dpi. This indicates that the *G. orontii* qPCR system has sufficient sensitivity to accurately reflect the slower disease progression in this system.

Plant cell death responses and tissue collapse in the case of necrotrophic fungi can lead to an overestimation of relative fungal biomass (Brouwer et al., 2003; Gachon and Saindrenan, 2004). Two mutants showing localized cell death at the penetration site after powdery mildew inoculation (*edr1* (Frye and Innes, 1998) and *pmr4* (Vogel and Somerville, 2000), did however not display unexpected variations in relative DNA abundance. Previously, a similar reduction in hyphal length for *mlo2* (=*pmr2*) and *pmr4* in comparison to the wild type had been observed (Vogel and Somerville, 2000), and this was also detected in the assay (Figure 2). Additionally, the relative fungal DNA abundance on *edr1* was indistinguishable from the wild type at 5 dpi. This is in agreement with previous observations of the *edr1* mutant, which permits extensive hyphal growth (similar to wild type), but no conidiation (Frye and Innes, 1998). Thus, the qPCR assay faithfully reflects fungal development even in the context of powdery mildew-triggered host cell death. The possibility that a somewhat reduced plant DNA yield owing to localized cell death responses results in a slight overestimation of fungal biomass can however not be excluded in these instances.

3.1.2 Spore counts are a valid method to determine *G. orontii* reproductive success

Spore formation is the final stage of powdery mildew biogenesis and thus suitable to detect even small differences in susceptibility. I thus adopted a frequently used protocol for spore counts of another Arabidopsis infecting obligate biotrophic pathogen, the oomycete *Hpa* (Feys et al., 2005; Stuttmann et al., 2011) to the requirements of powdery mildew research. The results of the spore count assay accurately reflected the previously described phenotypes of the mutants used. While *eds1* plants were found to allow 2-fold increased spore production relative to the wild-type, spore production dropped to 10% and 0% of the wild type in *mlo2* and *mlo2 mlo6 mlo12* plants. This proportion exceeds, however, a previous report using conidiophore counts at the same time point (Consonni et al., 2006), probably due to the averaging effect on tissue types of different susceptibility, some of which are deliberately excluded from penetration and conidiophore counts. Six days after infection was chosen for the quantification, as macroscopic symptoms between *eds1* and the wild type were most easily distinguished at this time. The assay has a high dynamic range of four to five orders of magnitude (0 to about 120.000 spores/g fresh weight) and can thus reveal even small differences in susceptibility between genotypes. In subsequent experiments (Figure 14), I realized that by harvesting at 7 dpi the centrifugation step of the protocol could be omitted without compromising the reproducibility of results.

Both assays developed here yielded comparable results for the susceptibility of the genotypes tested and can easily be adapted to other Arabidopsis-infecting powdery mildew species and

other plant-powdery mildew patho-systems. Both methods require similar amounts of time for data generation. The qPCR method is intrinsically more cost-intensive but allows simultaneous DNA extraction and PCR analysis of many samples. Spore counts are more cost-effective and, owing to the lower number of practical steps involved, offer less possibilities for experimental error (Supplemental Figure 6). In addition, the spore count assay is based on many seedlings rather than few mature plants, which offers the advantage of an averaging effect, lowering the possibility of experimental outliers. This assay was therefore used for the subsequent analysis of mutant lines.

3.1.3 Comparison of developed to existing methods of powdery mildew quantification

Currently, powdery mildew infection is either assessed semi-quantitatively by coarse categorization and thus macroscopic symptoms or quantitatively by microscopic penetration rate counts at early, hyphal area quantification at intermediate and/or conidiophore counts at late stages (Table 3). Macroscopic symptom assessment is prone to subjectivity and can only reveal large differences in susceptibility. The other methods require staining, mounting and microscopy and are therefore time-consuming and labor-intensive. I thus developed two complementing assays that could overcome the limitations of the currently used experimental protocols.

Table 3: Comparison of methods to assess powdery mildew infection.

	Macroscopic categorization	Host cell entry counts	Conidiophore counts	Hyphal area quantification	qPCR	Conidia counts
Assays type	semi-quantitative	quantitative	quantitative	quantitative	quantitative	quantitative
Staining required?	no	yes	yes	yes	no	no
Microscopy required?	no	yes (hundreds of interaction sites)	yes (multiple colonies)	yes (multiple colonies)	no	yes
Stage of patho-genesis scored	late (conidiation)	early (host cell entry)	late (conidiation)	early to late (host cell entry to conidiation)	middle to late (hyphal expansion to conidiation)	late (conidiation)
Importance of equal inoculation density	high (no normalization)	low (internal normalization)	low (internal normalization)	low (internal normalization)	low (internal normalization)	medium (averaging effect of scoring multiple plants at once)
Suitable for high-throughput analysis	yes	no	no	no	yes	yes
Reference	(Humphry et al., 2010; Reuber et al., 1998)	(Consonni et al., 2010; Consonni et al., 2006)	(Reuber et al., 1998; Vogel and Somerville, 2000)	(Baum et al., 2011; Seiffert and Schweizer, 2005)	this publication	this publication

Both assays introduced here are quantitative and are applied at late stages of infection when differences between genotypes are more pronounced. In addition, these assays quantify fungal development, rather than disease symptoms, and can therefore also discriminate macroscopically not detectable phenotypes. They do not require staining, are easy to perform and can generate quantitative data for larger numbers of genotypes (Table 3). These assays can therefore complement and overcome limitations of currently used methods of powdery mildew

quantification. They might be particularly suitable for the assessment of larger number of different mutant lines, e.g. in the course of follow-up analyses of genes identified by –omics approaches.

3.2 Transcriptome analysis of enriched *G. orontii* haustoria

3.2.1 Assembly and annotation of the haustorial library

In the current study, next generation sequencing of a haustorial cDNA library of the Arabidopsis-infecting powdery mildew *G. orontii* was used to characterize the types of transcripts and their abundance in these infection structures. Using a cut-off of >5-fold AC, 7,077 distinct contigs were obtained, for which ~46% of the predicted proteins did not have any homologs in other organisms. Similarly, in a comparative transcriptomics study, 50% of transcripts from *Bgh* were found to lack homologs in the completed genomes of a range of ascomycete phytopathogens (Soanes and Talbot, 2006). This was the lowest number in the comparison and was attributed to the high specialization of the fungus, the only obligate biotroph in the study. A comparatively low number of genes with homologs is also within the range of reports from rust (*Puccinia striiformis* f.sp. *tritici*) haustorial cDNA libraries (Xu et al., 2011; Yin et al., 2009). The genome of *Bgh* contains 5,854 curated genes, a low number in comparison to other fungi (Schmidt and Panstruga, 2011; Spanu et al., 2010). A similar number of genes can be expected for related powdery mildews such as *G. orontii*. The ~3,100 protein-coding transcripts with hits in the NCBInr database, in combination with the ~3,250 transcripts that are seemingly specific to *G. orontii*, therefore probably comprise the complete haustorial transcriptome (excluding presumptive retrotransposon transcripts). This was expected due to the high sequencing depth that is typically reached by next generation sequencing technologies.

The biological source material for the present analysis comprised an enriched preparation of haustorial complexes that were isolated from infected Arabidopsis plants at 4-6 dpi. At this stage of pathogenesis, fungal mycelia are fully developed and conidiophores emerge, but the colonies contain mixtures of juvenile and mature haustoria. The preparation of haustorial complexes, and thus the haustorial cDNA library, therefore derives from a blend of different developmental and likely functional stages. The purification protocol represents a second limitation of the analysis. The isolation and enrichment of haustorial complexes takes several hours, and although performed in cold conditions, this procedure may alter the physiological state of haustoria and/or might cause damage. The observation of intact extrahaustorial membranes around extracted haustoria (Figure 5B and C) however indicates limited mechanical damage during the isolation process. Nevertheless, the possibility remains that the transcript abundance seen in the haustorial cDNA library does not fully reflect the authentic *in vivo* situation. Despite attempts to exclude conidiospores during the preparation of haustoria, the final eluate still contained a significant amount of spores, although most were found to contain no cytoplasm (Cristina Micali, unpublished). In addition, bias during cDNA library construction and/or subsequent pyrosequencing may have further skewed the data. Indeed, results of qRT-PCR experiments revealed some differences in relative transcript abundance of selected genes compared to their relative transcript abundance in the haustorial cDNA library (Figure 6). Although it cannot be

stated with certainty which of the two data sets is more representative of biological reality, the quantitative aspects of the pyrosequencing approach might be regarded with caution.

3.2.2 Transcripts of primary metabolism dominate the haustorial transcriptome

Previously, haustorial transcriptomes of obligate biotrophic rust fungi have been shown to contain many transcripts involved in metabolism and protein synthesis as well as virulence (Catanzariti et al., 2006; Hahn and Mendgen, 1997; Xu et al., 2011; Yin et al., 2009). Similarly, elements of gene expression and protein turnover were found to be the most abundant transcripts in the library (Figure 4 and Supplemental Table 2). In addition, electron microscopic analyses revealed a high abundance of ribosomes in isolated haustorial complexes (Figure 5B and C). This observation has also been reported for haustoria of *Bgh in planta* (Hippe, 1985). Notably, genes and proteins involved in protein synthesis have been found in high numbers in both proteomic and transcriptomic studies at all stages of *Bgh* development (Bindschedler et al., 2009; Noir et al., 2009; Thomas et al., 2001). In a microarray study on *Bgh* development however, transcripts involved in protein biosynthesis were the most prominently up-regulated of all functional categories in post- relative to pre-penetration stages (Both et al., 2005b). The authors speculated that this effect is due to the switch from storage compound hydrolysis by preformed enzymes in spores to extensive invasive growth after penetration, which is most probably also the case for *G. orontii*. Similar observations were made in the rust fungi *Uromyces fabae, Hemileia vastatrix* and *Melampsora larici-populina*, where ribosomal transcripts were present at elevated levels in biotrophic mycelium compared to spores (Duplessis et al., 2011b; Fernandez et al., 2012; Jakupovic et al., 2006). Additionally, components of protein biosynthesis are significantly overrepresented in transcripts of ascomycete phytopathogens in comparison to non-pathogenic ascomycete fungi (Soanes and Talbot, 2006), indicating a general role of high translational activity during adaption to the host environment.

In the enrichment analysis, elements of the respiratory chain were overrepresented in the highly expressed genes (Figure 5A, Supplemental Table 3), which suggests the occurrence of extensive oxidative processes in haustoria. This assumption is supported by electron microscopic analysis of the material used for the generation of this library, which revealed mitochondria to be the most prevalent haustorial organelles (Figure 5B and C and Micali et al., (2011)). Together, these findings indicate a high energy demand of these fungal infection structures. This is further underlined by the high percentage of sequences related to energy production in the cDNA library (Figure 4B).

3.2.3 Haustoria produce multiple ROS scavenging molecules

In the EST assembly several highly expressed genes coding for enzymes involved in ROS detoxification and tolerance were identified. The local generation of ROS at the cell wall is a

frequent plant response to pathogens and ROS production is also typically observed during the hypersensitive response. The latter often coincides with localized cell death that occurs in response to pathogens and is correlated with effective defense against *Bgh* (Hückelhoven and Kogel, 2003). ROS production after *G. orontii* infection has also been observed in Arabidopsis, although a role in penetration resistance could not be detected (Göllner et al., 2008). RPW8.2, one of the two R-protein isoforms effective against Arabidopsis powdery mildew fungi, also enhances localized ROS accumulation around the haustorium (Wang et al., 2009). In response, fungi express ROS-detoxifying enzymes, presumably to cope with and even disturb the plant ROS production. In this study high transcript levels of thioredoxin H, a TSA/AhpC family protein, a Mn-type superoxide dismutase, a mannitol dehydrogenase, a gluthatione peroxidase and a putative Fe-type superoxide dismutase were found. These results are congruent with a microarray study of the bean rust fungus, *Uromyces fabae*, in which genes coding for a mannitol dehydrogenase, a manganese superoxide dismutase and a metallothionein were among the most highly up-regulated genes in rust-infected leaves compared to germinated spores (Jakupovic et al., 2006). *Uromyces fabae* has been shown to produce the ROS-scavenging compounds mannitol and arabitol during infection and to release these compounds into the plant apoplastic space, implicating mannitol dehydrogenases in ROS detoxification (Link et al., 2005). The presumed vital role of ROS scavenging during infection is further underlined by the discovery of several enzymes involved in the response to oxidative stress in proteomic studies on *Bgh* haustoria (Bindschedler et al., 2009; Bindschedler et al., 2011; Godfrey et al., 2009). The maize smut fungus *Ustilago maydis* also secretes Pep1, an effector that suppresses the oxidative burst by inhibiting host peroxidases (Hemetsberger et al., 2012). Additionally, transcripts of sequences related to cell rescue, defense, death and ageing are overrepresented in transcriptomes of phytopathogenic ascomycetes, indicating an important role of these protein classes in plant colonization (Soanes and Talbot, 2006). A putatively secreted Cu/Zn-type superoxide dismutase was also detected, which in comparison to the other detoxification enzymes has a rather low expression level (Supplemental Table 4). The qRT-PCR results however indicate higher expression levels of the respective gene at pre-penetration stages (Figure 6). The presumed early secretion of this enzyme would allow the detoxification of plant produced superoxide in the apoplast.

3.2.4 Transporter transcripts are not abundant in the haustorial cDNA library

Unexpectedly, only one transporter was among the Top50 transcripts encoding transmembrane proteins. The identified phosphate transporter is a member of the Pho88 group of inorganic phosphate transporters, which have not been attributed any specific function so far. The strong expression of this gene in haustoria could not be validated by qRT-PCR, but our time course analysis indicates that this transcript is constantly present throughout fungal development. Interestingly, in *Bgh*, a phosphate transporter homolog has been identified as part of a co-regulon of virulence-related genes (Both et al., 2005b). Phosphate metabolic genes are overrepresented

in ESTs from phytopathogenic versus non-pathogenic ascomycetes, suggesting an important role of phosphate metabolism in fungal pathogenesis (Soanes and Talbot, 2006). In addition, phosphate uptake is increased in powdery mildew infected barley plants, suggesting an induction of this process by fungal infection (Walters and Ayres, 1981).

Glucose seems to be the main carbon source of monocot-infecting powdery mildews (Sutton et al., 1999). Notably, no highly abundant transcripts coding for sugar transporters could be identified in the EST assembly. This contrasts with transcriptomic analysis of rust fungi, in which genes encoding hexose and amino acid transporters were highly represented in transcripts from infected leaves (Duplessis et al., 2011a; Duplessis et al., 2011b; Hahn and Mendgen, 1997; Jakupovic et al., 2006). I therefore carefully analyzed the *G. orontii* transcript library for homologies to known sugar and amino acid transporters but did not detect any highly represented transcripts (Supplemental Table 5). In agreement, proteomic studies of *Bgh* haustoria did not identify any sugar transporters (Bindschedler et al., 2009; Godfrey et al., 2009). However, both proteomic studies did detect PMA1, a plasma-membrane resident H^+-ATPase that is believed to generate the proton gradient needed to drive sugar import. The transcript of this gene is present at the same level in our library as transcripts coding for the MFS-type sugar transporters. Transcripts coding for PMA1 and a MFS maltose transporter were among the three transcripts that were found by qRT-PCR to be induced in late stages of fungal development (Figure 6B). While transcript abundance does not solely determine protein levels, the low transcript levels in *G. orontii* and the lack of identification in proteomic studies in *Bgh* indicate that powdery mildews probably use low abundance sugar transporters for carbohydrate uptake. These might have very high substrate affinity, as recently evidenced for *Um*SRT1, a sucrose transporter of *Ustilago maydis* that is required for virulence (Wahl et al., 2010). Alternatively, powdery mildews may exploit atypical ways of nutrient absorption.

3.2.5 Conserved pathogenicity genes are expressed in *G. orontii* haustoria

The extrahaustorial matrix is believed to represent the major battleground of the powdery mildew–plant interaction (Panstruga and Dodds, 2009). Haustorial transcripts are therefore expected to comprise large numbers of virulence determinants. Indeed, “Pathogenesis” is among the significant GOSlim categories, supporting the notion that specific processes for host colonization take place in the haustorium. These sequences contain a large percentage of transcripts coding for proteins involved in signal transduction, including homologs of G-proteins, Rho GTPases, MAP kinases and elements of cyclic AMP signaling (Supplemental Table 6). This includes a homolog of *Magnaporthe grisea* PMK1, a MAP kinase that is essential for appressorium formation and infectious growth (GoEST_c4866) (Xu and Hamer, 1996). Several homologs of pathogenicity genes were also not correctly annotated by Blast2GO. Abundant transcripts for a homolog of the *Colletotrichum gloeosporioides CAP20* gene, which is expressed during appressorium formation and whose knock-out severely reduces virulence of the fungus

(Hwang et al., 1995), were identified (Supplemental Table 2). In the qRT-PCR analysis, transcripts of this gene were most abundant at 12 hpi (Figure 6). This is similar to *Bgh*, where a homolog of this gene shows highest transcript accumulation during appressorium formation (Both et al., 2005b). Additionally, transcripts of many secreted putative pathogenicity factors, e.g. a cell wall-linked protein that is a homolog of the EMP1 pathogenicity factor from *M. grisea* (Ahn et al., 2004), were also frequently detected. This protein likely functions in the adhesion of the appressorium to the host surface and respective knock-out lines display strongly reduced appressorium formation and virulence (Ahn et al., 2004). In a comparative genomics study, *EMP1* was found to be conserved in the genomes of filamentous ascomycetes, while lacking in yeasts (Soanes et al., 2008). Homologs of *EMP1* have been identified in many plant-pathogenic fungi (Cornelissen and Haring, 2001; Soanes et al., 2008), and the DRMIP-HESP domain (PF10342) present in this protein and GoEST_c4284 is also present in a haustorially expressed gene coding for a secreted protein of flax rust (Catanzariti et al., 2006). While one member of this protein class has been implicated in cell differentiation of *Lentinula edodes* (Szeto et al., 2007), DRMIP-HESP domain containing proteins have been found to be enriched in the secretomes of rust fungi (Saunders et al., 2012). Overall, this suggests an important role of these proteins during pathogenesis of haustoria forming pathogens that is conserved across fungal phyla.

In our analysis, two transcripts encoding secreted cell wall-modifying enzymes were detected, a putative chitinase and a glucanosyltransferase. The secreted glucanosyltransferase is a homolog of GEL1, a protein that is involved in fungal cell wall biogenesis and virulence of *Aspergillus fumigatus* and *Fusarium oxysporum* (Caracuel et al., 2005; Nierman et al., 2005). Interestingly, the *Bgh* homolog of this gene has a virulence function, as shown by transient silencing assays (Nowara et al., 2010). Overall, only very few transcripts coding for lytic enzymes were detected at the haustorial stage, which is in line with the reduced set of these genes in the genomes of powdery mildew fungi (Spanu et al., 2010). Taken together, many general virulence factors seem to be conserved between *G. orontii*, *Bgh* and other pathogenic fungi. However, also many species- and even isolate-specific fungal virulence factors have been described (Stergiopoulos and de Wit, 2009). The repertoire of these effectors encoded by *G. orontii* will be discussed in the subsequent section.

3.3 Functional characterization of *G. orontii* effector candidates.

Effectors allow plant pathogens to suppress host immune responses and thus prepare the plant for colonization (Ellis et al., 2009; Feng and Zhou, 2012). While these effectors have been first identified by their avirulence functions, their virulence functions are now also being elucidated (de Jonge et al., 2011; Stergiopoulos and de Wit, 2009). The analysis of effector functions and targets has yielded important insights into the coevolution of pathogens and their hosts in many patho-systems (Boch et al., 2009; Jones and Dangl, 2006; Ma et al., 2010; Moscou and Bogdanove, 2009). For the powdery mildew fungi, effector biology is still in its infancy as only few effector proteins have been cloned and or functionally characterized from the barley powdery mildew *Bgh* (Schmidt, 2010; Spanu et al., 2010; Zhang et al., 2012). The Blumeriae species form a specific, Poaceae (grasses) infecting clade within the *Erysiphales*, while the vast majority of powdery mildew host plants (>90%) are dicotyledonous (Glawe, 2008; Takamatsu, 2004). The infection of Arabidopsis with powdery mildews has therefore recently been established as a model system for dicotyledonous plants (Micali et al., 2008). I used the haustorial cDNA described above to predict, clone and functionally characterize effectors of the Arabidopsis infecting powdery mildew *G. orontii*. The effectors analyzed in this study could potentially become the starting point for future research on effectors of dicot-infecting powdery mildews in general.

3.3.1 OECs display common features of effector proteins

In my analysis, I predicted 115 effector candidates, 19 of which are among the Top50 transcripts encoding secreted proteins in the haustorial library. The proteins encoded are considerably shorter than the residual secretome, are often cysteine-rich and contain only few recognizable domains, qualities that have been observed for effector proteins in general (Catanzariti et al., 2006; Godfrey et al., 2010; Spanu et al., 2010). Cysteine-rich effectors have mostly been found to act in the apoplast as protease inhibitors and protectors or scavengers of chitin (de Jonge et al., 2010; Tian et al., 2005; Tian et al., 2004; van den Burg et al., 2006). While several cysteine-rich effectors were identified, domains of protease inhibitors or chitin-binding proteins were not detected. For subsequent assays and reason of simplicity, I therefore assumed a cytoplasmic localization of the effectors. This might have prevented the accurate functional characterization of apoplastic OECs. Similar to reports on *Bgh* and the wheat stem rust *Puccinia graminis* f.sp. *tritici* a subset of 26 OECs contained a Y/F/WxC motif in their N-terminal region. This motif has been previously identified by effector analysis of *Bgh* and proposed to be involved in effector uptake by the host. It is however also widely present in both candidate effectors and non-secreted proteins of poplar rust, making a role in effector uptake unlikely (Duplessis et al., 2011a). Therefore, the role of this motif was not analyzed further.

In comparison to the 115 OECs, the effector arsenal of *Bgh* has recently been extended to 491 CSEPs (Pedersen et al., unpublished results). The discrepancy to this publication is probably due to the prediction of effectors from genomic DNA in *Bgh* in comparison to a single haustorial cDNA

library in the current study. Using an extensive set of RNAseq and cDNA libraries, most of the *Bgh* CSEPs were however found to be expressed at the haustorial stage (Spanu et al., (2010) and Pedersen et al, unpublished results). The limited number of OECs can also explain the few effector families detected, as additional family members possibly present in the *G. orontii* genome might have too low expression levels for contigs to be accurately assembled and/or might be expressed predominantly at different stages of development. In general, a more comprehensive analysis of the *G. orontii* effector arsenal would require an enhanced quality of the genome assembly and/or sequencing of transcriptome libraries representing additional stages of the *G. orontii* life-cycle.

Of the 115 OECs identified, 50 and 13 had homologs in the closer and more distantly related powdery mildews *E. pisi* and *Bgh*, respectively. This clearly reflects the evolutionary distance of the three pathogens but also indicates the existence of a core set of evolutionary ancient powdery mildew effectors that were retained in approx. 70 million years of divergent evolution (Spanu et al., 2010; Takamatsu, 2004). Of the eight OECs with predicted structural domains, three were similar to “Microbial Ribonucleases” (IPR016191) and each of these had homologies in the *E. pisi* genome and *Bgh* CSEPs. The microbial ribonuclease fold has been suggested as a stable structural template for effector sequence diversification in *Bgh* (Pedersen et al., unpublished results). Ancestral powdery mildew effectors that originated from a ribonuclease fold might thus be the basis of a shared powdery mildew effector set.

3.3.2 Cell death suppression by OECs

Localized cell death is the most effective defense response against powdery mildew fungi (Panstruga and Schulze-Lefert, 2002). For several pathogen effectors, the suppression of cell death has been described and was therefore also examined for the OECs (Dou et al., 2008; Kelley et al., 2010; Kleemann et al., 2012; Wang et al., 2011). Co-infiltration experiments with Agrobacteria harboring OEC- or *Ch*NLP1-expression vectors revealed a frequent (72%) suppression of cell death by OECs (Figure 8 and Table 1). The suppression of *Pi*INF1 triggered cell death, by contrast, was only detected for OEC63 and OEC66 and no OEC could inhibit R3a triggered HR. This is in line with the absence of *R* gene-triggered immunity to *G. orontii* in Arabidopsis (Micali et al., 2008). In a similar set-up using biotrophy-associated effectors of *Colletotrichum higgansianum*, from which NLP1 originates, five of eight (62%) tested effectors suppressed *Ch*NLP1-triggered cell death but none could suppress INF1-induced cell death. The necrosis-inducing peptides and R3a trigger different but overlapping downstream signaling pathways. While all require *Nb*SGT1 and *Nb*HSP90, the JA co-receptor COI1, the mitogen activated protein kinase *Nb*MEK2 and the two SA-signaling proteins *Nb*NPR1 and *Nb*TGA2.2 are only required for cell death triggered by *Pi*NPP1.1 and not *Pi*INF1 (Kanneganti et al., 2006). At least *Nb*NPR1 is also not required for R3a induced HR (Cui et al., 2009). Cell death triggered by *Pi*INF1 in turn requires the E3 ligase *Nb*CMPG1 and the BAK1 homolog *Nb*SERK3, while

*Nb*CMPG1 is not required for R3a triggered HR (Chaparro-Garcia et al., 2011; González-Lamothe et al., 2006; Gilroy et al., 2011). The contribution of these components to NLP-triggered cell death is unknown. The *Pi* effector SNE1 can suppress cell death triggered by both *Pi*NPP1.1 and R3a, indicating that NLPs and R proteins also share common signaling cascades (Kelley et al., 2010). Taken together, OECs, similarly to *Ch* effectors, predominantly suppress a cell death signaling pathway elicited by *Ch*NLP that requires MAP kinase, JA and SA signaling but not CMPG1.

3.3.3 The virulence enhancing effect of OECs

In general, it has been difficult to define virulence contributions to single effectors, probably due to the small effect of most single effectors and their functional redundancy. The reassembly of the full *Pst* effector repertoire from an effectorless mutant also revealed interdependences between effectors, further complicating the picture (Cunnac et al., 2011). For obligate biotrophic pathogens, the challenges of defining effector contributions to virulence are even greater, due to the lack of efficient transformation techniques and the sheer size of the effector arsenal. The delivery of OECs to the plant cell by phytopathogenic bacteria was therefore used as a tool for OEC characterization (Sohn et al., 2007). Six effectors (OEC25, 48, 60, 61, 63 and 65 (~20% of the tested OECs)) were found to reliably and significantly enhance bacterial growth relative to the YFP control and, together with the nuclear effector OEC56, shortlisted for subsequent assays. Similarly, in a previous study on *Hpa* RXLR effectors, enhanced bacterial growth on Col-0 was detected for approximately 45% of 62 tested proteins (Fabro et al., 2011). The authors however implemented a less stringent threshold for scoring growth as being enhanced. In this study, several effectors also restricted bacterial growth, indicating recognition by *R* genes. In contrast to *Hpa*, *G. orontii* does not seem to have a long coevolution history with Arabidopsis and thus, no corresponding *R* genes are described in Arabidopsis (Micali et al., 2008). Accordingly, no OEC restricted growth of the delivering bacterial strain. An enhanced growth of already virulent, OEC-delivering *Pst* strains points to a strong role in MTI suppression of the OECs that utilizes different mechanisms or targets than *Pst*. Accordingly, two (OEC56 and 65) of the seven shortlisted effectors suppressed callose deposition, a characteristic MTI response that can also be suppressed by several *Pst* effectors (DebRoy et al., 2004; Hauck et al., 2003; Zhang et al., 2007). Interestingly, callosic encasements of haustoria are always detected for the non-adapted powdery mildew *Bgh* in Arabidopsis and in about 20% of cases for *G. orontii*, indicating that the fungus can indeed partially suppress this response (Jacobs et al., 2003; Meyer et al., 2009). Another adapted powdery mildew species, *G. cichoracearum,* can completely suppress callose depositions, suggesting that it is even better adapted to interfering with cell wall based defenses of its host (Koh et al., 2005). Investigating *G. cichoracearum* effectors for their callose suppression activity would therefore be an interesting task. For *Hpa* effectors, as many as 78% of virulence enhancing effectors could also suppress callose deposition after delivery by *Pst* ΔCEL (Fabro et al., 2011), indicating that several effectors were potentially missed in my screen due to

the high variability of the assay. It has to be noted that *Hpa* still elicits callose deposits, these do however not seem to co-localize with haustorial encasements completely, indicating that *Hpa* can also manipulate their localization (Meyer et al., 2009). MTI responses are not limited to callose deposition and specific interference with the execution of other branches of MTI could not be analyzed with this assay. Assessment of additional MTI responses like ROS spiking or MAP kinase activation would also require the generation of transgenic Arabidopsis lines, which was unsuccessful in my hands.

3.3.4 Lessons from OEC localization

The OECs tested mostly localized to the cytoplasm and nucleus of *N. benthamiana* epidermal cells (Figure 10). The size of effector-fusion constructs was below the size exclusion limit of the nucleus, indicating that these proteins can enter via passive diffusion. OEC56 was localized exclusively to the nucleus, while OEC63 localized to net-like structures indicative of the ER. OEC65 was actively excluded from the nucleus and localized to the cytoplasm and several distinct foci. The diverse localization of this limited effector set indicates a number of different effector virulence targets within specific subcellular compartments. Effectors of diverse plant pathogens have also been found to localize to the nucleus, ER, Golgi, PM and the chloroplast where they exert different functions (Bartetzko et al., 2009; Caillaud et al., 2012; Deslandes et al., 2003; Jelenska et al., 2007; Nimchuk et al., 2000; Nomura et al., 2011; Schornack et al., 2010). A screen for *Hpa* effector localization revealed the nuclear/-cytoplasmic localization of 33% of tested candidates, while an additional 33% localized exclusively to the nucleus and 26% localized to different membranes (Caillaud et al., 2012). It is interesting to note that a canonical NLS was only predicted for 40% of strictly nuclear *Hpa* effectors (Caillaud et al., 2012), indicating that mere bioinformatic analysis cannot accurately predict the localization of OECs. Therefore, a systematic localization analysis of OECs should be undertaken in the future. Localization information can also be used to predict effector function. In the most striking example, the detection and confirmation of a NLS in the *Xanthomonas* AvrBs3 effector family (Van den Ackerveken et al., 1996; Yang and Gabriel, 1995) and the subsequent discovery of transcriptional activator functions for these proteins (Gu et al., 2005; Zhu et al., 1999) led to the discovery of specific TF activities of AvrBs3 (Kay et al., 2007; Römer et al., 2007). Subsequently, detailed studies revealed the molecular basis of DNA recognition by these effectors (Boch et al., 2009; Moscou and Bogdanove, 2009). This code can now be used to design specific DNA-binding motifs for different applications (Morbitzer et al., 2010).

3.3.5 Expression of OECs – do effectors come in waves?

For most of the tested OECs (OEC25, OEC48, OEC63) a preferential expression before haustorium formation was detected (Figure 11). In the expression profiles I cannot distinguish preformed from plant-induced transcripts, as 0 hpi samples were taken after inoculation and no pure spore sample was included. The predominant early expression of these genes contrasts

their identification from a haustorial library, but might be explained by contaminations of the material used for library generation, as discussed above (see 3.2.1). Additional effectors were transcriptionally induced after haustorium formation (OEC56 at 24 hpi), at the sporulation stage (OEC61 at 7 dpi) or expressed throughout pathogenesis (OEC65). Due to the low sample size (six effectors) a general statement on effector expression in *G. orontii* cannot be made. The distinct expression patterns of the OECs are however reminiscent of the effector expression in waves that has been detected in other patho-systems. In the poplar rust *Melampsora larici-populina*, large sets of candidate effectors displayed distinct expression patterns, including expression at the spore stage and/or germination and subsequent down-regulation as well as up-regulation *in planta* at early and late stages of infection (Duplessis et al., 2011b). The authors suggest that effectors preformed in spores or induced at germination might be prime candidates for suppression of early host defenses. For *P. sojae*, a similar observation was made. Many effectors were already expressed in the inoculum and expression increased subsequently while another subset was only induced *in planta* (Wang et al., 2011). In this study, preformed effectors seemed to be associated with the suppression of ETI, thereby paving the way for PTI suppression by *in planta*-induced effectors. These results indicate that early-induced or preformed effectors are important virulence components that should be investigated more thoroughly, especially as most effectors characterized to date are induced *in planta* (Hahn and Mendgen, 1997; Mosquera et al., 2009; Spanu et al., 2010; Torto et al., 2003). Exploring early-acting effectors will probably generate important insights into the first molecular events of pathogen recognition by the plant. Additionally, characterizing the functions of effectors induced late in the life cycle could reveal host processes specifically target to meet the increased metabolic demand of pathogens at the sporulation stage.

3.3.6 The OEC-Arabidopsis interactome reveals potential virulence targets

Effectors mostly exert their function through the manipulation of host targets (Feng and Zhou, 2012). Protein-protein interaction assays have therefore been extremely useful for defining effector targets and functions in bacteria. Y2H approaches have for instance uncovered the interaction of AvrPto with Pto (Tang et al., 1996), RIN4 with AvrB and AvrRpm1 (Mackey et al., 2002) and HopM1 with AtMIN7 (Nomura et al., 2006). The first described intracellular host target of a filamentous pathogen effector, *Nb*CMPG1 targeted by *Pi*Avr3a was also discovered by Y2H (Bos et al., 2010). Recently, this technique was used to systematically map host targets of both *Psy* and *Hpa* effectors (Mukhtar et al., 2011). This prompted us to also generate an interactome of the 84 cloned *G. orontii* effectors. Using a high-quality Y2H pipeline (Dreze et al., 2010), 132 high confidence interactions of 61 Arabidopsis proteins with 47 OECs were obtained (Figure 12A and Supplemental Table 10). Most OECs and Arabidopsis proteins only had few interactors, while a few proteins with many interactors were also detected. This is in line with observations from the *Hpa* and *Psy* interactome (Mukhtar et al., 2011) and suggests the existence of a few very important virulence targets in the host as well as promiscuous effectors in the pathogen. For *Pst*,

redundant targeting of host component has already been confirmed. At least four independent effectors (AvrRpm1, AvrB, AvrRpt2 and HopF2) target the host component RIN4 to suppress MTI and ETI (Kim et al., 2005a; Kim et al., 2005b; Mackey et al., 2002; Wilton et al., 2010). Conversely, AvrRpt2 cleaves at least five Arabidopsis proteins (Chisholm et al., 2005; Takemoto and Jones, 2005). Overall, effector targets were clearly enriched for protein binding and TF activities as well as nuclear and ER-resident proteins, while depleted in components of protein metabolism. Interestingly, only three proteins with described roles in the defense response (PRA1.F2, PRA1.F3 and Fibrillin) were directly targeted by effectors. Primary effector targets were however often found to interact with defense-related proteins, indicating indirect manipulations of immunity by *G. orontii*. Similar observations were made for *Hpa* and *Psy* (Mukhtar et al., 2011). It is interesting to note that 15 of the direct effector targets also interact with NB-LRR proteins. The recognition of effector activity, rather than the effector itself is proposed by the guard hypothesis (Dangl and Jones, 2001; Van Der Biezen and Jones, 1998). This would suggest the recognition of OEC activity by Arabidopsis, but again, no canonical R protein conferring resistance to *G. orontii* has been detected even after screening of multiple Arabidopsis accessions (Göllner et al., 2008). Therefore, these interactions either do not happen *in vivo*, due to different compartmentalization and/or expression patterns, or the guard recognizes other modifications of the guardee than those by OECs. This has been observed for RIN4, where RPM1 recognizes RIN4 phosphorylation induced by AvrRpm1 and AvrB but not RIN4 cleavage by AvrRpt2 which is detected by RPS2 instead (Chisholm et al., 2005; Day et al., 2005; Kim et al., 2005a; Mackey et al., 2002).

The screen results are certainly incomplete, as only a subset of the ~27.000 protein-coding genes of Arabidopsis were surveyed and additional OECs remain to be discovered and/or cloned. Still, significant convergence of the OECs onto a limited set of host proteins could be detected (Figure 12C), as previously found for *Hpa* and *Psy* effectors (Mukhtar et al., 2011). It is interesting to note that for a small set of effectors from *Phytophthora infestans*, for which Arabidopsis is a non-host, convergence was not detected (Pascal Braun, personal communication). Therefore, this phenomenon might be associated with adaptation to the host and thus the ability for MTI suppression.

3.3.7 Unrelated phytopathogens converge onto hubs in the plant cellular network

In the analysis of the integrated interaction network of *Psy*, *Hpa* and *G. orontii* effectors, it became apparent that different pathogens mostly target separate proteins in the host (Figure 13). This is conceivable, as all three pathogens show different lifestyles and/or routes of colonization, indicating that they might manipulate different processes in the cell and/or different cell types to promote susceptibility. *Pseudomonas syringae* is a hemibiotrophic bacterial pathogen that enters the leaf through wounds or stomata and subsequently proliferates in the apoplast where it

promotes nutrient leakage from mesophyll cells (Katagiri et al., 2002). *Hpa*, by contrast, is an obligate biotrophic oomycete that penetrates the leaf through anticlinical epidermal cell walls into the mesophyll, where it establishes haustoria and hyphal elongation takes place (Koch and Slusarenko, 1990). Sporulation occurs then by the outward growth of sporangiophores through stomata. *G. orontii* in turn completes its lifecycle on top of the epidermal cell layer and acquires all its nutrients through haustoria in epidermal cells (Micali et al., 2008). These cell types are different in both their morphology and gene expression profile (Brandt et al., 2002), possibly requiring distinct manipulation for susceptibility by the fungus. *Psy* effectors also target more defense compounds directly relative to *Hpa* and *G. orontii*. This observation can however be explained by a bias in the literature for defense proteins identified through the study of *Pseudomonas* and its effectors (Feng and Zhou, 2012).

Strikingly, the three pathogens examined also have nine host targets in common (Figure 13), indicating that they also manipulate common host processes in the plant. All three pathogens have to suppress MTI in order to be pathogenic, which suggests that common targets function in the MTI pathway. Most common targets are TFs or involved in transcriptional processes, indicating that they might interfere with MAMP-triggered transcriptional reprogramming rather than perception or signaling. This is in contrast to previous data on *Pseudomonas* effectors, which mostly interfere with MAMP-signaling directly at or immediately after MAMP-perception (Feng and Zhou, 2012). For filamentous pathogens, effector targets are mostly unknown. None of the common targets has been explicitly implicated in the defense response to any of these pathogens so far, indicating that in depth analysis of their contribution to resistance can reveal important insights into the defense response of Arabidopsis. Only for JAZ3 a link to defense processes is obvious. JAZ proteins are repressors of the JA signaling pathway which perceive JA in a complex with COI1 and are subsequently ubiquitinated by the SCF^{COI1} complex and degraded (Chini et al., 2007; Sheard et al., 2010; Thines et al., 2007; Yan et al., 2007). This allows the induction of JA-responsive genes by the TF MYC2. While JA induced defenses are usually attributed to defense against necrotrophic pathogens, they can also be effective against *G. orontii* (Glazebrook, 2005; Zimmerli et al., 2004). *Pst* utilizes the phytotoxin coronatine, a structural analog of JA-isoleucine, to induce JA signaling (Weiler et al., 1994; Yan et al., 2009). This leads to increased susceptibility owing to the suppression of SA-induced responses by hormonal crosstalk (Brooks et al., 2005; Uppalapati et al., 2007). It is therefore conceivable that *Hpa*, *G. orontii* and *Psy* target JAZ3 to promote JA- and thereby inhibit SA signaling. Transposon-insertion lines of *JAZ3* did however not display an infection phenotype with *G. orontii* (Figure 14), probably due to redundancy of the twelve JAZ proteins in Arabidopsis.

The common targets of the three pathogens have a high degree in AI-1 and four of them (CSN5a, TCP14, TCP13, APC8), are actually hubs within the cellular network. The high degree of the common targets provokes the idea of “sticky” proteins for which the interaction with effectors is not specific. It is therefore important to note that only four of the 15 hubs in AI-1 were targeted

commonly by the three pathogens. In addition, the targeting of hubs has been frequently observed for the interaction of bacteria and viruses with their human host, indicating a specific virulence strategy (Calderwood et al., 2007; Dyer et al., 2008; Dyer et al., 2010; Pfefferle et al., 2011; Simonis et al., 2012).

3.3.8 Hubs are involved in the defense response

Cellular interaction networks of all organisms examined so far resemble a scale-free network (Arabidopsis Interactome Mapping Consortium, 2011; Giot et al., 2003; Ito et al., 2001b; Li et al., 2004; Rual et al., 2005; Stelzl et al., 2005; Uetz et al., 2000). Network theory has shown that scale-free networks, like social networks, the internet or cells are resilient to perturbations of random proteins but very susceptible to attacks on their hubs (Albert et al., 2000). The common targeting of highly connected nodes by three unrelated phytopathogens evoked the question if immune responses could be compromised by node removal. I thus assembled a set of T-DNA insertion mutants for these genes and systematically screened them for altered susceptibility to *G. orontii,* which was detected in nine of the 38 tested lines (Figure 14). While insertion mutants of *CSN5a*, *PRA1.F3*, an unknown gene (At1G55170) and *BIM1* decreased susceptibility to *G. orontii*, the susceptibility was increased in mutants of *TCP14*, *TCP13*, *APC8*, *TCP15* and a gene encoding a SBP-family protein. The *csn5a* mutant shows dwarfism and other pleiotropic phenotypes due to the multitude of process regulated by the COP9 signalosome (Gusmaroli et al., 2007). Reduced expression of either one of the CUL3 isoforms in the *csn5a* background can however restore most of these pleiotropic phenotypes to wild type (Gusmaroli et al., 2007) and *csn5a-2 cul3a* plants display enhanced resistance to *Hpa* (Mukhtar et al., 2011), suggesting that CSN5A is specifically involved in plant immunity. These lines were however not tested for susceptibility to *G. orontii*. Furthermore, the expression of *CSN5* was induced 18-fold by *G. orontii* infection in local tissue, suggesting a specific role of this protein in the defense response (Chandran et al., 2010).

The CSN5 subunits of the COP9 signalosome catalyze the removal of the RUB moiety (Related to ubiquitin, called Nedd8 in yeast and animals) from CUL1, CUL3 and CUL4 (Gusmaroli et al., 2007; Lyapina et al., 2001). Cullins are one subunit of the cullin RING (Really interesting new gene) ligases (CRLs), the largest group of E3 ligases, which catalyze the transfer of ubiquitin to target proteins. Cycles of rubylation and derubylation seem to control the activity of these protein complexes (Hotton and Callis, 2008). CUL1 is part of the four subunit SCF complexes. In Arabidopsis, up to 700 F-box proteins have been detected, and these create the specificity of the complex (Hua et al., 2011). SCF complexes comprise, among many others, SCF^{COI1}, SCF^{TIR1} and SCF^{GID2}, which perceive the plant hormones JA, auxin and GA, respectively (Santner and Estelle, 2009) as well as and $SCF^{ETP1/2}$ and $SCF^{EBF1/2}$, which regulate ethylene responses (Guo and Ecker, 2003; Potuschak et al., 2003). Finally, an CUL3 based complex is involved in SA perception (Fu et al., 2012). Targeting of CSN5a might thus allow the manipulation of single or

several hormonal pathways simultaneously. Silencing of *CSN5* in tomato, for example, leads to increased JA but unaltered SA levels, making plants more resistant to herbivore and necrotrophic pathogen attack (Hind et al., 2011). It has to be noted that a first attempt to confirm the interaction of OEC61 and CSN5a by BiFC was successful. The interaction of CSN5a with *Hpa* effectors has however been confirmed (Yatusevich et al., unpublished results). Generally, it is not likely that pathogen effectors induce CSN5a degradation, as lack of this subunit leads to destabilization of the CSN complex and strong pleiotropic phenotypes (Gusmaroli et al., 2007). The geminivirus coat protein C2, for instance, targets CSN5a to interfere with CUL1 derubylation and several hormonal responses without disrupting the CSN complex. Most specifically, this leads to the repression of JA-responsive genes. JA application, in turn, induces resistance to the virus, indicating a specific repression of the JA response via CSN5a by the virus to promote susceptibility (Lozano-Durán et al., 2011).

PRA1.F3, whose knock-out leads to reduced susceptibility of Arabidopsis to *G. orontii*, and its two close homologs PRA1.F1 and PRA1.F2 interacted with OEC65 in Y2H and BiFC (Figure 12 and Figure 15). PRA1 proteins form a 19 member gene family in Arabidopsis which has expanded relative to green algae and other eukaryotes (Alvim Kamei et al., 2008). The F clade is specifically targeted by OECs. PRA1 proteins are involved in vesicle trafficking by regulating the insertion of small GTPases into the membrane (Dirac-Svejstrup et al., 1997; Sivars et al., 2003). The human bacterial pathogen *Legionella pneumophila* also uses the effector SidM, which has both PRA and GEF activity to manipulate the human Rab GTPase Rab1 and recruit membrane material from the ER. This leads to the establishment of a pathogen-induced compartment, the *Legionella*-containing vacuole, underlining the importance of the PRA system for the structure of the endomembrane system (Ingmundson et al., 2007; Machner and Isberg, 2007; Zhu et al., 2010). The BiFC signal of OEC65 and its interacting PRA1.F proteins was localized in spots close to the cell periphery (Figure 15), indicating a specific interaction at an unknown endomembrane compartment. PRA1.F1 co-localizes almost exclusively with a marker of the endosomal and prevacuolar compartment (PVC), RabF2b, suggesting that the interaction of OEC65 and the PRA1 proteins take place there (Alvim Kamei et al., 2008). This is in line with reports from humans, where PRA1 localizes to the Golgi apparatus and endosomes. Without co-localization studies of compartmental marker proteins with the BiFC signal however, no final conclusions can be drawn.

The question thus remains how the lack of PRA1.F3 generates enhanced resistance to *G. orontii*. It is unlikely that PRA proteins are negative regulators of defense signaling, as their biochemical activity is well described, at least in humans (Sivars et al., 2003). Recently, a negative role for AtPRA1.B6 in ER to Golgi trafficking has been established (Lee et al., 2011). The vacuolar and PM trafficking of a subset of marker proteins were inhibited at the ER to an extent proportional to PRA1.B6 protein level. Steady-state PRA1.B6 levels were in turn found to be controlled by proteasome-mediated degradation. It can thus be imagined that PRA1.F proteins function in the

negative regulation of defense component trafficking towards the fungal penetration site. Due to the localization of PRA1.F1 to the endosome/PVC, these trafficking events might involve MVBs, which have been detected at powdery mildew penetration sites in both Arabidopsis and barley (An et al., 2006; Bushnell, 1972; Micali et al., 2011). OEC65 might stabilize the PRA1.F proteins to exploit their inhibitory role and increase susceptibility. In this scenario, insertion mutants of *PRA1.F3* would show enhanced resistance due to increased defense component trafficking, as experimentally determined (Figure 14). Components of defense-related trafficking and the glucosinolate response could also be affected by this process as PEN1, VAMP722 and PEN3 have been found to localize to haustorial encasements and might be transported there by MVBs (Meyer et al., 2009). Interestingly, rat PRA1 also interacts with the v-SNARE VAMP2, potentially interconnecting VAMP and Rab functions in vesicle trafficking (Martincic et al., 1997). Recently, two ARF1 proteins were shown to control callose deposition at the infection site in barley (Böhlenius et al., 2010). These proteins were found to co-localize with *At*RabF2b in barley, but the significance of this signal is currently under debate (Robinson et al., 2011). Expression of dominant negative versions of the ARFs resulted in a lack of callose deposits at the infection site. PRA1.F3 also interacts with three ARF-GTPases (Arabidopsis Interactome Mapping Consortium, 2011). Taken together, the interaction of OEC65 with PRA1.F3, the interaction of PRA1.F3 with several ARF-GTPases and its presumably similar localization to ARF1 as well as the reduction of callose deposits observed after bacterial delivery of OEC65 provokes a scenario in which stabilization of PRA1.F proteins by OEC65 interferes with ARF-mediated trafficking events leading to callose deposition. The accuracy of this model remains to be determined.

BIM1 is also involved in the defense response to *G. orontii*, as an insertion mutant line displayed enhanced resistance to the fungus. This basic helix-loop-helix TF is involved in BR-signaling by binding to E-boxes upstream of BR-induced genes and synergistically activating these genes together with another TF, BES1 (Yin et al., 2005). The role of BR in defense responses is currently not clearly determined. While BR application increases resistance to pathogens in tobacco and rice (Nakashita et al., 2003), the effect of BR signaling on MTI in Arabidopsis is still under debate (Albrecht et al., 2012; Albrecht et al., 2008; Belkhadir et al., 2012). The effect of the *bim1* mutant on BR signaling is subtle. BIM1 also interacts with two TF involved in embryo patterning, DORNRÖSCHEN and DORNRÖSCHEN-LIKE, and the mutant also has an embryo patterning phenotype (Chandler et al., 2009), suggesting that it is involved in several different transcriptional complexes. Dissecting the pathways leading to enhanced resistance to *G. orontii* in *bim1* will thus be challenging.

Apart from three *TCP* genes, which will be discussed below, mutants in *APC8* and a gene encoding a SBP-family protein displayed enhanced susceptibility towards *G. orontii*. No function has been attributed to the SBP-family protein (At4G17680) yet. *SBP* genes have first been identified as interactors of S-RNase, one of the major components of gametophytic self-incompatibility (Sims and Ordanic, 2001). They do contain a RING domain, implicating a role in

ubiquitin-based degradation of target proteins. Not surprisingly, the protein encoded by AT4G17680 interacts, among others, with an F-box protein (Mukhtar et al., 2011). An interaction with two TCP TFs, TCP11 and TCP14 has also been detected. The insertion mutant of the gene is more resistant to a compatible *Hpa* isolate. This suggest an opposite role of this protein in defense against *G. orontii* and *Hpa*, which is surprising given that both are obligate biotrophic pathogens.

APC8 is a subunit of the anaphase promoting complex, an E3 ligase which regulates cell cycle progression by the ubiquitination of cell cycle regulators (Peters, 2006). Interestingly, the APC contains two subunits with a cullin and RING finger domain, respectively, suggesting a structural relationship to SCF complexes (Kramer et al., 1998; Yu et al., 1998; Zachariae et al., 1998). Disruptive knock-outs of the APC are lethal in higher organisms. APC8 contains several tetratrico peptide repeats (TPRs) and has been shown to bind the APC coactivator CCS52 (CDH1 in human) and CDC20, which are the substrate binding proteins of the E3 ligase complex (Matyskiela and Morgan, 2009). Interestingly, the APC is targeted by many human viruses, most probably to induce a S-phase like state that is conducive for viral replication (Mo et al., 2012). The APC also has a role in endoreduplication (Cebolla et al., 1999; Serralbo et al., 2006), a process that is induced by and important for *G. orontii* infection (Chandran et al., 2010). An insertion mutant of *APC8* displays reduced effectiveness of R protein-triggered immunity against *Hpa* (Mukhtar et al., 2011). Recently, an *apc8* mutant was isolated from an Ethylmethylsulfonate (EMS) mutagenized population and shown to display strong developmental phenotypes (Zheng et al., 2011). This sheds doubt on the effect of the transposon insertion mutant used in this study, which was developmentally normal, that still need to be resolved.

I found that *TCP* genes play an important role in the defense against *G. orontii*. Collectively, TCP TFs were targeted 36 times by OECs, with 23 OECs targeting TCP14 (Table 2). This TF was also targeted by 25 *Hpa* and 4 *Psy* effectors, indicating preferential targeting by filamentous and/or obligate biotrophic pathogens. Accordingly, insertion mutant lines of *TCP14* and *TCP13* show enhanced susceptibility to *Hpa* infection (Petra Epple, personal communication). The insertion mutant lines of all *TCPs* tested (*TCP14*, *TCP13*, *TCP15, TCP20*) displayed enhanced susceptibility to *G. orontii*, with *tcp14* showing the most prominent effect. Previously, only very mild or no developmental phenotypes have been observed for TCP single mutants, probably due to functional redundancy (Hervé et al., 2009; Kieffer et al., 2011; Li et al., 2012). The prominent infection phenotype of the single knock-out lines with *G. orontii* thus indicates an important role of these TFs in the defense response. TCP14, TCP15 and TCP20 are class I TCPs, while TCP13 is a member of the CIN subclade of class II TCPs (Martín-Trillo and Cubas, 2010). The TCP TFs have generally been associated with developmental processes and class I and II TCPs seem to act antagonistically (Danisman et al., 2012; Li et al., 2005). The role of type I genes in development has been mostly investigated for TCP20. This TF was found to be involved in the coordination of cell expansion, cell division, and cell growth genes (Hervé et al., 2009; Li et al.,

2005; Tatematsu et al., 2005). TCP14 and TCP15 were found to have redundant functions in the regulation of cell proliferation and the entry into the endocycle (Kieffer et al., 2011) and TCP15 was recently found to regulate endoreduplication (Li et al., 2012). The type II TF TCP13 is localized to both the nucleus and chloroplast and regulates the expression of a photosystem subunit (Baba et al., 2001; Suzuki et al., 2001). Together with other CIN-type TCPs, it is also involved in regulating the morphology of leafs (Efroni et al., 2008; Koyama et al., 2007). TCP14 and TCP13 interact in Y2H (Arabidopsis Interactome Mapping Consortium, 2011), although heterodimerization has previously only been reported for members of the same class (Kosugi and Ohashi, 2002). Accordingly, TCP20 was found to interact with TCP14, TCP15 and several other class I TCPs (Danisman et al., 2012). Several TCP TFs might thus function in a defense-related transcriptional complex to fine tune defense responses. The TCPs interact with several other TFs (Arabidopsis Interactome Mapping Consortium, 2011) and hetero-dimers of TCPs bind DNA more efficiently than homo-dimers (Kosugi and Ohashi, 2002). The site II element bound by TCP genes is also often associated with other *cis*-acting elements (Hervé et al., 2009; Vandepoele et al., 2006), further strengthening the idea of a transcriptional complex involving TCP TFs. Site II elements have been detected with high frequency in 5-10% of Arabidopsis gene promoters, indicating that TCP TFs can regulate a substantial subset of the transcriptome (Welchen and Gonzalez, 2006). But how do these developmental TFs influence the plant response to *G. orontii*?

Several scenarios are possible. Initially, TCP proteins could be regulated by and cooperate with their interactors to induce defense responses. TCP14 and TCP13 interact with each other and WRKY36, a TF that is differentially regulated during defense responses and could potentially bind to W-boxes in defense-related genes (Rushton et al., 2010). Currently, I am therefore investigating the contribution of WRKY36 to the defense against *G. orontii*. TCP14 also interacts with MPK3, a MAP kinase involved in MTI signal transduction (Pitzschke et al., 2009). MPK3 has been shown to phosphorylate and thus activate the defense-related TF WRKY33 (Mao et al., 2011) and the inhibition of MPK3, MPK4 and MPK6 by the *Pseudomonas* effector HopAI1 leads to enhanced bacterial virulence, demonstrating the importance of MAP kinase signaling for plant immunity (Zhang et al., 2007). Proteins involved in calcium-signaling, redox-maintenance and other processes with implications for pathogen defense also interact with TCP14, possibly regulating its activity (Mukhtar et al., 2011). The initiation of defense responses is a costly process for the plant, as it leads to reduced fitness (Bolton, 2009). TCP TFs might constitute a platform for the integration of defense and developmental signals, thus fine-tuning the trade-off between growth and immunity.

Currently, I can envision different but connected scenarios for the downstream targets of the TCP transcriptional complex. One potential mechanism is the control of JA levels in the plant. TCP20 has been found to bind to the promoter and along with TCP9 to repress the expression of *LOX2*, a key gene of JA biosynthesis (Danisman et al., 2012). Transposon insertion mutants of class I

TCP genes might thus examine increased JA levels and a JA-based repression of SA responses. The opposite scenario has been described for CIN-type TCPs like TCP13, which are positive regulators of JA biosynthetic genes (Schommer et al., 2008). These proteins are targeted by the phytoplasma effector SAP11, which destabilizes several CIN type TCPs to reduce JA levels in the plant, thus rendering it more susceptible to its insect vector, a grass hopper species (Sugio et al., 2011). A detailed analysis of SA and JA accumulation in the TCP mutants could help to reconcile the similar and opposing roles of class I and II TCPs in the regulation of susceptibility to *G. orontii* and JA biosynthesis. Interestingly, some JA-responsive genes are induced locally at the *G. orontii* infection site (Chandran et al., 2010) and JA-based defenses are effective against *G. orontii* when triggered extensively (Zimmerli et al., 2004), further complicating this scenario.

An additional scenario involves the regulation of the cell cycle by TCP TFs, most importantly the repression of endoreduplication. The endocycle is induced by several cues, including symbiotic interactions with arbuscular mycorrhizal fungi and rhizobia as well as parasitic interactions with nematodes and *G. orontii* (Bainard et al., 2011; Cebolla et al., 1999; Chandran et al., 2010; Williamson and Hussey, 1996). An inhibition of endoreduplication leads to decreased colonization by both pathogens and symbionts, illustrating its importance for successful infection (Chandran et al., 2010; Vinardell et al., 2003). Endoreduplication is achieved by a modification of the cell cycle, leading to DNA replication but an omission of mitosis, thus doubling cellular DNA content (De Veylder et al., 2011). The class I TCPs positively control cell cycle gene expression, thus linking them to endoreduplication conceptually. The B-type cyclins and cyclin-dependent kinases (CDKs) in particular are key regulators of G2 to M phase transition (G2-M) and their inhibition is associated with progression into the endocycle (Boudolf et al., 2004; Porceddu et al., 2001; Schnittger et al., 2002). Notably, the expression of some of these genes is repressed at the *G. orontii* infection site (Chandran et al., 2010). TCP20 partially controls *CyclinB1;1* expression at G2-M by directly binding to its promoter (Li et al., 2005). Additionally, insertion mutants of *TCP14* and *TCP15* show reduced expression of several cell cycle genes along with signs of increased ploidy (Kieffer et al., 2011). Recently, transcriptional repressor fusions or overexpression of *TCP15* were also found to increase and reduce endoreduplication, respectively (Li et al., 2012). This is achieved by binding of TCP15 to the promoters of *Retinoblastoma-related 1* (*Rbr1*) and *CyclinA2.3*, which are involved in the negative regulation of endoreduplication (Li et al., 2012). The endoreduplication observed after *G. orontii* infection is dependent on the Myb three repeat (MYB3R) TF MYB3R4 (Chandran et al., 2010). Unfortunately, this protein was not included in the Y2H library, so information on direct MYB – TCP interaction is not available. MYB3R TFs do however also control the expression of G2-M expressed genes, including B-type cyclins, linking them to TCP TFs mechanistically (Haga et al., 2007; Ito et al., 2001a). The transcriptional control is mediated through binding to the M-phase specific activator (MSA) element and its repressor or activator function is controlled by phosphorylation (Haga et al., 2007). Interestingly, the MSA and the site II element that is bound by TCP TFs have cooperative functions in the promoter of *CyclinB1;1* (Li et al., 2005). This could indicate that MYB3R4 and TCP TFs act cooperatively to

regulate the transcription of a specific gene set. Insertion mutant lines of MYBR3A and the TCP TFs do however show contrary phenotypes. While MYBR3A is required for full susceptibility (Chandran et al., 2010), the TCP TFs limit the susceptibility of the host. This is in line with the positive and negative regulatory roles of MYBR3A and TCP TFs in the initiation of endoreduplication, underlining the importance of this process during *G. orontii* pathogenesis. The opposing actions of the TFs could be balanced in the transcriptional complex containing them. Both site II and MSA elements are enriched in promoters of genes differentially regulated at the *G. orontii* infection site, further strengthening this model (Chandran et al., 2010). Interestingly, a SCF complex also partially regulates the switch from cell division to endoreduplication (del Pozo et al., 2006) and the APC marks mitotic cyclins for degradation, thereby promoting endoreduplication (Peters, 2006). Finally, JA also modulates the cell cycle (Pauwels et al., 2008). Several distinct effector targets might therefore be involved for the induction of endoreduplication. At least for nematodes, the specific induction of their multinucleate feeding organs by the manipulation of plant developmental pathways has been described (reviewed in (Gheysen and Mitchum, 2011)). However, it still remains to be investigated if the induction of endoreduplication is cause or consequence of *G. orontii* induced cellular changes.

Endoreduplication in general leads to enhanced expression of genes involved in protein synthesis, carbohydrate metabolism and energy generation as well as increased cell surface area and might thus increase nutrient availability for the pathogen or symbiont (Wildermuth, 2010). These processes are also induced by *G. orontii* infection (Chandran et al., 2010) and, together with the observed down-regulation of photosynthesis-related genes, turn the infection site from a nutrient source to a nutrient sink (Berger et al., 2007; Chandran et al., 2010; Chandran et al., 2009; Swarbrick et al., 2006). The infection by powdery mildews also induces the transcriptional activation of genes coding for cell wall invertases and hexose transporters, further increasing nutrient availability (Chandran et al., 2010; Chen et al., 2010; Swarbrick et al., 2006). The presumed induction of endoreduplication by *G. orontii* effectors would thus help to generate a suitable metabolic environment for colonization. This model requires the translocation of OECs from the fungus to epidermal cells and subsequently to adjacent mesophyll cells. While not described in powdery mildew fungi, the cell-to-cell movement of effectors has been detected in other patho-systems (Djamei et al., 2011; Khang et al., 2010).

The susceptibility phenotypes of the insertion mutants seem to indicate a direct role of host targets in the defense response. This is corroborated by the enhanced susceptibility of *eds1*, which is comprised in both SA-dependent and independent defense pathways. Effector virulence functions have often been investigated for their role in suppressing the defense response, and this approach has been successful in uncovering important components of host immunity (Feng and Zhou, 2012). However, it is also conceivable that these mutants induce a cellular state more permissive to *G. orontii* infection. This has been described for TAL-effectors of the rice pathogen *Xanthomonas oryzae* pv. *oryzae* (Antony et al., 2010; Yang et al., 2006) which induce the

transcription of genes coding for SWEET type glucose transporters, presumably to increase glucose availability in the apoplast (Chen et al., 2010). In Arabidopsis, SWEET transporters are also induced by *Pst* and powdery mildew infection (Chen et al., 2010). Importantly, a subset of *SWEETs* is induced in a T3SS-dependent manner, implicating effectors in their induction. Another TAL effector, AvrBs3, induces hypertrophy (increased cell size) of mesophyll cells, probably to facilitate bacterial release from the plant (Marois et al., 2002). Hypertrophy is often associated with endoreduplication (Breuer et al., 2010), but the ploidy level of hypertrophic mesophyll cells remains to be determined. In the future, fungal effectors needed for the induction of nutrient leakage and haustorium formation will certainly be uncovered.

In this study, I characterized the functions of host proteins in the defense response after the assessment of insertion mutant lines. While frequently and successfully used in the past, this tool does have a pitfall. In network terms, insertion mutants lead to node removal (absence of the protein and all its interactions), rather than the loss or change of edges (differences in protein affinity or specificity) (Dreze et al., 2009; Zhong et al., 2009). For pathogen effectors, at least of bacteria, the manipulation of host proteins is as important as degradation (Feng and Zhou, 2012). Many interesting virulence targets might thus be missed by insertion mutant screens. Accordingly, more than 50% of human diseases are associated with amino acid changes (~edgetic perturbation) rather than severe truncations of proteins (~node removal), suggesting that alterations in protein affinity can have strong impacts on cellular networks (Zhong et al., 2009).

3.3.9 Y2H interactions can be confirmed by BiFC

Finally, I attempted to confirm the interaction of shortlisted OECs with their respective targets derived from Y2H. Four of twelve tested interactions could be confirmed (Figure 15), a ratio expected from previous large scale interactome confirmation attempts (Braun et al., 2009; Venkatesan et al., 2009). Unfortunately, the interactions of OECs with CSN5a, TCP14 and TCP13 were not among the confirmed interactions. These proteins are targeted by several other effectors and the additional interactions remain to be confirmed. The interaction of OEC65 and PRA1.F1, PRA1.F2 and PRA1.F3 gave positive signals in BiFC, making these proteins prime candidates for further characterization (for discussion see above). In addition, I could confirm the interaction of OEC56 and NAP1.1. NAP1.1 and its three paralogs NAP1.2-4 are putative histone chaperones (Park and Luger, 2006) and have been found to bind H2A *in vitro* (Liu et al., 2009b). NAP1.1 and its paralogs are primarily localized to the cytoplasm, where the interaction with OEC56 was observed. A fusion protein of OEC56 and Citrine was however detected almost exclusively in the nucleus (Figure 10). Binding of OEC56 to NAP1.1 might thus mask its NLS or induce a NAP1.1-mediated exclusion of the hybrid from the nucleus, thereby shifting the balance between nuclear and cytoplasmic pools of both OEC56 and NAP1.1. Currently, these two scenarios cannot be discriminated. Also, no infection phenotype was detected for the *nap1.1* insertion mutant (Figure 14), in line with the genetic redundancy and compensatory expression

observed for the *NAP1* paralogs (Liu et al., 2009b). Roles for NAP1 proteins in nucleotide excision repair, transcriptional processes, homologous recombination and ABA responses have been described (Gao et al., 2012; Liu et al., 2009a; Liu et al., 2009b). The role of NAP1 proteins in these processes can be explained by the regulation of chromatin accessibility. The role of chromatin modifications in defense signaling is only beginning to be elucidated, but defense gene expression is certainly relying on a permissive chromatin state (Berr et al., 2012). OEC56 might thus modify NAP1.1-dependent H2A/B insertions to repress the expression of certain genes. The expression of this effector is induced rather late (>24 hpi), suggesting it interferes with late host responses. Interestingly, NAP1.1 has been found to interact with PNM1 (PPR protein localized to the nucleus and mitochondria 1) in the nucleus and this protein in turn interacts with TCP8 (Hammani et al., 2011). This interaction could link NAP1.1 to the TCP-dependent transcriptional processes described above.

3.4 Concluding remarks

In this thesis, I have established new protocols for the quantification of powdery mildew pathogenesis on Arabidopsis and analyzed the haustorial transcriptome of *G. orontii.* In addition, I have identified and characterized a subset of the effector arsenal used by the biotrophic powdery mildew fungus *G. orontii*. Some of these effectors can suppress cell death and enhance the virulence of bacteria delivering them to the plant. I have characterized the subcellular localization and expression profiles of selected candidates and subsequently determined the host-pathogen interactome of the OECs. This uncovered a multitude of host processes targeted by effectors, among them vesicle trafficking, protein degradation, hormone signaling and endoreduplication. The screen complements previously described interactomes and revealed common host targets of three unrelated phytopathogens. These targets are highly connected in the host interactome and are required for an efficient immune response against *G. orontii*, further corroborating the hypothesis that pathogens specifically target hubs to promote susceptibility. The effector targets identified will therefore form the basis of subsequent effector research in this patho-system. Additionally, a network analysis of plant-pathogen interactions will hopefully provide a tool for an integrated view of the multiple evolutionary forces shaping the plant immune response at the systems level.

4 Materials and Methods

4.1 Materials

4.1.1 Plant material

In this study the *Arabidopsis thaliana* Col-0 genotype and the *edr1*-1 (Frye and Innes, 1998), *eds1*-2 (Bartsch et al., 2006), *pmr4*-1 (Vogel and Somerville, 2000), *mlo2*-6 single and *mlo2*-5 *mlo6*-2 *mlo12*-1 triple mutants (Consonni et al., 2006) in the Col-0 genetic background were used. Additionally, a transgenic line expressing *NahG* (Gaffney et al., 1993) in the Col-0 genetic background was employed. The set of homozygous T-DNA insertion lines screened is described in Supplemental Table 11. Two different plant densities were used for growing. Either approximately 100 seeds were sown per pot of soil substrate and five pots were used per genotype (quantification of powdery mildew infection) or five plants/ pot were used (EDV assays, qRT-PCR). After stratification for 2 d at 4°C in darkness plants were grown for 18 d (quantification) or 4-5 weeks at a day/night cycle of 10/14 h in a light chamber with 22°C/20°C day/night temperature and a relative humidity of 60%.

4.1.2 Strains and plasmids

Below the bacterial and yeast strains as well as cloning and expression vectors used in this study are presented. *Escherichia coli*, *Agrobacteria, Pseudomonas* and yeast were grown at 37°C, 28°C, 28°C (all 220rpm) and 30°C (180rpm), respectively.

Table 4: Strains of microorganisms used in this study.

Organism	Strain	Source	Resistance
E. coli	DH5α	Invitrogen, Heidelberg, Germany	Nalidixic acid
E. coli	DB3.1	Invitrogen, Heidelberg, Germany	Spec Strep
E. coli	TOP10	Invitrogen, Heidelberg, Germany	Spec Strep
E. coli	HB101 pRK2013	Jonathan Jones, Sainsbury Lab, Norwich, UK	Kan
Agrobacterium tumefaciens	GV3101 pMP90RK	Csaba Conz, MPIPZ, Cologne, Germany	Rif Kan
A. tumefaciens	C58C1 pGV2260	Csaba Conz, MPIPZ, Cologne, Germany	Rif Carb
Pseudomonas syringae pv. *tomato* (*Pst*)	DC3000	Roger Innes, Indiana University, USA	Rif
Pst	LUC	Jonathan Jones, Sainsbury Lab, Norwich, UK	Rif Kan
Pst	ΔCEL	Jonathan Jones, Sainsbury Lab, Norwich, UK	Rif Spec Strep
Saccharomyces cerevisiae	Y8800	Pascal Braun, Dana-Farber Cancer Institute, Boston, USA	
S. cerevisiae	Y8930	Pascal Braun, Dana-Farber Cancer Institute, Boston, USA	

Table 5: Vectors used in this study.

Vector	Source	Resistance
p35S-GW-Citrine	Anja Reinstädler, MPIPZ, Cologne, Germany	Amp
pAM-PAT-GW-3xHA	Anja Reinstädler, MPIPZ, Cologne, Germany	Amp
pB7WG2-Strep-HA-GW	Jaqueline Bautor, MPIPZ, Cologne, Germany	Spec Strep
pB7WG2-*Ch*NLP1	Jochen Kleeman, MPIPZ, Cologne, Germany	Spec Strep
pB7WG2-Strep-HA-*Pi*INF1	Jaqueline Bautor, MPIPZ, Cologne, Germany	
pCR8/GW/TOPO	Invitrogen, Heidelberg, Germany	Spec Strep
pDON201	Invitrogen, Heidelberg, Germany	Kan
pEDV6	Jonathan Jones, Sainsbury Lab, Norwich, UK	Gent
pUBC-nYFP	Christopher Grefen, University of Glasgow, UK	Spec Strep
pUBC-cYFP	Christopher Grefen, University of Glasgow, UK	Spec Strep
pDEST-AD	Pascal Braun, Dana-Farber Cancer Institute, Boston, USA	Spec Strep/ TRP1
pDEST-DB	Pascal Braun, Dana-Farber Cancer Institute, Boston, USA	Spec Strep/ LEU2

4.1.3 Reagents, chemicals and antibiotics

Restriction enzymes were purchased from New England Biolabs (NEB, Frankfurt/Main, Germany) and Fermentas (St. Leon-Rot, Germany). Restriction digestions were performed following the manufacturer's instructions, using the provided 10 x reaction buffer.

Laboratory grade chemicals and reagents were purchased from Sigma-Aldrich (Deisenhofen, Germany), Roche (Mannheim, Germany), Roth (Karlsruhe, Germany), Merck (Darmstadt, Germany), Invitrogen (Karlsruhe, Germany), Serva (Heidelberg, Germany), Duchefa (Haarlem, The Netherlands) and Thermo Fisher Scientific (Rockford, USA) unless otherwise stated.

The antibiotics used and their stock concentration are listed below.

Table 6: Antibiotics used in this study.

Antibiotic	Stock	Solvent	Source
Ampicilin	50 mg/mL	H20	Roth
Carbencilin	50 mg/mL	H20	Sigma
Gentamycin	25 mg/mL	H20	Sigma
Kanamycin	50 mg/mL	H20	Sigma
Rifampicin	100 mg/mL	DMSO	Sigma
Spectinomycin	50 mg/mL	H20	Duchefa
Streptomycin	25 mg/mL	H20	Sigma

4.1.4 Antibodies

Primary and secondary antibodies used in this study are listed below.

Table 7: Antibodies used in this study.

Antibody	Source	Conjugate	Dilution	Source
anti-HA	rat, monoclonal		1:5000	Roche
anti-GFP	mouse, monoclonal (7.1 and 13.1)		1:5000	Roche
anti-rat IgG	goat, polyclonal	Horseradish peroxidase (HRP)	1:5000	Santa Cruz Biotechnology
anti-mouse IgG	rabbit, polyclonal	HRP	1:5000	Sigma

4.1.5 Media

Sterilized media were used for growing bacteria or yeast. For sterilization, media were autoclaved for 20 min at 121°C and cooled down prior to adding heat instable antibiotics or other supplements. Heat instable compounds were filter-sterilized before use. Agar for 1.5 % agar plate preparation was purchased from Becton (Franklin Lakes, USA). Bacterial media compositions are outlined below.

NYG medium (*Pst)*		LB medium (*E.coli*)		YEB medium (*A.tumefaciens*)	
Bactopeptone	5 g/l	Tryptone	10 g/l	Beef extract	5 g/l
Yeast extract	3 g/l	Yeast extract	5 g/l	Yeast extract	1 g/l
Glycerol	20 ml/l	NaCl	5 g/l	Tryptone	3 g/l
pH 7.0		pH 7.0		Sucrose	5 g/l
				pH 7.2	

For a detailed description of yeast media see Dreze et al. (2009).

4.2 Methods

4.2.1 Standard molecular and biochemical methods

4.1.2.1 Agarose gel electrophoresis

DNA fragments were separated by agarose gel electrophoresis in gels of 1 - 2 % (w/v) agarose (Bio-Budget Technologies, Krefeld, Germany) supplied with ethidium bromide solution (1:40000) in TAE buffer (400 mM Tris-HCl; 10 mM Na_2-ethylenediamine tetraacetic acid (EDTA); 200 mM acetic acid; pH 8.5).

4.1.2.2 DNA sequencing

DNA sequences were determined by the “Automated DNA isolation and sequencing” (ADIS) service unit at the Max-Planck Institute for Plant Breeding Research (Cologne, Germany) on Abi Prism 377 and 3700 sequencers (Applied Biosystems, Weiterstadt, Germany) using Big Dye-terminator chemistry. Sequence data were analyzed using LaserGene suite version 8.00 (DNAStar, Madison, USA).

4.1.2.3 Polymerase chain reaction (PCR)

For non-cloning purposes, PCR reactions were performed using home-made *Taq* DNA polymerase in a DNA engine Tetrad 2 (Bio-Rad, Munich, Germany). A 10 x PCR buffer containing 750mM Tris-HCl pH 8.8; 200 mM $(NH_4)_2SO_4$; 0.1 % (v/v) Tween 20; 25 mM $MgCl_2$ was used. For cloning of OECs and Arabidopsis genes, a proof-reading polymerase (Phusion, NEB) was used according to the manufacturer's instructions. For a list of primers used see Supplemental Table 1.

4.1.2.4 Total plant protein extract

Plant material was frozen in liquid nitrogen and homogenized in lysis buffer (20 mM HEPES pH 7.5; 13 % Sucrose; 1 mM EDTA; 1 mM DTT; 0.01 % Triton, 1x complete protease inhibitor cocktail (Roche)) using a concentric drill. Samples were centrifuged at 13,000 rpm, 4 °C for 10 min and the supernatant retained. Subsequently, 2x loading buffer (125 mM Tris-HCl pH 6.8; 5 % sodium dodecyl sulfate (SDS); 25 % Glycerol (v/v); 0,025 % Bromphenol blue (w/v); 0.2 M DTT) was added, samples incubated at 96°C for 5 min and used for SDS-polyacrylamide gel electrophoresis (SDS-PAGE).

4.1.2.5 SDS-PAGE and immunoblotting

Denaturing SDS-PAGE was carried out using the Mini-PROREAN® 3 system (Bio-Rad, Hercules, USA) and discontinuous SDS-polyacrylamide gels according to standard procedures (Laemmli, 1970). A separating gel (Table 8) was poured between two glass plates and overlaid with isopropanol. After polymerization the isopropanol was removed and a stacking gel was poured onto the separating gel (Table 8). The gel was placed into the electrophoresis tank and submerged in 1x SDS running buffer (25 mM Tris-HCl; 250 mM Glycine; 0.1 % SDS). A pre-stained molecular weight marker (Precision plus protein standard dual color, Bio-Rad) and 35µl denatured protein samples were loaded onto the gel and run at 100 V (stacking gel) and 130 V (separating gel).

Proteins were transferred to a Hybond™-ECL™ nitrocellulose membrane (Amersham Biosciences, Buckinghamshire, UK) in a Mini Trans-Blot® Cell (Bio-Rad) according to the manufacturer's instruction. The transfer was carried out in 1 x transfer buffer (15 mM $NaPO_4$; 0.05 % SDS; 20 % Ethanol) at 100 V for 1 h or 30mA o/n. Subsequently, membranes were stained with Ponceau S (0.5 % Ponceau S (w/v) in 5 % (v/v) acetic acid) for 10 min, washed 3 x 5 min with TBS-T (10 mM Tris, 1.5 mM NaCl, pH 7.5, 0.05% (v/v) Tween20) and blocked for 1 h in TBS-T containing 5 % (w/v) non-fat dry milk (AppliedChem, Germany). The blocking solution was removed and membranes were washed 3 x 5 min with TBS-T. Incubation with primary antibodies was carried out overnight by slowly shaking at 4 °C in TBS-T or 2h at RT. Membranes were washed 3 x 5 min with TBS-T at room temperature. Bound primary antibodies were detected using HRP-conjugated secondary antibodies diluted in TBS-T for 1 h at room temperature. For antibodies see

Table 7. Membranes were washed 3 x 5 min with TBS-T. Finally, bands were visualized using a 1:1 mixture of Super Signal West Pico and Femto kit (Thermo Fisher Scientific) and imaged with Kodak scientific imaging film.

Table 8: Composition of SDS-PAGE gels used in this study.

	Separating Gel			Stacking Gel	
	8%	10%	12%		
H_2O	9,2 ml	4 ml	3 ml	H_2O	6,8 ml
Polyacrylamide 30%	5,4 ml	5 ml	6 ml	Polyacrylamide 30 %	1,66 ml
1M Tris pH8,8	5,0 ml	5,7 ml	5,7 ml	1 M Tris pH6,8	1,26 ml
10% SDS	0,2 ml	150 µl	150 µl	10% SDS	100 µl
10% APS	0,2 ml	150 µl	150 µl	10% APS	100 µl
TEMED	12 µl	6 µl	6 µl	TEMED	10 µl

4.1.2.6 Trypan Blue staining

Trypan Blue staining was used to reveal the occurrence of plant cell death. Before the experiment, a Trypan Blue Stock solution (10 mg Trypan Blue (Sigma) in 40 ml lactophenol) was diluted 1:1 with ethanol. Leaves were boiled for 1 min in 500 µl of fresh trypan blue working solution, destained for 1 h in 4 ml chloral hydrate and destained a second time o/n with gentle agitation. Finally, chloral hydrate was removed and samples were stored in 70% glycerol.

4.1.2.7 Coomassie staining

For the visualization of fungal structures, seedlings were harvested at indicated time points and destained and stored in ethanol: glacial acetic acid 3:1 (v/v). Fungal structures were stained with 0,6% Coomassie Brilliant Blue in ethanol as described previously (Göllner et al., 2008) and brightfield images obtained using an AxioImager.A2 system with an AxioCam HRc (Zeiss, Jena, Germany).

Powdery mildew inoculations

The *G. orontii* isolate MPIPZ was propagated on four week old *eds1* plants and conidia were used at 11-21 dpi. Inoculations were either performed by brush inoculations (Göllner et al., 2008) or by using a simple 80 cm high cardboard settling tower whose opening was covered with a 80 µm nylon mesh (Reuber et al., 1998). The tower contained up to nine pots per inoculation. Therefore, consecutive rounds of infection had to be used. In each round, pots of different genotypes were included. A fine paint brush was used to harvest conidia from four heavily infected leaves and to separate the conidia by brushing them through the nylon mesh. Inoculation

density was approximately 750 spores/cm^2. Newly inoculated plants were then returned to the growth chamber.

4.2.2 Quantification of powdery mildew infection

4.2.2.1 Genomic DNA extraction

Ten seedlings per genotype were harvested across pots and frozen in liquid nitrogen. Genomic DNA was extracted essentially as previously described (Brouwer et al., 2003). Approximately 15 1 mm and 100 mg 0.2 mm diameter glass beads were added and the frozen material was disrupted in a MM400 mixer mill (Retsch, Haan, Germany) for 2x 1 min at 30 Hz. Subsequently, 300 µl lysis buffer (2.5 M LiCl, 50 mM Tris-HCl, 62.5 mM EDTA, and 4.0% Triton X-100, pH 8.0) and an equal volume of phenol:chloroform:isoamyl alcohol (25:24:1 v/v, Roth) were added and samples were homogenized for 30 s at 30 Hz in the mixer mill. After centrifugation (5 min, 16.000 g) the supernatant was recovered and the genomic DNA was precipitated by the addition of two volumes of 100% ethanol, incubation for 15 min at -20°C and another round of centrifugation. The DNA pellet was washed with 70% ethanol, air dried and resuspended in Millipore water. DNA quality and concentration were inspected on a Nanodrop system (Thermo Scientific).

4.2.2.2 qPCR on genomic DNA

For qPCR 15 µl samples were prepared using the Brilliant Sybr Green QPCR Reagent Kit (Stratagene, Waldbronn, Germany) according to the manufacturer's protocol. The *Taq* DNA polymerase provided was replaced by another *Taq* polymerase (Ampliqon, Odense, Denmark) and the according standard buffer. Final primer concentration of 0.4 µM and three technical replicates per sample were employed. qPCR was carried out according to the following protocol: denaturation at 95°C for 3 min, 40 repeats of 95°C for 20 s, 61°C for 20 s and 72°C for 15 s. A melting curve analysis was conducted from 55°C-95°C in 0.5°C steps and 10 s dwell time to confirm the amplification of single amplicons. Additionally, amplicon size and identity were confirmed on a 2% agarose gel and by DNA sequencing, respectively. The ratio of *G. orontii* to Arabidopsis genomic DNA was calculated using the ΔΔCt method (Pfaffl, 2001).

4.2.2.3 Spore counts

For the establishment of the method the following protocol was used: At 6 dpi, three samples of approximately 500 mg of seedlings were harvested per genotype. Five ml H_2O was added and spores liberated by vortexing for 30 s at maximum speed. The spore solution was filtered through Miracloth (Merck, Darmstadt, Germany) to remove large debris and spores were 4-fold concentrated by centrifugation (5 min, 4000g). For each sample, spores were counted in eight 1 mm^2 fields of a Neubauer-improved haemocytometer (Marienfeld, Lauda-Königshofen, Germany) and results were averaged. Finally, spore counts were normalized to the initial weight of seedlings.

During the continued application of the method I realized that sampling at 7dpi is generally more reliable and allows omitting the centrifugation step. Therefore this modified protocol was used for the results in Figure 14 and Supplemental Figure 5.

4.2.3 Generation and analysis of the haustorial library

The isolation of haustorial complexes and library generation was performed and partially described previously (Micali et al., 2011). Briefly, infected leaves of *NahG*-expressing plants were harvested at 4-6 dpi, homogenized, and haustorial complexes were isolated by isopycnic centrifugation on a Percoll cushion. RNA was extracted from the haustorial fraction using the RNeasy Plant Miniprep Kit (Qiagen, Hilden, Germany) according to the manufacturer's instructions. A non-normalized cDNA library was synthesized from 3.5 µg total RNA with the Mint-Universal kit (Evrogen, Moscow, Russia). 454 sequencing libraries were constructed by using self-made adaptors with Multiplex Identifiers (MIDs) following Roche's technical bulletin TCB 09004 introducing *Sfi*I restriction sites (Knaust et al., unpublished results). The so obtained 454 libraries were immobilized on beads and clonally amplified using the GS FLX Titanium LV emPCR Kit. The libraries were then sequenced using the GS FLX Titanium Sequencing Kit XLR70 and GS FLX Titanium PicoTiterPlate Kit on a GS FLX Instrument (Roche 454 Life Sciences, Mannheim, Germany). All kits used were purchased from Roche 454 Life Sciences and used according to the manufacturer's protocol.

Only reads were included in the assembly that mapped with at least 100 bases (BLASTN, ≥95% identity) to the draft genome assembly of *G. orontii*, leaving 679,000 reads. Adapters were removed using the cross_match algorithm (minmatch=8, minscore=12). In total, 620,000 reads were placed into 31,051 contigs by the MIRA assembler version 3 (job='denovo,est,normal,454', 454_SETTINGS '-LR:mxti=no -CL:qc=no:mbc=yes') (http://sourceforge.net/projects/mira-assembler/). For contigs that aligned to the same regions of the genome (best BLASTn hit) only the contig with the highest AC was selected, which resulted in a set of 20,259 unique contigs. Open reading frames were predicted from these contigs using BestORF with the *Sclerotinia sclerotiorum* matrix (Softberry, Mount Kisco, NY, U.S.A.). Predicted proteins were then annotated by Blast2GO (Conesa et al., 2005) using default parameters. Briefly, sequences were compared to the non-redundant database at NCBI by BLASTp (e<1e-5) (Altschul et al., 1990), Gene ontology (GO) terms were retrieved from the Top20 BLAST hits and, together with GO terms obtained by InterProScan analysis (InterPro version 29.0), used for *de novo* functional annotation of predicted proteins. If necessary, categorization was completed by hand. Only contigs with ≥5 AC were used for subsequent analysis. For visualization, sequences were grouped into categories according to the GOSlim file for *Candida albicans* (http://www.candidagenome.org/download/go/go_slim/). Secreted proteins were predicted from Open reading frames (ORFs) containing a genuine start codon by SignalP 3.0 (HMM_Sprob≥0.9) (Bendtsen et al., 2004). Transmembrane proteins were excluded by TMHMM analysis

(http://www.cbs.dtu.dk/services/TMHMM) of protein sequences lacking the first 20 amino acids (to prevent the false-positive assignment of N-terminal signal peptides as transmembrane domains).

The enrichment analysis was performed using the Blast2GO Fisher's exact test plugin with default parameters.

4.2.4 qRT-PCR

Four to five week old plants were infected with *G. orontii* by brush inoculation and total leaf material was harvested at indicated time points. For the samples containing total mycelium, eight infected leaves from four different wild type plants were harvested per time point, pooled, and directly frozen in liquid nitrogen. For mycelium-removed samples, cellulose acetate peelings were performed at 24 hpi and subsequent time points (72 hpi, 7 dpi) by painting ~15 leaves from 8 plants with 5% cellulose acetate in acetone using a fine brush. After the evaporation of acetone the mycelium was peeled off, the leaves were pooled and directly frozen in liquid nitrogen. The experiment was repeated once with wild type and once with *NahG* transgenic plants. For both sample types, total RNA was extracted from 100 mg tissue with the RNeasy Plant Miniprep Kit (Qiagen) according to the manufacturer's instructions. cDNA was synthesized using Superscript II Reverse Transcriptase (Roche) with oligo-dT primers according to the manufacturer's instructions. qRT-PCR was carried out with three technical replicas of cDNA corresponding to 75 ng RNA in an iQ5Cycler (Bio-Rad). The iQSybr Mastermix (Bio-Rad) was used with 0.5 µM final concentration of each primer and amplification conducted according to the following protocol: denaturation at 95°C for 3 min, then 40 repeats of 95°C 20 s, 55°C 20 s, 72°C 10 s. Subsequently, a melting curve analysis of 55-95°C in 0.5°C steps with a dwell time of 10 s per step was used to verify the amplification of single amplicons. In addition, amplicons were visualized on a 2% agarose gel and their identity confirmed by DNA sequencing. Expression was calculated relative to *Go β-tubulin* (GoEST_4780) using the ΔΔCt method (Pfaffl, 2001). Sequences and amplification efficiencies of oligonucleotide primers used are given in Supplemental Table 1.

4.2.5 Transmission electron microscopy

Preparation of samples (high pressure freezing, freeze substitution, embedding and sectioning) and transmission electron microscopy of haustorial complexes was performed as described in Micali et al. (2011).

4.2.6 Prediction and bioinformatic analysis of effectors

The set of secreted proteins identified in the analysis of the haustorial cDNA library (4.2.3) was used as the starting point of OEC prediction. The set of candidates was extended by lowering the SignalP threshold to 0.8 and using all contigs with ≥2 AC. Additionally, a size cut-off of ≥60 amino acids was implemented. The absence of homologs for these proteins in unrelated species was

confirmed by repeated BLAST analysis. In a second round of predictions, the set 491 *Bgh* CSEPs (Pedersen et al., unpublished) and effector candidates from the first round were used as templates for the tBLASTn and BLASTp analysis of the haustorial cDNA library . Putative homologs or paralogs of predicted effectors were then subjected to SignalP and TMHMM analysis to prevent false positives. This process was repeated twice to generate a list of 115 OECs. These effector candidates were then analyzed for their cysteine content, occurrence of the YxC motif (Godfrey et al., 2010) and the presence of putative NLS by NLStradamus and NucPred (Brameier et al., 2007; Nguyen Ba et al., 2009). Finally, the conservation of OECs in the genomes of *Bgh* and *E. pisi* was queried by tBLASTn (Spanu et al., 2010). A multiple sequence alignment of the OECs was created by ClustalW (http://www.ebi.ac.uk/Tools/msa/clustalw2/) and imported into MEGA4 (Tamura et al., 2007). The phylogeny was computed with default parameters using the Neighbor-joining algorithm and a p-distance model for amino acid substitutions.

4.2.7 *Pseudomonas* EDV assays

Transgenic *Pst* clones were prepared by standard triparental mating. *Pst* or *Pst* ΔCEL, *E. coli* carrying pEDV6-OEC constructs and the *E. coli* helper strain HB101 (pRK2013) were grown on plate overnight (o/n), mixed 2:1:1 in H_2O, washed once and transferred onto 1 % agar LB plates without antibiotics. After o/n incubation the mixture was streaked onto selective NYGA plates and grown 2-3 days. Three independent single colonies were restreaked and analyzed by colony PCR. Positive clones were checked for luciferase and EDV construct expression.

Luciferase expression was determined by growing strains in 1 mL of NYG o/n, 20-fold dilution with fresh medium and further growth until OD_{600nm} 0.2. Cultures were then diluted to OD_{600nm} 0.15, 0.1 and 0.05 and luciferase activity was measured for 10s in a luminometer (Centro LB 960 microplate luminometer, Berthold Technologies, Wildbach, Germany).

The expression of AvrRPS4-HA-OEC fusion proteins was determined by an *in vitro* secretion assay similar to previously described (Fabro et al., 2011). *Pst* strains were grown o/n in 25 ml liquid media to high density, centrifuged, washed twice with 10 mM $MgCl_2$ and diluted to OD_{600nm} 0.3 in 20 ml minimal media (50 mM potassium phosphate buffer, 7.6 mM $(NH_4)2SO_4$, 1.7 mM $MgCl_2$, 1.7 mM NaCl, pH 6.0, with 20 mM glucose added). The cultures were incubated at 22°C and 200 rpm o/n to a final OD_{600nm} of 1.0. Cells were harvested from 1mL culture, resuspended in 2x loading buffer, lysed at 96°C for 10min and used for Western Blotting (pellet fraction). The residual culture was spun down (5200g, 15min, 4°C), the supernatant was retained and filtered through a 0.2µm pore filter. The supernatant was then concentrated to 2ml final volume in 9kDa cut-off protein concentrator columns (Thermo Fisher Scientific) by sequential centrifugations (5200g, 4°C, 20min). Proteins in the concentrated supernatant were precipitated using 10 µl Strataclean beads (Stratagene, Santa Clara, USA) per ml supernatant. The mixture was incubated 15 min at 4°C inverting gently, centrifuged at 2000 g for 2 min and re-suspended in 60 µl 2x loading buffer containing 0.1 M NaOH (supernatant fraction). Samples were boiled for 5

minutes at 96°C and centrifuged at 12.000 rpm for 30s minutes before loading. The pellet and supernatant fractions were analyzed by SDS–PAGE, electro blotted onto nitrocellulose membrane, and probed with anti-HA and the secondary anti-rat IgG antibody.

The preliminary Luciferase-based screen was carried out as follows. Fresh bacteria were diluted in H_2O, plated on selective media and incubated o/n. Before spraying, plants were incubated in a high humidity environment for 3h to open stomata. The bacteria were harvested in 10 mM $MgCl_2$, OD_{600nm} adjusted to 0.2 in 10 mM $MgCl_2$ with 0.04% Silwet L-77 (Lehle seeds, USA) and sprayed onto plants until droplet run-off. Leaves were allowed to dry and plants incubated for three days in a growth cabinet with a 10/14 h day/night cycle at 23°C. Four leaves were harvested from three replicated pots, washed in 70% ethanol and two times in H_2O. One leaf disc was punched from each leaf and measured in a luminometer for 10 s. Means and standard errors were calculated. *Pst* pEDV-OEC strains with ≥ 10-fold enhanced growth relative to the pEDV-YFP control (provided by Jaqueline Bautor, MPIPZ) in three of four repeated experiments were selected for subsequent bacterial titer analyses.

For bacterial titer analysis, infections were performed as described above. At day zero, three biological replicates with three leafs per replicate were harvested, surface sterilized and leaf discs isolated. These were collected in 1 mL 10 mM $MgCl_2$ with 0.01% Silwet L-77 and bacteria isolated by shaking at 28°C, 650 rpm. 20 µl aliquots were plated on selective plates and scored after two days at 28°C. At day three, bacteria were isolated using the same procedure but only 500 µl 10 mM $MgCl_2$ with 0.01% Silwet. After isolation, a five step 10-fold dilution series in 10 mM $MgCl_2$ was prepared. 20 µl aliquots were plated on selective plates and incubated at 28°C. Colonies were counted two days later. Means and standard errors were calculated and significant differences determined by a two-tailed Student's t-test. Only strains with 10-fold enhanced growth relative to the pEDV-YFP control were used for subsequent analyses.

To determine if OECs could suppress callose deposition, *Pst*, *Pst* ΔCEL and *Pst* ΔCEL pEDV clones were used. Bacteria and plants were prepared as described above, but Silwet L77 was omitted. Leaves were infiltrated with bacteria or 10 mM $MgCl_2$ using a 1 ml syringe and plants were stored in the lab until harvest. At 12-14 hpi, 20 leaves were harvested per *Pst* strain, and destained in 100% Methanol three times. Callose was stained with 0.05% Aniline blue in 50 mM Phosphate buffer (pH 8.5) for at least 24 hrs. Samples were analyzed on an AxioImagerA2 system at 10x magnification. Callose foci were counted by automated image analysis using ImageJ (Abramoff et al., 2004). Parameters applied were Treshold low=9000 high=1683; Analyze Particles size=10-150, circularity 0.5-1. The mean and standard deviation was calculated and three independent experiments were integrated to generate Figure 9B.

4.2.8 Transient expression assays

4.8.2.1 Transient expression in *N. benthamiana*

For transient expression studies in *N. benthamiana*, OECs were transferred into pAM-PAT-GW-3xHA, p35S-GW-Citrine or pUBC-GW-cYFP vectors by recombination. Arabidopsis proteins were cloned into pDONR201 and transferred to pUBC-GW-nYFP. Recombinant plasmids were isolated and transformed into *A. tumefaciens* GV3101 pMP90RK (pAM-PAT and p35S vectors) or C58C1 pGV2260 (pUBC vectors). Positive clones were used for subsequent experiments.

The infiltration protocol used for cell death assays and localization studies is derived from (Kleemann et al., 2012). To analyze the necrosis-suppressing function of OECs, Agrobacteria containing vectors for either OEC, YFP or necrosis-necrosis inducing peptide expression were grown overnight to stationary phase, harvested (5000g, 15min, RT) and resuspended to OD_{600nm} 0.5 (OECs) and 1 (necrosis-inducing peptides) in infiltration buffer (10 mM 2-(*N*-morpholino)ethanesulfonic acid (MES), pH 5.6; 10 mM $MgCl_2$; 200 µM Acetosyringon). After incubation at RT for 4h, Agrobacteria solutions harboring the inducing peptides were mixed with OEC or YFP strains 1:10. The mixtures were then infiltrated into the abaxial side of leaves of five week old *N. benthamiana* plants using a needle-less syringe. Combinations of YFP or OEC and the necrosis-inducing peptide were infiltrated on opposite sides of the same leaf. Subsequently, plants were incubated in a controlled environment chamber (19 °C/21 °C day/night temperature cycles and 16-h-light/8-h-dark cycles. Macroscopic symptoms on three leaves from three different plants were documented per OEC at 7 dpi.

A similar protocol was used for the localization studies. Infiltration cultures were prepared from Agrobacteria carrying OEC-Citrine fusions (OD_{600nm} 0.5) and the p19 silencing suppressor (final OD_{600nm} 0.1) (Voinnet et al., 2003), respectively. The mixtures were infiltrated and plants incubated as described above. At 2dpi, Citrine fluorescence was visualized by CLSM on a Zeiss LSM 510 Meta for at least three epidermal cells on two different leaves.

For the BiFC analysis, a modified protocol was employed as described (Grefen et al., 2010). Agrobacterium cultures were grown to early stationary phase (OD_{600nm} ~2.5) and diluted 1:10 in fresh medium. After 6 h incubation (28°C, 220rpm, OD_{600nm} 1-2), bacteria were harvested (5000g, 15min, RT) and resuspended to OD_{600nm} 0.4 in infiltration buffer. Agrobacteria solutions of corresponding BiFC candidates were mixed 1:1 and directly used for leaf infiltrations. BiFC signals were visualized at 3 dpi, which corresponds to the highest expression from the vectors used (Grefen et al., 2010), by CLSM on a Zeiss LSM 510 Meta for at least three epidermal cells on two different leaves.

4.8.2.2 Particle bombardment of Arabidopsis

Ballistic transformation of single Arabidopsis epidermal cells was performed similar to previously described (Schweizer et al., 1999; Shirasu et al., 1999). Briefly, gold particles of 1 µm diameter (Bio-Rad) were coated with 1 µg OEC-Citrine and mCherry plasmids and biolisticly delivered into detached leaves of 4 week old Arabidopsis plants using a particle gun equipped with a Hepta adapter (Biolistic PDS-1000/He, Bio-Rad). At 2 dpi, fluorescence was visualized by CLSM on a Zeiss LSM 510 Meta for at least three epidermal cells on two different leaves.

4.2.9 Yeast-two-hybrid

A detailed protocol of the Y2H pipeline used is presented in (Dreze et al., 2010). I will summarize the protocol below.

The 84 cloned OECs were transferred into pDest-AD and pDest-DB vectors by recombination. Successful recombination was confirmed by PCR analysis. Isolated destination clones were transferred into *S. cerevisiae* Y8930 (for DB clones; MATα) and *S. cerevisiae* Y8890 (for AD clones; MATa) by Lithium-Acetate based transformation. Transgenic clones were selected on selective medium and stored in 20% glycerol at -80°C before use. For autoactivator removal, DB- and AD-OEC clones were mated with yeast clones containing an empty bait or prey vector on YPED medium. After o/n incubation, colonies were transferred to selective media for diploid yeast (Sc–Leu–Trp) and incubated o/n. Then, diploid colonies were transferred to interaction media (Sc–Leu–Trp–His + 3-Amino-1,2,4-triazole (3-AT)), incubated o/n and replica-cleaned (excess yeasts were removed by pushing plates onto a fine velvet on a replica plating block). Three days later, growth phenotypes were scored and autoactivators removed from the OEC libraries. The AD-OEC yeast clones were pooled by separately growing o/n and unification into one solution. Equal representation of clones in pools was confirmed by plating and colony PCR on 30 colonies. The Arabidopsis library used is described in (Arabidopsis Interactome Mapping Consortium, 2011; Mukhtar et al., 2011). For the screen, single DB-OEC clones were mated with pools of 192 AD-At clones, while single DB-At clones were screened against the AD-OEC pool. The screen was repeated once. Five µl of freshly grown DB- and AD- yeast were spotted on top of each other on YPED medium using a robotic fluid handling device. Plates were incubated o/n, colonies replated onto interaction medium as well as autoactivator test plates, incubated o/n and replica-cleaned. After five days incubation, single colonies were isolated and rearrayed into 96-well plates. These primary positive interactors were reevaluated in a secondary screen. They were plated onto diploid-selection medium, incubated two days, and transferred to interaction medium plates (Sc–Leu–Trp–His+3-AT). Three autoactivator plates (Sc-Leu-His + 1 mM 3-AT + CHX (1 mg/l) were also included. Plates were replica-cleaned and incubated three days. Positive clones were restreaked to diploid selection medium, incubated two days and lysed. PCR was used to obtain sequence information on corresponding AD- and DB-clones per colony. The interactors were identified by BLAST searches, single clones of these interactors retrieved from the stock

and rearrayed for the retest screen. Matings of single clones were performed as described above, but phenotypes were scored on both Sc–Leu–Trp–His +3-AT and Sc–Leu–Trp–Ade plates. Interactions were scored as confirmed when they were positive in three of four repeated matings and autoactivation was never detected. For all matings performed, a set of six control interactors was used to confirm expected phenotypes.

4.2.9.1 Statistical analysis of Y2H results

First, the probability of the observed number of OEC targets occurring by chance was calculated. To estimate the probability of a specific number of targets dependent on a subset of interactions (i.e. interactions between a specific effector and an Arabidopsis protein being represented in AI-1) between pathogen effectors and Arabidopsis targets, a Monte-Carlo-Simulation was conducted. The number of interactions with targets being represented in AI-Main was counted, then that number of targets was selected at random from a list of AI-1 with replacement. In this list, a protein occurs as often as it shows interactions in AI-1, dependent on its degree. Subsequently, for each sample the total number of different targets was calculated and summarized in a Monte-Carlo-Ranking. For visualization, the frequency of a certain number was counted and the p-value for the observed total number of targets was calculated based on the ranking.

Secondly, the probability of the observed number of shared targets between all three pathogens occurring by chance was calculated. To estimate the probability of a specific number of shared targets in intersections between different pathogens, a Monte-Carlo-Simulation was conducted. First, random samples of targets were created for each pathogen according to the observed total number of targets. Then, random samples were chosen and the intersection of targets, based on all proteins in AI-1, was calculated. This was done 1000 times. Subsequently, the total number of targets being shared was summarized in a Monte-Carlo-Ranking for calculating the p-value of the observed shared targets.

All network representations were drawn using Cytoscape (Shannon et al., 2003). Statistical analysis of network properties was performed by Christine Gläßer, Helmholtz Center Munich, Germany using R (Team, 2008).

5 References

Aarts, N., et al., 1998. Different requirements for EDS1 and NDR1 by disease resistance genes define at least two R gene-mediated signaling pathways in Arabidopsis. Proc. Natl. Acad. Sci. USA. 95, 10306-10311.

Abramoff, M. D., et al., 2004. Image processing with ImageJ. Biophotonics Int. 11, 36-42.

Adam, L., et al., 1999. Comparison of *Erysiphe cichoracearum* and *E. cruciferarum* and a survey of 360 *Arabidopsis thaliana* accessions for resistance to these two powdery mildew pathogens. Mol. Plant-Microbe Interact. 12, 1031-1043.

Ahn, N., et al., 2004. Extracellular matrix protein gene, EMP1, is required for appressorium formation and pathogenicity of the rice blast fungus, *Magnaporthe grisea*. Mol. Cells. 17, 166-173.

Albert, R., et al., 2000. Error and attack tolerance of complex networks. Nature. 406, 378-382.

Albrecht, C., et al., 2012. Brassinosteroids inhibit pathogen-associated molecular pattern–triggered immune signaling independent of the receptor kinase BAK1. Proc. Natl. Acad. Sci. USA. 109, 303-308.

Albrecht, C., et al., 2008. Arabidopsis SOMATIC EMBRYOGENESIS RECEPTOR KINASE proteins serve Brassinosteroid-dependent and -independent signaling pathways. Plant Physiol. 148, 611-619.

Altschul, S. F., et al., 1990. Basic local alignment search tool. J. Mol. Biol. 215, 403-410.

Alvim Kamei, C. L., et al., 2008. The PRA1 gene family in Arabidopsis. Plant Physiol. 147, 1735-1749.

An, Q., et al., 2006. Multivesicular bodies participate in a cell wall-associated defence response in barley leaves attacked by the pathogenic powdery mildew fungus. Cell. Microbiol. 8, 1009-1019.

Anderson, J. P., et al., 2004. Antagonistic interaction between Abscisic Acid and Jasmonate-Ethylene signaling pathways modulates defense gene expression and disease resistance in Arabidopsis. The Plant Cell Online. 16, 3460-3479.

Antony, G., et al., 2010. Rice xa13 recessive resistance to bacterial blight Is defeated by induction of the disease susceptibility gene Os-11N3. The Plant Cell Online. 22, 3864-3876.

Arabidopsis Interactome Mapping Consortium, 2011. Evidence for network evolution in an Arabidopsis interactome map. Science. 333, 601-607.

Armstrong, M. R., et al., 2005. An ancestral oomycete locus contains late blight avirulence gene Avr3a, encoding a protein that is recognized in the host cytoplasm. Proc. Natl. Acad. Sci. USA. 102, 7766-7771.

Ausubel, F. M., 2005. Are innate immune signaling pathways in plants and animals conserved? Nat Immunol. 6, 973-979.

Baba, K., et al., 2001. Involvement of a nuclear-encoded basic helix-loop-helix protein in transcription of the light-responsive promoter of psbD. Plant Physiol. 125, 595-603.

Bainard, L. D., et al., 2011. Mycorrhizal symbiosis stimulates endoreduplication in angiosperms. Plant, Cell Environ. 34, 1577-1585.

Bartetzko, V., et al., 2009. The *Xanthomonas campestris* pv. *vesicatoria* type III effector protein XopJ inhibits protein secretion: Evidence for interference with cell wall–associated defense responses. Mol. Plant-Microbe Interact. 22, 655-664.

Bartsch, M., et al., 2006. Salicylic acid independent ENHANCED DISEASE SUSCEPTIBILITY1 signaling in Arabidopsis immunity and cell death is regulated by the monooxygenase FMO1 and the nudix hydrolase NUDT7. Plant Cell. 18, 1038-1051.

Baum, T., et al., 2011. HyphArea—Automated analysis of spatiotemporal fungal patterns. J. Plant Physiol. 168, 72-78.

Bednarek, P., et al., 2009. A Glucosinolate metabolism pathway in living plant cells mediates broad-spectrum antifungal defense. Science. 323, 101-106.

Belkhadir, Y., et al., 2012. Brassinosteroids modulate the efficiency of plant immune responses to microbe-associated molecular patterns. Proc. Natl. Acad. Sci. USA. 109, 297-302.

Bendahmane, A., et al., 1999. The Rx Gene from Potato Controls Separate Virus Resistance and Cell Death Responses. The Plant Cell Online. 11, 781-791.

Bendtsen, J. D., et al., 2004. Improved Prediction of Signal Peptides: SignalP 3.0. J. Mol. Biol. 340, 783-795.

Berger, S., et al., 2007. Plant physiology meets phytopathology: plant primary metabolism and plant–pathogen interactions. J. Exp. Bot. 58, 4019-4026.

Berr, A., et al., 2012. Chromatin modification and remodelling: a regulatory landscape for the control of Arabidopsis defence responses upon pathogen attack. Cell. Microbiol. 14, 829-839.

Bindschedler, L., et al., 2009. In planta proteomics and proteogenomics of the biotrophic barley fungal pathogen *Blumeria graminis* f. sp. *hordei*. Mol. Cell. Proteomics. 8, 2368.

Bindschedler, L. V., et al., 2011. Proteogenomics and in silico structural and functional annotation of the barley powdery mildew *Blumeria graminis* f. sp. *hordei*. Methods. 54, 432-441.

Boch, J., et al., 2009. Breaking the code of DNA binding specificity of TAL-type III effectors. Science. 326, 1509-1512.

Böhlenius, H., et al., 2010. The Multivesicular Body-Localized GTPase ARFA1b/1c Is Important for Callose Deposition and ROR2 Syntaxin-Dependent Preinvasive Basal Defense in Barley. The Plant Cell Online. 22, 3831-3844.

Boller, T., Felix, G., 2009. A Renaissance of Elicitors: Perception of Microbe-Associated Molecular Patterns and Danger Signals by Pattern-Recognition Receptors. Annu. Rev. Plant Biol. 60, 379-406.

Bolton, M. D., 2009. Primary Metabolism and Plant Defense—Fuel for the Fire. Mol. Plant-Microbe Interact. 22, 487-497.

Bolton, M. D., et al., 2008. The novel Cladosporium fulvum lysin motif effector Ecp6 is a virulence factor with orthologues in other fungal species. Mol. Microbiol. 69, 119-136.

Bos, J. I. B., et al., 2010. *Phytophthora infestans* effector AVR3a is essential for virulence and manipulates plant immunity by stabilizing host E3 ligase CMPG1. Proc. Natl. Acad. Sci. USA.

Bos, J. I. B., et al., 2006. The C-terminal half of *Phytophthora infestans* RXLR effector AVR3a is sufficient to trigger R3a-mediated hypersensitivity and suppress INF1-induced cell death in *Nicotiana benthamiana*. The Plant Journal. 48, 165-176.

Both, M., et al., 2005a. Gene expression profiles of *Blumeria graminis* indicate dynamic changes to primary metabolism during development of an obligate biotrophic pathogen. Plant Cell. 17, 2107-2122.

Both, M., et al., 2005b. Transcript profiles of *Blumeria graminis* development during infection reveal a cluster of genes that are potential virulence determinants. Mol. Plant-Microbe Interact. 18, 125-133.

Boudolf, V., et al., 2004. The plant-specific Cyclin-dependent kinase CDKB1;1 and transcription factor E2Fa-DPa control the balance of mitotically dividing and endoreduplicating cells in Arabidopsis. The Plant Cell Online. 16, 2683-2692.

Bozkurt, T. O., et al., 2012. Oomycetes, effectors, and all that jazz. Curr. Opin. Plant Biol. 15, 483-492.

Bozkurt, T. O., et al., 2011. *Phytophthora infestans* effector AVRblb2 prevents secretion of a plant immune protease at the haustorial interface. Proc. Natl. Acad. Sci. USA. 108, 20832-20837.

Brameier, M., et al., 2007. NucPred—Predicting nuclear localization of proteins. Bioinformatics. 23, 1159-1160.

Brandt, S., et al., 2002. Using array hybridization to monitor gene expression at the single cell level. J. Exp. Bot. 53, 2315-2323.

Braun, P., et al., 2009. An experimentally derived confidence score for binary protein-protein interactions. Nat Meth. 6, 91-97.

Breuer, C., et al., 2010. Developmental control of endocycles and cell growth in plants. Curr. Opin. Plant Biol. 13, 654-660.

Brooks, D. M., et al., 2005. The *Pseudomonas syringae* phytotoxin coronatine promotes virulence by overcoming salicylic acid-dependent defences in *Arabidopsis thaliana*. Mol. Plant Pathol. 6, 629-639.

Brouwer, M., et al., 2003. Quantification of disease progression of several microbial pathogens on *Arabidopsis thaliana* using real-time fluorescence PCR. FEMS Microbiol. Lett. 228, 241-248.

Brutus, A., et al., 2010. A domain swap approach reveals a role of the plant wall-associated kinase 1 (WAK1) as a receptor of oligogalacturonides. Proc. Natl. Acad. Sci. USA.

Büschges, R., et al., 1997. The barley Mlo gene: A novel control element of plant pathogen resistance. Cell. 88, 695-705.

Bushnell, W. R., 1972. Physiology of fungal haustoria. Annu. Rev. Phytopathol. 10, 151-176.

Cabral, A., et al., 2012. Nontoxic Nep1-like proteins of the downy mildew pathogen *Hyaloperonospora arabidopsidis*: Repression of necrosis-inducing sctivity by a surface-exposed region. Mol. Plant-Microbe Interact. 25, 697-708.

Caillaud, M.-C., et al., 2012. Subcellular localization of the *Hpa* RxLR effector repertoire identifies a tonoplast-associated protein HaRxL17 that confers enhanced plant susceptibility. The Plant Journal. 69, 252-265.

Calderwood, M. A., et al., 2007. Epstein–Barr virus and virus human protein interaction maps. Proc. Natl. Acad. Sci. USA. 104, 7606-7611.

Cao, H., et al., 1994. Characterization of an Arabidopsis mutant that is nonresponsive to inducers of systemic acquired resistance. The Plant Cell Online. 6, 1583-1592.

Caracuel, Z., et al., 2005. *Fusarium oxysporum gas1* encodes aputative β-1, 3-glucanosyltransferase required for virulence on tomato plants. Mol. Plant-Microbe Interact. 18, 1140-1147.

Catanzariti, A.-M., et al., 2006. Haustorially expressed secreted proteins from flax rust are highly enriched for avirulence elicitors. Plant Cell. 18, 243-256.

Cebolla, A., et al., 1999. The mitotic inhibitor ccs52 is required for endoreduplication and ploidy-dependent cell enlargement in plants. EMBO J. 18, 4476-4484.

Chandler, J., et al., 2009. BIM1, a bHLH protein involved in brassinosteroid signalling, controls Arabidopsis embryonic patterning via interaction with DORNRÖSCHEN and DORNRÖSCHEN-LIKE. Plant Mol. Biol. 69, 57-68.

Chandran, D., et al., 2010. Laser microdissection of Arabidopsis cells at the powdery mildew infection site reveals site-specific processes and regulators. Proc. Natl. Acad. Sci. USA. 107, 460-465.

Chandran, D., et al., 2009. Temporal Global Expression Data Reveal Known and Novel Salicylate-Impacted Processes and Regulators Mediating Powdery Mildew Growth and Reproduction on Arabidopsis. Plant Physiol. 149, 1435-1451.

Chaparro-Garcia, A., et al., 2011. The receptor-like kinase SERK3/BAK1 is required for basal resistance against the late blight pathogen *Phytophthora infestans* in *Nicotiana benthamiana*. PLoS ONE. 6, e16608.

Chen, L.-Q., et al., 2010. Sugar transporters for intercellular exchange and nutrition of pathogens. Nature. 468, 527-532.

Cheng, W., et al., 2011. Structural analysis of *Pseudomonas syringae* AvrPtoB bound to host BAK1 reveals two similar kinase-interacting fomains in a type III effector. Cell Host & Microbe. 10, 616-626.

Chinchilla, D., et al., 2007. A flagellin-induced complex of the receptor FLS2 and BAK1 initiates plant defence. Nature. 448, 497-500.

Chini, A., et al., 2007. The JAZ family of repressors is the missing link in jasmonate signalling. Nature. 448, 666-671.

Chisholm, S. T., et al., 2005. Molecular characterization of proteolytic cleavage sites of the Pseudomonas syringae effector AvrRpt2. Proc. Natl. Acad. Sci. USA. 102, 2087-2092.

Clay, N. K., et al., 2009. Glucosinolate metabolites required for an Arabidopsis innate immune response. Science. 323, 95-101.

Clough, S. J., et al., 2000. The Arabidopsis dnd1 “defense, no death” gene encodes a mutated cyclic nucleotide-gated ion channel. Proc. Natl. Acad. Sci. USA. 97, 9323-9328.

Collins, N. C., et al., 2003. SNARE-protein-mediated disease resistance at the plant cell wall. Nature. 425, 973-977.

Conesa, A., et al., 2005. Blast2GO: a universal tool for annotation, visualization and analysis in functional genomics research. Bioinformatics. 21, 3674-3676.

Consonni, C., et al., 2010. Tryptophan-derived metabolites are required for antifungal defense in the Arabidopsis *mlo2* mutant. Plant Physiol. 152, 1544-1561.

Consonni, C., et al., 2006. Conserved requirement for a plant host cell protein in powdery mildew pathogenesis. Nat Genet. 38, 716-720.

Cornelissen, B., Haring, M., 2001. FEM1, a *Fusarium oxysporum* glycoprotein that is covalently linked to the cell wall matrix and is conserved in filamentous fungi. Mol. Genet. Genomics. 265, 143-152.

Cui, H., et al., 2010. *Pseudomonas syringae* effector protein AvrB perturbs Arabidopsis hormone signaling by activating MAP kinase 4. Cell host & microbe. 7, 164-175.

Cui, Y., et al., 2009. Studies on signal pathways of the potato late blight resistance gene R3a, RB using VIGS. Acta Horticulturae Sinica. 36, 997-1004.

Cunnac, S., et al., 2011. Genetic disassembly and combinatorial reassembly identify a minimal functional repertoire of type III effectors in *Pseudomonas syringae*. Proc. Natl. Acad. Sci. USA. 108, 2975-2980.

Cunnac, S., et al., 2009. *Pseudomonas syringae* type III secretion system effectors: repertoires in search of functions. Curr. Opin. Microbiol. 12, 53-60.

Dangl, J. L., Jones, J. D. G., 2001. Plant pathogens and integrated defence responses to infection. Nature. 411, 826-833.

Danisman, S., et al., 2012. Arabidopsis class I and class II TCP transcription factors regulate Jasmonic Acid metabolism and leaf development antagonistically. Plant Physiol. 159, 1511-1523.

Day, B., et al., 2005. Molecular basis for the RIN4 negative regulation of RPS2 disease resistance. The Plant Cell Online. 17, 1292-1305.

de Jonge, R., et al., 2011. How filamentous pathogens co-opt plants: the ins and outs of fungal effectors. Curr. Opin. Plant Biol. 14, 400-406.

de Jonge, R., et al., 2010. Conserved fungal LysM effector Ecp6 prevents chitin-triggered immunity in plants. Science. 329, 953-955.

De Veylder, L., et al., 2011. Molecular control and function of endoreplication in development and physiology. Trends Plant Sci. 16, 624-634.

DebRoy, S., et al., 2004. A family of conserved bacterial effectors inhibits salicylic acid-mediated basal immunity and promotes disease necrosis in plants. Proc. Natl. Acad. Sci. USA. 101, 9927-9932.

del Pozo, J. C., et al., 2006. The Balance between cell division and endoreplication depends on E2FC-DPB, transcription factors regulated by the Ubiquitin-SCFSKP2A pathway in Arabidopsis. The Plant Cell Online. 18, 2224-2235.

Deslandes, L., et al., 2003. Physical interaction between RRS1-R, a protein conferring resistance to bacterial wilt, and PopP2, a type III effector targeted to the plant nucleus. Proc. Natl. Acad. Sci. USA. 100, 8024-8029.

Dewdney, J., et al., 2000. Three unique mutants of *Arabidopsis* identify *eds* loci required for limiting growth of a biotrophic fungal pathogen. Plant J. 24, 205-218.

Dirac-Svejstrup, A. B., et al., 1997. Identification of a GDI displacement factor that releases endosomal Rab GTPases from Rab-GDI. EMBO J. 16, 465-472.

Dixon, M. S., et al., 2000. Genetic complexity of pathogen perception by plants: The example of Rcr3, a tomato gene required specifically by Cf-2. Proc. Natl. Acad. Sci. USA. 97, 8807-8814.

Djamei, A., et al., 2011. Metabolic priming by a secreted fungal effector. Nature. 478, 395-398.

Doares, S. H., et al., 1995. Oligogalacturonides and chitosan activate plant defensive genes through the octadecanoid pathway. Proc. Natl. Acad. Sci. USA. 92, 4095-4098.

Doehlemann, G., et al., 2009. Pep1, a secreted effector protein of *Ustilago maydis*, is required for successful invasion of plant cells. PLoS Pathog. 5, e1000290.

Dou, D., et al., 2008. Conserved C-terminal motifs required for avirulence and suppression of cell death by *Phytophthora sojae* effector Avr1b. Plant Cell. 20, 1118-1133.

Dreze, M., et al., 2009. 'Edgetic' perturbation of a C. elegans BCL2 ortholog. Nat Meth. 6, 843-849.

Dreze, M., et al., Chapter 12 - High-quality binary interactome mapping. In: W. Jonathan, et al., Eds.), Methods Enzymol. Academic Press, 2010, pp. 281-315.

Duplessis, S., et al., 2011a. Obligate biotrophy features unraveled by the genomic analysis of rust fungi. Proc. Natl. Acad. Sci. USA.

Duplessis, S., et al., 2011b. *Melampsora larici-populina* transcript profiling during germination and timecourse infection of poplar leaves reveals dynamic expression patterns associated with virulence and biotrophy. Mol. Plant-Microbe Interact. 24, 808-818.

Durrant, W. E., Dong, X., 2004. Systemic Acquired Resistance. Annu. Rev. Phytopathol. 42, 185-209.

Dyer, M. D., et al., 2008. The landscape of human proteins interacting with viruses and other pathogens. PLoS Pathog. 4, e32.

Dyer, M. D., et al., 2010. The human-bacterial pathogen protein interaction networks of *Bacillus anthracis*, *Francisella tularensis*, and *Yersinia pestis*. PLoS ONE. 5, e12089.

Efroni, I., et al., 2008. A protracted and dynamic maturation schedule underlies Arabidopsis leaf development. The Plant Cell Online. 20, 2293-2306.

Ellis, J., et al., 2009. Recent progress in discovery and functional analysis of effector proteins of fungal and oomycete plant pathogens. Curr Opin Plant Biol. 12, 399 - 405.

Ellis, J. G., et al., 2007. Flax rust resistance gene specificity is based on direct resistance-avirulence protein interactions. Annu. Rev. Phytopathol. 45, 289-306.

Fabro, G., et al., 2011. Multiple candidate effectors from the oomycete pathogen *Hyaloperonospora arabidopsidis* suppress host plant immunity. PLoS Pathog. 7, e1002348.

Falk, A., et al., 1999. EDS1, an essential component of R gene-mediated disease resistance in Arabidopsis has homology to eukaryotic lipases. Proc. Natl. Acad. Sci. USA. 96, 3292-3297.

Feng, F., et al., 2012. A Xanthomonas uridine 5'-monophosphate transferase inhibits plant immune kinases. Nature. 485, 114-118.

Feng, F., Zhou, J.-M., 2012. Plant–bacterial pathogen interactions mediated by type III effectors. Curr. Opin. Plant Biol. 15, 469-476.

Fernandez, D., et al., 2012. 454-pyrosequencing of *Coffea arabica* leaves infected by the rust fungus *Hemileia vastatrix* reveals in planta-expressed pathogen-secreted proteins and plant functions in a late compatible plant–rust interaction. Mol. Plant Pathol. 13, 17-37.

Feys, B. J., et al., 2001. Direct interaction between the Arabidopsis disease resistance signaling proteins, EDS1 and PAD4. EMBO J. 20, 5400-5411.

Feys, B. J., et al., 2005. Arabidopsis SENESCENCE-ASSOCIATED GENE101 stabilizes and signals within an ENHANCED DISEASE SUSCEPTIBILITY1 complex in plant innate immunity. Plant Cell. 17, 2601-2613.

Flor, H. H., 1971. Current status of the gene-for-gene concept. Annu. Rev. Phytopathol. 9, 275-296.

Frye, C. A., Innes, R. W., 1998. An Arabidopsis mutant with enhanced resistance to powdery mildew. The Plant Cell Online. 10, 947-956.

Fu, Z. Q., et al., 2007. A type III effector ADP-ribosylates RNA-binding proteins and quells plant immunity. Nature. 447, 284-288.

Fu, Z. Q., et al., 2012. NPR3 and NPR4 are receptors for the immune signal salicylic acid in plants. Nature. 486, 228-232.

Gachon, C., Saindrenan, P., 2004. Real-time PCR monitoring of fungal development in *Arabidopsis thaliana* infected by *Alternaria brassicicola* and *Botrytis cinerea*. Plant Physiol. Biochem. 42, 367-371.

Gaffney, T., et al., 1993. Requirement of salicylic acid for the induction of systemic acquired resistance. Science. 261, 754-756.

Gao, J., et al., 2012. NAP1 family histone chaperones are required for somatic homologous recombination in Arabidopsis. The Plant Cell Online. 24, 1437-1447.

Gheysen, G., Mitchum, M. G., 2011. How nematodes manipulate plant development pathways for infection. Curr. Opin. Plant Biol. 14, 415-421.

Gil, F., Gay, J. L., 1977. Ultrastructural and physiological properties of the host interfacial components of haustoria of *Erysiphe pisi* in vivo and in vitro. Physiol. Plant Pathology. 10, 1-4, IN1-IN8, 5-12.

Gilroy, E. M., et al., 2011. CMPG1-dependent cell death follows perception of diverse pathogen elicitors at the host plasma membrane and is suppressed by *Phytophthora infestans* RXLR effector AVR3a. New Phytol. 190, 653-666.

Gimenez-Ibanez, S., et al., 2009. AvrPtoB targets the LysM receptor kinase CERK1 to promote bacterial virulence on plants. Curr. Biol. 19, 423-429.

Giot, L., et al., 2003. A protein interaction map of *Drosophila melanogaster*. Science. 302, 1727-1736.

Glawe, D. A., 2008. The powdery mildews: A review of the world's most familiar (yet poorly known) plant pathogens. Annu. Rev. Phytopathol. 46, 27-51.

Glazebrook, J., 2005. Contrasting mechanisms of defense against biotrophic and necrotrophic pathogens. Annu. Rev. Phytopathol. 43, 205-227.

Godfrey, D., et al., 2010. Powdery mildew fungal effector candidates share N-terminal Y/F/WxC-motif. BMC Genomics. 11, 317.

Godfrey, D., et al., 2009. A proteomics study of barley powdery mildew haustoria. Proteomics. 9, 3222 - 3232.

Göhre, V., et al., 2008. Plant pattern-recognition receptor FLS2 is directed for degradation by the bacterial ubiquitin ligase AvrPtoB. 18, 1824-1832.

Göllner, K., et al., 2008. Natural genetic resources of *Arabidopsis thaliana* reveal a high prevalence and unexpected phenotypic plasticity of *RPW8*-mediated powdery mildew resistance. New Phytol. 177, 725-742.

Gómez-Gómez, L., Boller, T., 2000. FLS2: An LRR receptor–like kinase involved in the perception of the bacterial elicitor flagellin in Arabidopsis. Mol. Cell. 5, 1003-1011.

Gómez-Gómez, L., et al., 1999. A single locus determines sensitivity to bacterial flagellin in Arabidopsis thaliana. The Plant Journal. 18, 277-284.

González-Lamothe, R., et al., 2006. The U-Box Protein CMPG1 Is Required for Efficient Activation of Defense Mechanisms Triggered by Multiple Resistance Genes in Tobacco and Tomato. The Plant Cell Online. 18, 1067-1083.

Goritschnig, S., et al., 2012. Computational Prediction and Molecular Characterization of an Oomycete Effector and the Cognate Arabidopsis Resistance Gene. PLoS Genet. 8.

Grefen, C., et al., 2010. A ubiquitin-10 promoter-based vector set for fluorescent protein tagging facilitates temporal stability and native protein distribution in transient and stable expression studies. The Plant Journal. 64, 355-365.

Grell, M. N., et al., 2003. A *Blumeria graminis* gene family encoding proteins with a C-terminal variable region with homologues in pathogenic fungi. Gene. 311, 181-192.

Griesbeck, O., et al., 2001. Reducing the Environmental Sensitivity of Yellow Fluorescent Protein. J. Biol. Chem. 276, 29188-29194.

Gu, K., et al., 2005. R gene expression induced by a type-III effector triggers disease resistance in rice. Nature. 435, 1122-1125.

Guo, H., Ecker, J. R., 2003. Plant Responses to Ethylene Gas Are Mediated by SCFEBF1/EBF2-Dependent Proteolysis of EIN3 Transcription Factor. Cell. 115, 667-677.

Gusmaroli, G., et al., 2007. Role of the MPN Subunits in COP9 Signalosome Assembly and Activity, and Their Regulatory Interaction with Arabidopsis Cullin3-Based E3 Ligases. The Plant Cell Online. 19, 564-581.

Haas, B., et al., 2009. Genome sequence and analysis of the Irish potato famine pathogen Phytophthora infestans. Nature. 461, 393 - 398.

Haga, N., et al., 2007. R1R2R3-Myb proteins positively regulate cytokinesis through activation of KNOLLE transcription in Arabidopsis thaliana. Development. 134, 1101-1110.

Hahn, M., Mendgen, K., 1997. Characterization of in planta—induced rust genes isolated from a haustorium-specific cDNA library. Mol. Plant-Microbe Interact. 10, 427-437.

Hammani, K., et al., 2011. An Arabidopsis Dual-Localized Pentatricopeptide Repeat Protein Interacts with Nuclear Proteins Involved in Gene Expression Regulation. The Plant Cell Online. 23, 730-740.

Hann, D. R., Rathjen, J. P., 2007. Early events in the pathogenicity of Pseudomonas syringae on Nicotiana benthamiana. The Plant Journal. 49, 607-618.

Hauck, P., et al., 2003. A Pseudomonas syringae type III effector suppresses cell wall-based extracellular defense in susceptible Arabidopsis plants. Proc. Natl. Acad. Sci. USA. 100, 8577-8582.

Heidrich, K., et al., 2011. Arabidopsis EDS1 Connects Pathogen Effector Recognition to Cell Compartment–Specific Immune Responses. Science. 334, 1401-1404.

Hemetsberger, C., et al., 2012. The *Ustilago maydis* effector Pep1 suppresses plant immunity by inhibition of host peroxidase activity. PLoS Pathog. 8, e1002684.

Herbers, K., et al., 1996. Salicylic acid-independent induction of pathogenesis-related protein transcripts by sugars is dependent on leaf developmental stage. FEBS Lett. 397, 239-244.

Hervé, C., et al., 2009. In Vivo Interference with AtTCP20 Function Induces Severe Plant Growth Alterations and Deregulates the Expression of Many Genes Important for Development. Plant Physiol. 149, 1462-1477.

Hind, S. R., et al., 2011. The COP9 signalosome controls jasmonic acid synthesis and plant responses to herbivory and pathogens. The Plant Journal. 65, 480-491.

Hippe, S., 1985. Ultrastructure of haustoria of *Erysiphe graminis* f. sp. *hordei* preserved by freeze-substitution. Protoplasma. 129, 52-61.

Hiruma, K., et al., 2010. Entry Mode–Dependent Function of an Indole Glucosinolate Pathway in Arabidopsis for Nonhost Resistance against Anthracnose Pathogens. The Plant Cell Online. 22, 2429-2443.

Hogenhout, S. A., et al., 2009. Emerging Concepts in Effector Biology of Plant-Associated Organisms. Mol. Plant-Microbe Interact. 22, 115-122.

Hotton, S. K., Callis, J., 2008. Regulation of Cullin RING Ligases. Annu. Rev. Plant Biol. 59, 467-489.

Houterman, P. M., et al., 2008. Suppression of Plant Resistance Gene-Based Immunity by a Fungal Effector. PLoS Pathog. 4, e1000061.

Hua, Z., et al., 2011. Phylogenetic Comparison of F-Box Gene Superfamily within the Plant Kingdom Reveals Divergent Evolutionary Histories Indicative of Genomic Drift. PLoS ONE. 6, e16219.

Huang, S., et al., 2005. Comparative genomics enabled the isolation of the R3a late blight resistance gene in potato. The Plant Journal. 42, 251-261.

Hückelhoven, R., Kogel, K.-H., 2003. Reactive oxygen intermediates in plant-microbe interactions: Who is who in powdery mildew resistance? Planta. 216, 891-902.

Hückelhoven, R., Panstruga, R., 2011. Cell biology of the plant–powdery mildew interaction. Curr. Opin. Plant Biol. 14, 738-746.

Huffaker, A., et al., 2006. An endogenous peptide signal in Arabidopsis activates components of the innate immune response. Proc. Natl. Acad. Sci. USA. 103, 10098-10103.

Humphry, M., et al., 2010. A regulon conserved in monocot and dicot plants defines a functional module in antifungal plant immunity. Proc. Natl. Acad. Sci. USA. 107, 21896-21901.

Hwang, C. S., et al., 1995. Cloning of a gene expressed during appressorium formation by *Colletotrichum gloeosporioides* and a marked decrease in virulence by disruption of this gene. Plant Cell. 7, 183-193.

Ingmundson, A., et al., 2007. Legionella pneumophila proteins that regulate Rab1 membrane cycling. Nature. 450, 365-369.

Ito, M., et al., 2001a. G2/M-Phase–Specific Transcription during the Plant Cell Cycle Is Mediated by c-Myb–Like Transcription Factors. The Plant Cell Online. 13, 1891-1905.

Ito, T., et al., 2001b. A comprehensive two-hybrid analysis to explore the yeast protein interactome. Proc. Natl. Acad. Sci. USA. 98, 4569-4574.

Jacobs, A. K., et al., 2003. An Arabidopsis Callose Synthase, GSL5, Is Required for Wound and Papillary Callose Formation. The Plant Cell Online. 15, 2503-2513.

Jakupovic, M., et al., 2006. Microarray analysis of expressed sequence tags from haustoria of the rust fungus *Uromyces fabae*. Fungal Genet. Biol. 43, 8-19.

Jelenska, J., et al., 2007. A J Domain Virulence Effector of Pseudomonas syringae Remodels Host Chloroplasts and Suppresses Defenses. Curr. Biol. 17, 499-508.

Jin, Q., He, S.-Y., 2001. Role of the Hrp Pilus in Type III Protein Secretion in Pseudomonas syringae. Science. 294, 2556-2558.

Joergensen, J. H., 1994. Genetics of Powdery Mildew Resistance in Barley. Crit. Rev. Plant Sci. 13, 97 - 97.

Jones, J. D. G., Dangl, J. L., 2006. The plant immune system. Nature. 444, 323-329.

Kamoun, S., et al., 1997. A Gene Encoding a Protein Elicitor of Phytophthora infestans Is Down-Regulated During Infection of Potato. Mol. Plant-Microbe Interact. 10, 13-20.

Kanneganti, T.-D., et al., 2006. Synergistic Interactions of the Plant Cell Death Pathways Induced by *Phytophthora infestans* Nep1-Like Protein PiNPP1.1 and INF1 Elicitin. Mol. Plant-Microbe Interact. 19, 854-863.

Katagiri, F., et al., 2002. The *Arabidopsis thaliana* - *Pseudomonas syringae* interaction. The Arabidopsis Book. e0039.

Kay, S., et al., 2007. A Bacterial Effector Acts as a Plant Transcription Factor and Induces a Cell Size Regulator. Science. 318, 648-651.

Kelley, B. S., et al., 2010. A secreted effector protein (SNE1) from *Phytophthora infestans* is a broadly acting suppressor of programmed cell death. The Plant Journal. 62, 357-366.

Kemen, E., Jones, J. D. G., 2012. Obligate biotroph parasitism: can we link genomes to lifestyles? Trends Plant Sci. 17, 448-457.

Kemen, E., et al., 2005. Identification of a protein from rust fungi transferred from haustoria into infected plant cells. Mol. Plant-Microbe Interact. 18, 1130-1139.

Khang, C. H., et al., 2010. Translocation of Magnaporthe oryzae Effectors into Rice Cells and Their Subsequent Cell-to-Cell Movement. Plant Cell. 22, 1388-1403.

Kieffer, M., et al., 2011. TCP14 and TCP15 affect internode length and leaf shape in Arabidopsis. The Plant Journal. 68, 147-158.

Kim, H.-S., et al., 2005a. The *Pseudomonas syringae* effector AvrRpt2 cleaves its C-terminally acylated target, RIN4, from Arabidopsis membranes to block RPM1 activation. Proc. Natl. Acad. Sci. USA. 102, 6496-6501.

Kim, M. G., et al., 2005b. Two *Pseudomonas syringae* Type III Effectors Inhibit RIN4-Regulated Basal Defense in Arabidopsis. Cell. 121, 749-759.

Kleemann, J., et al., 2012. Sequential Delivery of Host-Induced Virulence Effectors by Appressoria and Intracellular Hyphae of the Phytopathogen *Colletotrichum higginsianum*. PLoS Pathog. 8, e1002643.

Koch, E., Slusarenko, A., 1990. Arabidopsis is susceptible to infection by a downy mildew fungus. The Plant Cell Online. 2, 437-45.

Koh, S., et al., 2005. Arabidopsis thaliana subcellular responses to compatible *Erysiphe cichoracearum* infections. The Plant Journal. 44, 516-529.

Kosugi, S., Ohashi, Y., 2002. DNA binding and dimerization specificity and potential targets for the TCP protein family. The Plant Journal. 30, 337-348.

Koyama, T., et al., 2007. TCP Transcription Factors Control the Morphology of Shoot Lateral Organs via Negative Regulation of the Expression of Boundary-Specific Genes in Arabidopsis. The Plant Cell Online. 19, 473-484.

Kramer, K. M., et al., 1998. Budding yeast RSI1/APC2, a novel gene necessary for initiation of anaphase, encodes an APC subunit. EMBO J. 17, 498-506.

Krol, E., et al., 2010. Perception of the Arabidopsis Danger Signal Peptide 1 Involves the Pattern Recognition Receptor AtPEPR1 and Its Close Homologue AtPEPR2. J. Biol. Chem. 285, 13471-13479.

Kunze, G., et al., 2004. The N Terminus of Bacterial Elongation Factor Tu Elicits Innate Immunity in Arabidopsis Plants. The Plant Cell Online. 16, 3496-3507.

Kwon, C., et al., 2008. Co-option of a default secretory pathway for plant immune responses. Nature. 451, 835-840.

Lacombe, S., et al., 2010. Interfamily transfer of a plant pattern-recognition receptor confers broad-spectrum bacterial resistance. Nat Biotech. 28, 365-369.

Laemmli, U. K., 1970. Cleavage of Structural Proteins during the Assembly of the Head of Bacteriophage T4. Nature. 227, 680-685.

Lee, M. H., et al., 2011. An Arabidopsis Prenylated Rab Acceptor 1 Isoform, AtPRA1.B6, Displays Differential Inhibitory Effects on Anterograde Trafficking of Proteins at the Endoplasmic Reticulum. Plant Physiol. 157, 645-658.

Lee, S.-W., et al., 2009. A Type I–Secreted, Sulfated Peptide Triggers XA21-Mediated Innate Immunity. Science. 326, 850-853.

Leon-Reyes, A., et al., 2009. Ethylene Modulates the Role of NONEXPRESSOR OF PATHOGENESIS-RELATED GENES1 in Cross Talk between Salicylate and Jasmonate Signaling. Plant Physiol. 149, 1797-1809.

Li, C., et al., 2005. Arabidopsis TCP20 links regulation of growth and cell division control pathways. Proc. Natl. Acad. Sci. USA. 102, 12978-12983.

Li, S., et al., 2004. A Map of the Interactome Network of the Metazoan *C. elegans*. Science. 303, 540-543.

Li, Z.-Y., et al., 2012. The Arabidopsis Transcription Factor AtTCP15 Regulates Endoreduplication by Modulating Expression of Key Cell-cycle Genes. Molecular Plant. 5, 270-280.

Link, T., et al., 2005. Characterization of a novel NADP(+)-dependent D-arabitol dehydrogenase from the plant pathogen *Uromyces fabae*. Biochem. J. 389, 289-295.

Lipka, V., et al., 2005. Pre- and Postinvasion Defenses Both Contribute to Nonhost Resistance in Arabidopsis. Science. 310, 1180-1183.

Liu, Z.-Q., et al., 2009a. A Truncated Arabidopsis NUCLEOSOME ASSEMBLY PROTEIN 1, AtNAP1;3T, Alters Plant Growth Responses to Abscisic Acid and Salt in the *Atnap1;3-2* Mutant. Molecular Plant. 2, 688-699.

Liu, Z., et al., 2009b. Molecular and reverse genetic characterization of NUCLEOSOME ASSEMBLY PROTEIN1 (NAP1) genes unravels their function in transcription and nucleotide excision repair in Arabidopsis thaliana. The Plant Journal. 59, 27-38.

Lorenzo, O., et al., 2004. JASMONATE-INSENSITIVE1 Encodes a MYC Transcription Factor Essential to Discriminate between Different Jasmonate-Regulated Defense Responses in Arabidopsis. The Plant Cell Online. 16, 1938-1950.

Lorenzo, O., et al., 2003. ETHYLENE RESPONSE FACTOR1 Integrates Signals from Ethylene and Jasmonate Pathways in Plant Defense. The Plant Cell Online. 15, 165-178.

Lozano-Durán, R., et al., 2011. Geminiviruses Subvert Ubiquitination by Altering CSN-Mediated Derubylation of SCF E3 Ligase Complexes and Inhibit Jasmonate Signaling in Arabidopsis thaliana. The Plant Cell Online.

Lozano-Torres, J. L., et al., 2012. Dual disease resistance mediated by the immune receptor Cf-2 in tomato requires a common virulence target of a fungus and a nematode. Proc. Natl. Acad. Sci. USA. 109, 10119-10124.

Lu, D., et al., 2010. A receptor-like cytoplasmic kinase, BIK1, associates with a flagellin receptor complex to initiate plant innate immunity. Proc. Natl. Acad. Sci. USA. 107, 496-501.

Lyapina, S., et al., 2001. Promotion of NEDD8-CUL1 Conjugate Cleavage by COP9 Signalosome. Science. 292, 1382-1385.

Ma, L.-J., et al., 2010. Comparative genomics reveals mobile pathogenicity chromosomes in *Fusarium*. Nature. 464, 367-373.

Machner, M. P., Isberg, R. R., 2007. A Bifunctional Bacterial Protein Links GDI Displacement to Rab1 Activation. Science. 318, 974-977.

Macho, A. P., et al., 2010. The *Pseudomonas syringae* effector protein HopZ1a suppresses effector-triggered immunity. New Phytol. 187, 1018-1033.

Mackey, D., et al., 2002. RIN4 Interacts with *Pseudomonas syringae* Type III Effector Molecules and Is Required for RPM1-Mediated Resistance in Arabidopsis. Cell. 108, 743-754.

Mao, G., et al., 2011. Phosphorylation of a WRKY Transcription Factor by Two Pathogen-Responsive MAPKs Drives Phytoalexin Biosynthesis in Arabidopsis. The Plant Cell Online. 23, 1639-1653.

Marois, E., et al., 2002. The *Xanthomonas* Type III Effector Protein AvrBs3 Modulates Plant Gene Expression and Induces Cell Hypertrophy in the Susceptible Host. Mol. Plant-Microbe Interact. 15, 637-646.

Martín-Trillo, M., Cubas, P., 2010. TCP genes: a family snapshot ten years later. Trends Plant Sci. 15, 31-39.

Martincic, I., et al., 1997. Isolation and Characterization of a Dual Prenylated Rab and VAMP2 Receptor. J. Biol. Chem. 272, 26991-26998.

Matsuda, S., Takamatsu, S., 2003. Evolution of host-parasite relationships of Golovinomyces (Ascomycete: Erysiphaceae) inferred from nuclear rDNA sequences. Mol. Phylogen. Evol. 27, 314-327.

Matyskiela, M. E., Morgan, D. O., 2009. Analysis of Activator-Binding Sites on the APC/C Supports a Cooperative Substrate-Binding Mechanism. Mol. Cell. 34, 68-80.

Meyer, D., et al., 2009. Extracellular transport and integration of plant secretory proteins into pathogen-induced cell wall compartments. Plant J. 57, 986-999.

Micali, C., et al., 2008. The powdery mildew disease of Arabidopsis: A paradigm for the interaction between plants and biotrophic fungi. The Arabidopsis Book. 6, 1-19.

Micali, C. O., et al., 2011. Biogenesis of a specialized plant–fungal interface during host cell internalization of *Golovinomyces orontii* haustoria. Cell. Microbiol. 13, 210-226.

Miya, A., et al., 2007. CERK1, a LysM receptor kinase, is essential for chitin elicitor signaling in Arabidopsis. Proc. Natl. Acad. Sci. USA. 104, 19613-19618.

Mo, M., et al., 2012. How viruses affect the cell cycle through manipulation of the APC/C. Trends Microbiol. 20, 440-448.

Morbitzer, R., et al., 2010. Regulation of selected genome loci using de novo-engineered transcription activator-like effector (TALE)-type transcription factors. Proc. Natl. Acad. Sci. USA.

Moscou, M. J., Bogdanove, A. J., 2009. A Simple Cipher Governs DNA Recognition by TAL Effectors. Science. 326, 1501.

Mosquera, G., et al., 2009. Interaction Transcriptome Analysis Identifies *Magnaporthe oryzae* BAS1-4 as Biotrophy-Associated Secreted Proteins in Rice Blast Disease. The Plant Cell Online. 21, 1273-1290.

Mou, Z., et al., 2003. Inducers of Plant Systemic Acquired Resistance Regulate NPR1 Function through Redox Changes. Cell. 113, 935-944.

Mukhtar, M. S., et al., 2011. Independently Evolved Virulence Effectors Converge onto Hubs in a Plant Immune System Network. Science. 333, 596-601.

Mysore, K. S., Ryu, C.-M., 2004. Nonhost resistance: how much do we know? Trends Plant Sci. 9, 97-104.

Nakashita, H., et al., 2003. Brassinosteroid functions in a broad range of disease resistance in tobacco and rice. The Plant Journal. 33, 887-898.

Naseem, M., et al., 2012. Integrated Systems View on Networking by Hormones in Arabidopsis Immunity Reveals Multiple Crosstalk for Cytokinin. The Plant Cell Online. 24, 1793-1814.

Navarro, L., et al., 2008. DELLAs Control Plant Immune Responses by Modulating the Balance of Jasmonic Acid and Salicylic Acid Signaling. Current biology : CB. 18, 650-655.

Navarro, L., et al., 2004. The Transcriptional Innate Immune Response to flg22. Interplay and Overlap with Avr Gene-Dependent Defense Responses and Bacterial Pathogenesis. Plant Physiol. 135, 1113-1128.

Nguyen Ba, A., et al., 2009. NLStradamus: a simple Hidden Markov Model for nuclear localization signal prediction. BMC Bioinformatics. 10, 202.

Nierman, W. C., et al., 2005. Genomic sequence of the pathogenic and allergenic filamentous fungus *Aspergillus fumigatus*. Nature. 438, 1151-1156.

Nimchuk, Z., et al., 2000. Eukaryotic Fatty Acylation Drives Plasma Membrane Targeting and Enhances Function of Several Type III Effector Proteins from Pseudomonas syringae. Cell. 101, 353-363.

Nishimura, M. T., et al., 2003. Loss of a Callose Synthase Results in Salicylic Acid-Dependent Disease Resistance. Science. 301, 969-972.

Noir, S., et al., 2009. A proteomic analysis of powdery mildew (*Blumeria graminis* f. sp. *hordei*) conidiospores. Mol. Plant Pathol. 10, 223.

Nomura, K., et al., 2006. A Bacterial Virulence Protein Suppresses Host Innate Immunity to Cause Plant Disease. Science. 313, 220-223.

Nomura, K., et al., 2011. Effector-triggered immunity blocks pathogen degradation of an immunity-associated vesicle traffic regulator in Arabidopsis. Proc. Natl. Acad. Sci. USA.

Nowara, D., et al., 2010. HIGS: Host-induced gene silencing in the obligate biotrophic fungal pathogen *Blumeria graminis*. Plant Cell. 22, 3130-3141.

O'Connell, R. J., Panstruga, R., 2006. Tête à tête inside a plant cell: establishing compatibility between plants and biotrophic fungi and oomycetes. New Phytol. 171, 699-718.

Oh, S.-K., et al., 2009. In Planta Expression Screens of *Phytophthora infestans* RXLR Effectors Reveal Diverse Phenotypes, Including Activation of the *Solanum bulbocastanum* Disease Resistance Protein Rpi-blb2. The Plant Cell Online. 21, 2928-2947.

Ottmann, C., et al., 2009. A common toxin fold mediates microbial attack and plant defense. Proc. Natl. Acad. Sci. USA. 106, 10359-10364.

Panstruga, R., Dodds, P. N., 2009. Terrific protein traffic: The mystery of effector protein delivery by filamentous plant pathogens. Science. 324, 748-750.

Panstruga, R., Schulze-Lefert, P., 2002. Live and let live: insights into powdery mildew disease and resistance. Mol. Plant Pathol. 3, 495-502.

Park, Y.-J., Luger, K., 2006. The structure of nucleosome assembly protein 1. Proc. Natl. Acad. Sci. USA. 103, 1248-1253.

Pauwels, L., et al., 2010. NINJA connects the co-repressor TOPLESS to jasmonate signalling. Nature. 464, 788-791.

Pauwels, L., Goossens, A., 2011. The JAZ Proteins: A Crucial Interface in the Jasmonate Signaling Cascade. The Plant Cell Online. 23, 3089-3100.

Pauwels, L., et al., 2008. Mapping methyl jasmonate-mediated transcriptional reprogramming of metabolism and cell cycle progression in cultured Arabidopsis cells. Proc. Natl. Acad. Sci. USA. 105, 1380-1385.

Peters, J.-M., 2006. The anaphase promoting complex/cyclosome: a machine designed to destroy. Nat Rev Mol Cell Biol. 7, 644-656.

Pfaffl, M. W., 2001. A new mathematical model for relative quantification in real-time RT–PCR. Nucleic Acids Res. 29, e45.

Pfefferle, S., et al., 2011. The SARS-Coronavirus-Host Interactome: Identification of Cyclophilins as Target for Pan-Coronavirus Inhibitors. PLoS Pathog. 7, e1002331.

Pieterse, C., et al., 2009. Networking by small-molecule hormones in plant immunity. Nat Chem Biol. 5, 308 - 316.

Pitzschke, A., et al., 2009. MAPK cascade signalling networks in plant defence. Curr. Opin. Plant Biol. 12, 421-426.

Plotnikova, J. M., et al., 1998. Powdery mildew pathogenesis of *Arabidopsis thaliana*. Mycologia. 90, 1009-1016.

Porceddu, A., et al., 2001. A Plant-specific Cyclin-dependent Kinase Is Involved in the Control of G2/M Progression in Plants. J. Biol. Chem. 276, 36354-36360.

Potuschak, T., et al., 2003. EIN3-Dependent Regulation of Plant Ethylene Hormone Signaling by Two Arabidopsis F Box Proteins: EBF1 and EBF2. Cell. 115, 679-689.

Pré, M., et al., 2008. The AP2/ERF Domain Transcription Factor ORA59 Integrates Jasmonic Acid and Ethylene Signals in Plant Defense. Plant Physiol. 147, 1347-1357.

Qiao, H., et al., 2009. Interplay between ethylene, ETP1/ETP2 F-box proteins, and degradation of EIN2 triggers ethylene responses in Arabidopsis. Genes Dev. 23, 512-521.

Rehmany, A. P., et al., 2005. Differential Recognition of Highly Divergent Downy Mildew Avirulence Gene Alleles by RPP1 Resistance Genes from Two Arabidopsis Lines. The Plant Cell Online. 17, 1839-1850.

Reuber, T. L., et al., 1998. Correlation of defense gene induction defects with powdery mildew susceptibility in Arabidopsis enhanced disease susceptibility mutants. Plant J. 16, 473-485.

Richards, T. A., et al., 2006. Evolution of Filamentous Plant Pathogens: Gene Exchange across Eukaryotic Kingdoms. Curr. Biol. 16, 1857-1864.

Robatzek, S., et al., 2007. Molecular identification and characterization of the tomato flagellin receptor *LeFLS2*, an orthologue of Arabidopsis *FLS2* exhibiting characteristically different perception specificities. Plant Mol. Biol. 64, 539-547.

Robinson, D. G., et al., 2011. ARF1 Localizes to the Golgi and the Trans-Golgi Network. The Plant Cell Online. 23, 846-849.

Römer, P., et al., 2007. Plant Pathogen Recognition Mediated by Promoter Activation of the Pepper Bs3 Resistance Gene. Science. 318, 645-648.

Rooney, H. C. E., et al., 2005. *Cladosporium* Avr2 Inhibits Tomato Rcr3 Protease Required for Cf-2-Dependent Disease Resistance. Science. 308, 1783-1786.

Rual, J.-F., et al., 2005. Towards a proteome-scale map of the human protein-protein interaction network. Nature. 437, 1173-1178.

Rushton, P. J., et al., 2010. WRKY transcription factors. Trends Plant Sci. 15, 247-258.

Santner, A., Estelle, M., 2009. Recent advances and emerging trends in plant hormone signalling. Nature. 459, 1071-1078.

Saunders, D. G. O., et al., 2012. Using hierarchical clustering of secreted protein families to classify and rank candidate effectors of rust fungi. PLoS ONE. 7, e29847.

Schlaeppi, K., et al., 2010. Disease resistance of Arabidopsis to *Phytophthora brassicae* is established by the sequential action of indole glucosinolates and camalexin. The Plant Journal. 62, 840-851.

Schmidt, S. M., Identification and functional characterization of powdery mildew effectors. Faculty of Mathematics and Natural Sciences, Vol. Ph.D. University of Cologne, Cologne, Germany, 2010.

Schmidt, S. M., Panstruga, R., 2011. Pathogenomics of fungal plant parasites: what have we learnt about pathogenesis? Curr. Opin. Plant Biol. 14, 392-399.

Schnittger, A., et al., 2002. Ectopic B-Type Cyclin Expression Induces Mitotic Cycles in Endoreduplicating Arabidopsis Trichomes. Current biology : CB. 12, 415-420.

Schommer, C., et al., 2008. Control of Jasmonate Biosynthesis and Senescence by miR319 Targets. PLoS Biol. 6, e230.

Schornack, S., et al., 2010. Ancient class of translocated oomycete effectors targets the host nucleus. Proc. Natl. Acad. Sci. USA. 107, 17421-17426.

Schweizer, P., et al., 1999. Transient expression of members of the germin-like gene family in epidermal cells of wheat confers disease resistance. The Plant Journal. 20, 541-552.

Seiffert, U., Schweizer, P., 2005. A pattern recognition tool for quantitative analysis of *in planta* hyphal growth of powdery mildew fungi. Mol. Plant-Microbe Interact. 18, 906-912.

Serralbo, O., et al., 2006. Non-cell-autonomous rescue of anaphase-promoting complex function revealed by mosaic analysis of HOBBIT, an Arabidopsis CDC27 homolog. Proc. Natl. Acad. Sci. USA. 103, 13250-13255.

Shan, X., et al., 2012. Comparison of phytohormone signaling mechanisms. Curr. Opin. Plant Biol. 15, 84-91.

Shannon, P., et al., 2003. Cytoscape: A Software Environment for Integrated Models of Biomolecular Interaction Networks. Genome Res. 13, 2498-2504.

Sheard, L. B., et al., 2010. Jasmonate perception by inositol-phosphate-potentiated COI1-JAZ co-receptor. Nature. 468, 400-405.

Shen, Q.-H., et al., 2007. Nuclear activity of MLA immune receptors links isolate-specific and basal disease-resistance responses. Science. 315, 1098-1103.

Shirasu, K., et al., 1999. Cell-autonomous complementation of mlo resistance using a biolistic transient expression system. The Plant Journal. 17, 293-299.

Silvar, C., et al., 2005. Real-time polymerase chain reaction quantification of *Phytophthora capsici* in different pepper genotypes. Phytopathology. 95, 1423-1429.

Simonis, N., et al., 2012. Host-pathogen interactome mapping for HTLV-1 and -2 retroviruses. Retrovirology. 9, 26.

Sims, T. L., Ordanic, M., 2001. Identification of a S-ribonuclease-binding protein in *Petunia hybrida*. Plant Mol. Biol. 47, 771-783.

Sivars, U., et al., 2003. Yip3 catalyses the dissociation of endosomal Rab-GDI complexes. Nature. 425, 856-859.

Soanes, D. M., et al., 2008. Comparative genome analysis of filamentous fungi reveals gene family expansions associated with fungal pathogenesis. PLoS ONE. 3, e2300.

Soanes, D. M., Talbot, N. J., 2006. Comparative genomic analysis of phytopathogenic fungi using expressed sequence tag (EST) collections. Mol. Plant Pathol. 7, 61-70.

Sohn, K. H., et al., 2007. The downy mildew effector proteins ATR1 and ATR13 promote disease susceptibility in *Arabidopsis thaliana*. Plant Cell. 19, 4077-4090.

Solomon, P., Oliver, R., 2002. Evidence that y-aminobutyric acid is a major nitrogen source during *Cladosporium fulvum* infection of tomato. Planta. 214, 414-420.

Song, J., et al., 2009. Apoplastic effectors secreted by two unrelated eukaryotic plant pathogens target the tomato defense protease Rcr3. Proc. Natl. Acad. Sci. USA. 106, 1654-1659.

Spanu, P. D., et al., 2010. Genome expansion and gene loss in powdery mildew fungi reveal tradeoffs in extreme parasitism. Science. 330, 1543-1546.

Spoel, S. H., et al., 2003. NPR1 Modulates Cross-Talk between Salicylate- and Jasmonate-Dependent Defense Pathways through a Novel Function in the Cytosol. The Plant Cell Online. 15, 760-770.

Spoel, S. H., et al., 2009. Proteasome-Mediated Turnover of the Transcription Coactivator NPR1 Plays Dual Roles in Regulating Plant Immunity. Cell. 137, 860-872.

Stein, M., et al., 2006. Arabidopsis PEN3/PDR8, an ATP Binding Cassette Transporter, Contributes to Nonhost Resistance to Inappropriate Pathogens That Enter by Direct Penetration. The Plant Cell Online. 18, 731-746.

Stelzl, U., et al., 2005. A Human Protein-Protein Interaction Network: A Resource for Annotating the Proteome. Cell. 122, 957-968.

Stergiopoulos, I., de Wit, P. J. G. M., 2009. Fungal effector proteins. Annu. Rev. Phytopathol. 47, 233-263.

Stotz, H. U., et al., 2011. Role of camalexin, indole glucosinolates, and side chain modification of glucosinolate-derived isothiocyanates in defense of Arabidopsis against *Sclerotinia sclerotiorum*. The Plant Journal. 67, 81-93.

Stuttmann, J., et al., 2011. Perturbation of Arabidopsis amino acid metabolism causes incompatibility with the adapted biotrophic pathogen *Hyaloperonospora arabidopsidis*. Plant Cell. 23, 2788-2803.

Sugio, A., et al., 2011. Phytoplasma protein effector SAP11 enhances insect vector reproduction by manipulating plant development and defense hormone biosynthesis. Proc. Natl. Acad. Sci. USA. 108, E1254–E1263.

Sutton, P. N., et al., 1999. Glucose, and not sucrose, is transported from wheat to wheat powdery mildew. Planta. 208, 426-430.

Suzuki, T., et al., 2001. Two Types of Putative Nuclear Factors that Physically Interactwith Histidine-Containing Phosphotransfer (Hpt) Domains, SignalingMediators in His-to-Asp Phosphorelay, in Arabidopsisthaliana. Plant and Cell Physiology. 42, 37-45.

Swarbreck, D., et al., 2008. The Arabidopsis Information Resource (TAIR): gene structure and function annotation. Nucleic Acids Res. 36, D1009-D1014.

Swarbrick, P. J., et al., 2006. Metabolic consequences of susceptibility and resistance (race-specific and broad-spectrum) in barley leaves challenged with powdery mildew. Plant, Cell Environ. 29, 1061-1076.

Szeto, C. Y. Y., et al., 2007. Le.MAPK and its interacting partner, Le.DRMIP, in fruiting body development in Lentinula edodes. Gene. 393, 87-93.

Tada, Y., et al., 2008. Plant Immunity Requires Conformational Charges of NPR1 via S-Nitrosylation and Thioredoxins. Science. 321, 952-956.

Takai, R., et al., 2008. Analysis of Flagellin Perception Mediated by flg22 Receptor OsFLS2 in Rice. Mol. Plant-Microbe Interact. 21, 1635-1642.

Takamatsu, S., 2004. Phylogeny and evolution of the powdery mildew fungi (Erysiphales, Ascomycota) inferred from nuclear ribosomal DNA sequences. Mycoscience. 45, 147-157.

Takemoto, D., Jones, D. A., 2005. Membrane Release and Destabilization of Arabidopsis RIN4 Following Cleavage by Pseudomonas syringae AvrRpt2. Mol. Plant-Microbe Interact. 18, 1258-1268.

Takken, F. L. W., Tameling, W. I. L., 2009. To Nibble at Plant Resistance Proteins. Science. 324, 744-746.

Tamura, K., et al., 2007. MEGA4: Molecular evolutionary genetics analysis (MEGA) software version 4.0. Mol Biol Evol. 24, 1596 - 1599.

Tang, X., et al., 1996. Initiation of Plant Disease Resistance by Physical Interaction of AvrPto and Pto Kinase. Science. 274, 2060-2063.

Tatematsu, K., et al., 2005. Identification of cis-Elements That Regulate Gene Expression during Initiation of Axillary Bud Outgrowth in Arabidopsis. Plant Physiol. 138, 757-766.

Team, R. D. C., 2008. R: A Language and Environment for Statistical Computing.

Thines, B., et al., 2007. JAZ repressor proteins are targets of the SCFCOI1 complex during jasmonate signalling. Nature. 448, 661-665.

Thomas, S., et al., 2001. Gene identification in the obligate fungal pathogen *Blumeria graminis* by expressed sequence tag analysis. Fungal Gen Biol. 33, 195 - 211.

Thomma, B. P. H. J., et al., 1999a. Requirement of Functional Ethylene-Insensitive 2Gene for Efficient Resistance of Arabidopsis to Infection by *Botrytis cinerea*. Plant Physiol. 121, 1093-1101.

Thomma, B. P. H. J., et al., 1999b. Deficiency in phytoalexin production causes enhanced susceptibility of *Arabidopsis thaliana* to the fungus *Alternaria brassicicola*. The Plant Journal. 19, 163-171.

Thomma, B. P. H. J., et al., 2011. Of PAMPs and Effectors: The Blurred PTI-ETI Dichotomy. The Plant Cell Online. 23, 4-15.

Thomma, B. P. H. J., et al., 1999c. Disturbed correlation between fungal biomass and β-glucuronidase activity in infections of *Arabidopsis thaliana* with transgenic *Alternaria brassicicola*. Plant Sci. 148, 31-36.

Thordal-Christensen, H., 2003. Fresh insights into processes of nonhost resistance. Curr. Opin. Plant Biol. 6, 351-357.

Tian, M., et al., 2005. A Second Kazal-Like Protease Inhibitor from *Phytophthora infestans* Inhibits and Interacts with the Apoplastic Pathogenesis-Related Protease P69B of Tomato. Plant Physiol. 138, 1785-1793.

Tian, M., et al., 2004. A Kazal-like Extracellular Serine Protease Inhibitor from *Phytophthora infestans* Targets the Tomato Pathogenesis-related Protease P69B. J. Biol. Chem. 279, 26370-26377.

Töller, A., Studies of plant innate immunity provide new functional insights on class IIa WRKY transcription factors and reveals a role for two Glucan Synthase-Like genes in gametophyte

development. Faculty of Mathematics and Natural Sciences, Vol. Ph.D. University of Cologne, Cologne, Germany, 2010.

Torres, M. A., et al., 2006. Reactive Oxygen Species Signaling in Response to Pathogens. Plant Physiol. 141, 373-378.

Torto, T. A., et al., 2003. EST Mining and Functional Expression Assays Identify Extracellular Effector Proteins From the Plant Pathogen *Phytophthora*. Genome Res. 13, 1675-1685.

Tsuda, K., Katagiri, F., 2010. Comparing signaling mechanisms engaged in pattern-triggered and effector-triggered immunity. Curr. Opin. Plant Biol. 13, 459-465.

Tsuda, K., et al., 2009. Network Properties of Robust Immunity in Plants. PLoS Genet. 5, e1000772.

Uetz, P., et al., 2000. A comprehensive analysis of protein-protein interactions in *Saccharomyces cerevisiae*. Nature. 403, 623-627.

Underwood, W., et al., 2007. The *Pseudomonas syringae* type III effector tyrosine phosphatase HopAO1 suppresses innate immunity in *Arabidopsis thaliana*. The Plant Journal. 52, 658-672.

Uppalapati, S. R., et al., 2007. The Phytotoxin Coronatine Contributes to Pathogen Fitness and Is Required for Suppression of Salicylic Acid Accumulation in Tomato Inoculated with *Pseudomonas syringae* pv. *tomato* DC3000. Mol. Plant-Microbe Interact. 20, 955-965.

van Damme, M., et al., 2012. The Irish Potato Famine Pathogen *Phytophthora infestans* Translocates the CRN8 Kinase into Host Plant Cells. PLoS Pathog. 8, e1002875.

Van den Ackerveken, G., et al., 1996. Recognition of the Bacterial Avirulence Protein AvrBs3 Occurs inside the Host Plant Cell. Cell. 87, 1307-1316.

van den Burg, H. A., et al., 2006. *Cladosporium fulvum* Avr4 Protects Fungal Cell Walls Against Hydrolysis by Plant Chitinases Accumulating During Infection. Mol. Plant-Microbe Interact. 19, 1420-1430.

Van Der Biezen, E. A., Jones, J. D. G., 1998. Plant disease-resistance proteins and the gene-for-gene concept. Trends Biochem. Sci. 23, 454-456.

van der Hoorn, R. A. L., Kamoun, S., 2008. From Guard to Decoy: A New Model for Perception of Plant Pathogen Effectors. The Plant Cell Online. 20, 2009-2017.

van Loon, L. C., et al., 2006. Significance of Inducible Defense-related Proteins in Infected Plants. Annu. Rev. Phytopathol. 44, 135-162.

Vandepoele, K., et al., 2006. Identification of novel regulatory modules in dicotyledonous plants using expression data and comparative genomics. Genome Biology. 7, R103.

Venkatesan, K., et al., 2009. An empirical framework for binary interactome mapping. Nat Meth. 6, 83-90.

Vernoud, V., et al., 2003. Analysis of the Small GTPase Gene Superfamily of Arabidopsis. Plant Physiol. 131, 1191-1208.

Vinardell, J. M., et al., 2003. Endoreduplication Mediated by the Anaphase-Promoting Complex Activator CCS52A Is Required for Symbiotic Cell Differentiation in *Medicago truncatula* Nodules. The Plant Cell Online. 15, 2093-2105.

Vleeshouwers, V. G. A. A., et al., 2008. Effector Genomics Accelerates Discovery and Functional Profiling of Potato Disease Resistance and *Phytophthora infestans* Avirulence Genes. PLoS ONE. 3, e2875.

Voegele, R. T., Mendgen, K., 2003. Rust haustoria: nutrient uptake and beyond. New Phytol. 159, 93-100.

Vogel, J., Somerville, S., 2000. Isolation and characterization of powdery mildew-resistant *Arabidopsis* mutants. Proc. Natl. Acad. Sci. USA. 97, 1897-1902.

Vogel, J. P., et al., 2002. *PMR6*, a pectate lyase-like gene required for powdery mildew susceptibility in Arabidopsis. Plant Cell. 14, 2095-2106.

Voinnet, O., et al., 2003. An enhanced transient expression system in plants based on suppression of gene silencing by the p19 protein of tomato bushy stunt virus. The Plant Journal. 33, 949-956.

Wahl, R., et al., 2010. A novel high-sffinity sucrose transporter is required for virulence of the plant pathogen *Ustilago maydis*. PLoS Biol. 8, e1000303.

Walter, M., et al., 2004. Visualization of protein interactions in living plant cells using bimolecular fluorescence complementation. The Plant Journal. 40, 428-438.

Walters, D. R., Ayres, P. G., 1981. Phosphate uptake and translocation by roots of powdery mildew infected barley. Physiol. Plant Pathology. 18, 195-205.

Wan, J., et al., 2008. A LysM Receptor-Like Kinase Plays a Critical Role in Chitin Signaling and Fungal Resistance in Arabidopsis. The Plant Cell Online. 20, 471-481.

Wang, D., et al., 2007. Salicylic Acid Inhibits Pathogen Growth in Plants through Repression of the Auxin Signaling Pathway. Curr. Biol. 17, 1784-1790.

Wang, K. L.-C., et al., 2002. Ethylene Biosynthesis and Signaling Networks. The Plant Cell Online. 14, S131-S151.

Wang, Q., et al., 2011. Transcriptional Programming and Functional Interactions within the *Phytophthora sojae* RXLR Effector Repertoire. The Plant Cell Online.

Wang, R., Brattain, M. G., 2007. The maximal size of protein to diffuse through the nuclear pore is larger than 60kDa. FEBS Lett. 581, 3164-3170.

Wang, W., et al., 2009. Specific targeting of the Arabidopsis resistance protein RPW8.2 to the interfacial membrane encasing the fungal haustorium renders broad-spectrum resistance to powdery mildew. Plant Cell. 21, 2898-2913.

Wang, Y., et al., 2010. A *Pseudomonas syringae* ADP-Ribosyltransferase Inhibits Arabidopsis Mitogen-Activated Protein Kinase Kinases. The Plant Cell Online.

Wasternack, C., 2007. Jasmonates: An Update on Biosynthesis, Signal Transduction and Action in Plant Stress Response, Growth and Development. Ann. Bot. 100, 681-697.

Weiler, E. W., et al., 1994. The *Pseudomonas* phytotoxin coronatine mimics octadecanoid signalling molecules of higher plants. FEBS Lett. 345, 9-13.

Welchen, E., Gonzalez, D. H., 2006. Overrepresentation of Elements Recognized by TCP-Domain Transcription Factors in the Upstream Regions of Nuclear Genes Encoding Components of the Mitochondrial Oxidative Phosphorylation Machinery. Plant Physiol. 141, 540-545.

Whisson, S. C., et al., 2007. A translocation signal for delivery of oomycete effector proteins into host plant cells. Nature. 450, 115-118.

Wildermuth, M. C., 2010. Modulation of host nuclear ploidy: a common plant biotroph mechanism. Curr. Opin. Plant Biol. 13, 449-458.

Wildermuth, M. C., et al., 2001. Isochorismate synthase is required to synthesize salicylic acid for plant defence. Nature. 414, 562-565.

Williamson, V. M., Hussey, R. S., 1996. Nematode pathogenesis and resistance in plants. The Plant Cell Online. 8, 1735-45.

Wilton, M., et al., 2010. The type III effector HopF2 Pto targets Arabidopsis RIN4 protein to promote *Pseudomonas syringae* virulence. Proc. Natl. Acad. Sci. USA. 107, 2349-2354.

Wu, Y., et al., 2012. The Arabidopsis NPR1 Protein Is a Receptor for the Plant Defense Hormone Salicylic Acid. Cell Reports. 1, 639-647.

Xiao, S., et al., 2005. The atypical resistance gene, RPW8, recruits components of basal defence for powdery mildew resistance in Arabidopsis. The Plant Journal. 42, 95-110.

Xiao, S., et al., 2001. Broad-spectrum mildew resistance in *Arabidopsis thaliana* mediated by *RPW8*. Science. 291, 118-120.

Xie, D.-X., et al., 1998. COI1: An Arabidopsis Gene Required for Jasmonate-Regulated Defense and Fertility. Science. 280, 1091-1094.

Xu, J., Hamer, J., 1996. MAP kinase and cAMP signaling regulate infection structure formation and pathogenic growth in the rice blast fungus *Magnaporthe grisea*. Genes Dev. 10, 2696.

Xu, J., et al., 2011. Gene discovery in EST sequences from the wheat leaf rust fungus *Puccinia triticina* sexual spores, asexual spores and haustoria, compared to other rust and corn smut fungi. BMC Genomics. 12, 161.

Yamada, K., et al., 2003. Empirical Analysis of Transcriptional Activity in the Arabidopsis Genome. Science. 302, 842-846.

Yamaguchi, Y., et al., 2010. PEPR2 Is a Second Receptor for the Pep1 and Pep2 Peptides and Contributes to Defense Responses in Arabidopsis. The Plant Cell Online. 22, 508-522.

Yamaguchi, Y., et al., 2006. The cell surface leucine-rich repeat receptor for AtPep1, an endogenous peptide elicitor in Arabidopsis, is functional in transgenic tobacco cells. Proc. Natl. Acad. Sci. USA. 103, 10104-10109.

Yan, J., et al., 2009. The Arabidopsis CORONATINE INSENSITIVE1 Protein Is a Jasmonate Receptor. The Plant Cell Online. 21, 2220-2236.

Yan, Y., et al., 2007. A Downstream Mediator in the Growth Repression Limb of the Jasmonate Pathway. The Plant Cell Online. 19, 2470-2483.

Yang, B., et al., 2006. Os8N3 is a host disease-susceptibility gene for bacterial blight of rice. Proc. Natl. Acad. Sci. USA. 103, 10503-10508.

Yang, Y., Gabriel, D. W., 1995. *Xanthomonas* avirulence/pathogenicity gene family encodes functional plant nuclear targeting signals. Mol. Plant-Microbe Interact. 8, 627-631.

Yasuda, M., et al., 2008. Antagonistic Interaction between Systemic Acquired Resistance and the Abscisic Acid–Mediated Abiotic Stress Response in Arabidopsis. The Plant Cell Online. 20, 1678-1692.

Yin, C., et al., 2009. Generation and analysis of expression sequence tags from haustoria of the wheat stripe rust fungus *Puccinia striiformis* f. sp. *tritici*. BMC Genomics. 10, 626.

Yin, Y., et al., 2005. A New Class of Transcription Factors Mediates Brassinosteroid-Regulated Gene Expression in Arabidopsis. Cell. 120, 249-259.

Yu, H., et al., 1998. Identification of a Cullin Homology Region in a Subunit of the Anaphase-Promoting Complex. Science. 279, 1219-1222.

Zachariae, W., et al., 1998. Mass Spectrometric Analysis of the Anaphase-Promoting Complex from Yeast: Identification of a Subunit Related to Cullins. Science. 279, 1216-1219.

Zhang, J., et al., 2010. Receptor-like Cytoplasmic Kinases Integrate Signaling from Multiple Plant Immune Receptors and Are Targeted by a *Pseudomonas syringae* Effector. Cell Host & Microbe. 7, 290-301.

Zhang, J., et al., 2007. A *Pseudomonas syringae* Effector Inactivates MAPKs to Suppress PAMP-Induced Immunity in Plants. Cell Host & Microbe. 1, 175-185.

Zhang, W.-J., et al., 2012. Interaction of barley powdery mildew effector candidate CSEP0055 with the defence protein PR17c. Mol. Plant Pathol., n/a-n/a.

Zhang, Z., et al., 2004. *Blumeria graminis* secretes an extracellular catalase during infection of barley: potential role in suppression of host defence. Mol. Plant Pathol. 5, 537-547.

Zheng, B., et al., 2011. The Anaphase-Promoting Complex Is a Dual Integrator That Regulates Both MicroRNA-Mediated Transcriptional Regulation of Cyclin B1 and Degradation of Cyclin B1 during Arabidopsis Male Gametophyte Development. The Plant Cell Online. 23, 1033-1046.

Zhong, Q., et al., 2009. Edgetic perturbation models of human inherited disorders. Mol Syst Biol. 5.

Zhou, N., et al., 1998. PAD4 Functions Upstream from Salicylic Acid to Control Defense Responses in Arabidopsis. The Plant Cell Online. 10, 1021-1030.

Zhu, S., et al., 2011. SAG101 Forms a Ternary Complex with EDS1 and PAD4 and Is Required for Resistance Signaling against Turnip Crinkle Virus. PLoS Pathog. 7, e1002318.

Zhu, W., et al., 1999. The C Terminus of AvrXa10 Can Be Replaced by the Transcriptional Activation Domain of VP16 from the Herpes Simplex Virus. The Plant Cell Online. 11, 1665-1674.

Zhu, Y., et al., 2010. Structural mechanism of host Rab1 activation by the bifunctional *Legionella* type IV effector SidM/DrrA. Proc. Natl. Acad. Sci. USA. 107, 4699-4704.

Zimmerli, L., et al., 2004. Host and non-host pathogens elicit different jasmonate/ethylene responses in Arabidopsis. The Plant Journal. 40, 633-646.

Zipfel, C., et al., 2006. Perception of the Bacterial PAMP EF-Tu by the Receptor EFR Restricts Agrobacterium-Mediated Transformation. Cell. 125, 749-760.

Zipfel, C., et al., 2004. Bacterial disease resistance in Arabidopsis through flagellin perception. Nature. 428, 764-767.

6 Supplemental Data

6.1 Supplemental Figures

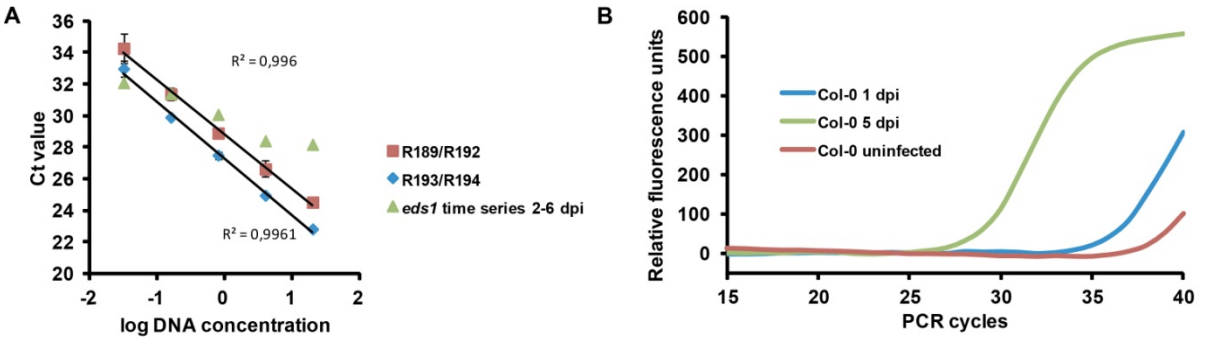

Supplemental Figure 1: Documentation of technical details related to the qPCR assay. (**A**) Primer efficiency calculations for primer sets R189/R192 (red) and R193/R194 (blue). Efficiency was calculated from a 5-fold dilution series. The respective correlation coefficients (R^2) are indicated. Ct values of *G. orontii* gDNA amplification from the *eds1* time series from 2-6 dpi are presented in green for comparison. (**B**) Comparison of amplification plots of *G. orontii*-infected Col-0 at 1 (blue) and 5 dpi (green) and the uninfected Col-0 control (red). Raw fluorescence data were exported and used for visualization. Ratios of *G. orontii* to Arabidopsis gDNA were determined by qPCR with primers R189/R192 and R193/R194, respectively.

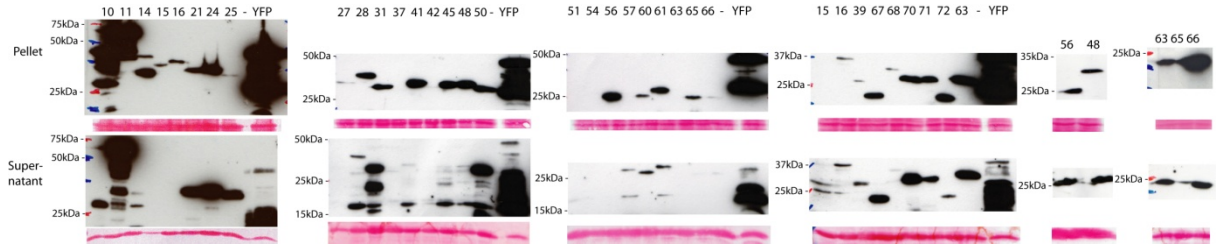

Supplemental Figure 2: In vitro secretion of OECs by transgenic Pseudomonas. *Pst* strains were grown in minimal media o/n and the pellet fraction was harvested by centrifugation. The supernatant fraction was obtained by filtering of total culture supernatant (0,2 µm filter), concentration to 1/10 volume and isolation of proteins using Strataclean beads. Both fractions were subjected to SDS-PAGE on 12% gels and immunoblotted. Blots were with anti-HA and the secondary anti-rat IgG antibody.

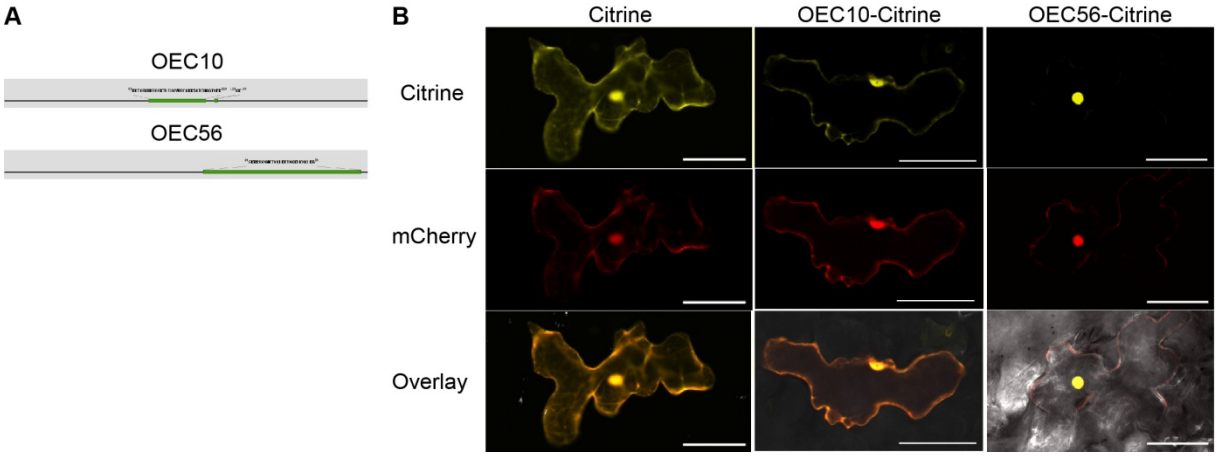

Supplemental Figure 3: Only OEC56 localizes exclusively to the nucleus in Arabidopsis. (**A**) Nuclear localization signals predicted for OEC10 and OEC56 by NLStradamus. (**B**)Biolistic transformation of single epidermal cells of Arabidopsis with vectors carrying Citrine, OEC10-Citrine or OEC56-Citrine. A construct carrying mCherry was cobombarded as a transformation

and localization control. Transformed cells were visualized by CLSM at 2dpi. 5 cells were imaged per transformation. Experiment was repeated once with similar results.

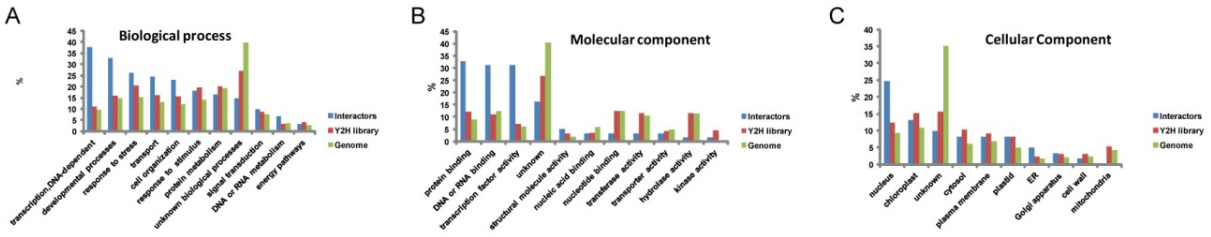

Supplemental Figure 4: Gene ontology distribution of OEC interacting Arabidopsis proteins. Gene Ontology distribution among OEC interactors (blue), Y2H library proteins (red) and the TAIR10 Arabidopsis proteome (green) for biological process (**A**), molecular component (**B**) and cellular component (**C**) categories. GO terms and distributions were retrieved from TAIR. Individual proteins may be represented in more than one category.

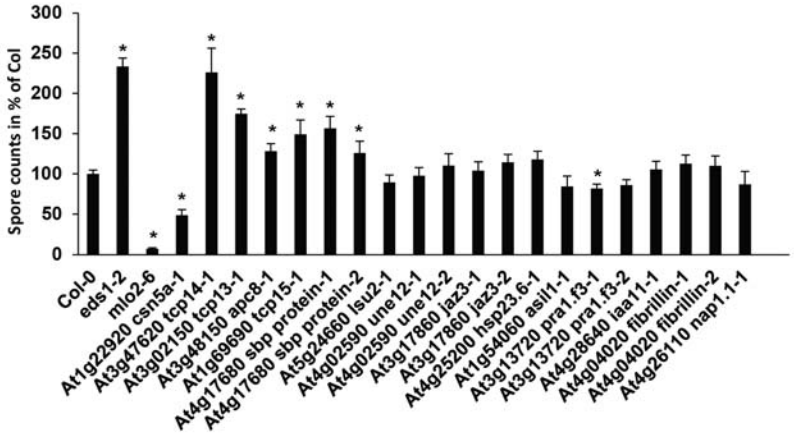

Supplemental Figure 5: Spore counts on additional lines. Spore numbers per seedling fresh weight were determined at 7dpi from three replicates per genotype and experiment, normalized to the average of Col-0 within each experiment and subsequently integrated. Bars represent the mean of three experiments ± SE. Asterisks indicate statistically significant differences to Col-0 in two-tailed Student's t-test ($p<0,05$).

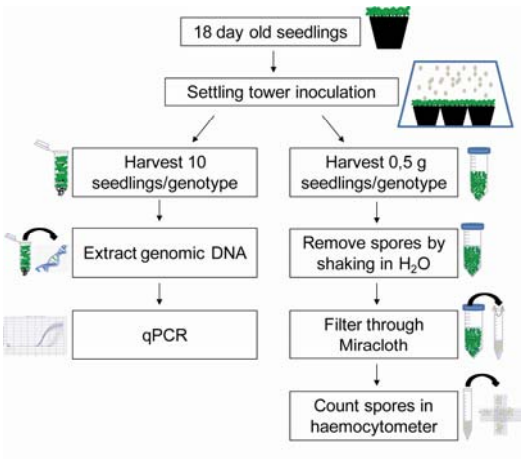

Supplemental Figure 6: Schematic overview of developed methods. Simplified view of the workflow of the qPCR- and spore count-based powdery mildew quantification procedures. For further details see main text.

6.2 Supplemental Tables

Supplemental Table 1: List of primers used in this study.

qRT-PCR Target	Name	Forward Primer	Reverse Primer
	OEC61	GCGAGAGCGGAAGATCTGTA	CAGGAAACCCTCGCCTGTAT
	OEC63	CCAGTTTCTGGCGCAAAT	GGACTTGCCATCGTCGTAGT
	OEC65	TCAAATTCTGGCGAATCCTC	ACAAGGTTCAACCAGCACCT
	OEC25	ACGTTTGCCTGGCTGTAAAT	GTCACCACCCAGGTAAGGAA
At3G21215	RNA-binding family protein	GAATCCACCCATACCACCAG	GAGGAGGAGGATGGTGATGA
AT1G16300	G-3-P dehydrogenase of plastid 2	AAGCACCTCCTGCTGTTCAT	CTTTCCACTGCTCCTTGACCR244
Go_V1_Contig3757	Plasma membrane ATPase 1	TCGCCGCTATATTTGGAGTC	CTGGGTCAGATGGTTCACCT
Go_V1_Contig76	GDSL-like lipase	TCTTGGTGGCACGAATGAC	AGTGCGAGAGTGGGACAGAC
GoEST_c2903	OEC70	ATCTTGGCCCTATTTGTCTC	GTATGGTGGTGGAGATGAGT
GoEST_c2438	OEC48	ACGCATCACATTCATTTCTC	TCTTGGGAATCGTAACTGTC
GoEST_c253	OEC56	ACTCAGGGGAATACTTCGAT	ATTCTTTCTTCTGCGTTTCC
GoEST_c501	Conserved hypothetical protein	CACTACCTCCAGCTTCATCT	TAGCAGCAAAATCCAAATCA
GoEST_c5204	PMA1	GCAACATTGAACAGCCTACT	TTGTAACGGCCTAGATTGTC
GoEST_c5054	MFS maltose permease	ACGTCGAACACTATTTGGAG	TCTTGTTCTTCATGCGAGTT
GoEST_c22345	GLTRN1	TCGGCGAAGAAGCTGTTAGT	CTTGGCGTTCATCCAGAAAT
GoEST_c311	GABA Permease	ACCGGGTGTATGGTACATGG	AACACCCGGACACCAGTAGT
GoEST_c1259	SOD	GGGAAAACACGGAAAGATCA	GGCTGTTCCATGGTGAAGTT
GoEST_c38	Phosphate transporter	GGATCACAAGAGGAGCCAAA	TTGCGACTTCAGAACCCTCT
GoEST_c886	CAP20	ACGGTGAAGCCAGACAGACT	TGTGCGGAGATATGGCAGTA
GoEST_c4780	β-Tubulin	TGTTGGAGATCAATTTACCG	TCACCCTCAGAGATAGAAGC
Sequencing			
pB7WG2		ATGACGCACAATCCCACTATCCTTCGCA	AGCGAAACCCTATAAGAA
pDest-AD		CGCGTTTGGAATCACTACAGGG	GGAGACTTGACCAAACCTCTGGCG
pDest-DB		GGCTTCAGTGGAGACTGATATGCCTC	see above
pEDV		TACACCCAAATCCCTATTGG	CGTTGTAAAACGACGGCCAGT
pUBQ	pUB-Vectors	cgaatttgtagattaatctgag	TCTGGGAACTACTCACAC
	pAM-PAT	ACAATCCCACTATCCTTC	
	pDONR201	TCGCGTTAACGCTAGCATGGATCTC	GTAACATCAGAGATTTTGAGACAC
Cloning			
AT3G47620noStop	TCP14	GGGGACAAGTTTGTACAAAAAAGCAGGCTTGATGCAAAAGCCAACATCAAG	GGGGACCACTTTGTACAAGAAAGCTGGGTAATCTTGCTGATCCTCCTCATC
AT5G24660noStop	LSU2	GGGGACAAGTTTGTACAAAAAAGCAGGCTTGATGGGGAAAGGAGGAAACTAT	GGGGACCACTTTGTACAAGAAAGCTGGGTACGGAGAGGCAGAGGCAG
AT4G24840noStop		GGGGACAAGTTTGTACAAAAAAGCAGGCTTGATGTCAGATCTGGTCGCGA	GGGGACCACTTTGTACAAGAAAGCTGGGTAAACACTAATTGAGTTTTGCCTA
AT3G21490noStop	Heavy metal transport/detoxification superfamily protein	GGGGACAAGTTTGTACAAAAAAGCAGGCTTGATGACGAAAGATAAGAAGAAAAAG	GGGGACCACTTTGTACAAGAAAGCTGGGTAAGAAATAGAACAAATGGCTTTG
AT4G26110noStop	NAP1.1	GGGGACAAGTTTGTACAAAAAAGCAGGCTTGATGAGCAACGACAAGGATAGC	GGGGACCACTTTGTACAAGAAAGCTGGGTACTGTTGCTTGCATTCGG
AT3G02150noStop	TCP13	GGGGACAAGTTTGTACAAAAAAGCAGGCTTGATGAATATCGTCTCTTGGAAAGA	GGGGACCACTTTGTACAAGAAAGCTGGGTACATATGGTGATCACTTCCTCTAC
AT4G17680noStop	SBP family protein	GGGGACAAGTTTGTACAAAAAAGCAGGCTTGATGCCCTTATTATCTGATAATGAAC	GGGGACCACTTTGTACAAGAAAGCTGGGTAAAATAAAACTTCGACACCGG
AT4G11790noStop	PH domain superfamily protein	GGGGACAAGTTTGTACAAAAAAGCAGGCTTGATGAGAGGAGTAAAACGCGC	GGGGACCACTTTGTACAAGAAAGCTGGGTATGAAGAAGGGGCGTATTCTT
AT1G17700noStop	PRA1.F1	GGGGACAAGTTTGTACAAAAAAGCAGGCTTGATGACAACATATGGCACCAATC	GGGGACCACTTTGTACAAGAAAGCTGGGTACGGATTTAAAAGACTGGTTTCT
AT1G55190noStop	PRA1.F2	GGGGACAAGTTTGTACAAAAAAGCAGGCTTGATGACGAACTACGGGGCG	GGGGACCACTTTGTACAAGAAAGCTGGGTACGACGAAGGGTATGACATCA
AT3G13720noStop	PRA1.F3	GGGGACAAGTTTGTACAAAAAAGCAGGCTTGATGACGAACTACGGTGCGA	GGGGACCACTTTGTACAAGAAAGCTGGGTAAGTCGACGGGTATGACGTC
AT3G47620	TCP14	see above	GGGGACCACTTTGTACAAGAAAGCTGGGTCTAATCTTGCTGATCCTCCTCATC
AT5G24660	LSU2	see above	GGGGACCACTTTGTACAAGAAAGCTGGGTTCACGGAGAGGCAGAGGCAG
AT4G24840		see above	GGGGACCACTTTGTACAAGAAAGCTGGGTCTAAACACTAATTGAGTTTTGCCTA
AT3G21490		see above	GGGGACCACTTTGTACAAGAAAGCTGGGTTCAAGAAATAGAACAAATGGCTTTG
AT4G26110	NAP1.1	see above	GGGGACCACTTTGTACAAGAAAGCTGGGTTACTGTTGCTTGCATTCGG
AT4G17680		see above	GGGGACCACTTTGTACAAGAAAGCTGGGTCTAAAATAAAACTTCGACACCGG
AT4G11790		see above	GGGGACCACTTTGTACAAGAAAGCTGGGTTCATGAAGAAGGGGCGTATTCTT
AT1G17700	PRA1.F1	see above	GGGGACCACTTTGTACAAGAAAGCTGGGTTTACGGATTTAAAAGACTGGTTTCT
AT1G55190	PRA1.F2	see above	GGGGACCACTTTGTACAAGAAAGCTGGGTTTACGACGAAGGGTATGACATCA
AT3G13720	PRA1.F3	PRA1.F3	GGGGACCACTTTGTACAAGAAAGCTGGGTTTAAGTCGACGGGTATGACGTC
OEC9noStop		GGGACAAGTTTGTACAAAAAAGCAGGCTTGATGGTTCCTCTTAACATCAATCTTG	GGGGACCACTTTGTACAAGAAAGCTGGGTATTCTTCGTTGTTGGTAGTC
OEC9		see above	GGGGACCACTTTGTACAAGAAAGCTGGGTCTATTCTTCGTTGTTGGTAGTCTC
OEC10noStop		GGGGACAAGTTTGTACAAAAAAGCAGGCTTGATGACCTATCATGAGGCCGACT	GGGGACCACTTTGTACAAGAAAGCTGGGTATTTCGGCCCGAATTTA
OEC10		see above	GGGGACCACTTTGTACAAGAAAGCTGGGTCTATTTCGGCCCGAATTTA
OEC11noStop		GGGGACAAGTTTGTACAAAAAAGCAGGCTTGATGGCTCCATTATCTCCGCTC	GGGGACCACTTTGTACAAGAAAGCTGGGTATACTTTCCACTCGCTTTTAGT
OEC11		see above	GGGGACCACTTTGTACAAGAAAGCTGGGTCTATACTTTCCACTCGCTTTTAG
OEC13short			GCTTTCGGTTGAGTAAGTTGG
OEC14noStop		GGGACAAGTTTGTACAAAAAAGCAGGCTTGATGATTTCTCCTGTTCAGGGCGAAC	GGGGACCACTTTGTACAAGAAAGCTGGGTACACACGAACGCATTGATGG
OEC14		see above	GGGGACCACTTTGTACAAGAAAGCTGGGTTCACACACGAACGCATTG
OEC15noStop		GGGACAAGTTTGTACAAAAAAGCAGGCTTGATGTACGTTGGCCTTAGAACACATTC	GGGGACCACTTTGTACAAGAAAGCTGGGTATTTACGATGATCTTCTTCG
OEC15		see above	GGGGACCACTTTGTACAAGAAAGCTGGGTCTATTTACGATGATCTTCTTCGC
OEC16noStop		GGGACAAGTTTGTACAAAAAAGCAGGCTTGATGCACGTCGCGTCTAGTACCGTG	GGGGACCACTTTGTACAAGAAAGCTGGGTAGTTACTGCGCCAACGACGG
OEC16		see above	GGGGACCACTTTGTACAAGAAAGCTGGGTTTAGTTACTGCGCCAACGA
OEC16a		ATGCACATCGTTACTCGCAGTGT	TTAATGCGGTTCCACTGTGC
OEC20		GGGGACAAGTTTGTACAAAAAAGCAGGCTTGATGGTTCCTCAACCCTGGCA	GGGGACCACTTTGTACAAGAAAGCTGGGTAGTCACTGTCATCCTTGTTACTT
OEC21noStop		GGGACAAGTTTGTACAAAAAAGCAGGCTTGATGACTTCCATTGGACGACTGGC	GGGGACCACTTTGTACAAGAAAGCTGGGTAGGACAGCTGCTCTACCGGAG
OEC21		see above	GGGGACCACTTTGTACAAGAAAGCTGGGTTCAGGACAGCTGCTCTACC
OEC22		ATGTCCTCAATAATTCCTTCTCATTC	TCATACGTTATTAAAGGTTCCTATGA
OEC23		ATGGTCGAGCCCCAGACTGTTGATG	TCATATTGGTCGAGATCTCGGTG
OEC23a		ATGGTTGCCGTCGAGCCCCC	TTATCGGTTGGGTAACTTTAATT
OEC23b		ATGGTTGCCGTTGAGCTCTATTA	TTATATTGGTGCAAATCTCGGT
OEC24noStop		GGGGACAAGTTTGTACAAAAAAGCAGGCTTGATGCCCACAAGGAATGTC	GGGGACCACTTTGTACAAGAAAGCTGGGTATCTGAAAATTCTAAAAATCCAAC
OEC24		see above	GGGGACCACTTTGTACAAGAAAGCTGGGTCTATCTGAAAATTCTAAAAATCCAAC
OEC25noStop		GGGGACAAGTTTGTACAAAAAAGCAGGCTTGATGCGCTCCAGGACCGAGG	GGGGACCACTTTGTACAAGAAAGCTGGGTAAAAATTACATTTCAAATTTCC
OEC25		see above	GGGGACCACTTTGTACAAGAAAGCTGGGTCTAAAAATTACATTTCAAATTTCC
OEC25b		ATGGCCAATAACCCACTCAATATT	TCAGGTCTTTGGTTTGCGGT
OEC27noStop		GGGACAAGTTTGTACAAAAAAGCAGGCTTGATGCAACCTTTTGATGCGTACGG	GGGGACCACTTTGTACAAGAAAGCTGGGTAGAATTTTTCACAAGCATGAATG
OEC27		see above	GGGGACCACTTTGTACAAGAAAGCTGGGTTTAGAATTTTTCACAAGCATGAA
OEC28noStop		GGGACAAGTTTGTACAAAAAAGCAGGCTTGATGACTCCATCAGGTTTGAACTTTTAC	GGGGACCACTTTGTACAAGAAAGCTGGGTAAACGTCCGAGTTCTGCATTG
OEC28		see above	GGGGACCACTTTGTACAAGAAAGCTGGGTTCAAACGTCCGAGTTCTGC
OEC29		ATGGAAGATCGTTTTTTTTGGTC	TCACAACTCAACACAAAGAAAATTTC
OEC30		ATGTTTCCCAAAAGGCAACAA	TCAGATATTTTGTTTCTGTTTCACCA
OEC31noStop		GGGACAAGTTTGTACAAAAAAGCAGGCTTGATGCAAATATTGCCCGTTCAAGTG	GGGGACCACTTTGTACAAGAAAGCTGGGTAAAGGTTGACCACTGCAGCAC
OEC31		see above	GGGGACCACTTTGTACAAGAAAGCTGGGTTTAAAGGTTGACCACTGCAG
OEC33		ATGGCTCCCTTACAAGAAAATCTG	TCAGTTTTGATCGTCTTCGTTC
OEC35		ATGTATGACCCACAACAGATAAC	TCACCAGGCAGTGACCGCTGTG
OEC36noStop		GGGACAAGTTTGTACAAAAAAGCAGGCTTGATGCAATTTGACTTCTTTGAGCAG	GGGGACCACTTTGTACAAGAAAGCTGGGTATAAAAGACCTTTTCTTGCTAAC
OEC36		see above	GGGGACCACTTTGTACAAGAAAGCTGGGTTTATAAAAGACCTTTTCTTGCTAAC
OEC37noStop		GGGGACAAGTTTGTACAAAAAAGCAGGCTTGATGCAAACGATACAACAAATCAAACA	GGGGACCACTTTGTACAAGAAAGCTGGGTAGATAAACGTACTCAAATCTTC
OEC37		see above	GGGGACCACTTTGTACAAGAAAGCTGGGTCTAGATAAACGTACTCAAATCTTC
OEC38		GGGACAAGTTTGTACAAAAAAGCAGGCTTGATGACTCAATTCTCTTATGCGCC	GGGGACCACTTTGTACAAGAAAGCTGGGTACATTGTACGTAGTTCTTCG
OEC39noStop		GGGGACAAGTTTGTACAAAAAAGCAGGCTTGATGCAACCTTTTGATGCGTACG	GGGGACCACTTTGTACAAGAAAGCTGGGTAGAGACAAAACGAATGCG
OEC39		see above	GGGGACCACTTTGTACAAGAAAGCTGGGTCTAGAGACAAAACGAATGC
OEC41noStop		GGGGACAAGTTTGTACAAAAAAGCAGGCTTGATGGTCGAGCCCCCGACTGTT	GGGGACCACTTTGTACAAGAAAGCTGGGTATCGGTTGGGTAACTTTAAT
OEC41		see above	GGGGACCACTTTGTACAAGAAAGCTGGGTCTATCGGTTGGGTAACTTTAA
OEC42noStop		GGGACAAGTTTGTACAAAAAAGCAGGCTTGATGAGACGTTCCCCCAAATATGTC	GGGGACCACTTTGTACAAGAAAGCTGGGTAGCCTGATCTGTGTGGATGTTG
OEC42		see above	GGGGACCACTTTGTACAAGAAAGCTGGGTTCAGCCTGATCTGTGTGGA
OEC43		ATGCATCCTACTCTTTATGAACG	TCAGCGCAGCCTCTGAGTTTTG
OEC44		ATGGTCAACAAGCCACCTACCTC	TCACAGTCCTGATTGGCGAT
OEC45noStop		GGGACAAGTTTGTACAAAAAAGCAGGCTTGATGCAGCCTAACCCGAATGCTGC	GGGGACCACTTTGTACAAGAAAGCTGGGTATCGTAACTCGGTTTCACAG
OEC45		see above	GGGGACCACTTTGTACAAGAAAGCTGGGTTTATCGTAACTCGGTTTCACA
OEC47		ATGCAGCGTCCTCGACGAAG	TCAATTTATGGAATTCACAATTT
OEC48		see above	GGGGACCACTTTGTACAAGAAAGCTGGGTTTATGCGTGTGCCTTTGG
OEC49		ATGTCACCAGTTTCTACCTTCATC	TCACAAACATCTCCCCACATGAATAAAC
OEC50noStop		GGGACAAGTTTGTACAAAAAAGCAGGCTTGATGGCTCCTCTATCTCCCCTTCC	GGGGACCACTTTGTACAAGAAAGCTGGGTAGAATCGGAATTCTGTGTCAG
OEC50		see above	GGGGACCACTTTGTACAAGAAAGCTGGGTTCAGAATCGGAATTCTGTGTC
OEC51noStop		GGGACAAGTTTGTACAAAAAAGCAGGCTTGATGGAAGCTACATCAAAAGCTAC	GGGGACCACTTTGTACAAGAAAGCTGGGTAAAAACATCGCACATCAGAATATG
OEC51		see above	GGGGACCACTTTGTACAAGAAAGCTGGGTTTAAAAACATCGCACATCAGA
OEC54noStop		GGGGACAAGTTTGTACAAAAAAGCAGGCTTGATGAGATATACACATAAATGCGAAATAAG	GGGGACCACTTTGTACAAGAAAGCTGGGTACCCACATCGCACACC
OEC54		see above	GGGGACCACTTTGTACAAGAAAGCTGGGTCTACCCACATCGCACACC
OEC55noStop		GGGGACAAGTTTGTACAAAAAAGCAGGCTTGATGTTTCCAGCCATACCCACG	GGGGACCACTTTGTACAAGAAAGCTGGGTAATGCGCGCTAGTATTC
OEC55		see above	GGGGACCACTTTGTACAAGAAAGCTGGGTCTAATGCGCGCTAGTATTC

Supplemental Table 1 (continued from last page)

Target	Name	Forward Primer	Reverse Primer
OEC56noStop		GGGACAAGTTTGTACAAAAAAGCAGGCTTGATGGCTCCTACAAGGGAAAGTAC	GGGGACCACTTTGTACAAGAAAGCTGGGTAGTAGCCCTTTAGTTTATTC
OEC56		see above	GGGGACCACTTTGTACAAGAAAGCTGGGTCTAGTAGCCCTTTAGTTTATTCT
OEC57noStop		GGGACAAGTTTGTACAAAAAAGCAGGCTTGATGGCTCCTCTGAACGTCATTCAG	GGGGACCACTTTGTACAAGAAAGCTGGGTATGTCGAGTAACTTGGCCTG
OEC57		see above	GGGGACCACTTTGTACAAGAAAGCTGGGTCTATGTCGAGTAACTTGGCCT
OEC59noStop		GGGGACAAGTTTGTACAAAAAAGCAGGCTTGATGGTCTCTGCTTCGCTCAATAAC	GGGGACCACTTTGTACAAGAAAGCTGGGTAGTGATTGTTAGAATTGTAGACTAAA
OEC59		ATGGTCTCTGCTTCGCTCAATAAC	TCAGTGATTGTTAGAATTGTAGACTAAA
OEC60noStop		GGGGACAAGTTTGTACAAAAAAGCAGGCTTGATGGAAGATCTGTATGATTCATCTGAAG	GGGGACCACTTTGTACAAGAAAGCTGGGTAGAATTTTCTCTTCAAAATCAA
OEC60		see above	GGGGACCACTTTGTACAAGAAAGCTGGGTCTAGAATTTTCTCTTCAAAATCA
OEC61noStop		see above	GGGGACCACTTTGTACAAGAAAGCTGGGTAAATTTTGGTTACCGATG
OEC61		see above	GGGGACCACTTTGTACAAGAAAGCTGGGTCTAAATTTTGGTTACCGATG
OEC63noStop		GGGACAAGTTTGTACAAAAAAGCAGGCTTGATGGCAAATCCAGTGGAGACGGC	GGGGACCACTTTGTACAAGAAAGCTGGGTATATTAACTCCAGTACGATTC
OEC63		GGGGACAAGTTTGTACAAAAAAGCAGGCTTGATGGCAAATCCAGTGGAGACG	GGGGACCACTTTGTACAAGAAAGCTGGGTATATTAACTCCAGTACGATTCTTAT
OEC63		see above	GGGGACCACTTTGTACAAGAAAGCTGGGTTTATATTAACTCCAGTACGATTCTTA
OEC65		GGGGACAAGTTTGTACAAAAAAGCAGGCTTGATGGAACCGCTTTCGCTATGT	GGGGACCACTTTGTACAAGAAAGCTGGGTCTAAGGCTGCCAAATTTTTTG
OEC66		GGGGACAAGTTTGTACAAAAAAGCAGGCTTGATGACTAGGACATACGATACACCAGG	GGGGACCACTTTGTACAAGAAAGCTGGGTAAAGCGCATCCTTGAAC
OEC66		see above	GGGGACCACTTTGTACAAGAAAGCTGGGTCTAAAGCGCATCCTTGAAC
OEC67		GGGGACAAGTTTGTACAAAAAAGCAGGCTTGATGAGTGGTGATGCTCATGATAGAA	GGGGACCACTTTGTACAAGAAAGCTGGGTATAGGTACCTTTTGGTGTTGTC
OEC67		see above	GGGGACCACTTTGTACAAGAAAGCTGGGTCTATAGGTACCTTTTGGTGTTGT
OEC68		GGGGACAAGTTTGTACAAAAAAGCAGGCTTGATGTTGCTAAATGAGACTCAATCTGT	GGGGACCACTTTGTACAAGAAAGCTGGGTACCATACAGTTGTAAAAACAGAG
OEC68		see above	GGGGACCACTTTGTACAAGAAAGCTGGGTCTACCATACAGTTGTAAAAACAGAG
OEC70		GGGGACAAGTTTGTACAAAAAAGCAGGCTTGATGACAGAGACCGTAACAGTGTCTGTC	GGGGACCACTTTGTACAAGAAAGCTGGGTAAATCAACATCGCTACAAACC
OEC70		see above	GGGGACCACTTTGTACAAGAAAGCTGGGTCTAAATCAACATCGCTACAAACC
OEC71		GGGGACAAGTTTGTACAAAAAAGCAGGCTTGATGGTTCCATCTCCAAACACTCCC	GGGGACCACTTTGTACAAGAAAGCTGGGTAATTTTTGAAATTGTAACGCTTG
OEC71		see above	GGGGACCACTTTGTACAAGAAAGCTGGGTCTAATTTTTGAAATTGTAACGCTTG
OEC75		ATGTGTTCTGAGAAAGAAGTTGGG	TCATGAGATCTTCAGAAGATAC
OEC76		ATGCACTATCGAGTCCTTTTAGAG	TCATTCTCCACCGTCAACTAA
OEC77		ATGAAATACACCAGTAAAGCGCTC	TTATGTTGCAGTAAGTCTGGG
OEC78		ATGATTGAGAGTCCCTTGCGTG	TTAAATGCGTGTAAAACGCGA
OEC81		ATGTCTGTACTAATCCTCAAATTTC	CTAAGGTTTCAGGTTGGGTC
OEC83		ATGGAACCAAATCAATCCGGACAA	TTATTTCAGGGAAAGTCCCGC
OEC84		ATGTCACGAAGCTACCGAAGATC	TCATGGAGAAACCTTCCCTTT
OEC85		ATGTGCAGGCCAAAATTGCGCT	TTACTTGGAGACTTTAACTGTC
OEC88		ATGTTGTACGTTCTTTCTTTTCACG	TCACCTGCCCTTGTCGCG
OEC89		ATGAACGAATGTTTACCTAATGTTC	TCATATGTTTTGTCCATTTACTC
OEC90		ATGCTTGAGCTATGCAGTTTCAAG	TCAGTGTGAAGTTGCCCAAAA
OEC92		ATGTTTCCCCTTTACAATTTTAGGT	TTACCTTGTTATTGCACAATCG
OEC96		ATGGAAGTGGACATCCAGAGCG	TTAACTAGGTTTTCTCTTCGG
OEC97		ATGCGGATGGTTTGGTGGTATG	TCATTTAAAGTGCTCAGATATTG
OEC99		ATGGCTTCGATGTCCAATCGCAA	CTATGGCGCGCAACGACCA
OEC101		ATGGTAAATATCATAGTATCATCGTA	CTAATGGGCAACGGCAAGA
OEC103		ATGAACATAAAAGCAGGCTTTAGAG	TCATCTCACGGGTATGCGTA
OEC104		ATGGCATTCATTCCATTGTTCACG	TCATAACAAAACCAAGATCTTAA
OEC105		ATGTTACCTGCATGGGGTGAATA	TTAGCAATCAAGTGCTCCTCC
OEC106		ATGTTTAATCCGACTTGTTTAACAAT	TCAAGCAGTACGGTCTGACTT
OEC107		ATGATTGAAACCTTAACACTGTTCA	TCAACTATCCATTCCATTTTTTTC
OEC108		ATGCAGCATATGATCGGCCGAC	TTATTCGGAGCATCTATTCGG
OEC109		ATGAAGTATTACAGCAATCTACAGC	TTATTCTGTGTCTCTTTTACAAA
OEC110		ATGACTGACATCCGTCAAACGAA	CTAAAAATTACATTGTACGTAGT
OEC111		ATGGAGAAACCGGATGCATACAA	TCACATAAAAATTAAGAAACCGA
OEC112		ATGACCTGCTGGTATCCTGATG	TTAGTTAACATATCGTATATCAAA
OEC113		ATGAGCCTCTATCACAGCATAGT	CTATCGATTCTTTTCTGAAATTG
OEC115		ATGCACGTCGTGTCTAAGGCC	CTATCCCCTGTGTGCCTTG
OEC116		ATGGCCTACCCAGAATTTGTCAG	TTACAAAGCTAATGCCAATCCG
OEC117		ATGAAGTTATCTAGTTGTTTCTACG	TTAGAATTTTTTCTTGTAAGTTTGA
OEC118		ATGGCTCCTGCTCCCCCTCC	CTAATTCTTGGAATCCATAGGTT
OEC119		ATGTATCCGTTACATTTCAACGAAA	CTATTCTGGTGTCTCATATGATT
OEC120		ATGTTAGTGACTCCAAACATTATAG	CTAGCGAGGTCTTAGCACC
OEC123		ATGTCTACCATCCTTTCCAGAGA	TTAGTCCGATACCGCCTTGC
OEC125		ATGACCTATCATGAGGCCGACT	TCATTTCGGCCCGAATTTACA

Supplemental Table 2: Top100 expressed transcripts of the *G. orontii* haustorial library

G. orontii EST contig[a]	Protein description[b]	Sequence length[c]	Average coverage[d]	E-value[e]	Gene Bank Id[f]	Species[g]
Translation						
GoEST_c352	40s ribosomal protein s25	97	975	9,84E-34	XP_001228474	*Sordaria macrospora*
GoEST_c802	60s ribosomal protein l21	160	604	5,42E-80	XP_001546444	*Sclerotinia sclerotiorum*
GoEST_c3518	60s ribosomal protein l28	160	581	9,59E-69	P78987	*Blumeria graminis*
GoEST_c1623	60s ribosomal protein l11	175	502	1,56E-93	XP_001586298	*Sclerotinia sclerotiorum*
GoEST_c1706	40s ribosomal protein s7	181	476	2,95E-75	XP_001586490	*Sclerotinia sclerotiorum*
GoEST_c1709	60s ribosomal protein l17	186	453	9,85E-96	XP_001586516	*Sclerotinia sclerotiorum*
GoEST_c320	60s ribosomal protein l24	181	448	8,13E-55	EEY15953	*Paracoccidioides brasiliensis*
GoEST_c1797	40s ribosomal protein s13	151	444	1,08E-78	XP_001245252	*Coccidioides immitis*
GoEST_c940	60s ribosomal protein l12	165	442	9,17E-76	XP_001557403	*Botryotinia fuckeliana*
GoEST_c1585	60s ribosomal protein l10a	203	430	1,54E-100	XP_001598446	*Sclerotinia sclerotiorum*
GoEST_c2309	60s ribosomal protein l10-b	221	425	2,80E-121	XP_001551814	*Botryotinia fuckeliana*
GoEST_c901	Elongation factor 1-gamma	240	419	4,61E-67	XP_001598134	*Sclerotinia sclerotiorum*
GoEST_c2009	60s ribosomal protein l16	202	418	1,42E-103	XP_001555732	*Botryotinia fuckeliana*
GoEST_lrc4678	60s ribosomal protein l23	153	387	1,59E-59	XP_001597937	*Coccidioides posadasii*
GoEST_c952	40s ribosomal protein s14	151	374	4,39E-59	XP_359539	*Magnaporthe oryzae*
GoEST_c181	60s ribosomal protein l27-a	135	361	6,20E-67	XP_001556037	*Botryotinia fuckeliana*
GoEST_lrc4680	40s ribosomal protein s18	157	354	4,50E-80	XP_001557449	*Botryotinia fuckeliana*
GoEST_lrc4676	60s ribosomal protein l15	203	324	1,85E-93	XP_001545571	*Botryotinia fuckeliana*
GoEST_c464	40s ribosomal protein s26	122	324	1,17E-55	XP_001802422	*Phaeosphaeria nodorum*
GoEST_c191	37s ribosomal protein s24	135	324	8,14E-46	XP_001551271	*Botryotinia fuckeliana*
GoEST_c1686	60s ribosomal protein l33	109	322	5,98E-50	EEQ88513	*Ajellomyces dermatitidis*
GoEST_c665	60s ribosomal protein l28	166	315	1,24E-44	XP_001590212	*Sclerotinia sclerotiorum*
GoEST_c602	40s ribosomal protein s9	196	313	1,37E-78	XP_001594205	*Sclerotinia sclerotiorum*
GoEST_c1337	40s ribosomal protein s5	208	310	9,68E-108	XP_001559487	*Botryotinia fuckeliana*
GoEST_c1603	60s ribosomal protein	156	307	1,85E-76	XP_766572	*Botryotinia fuckeliana*
GoEST_lrc4677	Conserved hypothetical protein	198	295	3,54E-27	XP_001597145	*Sclerotinia sclerotiorum*
GoEST_c424	60s acidic ribosomal protein p2	110	281	1,10E-16	XP_965172	*Sordaria macrospora*
GoEST_c873	Ribosomal protein l14	148	277	3,31E-48	XP_001551610	*Botryotinia fuckeliana*
GoEST_c898	60s ribosomal protein l22	125	268	7,32E-38	XP_001910994	*Podospora anserina*
GoEST_c379	40s ribosomal protein s3	242	266	1,18E-126	XP_001551365	*Botryotinia fuckeliana*
GoEST_c1029	Translation initiation factor	96	260	2,28E-31	XP_001270644	*Podospora anserina*
GoEST_c422	60s ribosomal protein l35	127	256	5,53E-54	XP_001556843	*Botryotinia fuckeliana*
GoEST_c82	40s ribosomal protein s11	161	252	4,59E-84	XP_001589541	*Botryotinia fuckeliana*
GoEST_lrc4687	40s ribosomal protein s20	117	234	4,41E-52	XP_360829	*Magnaporthe oryzae*
GoEST_c258	60s ribosomal protein l23	64	230	9,62E-29	NP_001003100	*Botryotinia fuckeliana*
GoEST_c156	60s ribosomal protein l7	251	225	4,32E-99	XP_001546001	*Botryotinia fuckeliana*
GoEST_c36	60s ribosomal protein l24	159	224	8,89E-58	EEY15953	*Coccidioides immitis*
GoEST_c59	60s ribosomal protein	192	222	2,11E-86	XP_381330	*Verticillium albo-atrum*
GoEST_c388	Eukaryotic translation initiation factor 5a-2	104	222	5,34E-47	EEU34377	*Ajellomyces capsulatus*
GoEST_c772	60s ribosomal protein l6	141	217	2,21E-48	XP_002151439	*Neurospora crassa*
GoEST_c91	Conserved hypothetical protein	206	216	2,21E-23	XP_001220058	*Chaetomium globosum*
GoEST_c2025	40s ribosomal protein s15	152	215	9,51E-56	EEH33640	*Paracoccidioides brasiliensis*
GoEST_c269	60s ribosomal protein l19	198	213	1,46E-78	XP_001554456	*Botryotinia fuckeliana*
GoEST_c40	60s ribosomal protein l38	83	209	1,78E-29	XP_001587153	*Sclerotinia sclerotiorum*
Protein modification process						
GoEST_c1962	Ubiquitin	128	702	2,27E-67	XP_002172615	*Schizosaccharomyces japonicus*
GoEST_c1599	Ubiquitin	155	415	1,31E-65	XP_001538961	*Ajellomyces capsulatus*
GoEST_c2788	Ubiquitin	68	381	2,01E-24	AAC64787	*Candida tropicalis*
GoEST_c816	Ubiquitin conjugating enzyme	149	376	3,89E-74	XP_001270622	*Aspergillus clavatus*
GoEST_c144	Ubiquitin conjugating enzyme	151	210	1,02E-46	EEY23952	*Verticillium albo-atrum*

Supplemental Table 2 (continued from last page)

G. orontii EST contig[a]	Protein description[b]	Sequence length[c]	Average coverage[d]	E-value[e]	Gene Bank Id[f]	Species[g]
Protein catabolic process						
GoEST_c104	Conserved hypothetical protein	79	875	1,45E-13	XP_001931052	*Pyrenophora tritici-repentis*
GoEST_lrc4675	Proteasome component y7	120	658	1,78E-33	EEQ31310	*Pyrenophora tritici-repentis*
GoEST_c1083	Aspartyl protease	61	464	7,49E-08	XP_001557997	*Botryotinia fuckeliana*
Protein folding						
GoEST_c1770	Peptidyl-prolyl cis-trans isomerase	149	301	2,58E-57	AAQ16572	*Botryotinia fuckeliana*
GoEST_c525	Peptidyl-prolyl cis-trans isomerase	174	259	1,20E-66	AAQ16572	*Botryotinia fuckeliana*
Lipid metabolic process						
GoEST_c1373	Protein	105	463	1,69E-24	XP_369287	*Magnaporthe oryzae*
GoEST_c445	Acyl carrier	128	292	1,07E-34	XP_001793316	*Phaeosphaeria nodorum*
GoEST_c916	Glutation s-transferase	140	258	5,14E-34	XP_001550749	*Botryotinia fuckeliana*
Nucleobase, nucleoside, nucleotide and nucleic acid metabolic process						
GoEST_c1856	Small nuclear ribonucleoprotein	93	380	2,47E-33	XP_748912	*Aspergillus terreus*
GoEST_c45	Adomet-dependent trna methyltransferase complex subunit	162	241	3,57E-39	EEU44619	*Nectria haematococca*
GoEST_lrc4686	Exosome complex exonuclease rrp41	72	232	2,16E-24	XP_001791170	*Phaeosphaeria nodorum*
Generation of precursor metabolites and energy						
GoEST_c1652	ATP synthase subunit	88	332	5,32E-08	XP_001592079	*Sclerotinia sclerotiorum*
GoEST_c116	ATP synthase d mitochondrial	159	325	4,90E-68	XP_001593857	*Sclerotinia sclerotiorum*
GoEST_c209	CHCH domain protein	153	218	1,51E-21	XP_001545865	*Botryotinia fuckeliana*
Organelle organization						
GoEST_c1342	Histone H3	136	472	5,35E-72	NP_001106556	*Xenopus (Silurana) tropicalis*
GoEST_c699	Profilin	129	458	7,78E-30	XP_386568	*Gibberella zeae*
GoEST_c400	Histone H4	103	440	6,60E-40	EEU42757	*Podospora anserina*
Cellular homeostasis						
GoEST_c351	TSA/AhpC family protein	161	467	3,01E-43	XP_001555759	*Penicillium marneffei*
GoEST_c612	Thioredoxin H	115	284	2,54E-20	XP_001829191	*Coprinus comatus*
Cell cycle						
GoEST_c245	HSP90 binding co-chaperone	160	290	6,23E-30	XP_370172	*Magnaporthe oryzae*
Ion transport						
GoEST_c38	Phosphate transporter	152	216	3,95E-62	XP_001597838	*Sclerotinia sclerotiorum*
Mycelium development						
GoEST_c1119	Conidiation-specific protein-8	83	947	4,53E-10	XP_001586299	*Sclerotinia sclerotiorum*
GoEST_c586	Conserved hypothetical protein	201	846	5,62E-46	XP_001590087	*Sclerotinia sclerotiorum*
GoEST_c886	CAP20 homolog	144	264	4,94E-51	AAK69534	*Blumeria graminis*
GoEST_c284	G-protein complex beta subunit	196	226	9,38E-68	EEU45366	*Magnaporthe oryzae*
Vitamin metabolic process						
GoEST_c729	Riboflavin kinase	218	283	7,98E-49	Q6M923	*Schizophyllum commune*
Pathogenesis						
GoEST_c231	Extracellular matrix protein	221	224	3,03E-22	CAQ16265	*Glomerella graminicola*
Protein localization						
GoEST_c32	Membrane biogenesis protein	171	292	1,34E-63	XP_001598487	*Phaeosphaeria nodorum*
No functional annotation						
GoEST_c2903	---NA---	102	1463			
GoEST_c2438	---NA---	108	925			
GoEST_c1507	---NA---	135	823			
GoEST_c2235	---NA---	18	695			
GoEST_c997	---NA---	171	666			
GoEST_c501	Conserved hypothetical protein	207	664	8,24E-15	XP_001595620	*Sclerotinia sclerotiorum*
GoEST_c2503	---NA---	101	635			
GoEST_c2918	---NA---	89	571			
GoEST_c1211	---NA---	91	453			
GoEST_c735	---NA---	69	453			
GoEST_c1162	---NA---	65	431			
GoEST_c1495	---NA---	58	406			
GoEST_c658	Conserved hypothetical protein	177	371	1,14E-20	XP_001556665	*Botryotinia fuckeliana*
GoEST_lrc4679	---NA---	139	349			
GoEST_c740	---NA---	35	309			
GoEST_c636	---NA---	168	306			
GoEST_c268	CFEM domain containing protein	154	305	1,30E-05	XP_001911616	*Podospora anserina*
GoEST_c484	Conserved hypothetical protein	113	287	1,44E-22	XP_002560580	*Sclerotinia sclerotiorum*
GoEST_c2693	---NA---	104	257			
GoEST_c641	Conserved hypothetical protein	159	256	1,03E-11	XP_001596723	*Sclerotinia sclerotiorum*
GoEST_c819	---NA---	45	234			
GoEST_c85	---NA---	163	223			
GoEST_c184	---NA---	141	218			

a: Identifier of assembled EST contigs
b: Description of haustorial genes derived from Blast2GO
c: Length of predicted proteins
d: Average coverage of transcripts
e: e-value as reported by blastp from Blast2GO
f: Gene identifier of best hit reported by Blast2GO
g: Species of best hit reported by Blast2GO

Supplemental Table 3: Top50 expressed transmembrane protein encoding genes of the *G. orontii* haustorial library.

G. orontii EST contig[a]	Protein description[b]	Sequence length[c]	Average coverage[d]	E-value[e]	Gene Bank Idf	Species[g]
Protein localization						
GoEST_c32	Membrane biogenesis protein Yop1	171	292	1,34E-63	XP_001598487	*Phaeosphaeria nodorum*
GoEST_c25	Synaptobrevin	121	173	1,21E-38	XP_002148838	*Penicillium chrysogenum*
GoEST_c1027	Mitochondrial import receptor subunit tom22	117	70	2,56E-19	XP_001598196	*Sclerotinia sclerotiorum*
GoEST_c282	Endosomal cargo receptor	210	68	7,54E-80	XP_001554064	*Botryotinia fuckeliana*
GoEST_c402	Mitochondrial import receptor subunit tom22	119	67	3,52E-20	XP_001598196	*Sclerotinia sclerotiorum*
Generation of precursor metabolites and energy						
GoEST_c183	Cytochrome c oxidase subunit V	176	144	8,75E-58	XP_001591171	*Chaetomium globosum*
GoEST_c208	Cytochrome c oxidase subunit VIa	117	136	1,16E-31	XP_001546435	*Botryotinia fuckeliana*
GoEST_c272	NADH:ubiquinone oxidoreductase subunit	125	133	3,03E-29	XP_001592645	*Sclerotinia sclerotiorum*
GoEST_c41	Cytochrome c	80	125	4,87E-21	XP_001546681	*Sclerotinia sclerotiorum*
GoEST_c11	Mitochondrial f1f0 atp synthase subunit f	101	121	4,24E-39	XP_001547689	*Botryotinia fuckeliana*
GoEST_c42	Succinate dehydrogenase cytochrome b560 subunit	163	111	3,21E-45	XP_001547075	*Botryotinia fuckeliana*
GoEST_c147	Cytochrome c oxidase assembly protein ctag	104	101	1,29E-20	XP_001545817	*Botryotinia fuckeliana*
GoEST_c515	Conserved hypothetical protein	281	84	4,14E-21	XP_001596851	*Sclerotinia sclerotiorum*
GoEST_c35	NADH-ubiquinone oxidoreductase 9,5 kda subunit	118	83	8,42E-23	XP_001552000	*Botryotinia fuckeliana*
GoEST_c4	NADH-ubiquinone oxidoreductase 213 kda subunit	192	80	1,72E-35	XP_001550622	*Coccidioides posadasii*
GoEST_c128	Cytochrome C1	281	70	2,46E-119	XP_001556506	*Botryotinia fuckeliana*
GoEST_c495	NADH-ubiquinone oxidoreductase 14 kda	92	65	6,71E-25	XP_002484810	*Paracoccidioides brasiliensis*
Lipid metabolic process						
GoEST_c103	C-4 methyl sterol oxidase	303	71	6,23E-126	XP_001547478	*Botryotinia fuckeliana*
Protein modification process						
GoEST_c477	Prenyl cysteine carboxyl methyltransferase	229	92	6,08E-28	XP_382626	*Gibberella zeae*
GoEST_c135	Dolichyl-phosphate mannosyltransferase polypeptide 3	92	66	7,76E-13	EEY23436	*Verticillium albo-atrum*
Response to stimulus						
GoEST_c69	Stress response rci	57	135	1,44E-13	XP_569421	*Coccidioides immitis*
GoEST_c478	Stress response rci	77	87	4,11E-13	CAP65494	*Magnaporthe oryzae*
GoEST_c569	Opsin 1	135	60	2,83E-58	XP_001597420	*Sclerotinia sclerotiorum*
Ion transport						
GoEST_c38	Phosphate transporter	152	216	3,95E-62	XP_001597838	*Sclerotinia sclerotiorum*
Mycelium development						
GoEST_c589	Integral membrane protein	112	63	7,88E-07	XP_001222747	*Chaetomium globosum*
Regulation of apoptosis						
GoEST_c70	Mitochondrial membrane fission protein	154	101	2,16E-61	XP_001548925	*Botryotinia fuckeliana*
GoEST_c53	Bax inhibitor family protein	125	63	2,93E-32	XP_001595227	*Sclerotinia sclerotiorum*

Supplemental Table 3 (continued from last page)

G. orontii EST contig[a]	Protein description[b]	Sequence length[c]	Average coverage[d]	E-value[e]	Gene Bank Idf	Species[g]
No functional annotation						
GoEST_lrc4907	---NA---	139	350			
GoEST_c636	---NA---	168	306			
GoEST_c641	Hypothetical protein	159	256	1,03E-11	XP_001596723	*Sclerotinia sclerotiorum*
GoEST_c184	---NA---	141	218			
GoEST_c17	Mitochondrial hypoxia responsive domain protein	167	104	5,83E-45	XP_001545600	*Botryotinia fuckeliana*
GoEST_c80	Conserved hypothetical protein	146	158	9,45E-30	XP_001560656	*Botryotinia fuckeliana*
GoEST_c133	Hypothetical protein	93	154	2,94E-14	XP_001586834	*Sclerotinia sclerotiorum*
GoEST_c450	Conserved hypothetical protein	201	149	5,82E-41	XP_001593371	*Sclerotinia sclerotiorum*
GoEST_c674	Conserved hypothetical protein	254	122	4,60E-58	XP_001560540	*Botryotinia fuckeliana*
GoEST_c249	Cytochrome b5	134	119	1,78E-36	XP_001585515	*Sclerotinia sclerotiorum*
GoEST_c504	Conserved hypothetical protein	237	111	3,15E-50	XP_001545677	*Botryotinia fuckeliana*
GoEST_c120	Conserved hypothetical protein	96	91	1,90E-23	XP_001588360	*Sclerotinia sclerotiorum*
GoEST_c7	Conserved hypothetical protein	165	86	5,38E-27	XP_001557757	*Botryotinia fuckeliana*
GoEST_c304	Staphylococcal nuclease domain containing protein	223	84	1,44E-74	XP_001559036	*Sclerotinia sclerotiorum*
GoEST_c108	NAD-binding domain 4 protein	409	83	8,46E-71	XP_001390934	*Aspergillus niger*
GoEST_c517	Ubiquitin-domain protein	237	76	6,87E-34	XP_001910410	*Podospera anserina*
GoEST_c568	Conserved hypothetical protein	126	71	1,44E-18	XP_001593081	*Sclerotinia sclerotiorum*
GoEST_c895	Hypothetical protein	76	61	1,98E-33	XP_001597584	*Sclerotinia sclerotiorum*
GoEST_c239	---NA---	90	61			
GoEST_c368	---NA---	237	60			
GoEST_c833	Conserved hypothetical protein	150	58	4,18E-10	XP_001560812	*Botryotinia fuckeliana*
GoEST_c678	---NA---	279	57			

a: Identifier of assembled EST contigs
b: Description of haustorial genes derived from Blast2GO
c: Length of predicted proteins
d: Average coverage of transcripts
e: e-value as reported by blastp from Blast2GO
f: Gene identifier of best hit reported by Blast2GO
g: Species of best hit reported by Blast2GO

Supplemental Table 4: Top50 expressed secreted protein encoding genes of the *G. orontii* haustorial library.

G. orontii EST contig[a]	Protein description[b]	Sequence length[c]	Average coverage[d]	E-value[e]	Gene Bank Idf	Species[g]	Effector candidate
No functional annotation							
GoEST_c2438	---NA---	108	925				x
GoEST_c997	---NA---	171	666				x
GoEST_c501	Conserved hypothetical protein	207	664	8,24E-15	XP_001595620	*Sclerotinia sclerotiorum*	
GoEST_lrc4679	---NA---	139	349				x
GoEST_c268	CFEM domain containing protein	154	305	1,30E-05	XP_001911616	*Podospora anserina*	
GoEST_c47	---NA---	28	188				
GoEST_c367	Hypothetical protein	91	180	1,80E-05	XP_001590989	*Sclerotinia sclerotiorum*	
GoEST_c500	---NA---	206	136				x
GoEST_c2239	---NA---	109	122				x
GoEST_c62	---NA---	133	118				x
GoEST_c253	---NA---	86	78				x
GoEST_c285	Conserved hypothetical protein	181	77	1,02E-25	EEU43966	*Gibberella zeae*	
GoEST_c392	Conserved hypothetical protein	216	66	5,54E-45	EEY18756	*Verticillium albo-atrum*	
GoEST_c348	---NA---	113	64				x
GoEST_c1080	---NA---	79	48				x
GoEST_c4732	---NA---	76	41				x
GoEST_c956	Carbonic anhydrase	281	41	6,74E-66	XP_001552065	*Botryotinia fuckeliana*	
GoEST_c821	Allergen asp f4	344	36	3,03E-54	XP_001559716	*Botryotinia fuckeliana*	
GoEST_c943	Conserved hypothetical protein	173	35	6,94E-29	XP_001597032	*Botryotinia fuckeliana*	
GoEST_c1195	---NA---	117	34				x
GoEST_c808	---NA---	213	33				x
GoEST_lrc11563	Conserved hypothetical protein	137	27	3,68E-25	XP_001593371	*Sclerotinia sclerotiorum*	
GoEST_c5169	---NA---	144	27				x
GoEST_c27130	---NA---	65	26				x
GoEST_c5274	---NA---	116	23				x
GoEST_c5194	Covalently-linked cell wall protein	329	20	2,65E-58	AAK95385	*Blumeria graminis*	
GoEST_c5773	---NA---	100	19				x
GoEST_c4872	---NA---	137	19				x
GoEST_c2118	---NA---	194	19				x
GoEST_c5051	---NA---	176	18				x
GoEST_c5962	---NA---	70	17				x
GoEST_c4284	Extracellular serine-threonine rich protein	291	17	2,25E-17	XP_001594618	*Sclerotinia sclerotiorum*	
GoEST_c5451	---NA---	202	15				x
Protein metabolic process							
GoEST_c424	60s acidic ribosomal protein p2	110	281	1,10E-16	XP_965172	*Sordaria macrospora*	
GoEST_c335	Peptidyl-prolyl cis-trans isomerase b	209	120	1,90E-66	XP_001556077	*Botryotinia fuckeliana*	
GoEST_c115	Aspartic endopeptidase pep2	396	81	7,22E-167	XP_001554261	*Botryotinia fuckeliana*	
GoEST_c13	Serine protease	358	57	9,10E-84	XP_001586618	*Sclerotinia sclerotiorum*	
GoEST_c262	FKBP-type peptidyl-prolyl cis-trans isomerase	168	55	9,29E-46	XP_001585920	*Sclerotinia sclerotiorum*	
GoEST_c5463	Oligosaccharyltransferase subunit ribophorin	136	23	3,32E-22	XP_001937381	*Sclerotinia sclerotiorum*	
Carbohydrate metabolic process							
GoEST_c4743	Beta-glucanosyltransferase GEL1	415	29	0,00E+00	XP_001550496	*Blumeria graminis*	
GoEST_c4968	Chitin deacetylase	324	27	1,90E-134	AAK84438	*Blumeria graminis*	
GoEST_c4808	Xylanase 3	378	18	2,24E-92	XP_001597291	*Sclerotinia sclerotiorum*	
Mycelium development							
GoEST_c260	CFEM-domain containing protein	210	195	2,64E-22	XP_001549293	*Botryotinia fuckeliana*	
Transport							
GoEST_c242	Endoplasmic reticulum vesicle protein	204	136	1,00E-69	XP_001588872	*Sclerotinia sclerotiorum*	
GoEST_c227	Endosomal cargo receptor	124	84	1,94E-24	XP_001545203	*Magnaporthe oryzae*	
GoEST_c583	Secretory pathway protein	220	50	3,19E-46	XP_001556350	*Botryotinia fuckeliana*	
Lipid metabolic process							
GoEST_c5560	Conserved hypothetical protein	157	24	6,29E-44	XP_001593645	*Sclerotinia sclerotiorum*	
Pathogenesis							
GoEST_c231	Extracellular matrix protein	221	224	3,03E-17	CAQ16265	*Glomerella graminicola*	
GoEST_c5330	Cell surface protein	365	16	6,45E-108	AAK25793	*Blumeria graminis*	
Superoxide metabolic process							
GoEST_c1259	Cu Zn superoxide dismutase	233	30	1,92E-63	XP_001556224	*Botryotinia fuckeliana*	

a: Identifier of assembled EST contigs
b: Description of haustorial genes derived from Blast2GO
c: Length of predicted proteins
d: Average coverage of transcripts
e: e-value as reported by blastp from Blast2GO
f: Gene identifier of best hit reported by Blast2GO
g: Species of best hit reported by Blast2GO

Supplemental Table 5: Transporter proteins present in the *G. orontii* haustorial library.

G. orontii EST contig[a]	Protein description[b]	Sequence length[c]	Average coverage[d]	E-value[e]	Gene Bank Id[f]	Species[g]
Sugar transporters						
GoEST_c5014	MFS sugar	256	26	3,38E-72	EEU39950	*Nectria haematococca*
GoEST_c5054	MFS maltose permease	247	17	2,00E-128	XP_002484658	*Talaromyces stipitatus*
GoEST_c5149	MFS sugar	215	16	2,60E-95	XP_001803583	*Phaeosphaeria nodorum*
GoEST_c5621	Sucrose transporter	152	16	7,99E-45	XP_001240500	*Coccidioides immitis*
GoEST_c5621	Sucrose transporter	152	16	7,99E-45	XP_001240500	*Coccidioides immitis*
GoEST_c6506	Maltose permease	323	11	1,52E-84	EEU35698	*Nectria haematococca*
GoEST_c6236	MFS monosaccharide	377	9	1,94E-164	XP_001590994	*Sclerotinia sclerotiorum*
GoEST_c6579	MFS sugar	95	9	5,04E-14	EDP48424	*Aspergillus fumigatus*
GoEST_c10133	High affinity glucose transporter rgt2	135	8	2,25E-31	XP_001594028	*Sclerotinia sclerotiorum*
GoEST_c8982	High-affinity glucose transporter	142	8	8,30E-42	XP_001594028	*Sclerotinia sclerotiorum*
Amino Acid transporters						
GoEST_c311	GABA permease	298	49	2,98E-116	XP_001552644	*Botryotinia fuckeliana*
GoEST_c4777	MFS amine	140	41	2,37E-28	XP_001523046	*Magnaporthe grisea*
GoEST_c4945	GABA permease	353	16	1,66E-154	XP_001592106	*Sclerotinia sclerotiorum*
GoEST_c6938	Amino acid permease	169	7	1,66E-94	XP_001554295	*Botryotinia fuckeliana*
GoEST_c8611	Large neutral amino acids transporter small subunit 2	174	6	1,98E-80	XP_001598606	*Sclerotinia sclerotiorum*
GoEST_c9414	Oligopeptide transporter	215	5	2,48E-68	CAI79386	*Blumeria graminis*
Drug Efflux transporters						
GoEST_c153	MFS drug efflux	314	60	2,41E-58	XP_660841	*Aspergillus nidulans*
GoEST_c1098	MFS multidrug	235	40	7,97E-26	XP_002486702	*Talaromyces stipitatus*
GoEST_c728	MFS multidrug	398	31	2,79E-97	XP_001550345	*Botryotinia fuckeliana*
GoEST_c755	MFS multidrug	344	30	1,52E-92	XP_383231	*Gibberella zeae*
GoEST_c5353	MFS multidrug	90	14	1,21E-70	XP_001559102	*Botryotinia fuckeliana*
GoEST_c7565	MFS multidrug transporter	272	12	3,02E-30	XP_002145814	*Penicillium marneffei*
GoEST_c7486	MFS drug efflux	365	10	2,74E-125	XP_001401988	*Aspergillus niger*
GoEST_c6501	MFS multidrug	80	9	1,91E-15	XP_001906690	*Podospora anserina*
Other transporters						
GoEST_c38	Phosphate transporter	152	216	8,60E-60	XP_001597838	*Sclerotinia sclerotiorum*
GoEST_c378	Izh family channel protein	389	58	1,08E-152	ACA43006	*Sporothrix schenckii*
GoEST_c4720	MFS monocarboxylic acid transporter	274	22	4,68E-72	XP_001555261	*Botryotinia fuckeliana*
GoEST_c5331	Sulfate transporter	303	17	6,00E-45	EEY21422	*Verticillium albo-atrum*
GoEST_c5530	Pantothenate transporter liz1	217	13	6,08E-45	XP_001593662	*Sclerotinia sclerotiorum*
GoEST_c6922	Potassium ion transporter	111	13	2,35E-28	XP_001558290	*Botryotinia fuckeliana*
GoEST_c7783	MFS	205	10	2,81E-43	EEY22694	*Verticillium albo-atrum*
GoEST_c7062	Voltage-gated chloride channel	218	9	1,40E-94	XP_001552228	*Botryotinia fuckeliana*
GoEST_c7409	High-affinity iron transporter	106	8	1,83E-64	XP_001597434	*Sclerotinia sclerotiorum*
GoEST_c7295	MFS transporter	339	8	2,62E-107	XP_001585932	*Sclerotinia sclerotiorum*
GoEST_c9403	Calcium ion transporter	179	7	2,03E-53	XP_001560775	*Botryotinia fuckeliana*
GoEST_c8512	C4-dicarboxylate transporter malic acid transport	277	7	1,00E-106	XP_001596399	*Sclerotinia sclerotiorum*
GoEST_c10216	MFS phosphate transporter	91	6	1,40E-49	XP_958868	*Neurospora crassa*
GoEST_c10623	Na+ H+ antiporter nha1	95	6	3,12E-33	XP_001598436	*Sclerotinia sclerotiorum*
GoEST_c7720	Urea transporter	231	6	1,01E-93	XP_964341	*Neurospora crassa*
GoEST_c11501	Membrane transporter	88	5	1,89E-18	XP_001585435	*Sclerotinia sclerotiorum*

a: Identifier of assembled EST contigs
b: Description of haustorial genes derived from Blast2GO
c: Length of predicted proteins
d: Average coverage of transcripts
e: e-value as reported by blastp from Blast2GO
f: Gene identifier of best hit reported by Blast2GO
g: Species of best hit reported by Blast2GO

Supplemental Table 6: Pathogenesis-related transcripts identified in the *G. orontii* haustorial library.

G. orontii EST contig[a]	Protein description[b]	Sequence length[c]	Average coverage[d]	E-value[e]	Gene Bank Idf	Species[g]
Pathogenesis						
GoEST_c136	Autophagic death protein aut7	89	130	8,4E-36	XP_001909318	*Trichophyton verrucosum*
GoEST_c41	Cytochrome C	80	125	4,9E-21	XP_001546681	*Sclerotinia sclerotiorum*
GoEST_c126	Exosome complex subunit	233	91	7,6E-80	XP_001554662	*Botryotinia fuckeliana*
GoEST_c615	Fungal specific transcription	113	53	4,3E-17	XP_002144445	*Talaromyces stipitatus*
GoEST_c139	G-protein alpha subunit	206	51	2E-108	CAC10177	*Blumeria graminis*
GoEST_c1044	gEgh16	208	37	2,7E-83	AAB05211	*Blumeria graminis*
GoEST_c4898	ER lumen protein retaining	106	36	1,5E-33	XP_001597574	*Sclerotinia sclerotiorum*
GoEST_c730	Adenylate cyclase	286	32	2E-119	CAC19663	*Blumeria graminis*
GoEST_c4866	Mitogen-activated protein kinase	246	24	2E-133	AAG53654	*Blumeria graminis*
GoEST_c4904	Peroxisomal hydratase-dehydrogenase-epimerase	275	22	7,1E-94	XP_001589313	*Sclerotinia sclerotiorum*
GoEST_c4882	Guanine nucleotide-binding protein beta subunit	149	20	2,5E-77	XP_001595393	*Sclerotinia sclerotiorum*
GoEST_c1475	Rho GTPase	199	20	5E-103	XP_366655	*Magnaporthe oryzae*
GoEST_c5253	Neutral trehalase	329	18	4E-139	XP_001593547	*Sclerotinia sclerotiorum*
GoEST_c5330	Cell surface protein	365	16	6E-113	AAK25793	*Blumeria graminis*
GoEST_c5597	Hypothetical protein	207	14	2,4E-47	XP_001554384	*Botryotinia fuckeliana*
GoEST_c6529	Polymerase zeta subunit	136	14	6,2E-56	EEU47080	*Nectria haematococca*
GoEST_c6706	Guanine nucleotide-binding protein beta subunit	89	11	1,5E-23	AAL90861	*Botryotinia fuckeliana*
GoEST_c6115	Transcription factor stea	331	11	9,6E-78	ACJ06644	*Botryotinia fuckeliana*
GoEST_c6291	Hypothetical protein	87	11	1,2E-22	XP_001587154	*Sclerotinia sclerotiorum*
GoEST_c7421	cAMP-dependent protein kinase catalytic subunit 1	91	10	1,3E-42	CAB61490	*Blumeria graminis*
GoEST_c6322	Carnitine o-acetyltransferase	395	10	0	XP_001547114	*Botryotinia fuckeliana*
GoEST_c6555	Phosphoenolpyruvate carboxykinase	394	9	0	XP_001596065	*Sclerotinia sclerotiorum*
GoEST_c7900	Neutral trehalase	165	9	1,6E-73	XP_001547841	*Podospora anserina*
GoEST_c7068	Hypothetical protein	414	8	2E-118	XP_001561172	*Botryotinia fuckeliana*
GoEST_c7493	Hypothetical protein	223	8	2,7E-57	XP_001405070	*Magnaporthe oryzae*
GoEST_c7138	Yt521-b-like splicing	326	8	4,6E-95	XP_001553612	*Botryotinia fuckeliana*
GoEST_c6762	Dual specificity protein kinase pom1	151	7	8,9E-82	EEY14178	*Sordaria macrospora*
GoEST_c6908	Developmental regulator flba	143	7	1,2E-47	XP_001589336	*Sclerotinia sclerotiorum*
GoEST_c8367	RNApii degradation factor	113	6	7,4E-11	XP_001592227	*Sclerotinia sclerotiorum*
GoEST_c12113	S-adenoslymethionine synthetase	82	6	1E-37	XP_001556886	*Botryotinia fuckeliana*
GoEST_c9383	Rho-like gtpase cdc42	194	6	1E-104	XP_368778	*Magnaporthe oryzae*
GoEST_c8081	Rhomboid family membrane protein	227	6	2,9E-65	XP_001553034	*Podospora anserina*
GoEST_c9267	Hypothetical protein	249	5	1,2E-93	XP_001588481	*Sclerotinia sclerotiorum*
GoEST_c8707	Peroxisomal multifunctional beta-oxidation protein	187	5	5,1E-82	XP_001400728	*Sclerotinia sclerotiorum*
GoEST_c9724	Serine threonine protein kinase	187	5	3,3E-55	XP_001556061	*Botryotinia fuckeliana*
GoEST_c10398	SH3 domain protein	124	5	5,3E-59	XP_961833	*Sordaria macrospora*

a: Identifier of assembled EST contigs
b: Description of haustorial genes derived from Blast2GO
c: Length of predicted proteins
d: Average coverage of transcripts
e: e-value as reported by blastp from Blast2GO
f: Gene identifier of best hit reported by Blast2GO
g: Species of best hit reported by Blast2GO

Supplemental Table 7: Prediction and bioinformatic analysis of OECs.

OEC	Cloned	Identified from	AverageCoverage	Length in AA	InterProScan results	# of cysteins	Cysteins/100AA	NLStradamus	NucPred	YxC motiv	FxC motiv	tBLASTn vs. *Bgh* genome	E-value	BLASTp vs. *Bgh* CSEPs	E-value	tBLASTn vs. *E. pisi* genome	E-value
OEC10	x	Go_EST_c500	135,69	221	-	8	3,6	Y 88	0.71		x			CSEP0078	3E-08	Contig1659.1	1E-25
OEC100		Go_EST_c3141	3,2	87	-	0	0,0	N	0.07								
OEC101	x	Go_EST_c16200	2,21	87	WD40/YVTN_repeat-like_dom	0	0,0	N	0.02			cabog_capped_contig_008640	8e-24			Contig9307.1	4E-27
OEC102		Go_EST_c5416	19,75	89	-	0	0,0	N	0.00			cabog_capped_contig_005335	2e-07	CSEP0051	2E-14	Contig18986.1	9E-20
OEC103	x	Go_EST_c10818	3,93	92	-	0	0,0	N	0.15							Contig11598.1	6E-09
OEC104	x	Go_EST_c13637	2,43	93	-	2	2,2	N	0.01								
OEC105	x	Go_EST_c4925	25,76	94	-	7	7,4	N	0.16	x		cabog_capped_contig_000032	7e-20	CSEP0277	2E-17	Contig10737.1	7E-15
OEC106	x	Go_EST_c9662	4,7	94	-	5	5,3	N	0.13								
OEC107	x	Go_EST_c216658	1,52	100	-	4	4,0	N	0.39								
OEC108	x	Go_EST_c2987	4,87	102	-	4	3,9	N	0.37		x						
OEC109	x	Go_EST_c19201	1,79	103	-	4	3,9	N	0.07								
OEC11	x	Go_EST_c11509	4,25	219	-	1	0,5	N	0.24					CSEP0420	2E-09	Contig1756.1	2E-22
OEC110	x	Go_EST_c9925	5,81	107	-	4	3,7	N	0.07								
OEC111	x	Go_EST_c5455	13,18	109	-	0	0,0	N	0.04							Contig3715.1	5E-07
OEC112	x	Go_EST_c3523	2,42	112	-	11	9,8	N	0.12			cabog_capped_contig_004399	2e-21			Contig10858.1	5E-35
OEC113	x	Go_EST_c1107	41,31	113	-	4	3,5	N	0.05							Contig4396.1	2E-10
OEC114		Go_EST_lrc29590	2,77	126	-	3	2,4	N	0.06			cabog_capped_contig_005736	7e-14			Contig16310.1	4E-21
OEC115	x	Go_EST_c62	117,58	133	-	6	4,5	N	0.14		x					Contig5879.1	7E-15
OEC116	x	Go_EST_c1507	823,48	135	-	1	0,7	N	0.06					CSEP0040	4E-29	Contig11903.1	7E-25
OEC117	x	Go_EST_c12607	3,74	136	-	2	1,5	N	0.26							Contig15401.1	2E-07
OEC118	x	Go_EST_c4872	19,27	137	-	0	0,0	N	0.12							Contig4163.1	1E-13
OEC119	x	Go_EST_c10851	4,18	141	-	1	0,7	N	0.41								
OEC120	x	Go_EST_c7101	11,64	148	-	3	2,0	N	0.35								
OEC121		Contig3216.1		171	-	3	1,8	N	0.47								
OEC122		Go_EST_c1061	24,44	170	-	6	3,5	N	0.15			cabog_capped_contig_004165	7e-07			Contig8728.1	2E-20
OEC123	x	Bgh02945		178	Microbial ribonucleases	6	3,4	N	0.32			cabog_capped_contig_004470	1e-11	CSEP0078	6E-16	Contig6127.1	1E-25
OEC124		Bgh01675		194	-	7	3,6	N	0.46		x			CSEP0078	2E-08	Contig5879.1	6E-24
OEC125	x	Go_EST_c3174	14,07	104	-	1	1,0	Y	0.66		x			CSEP0078	3E-08	Contig1659.1	5E-27
OEC126	x	Go_EST_c1130		146	-	3	2,1	N	0.14								
OEC127		Contig1310.1		127	-	7	5,5	N	0.13								
OEC13		Go_EST_c808	33,41	259	-	4	1,5	N	0.26							Contig11556.1	2E-06
OEC14	x	Go_EST_c5451	15,37	202	Coiled-coil domain	5	2,5	N	0.36	x						Contig4588.1	4E-11
OEC15	x	Go_EST_c6319	12,11	198	Microbial ribonucleases	6	3,0	N	0.20					CSEP0342	3E-16	Contig2823.1	3E-24
OEC16	x	Go_EST_c2118	18,93	194	Ribonuclease/ribotoxin	7	3,6	N	0.46		x			CSEP0078	2E-08	Contig5879.1	6E-24
OEC16a	x	Contig213.1		212	-	10	4,7	N	0.29								
OEC17		Go_EST_c2239	121,57	192	-	2	1,0	N	0.11			cabog_capped_contig_006863	1e-32			Contig11266.1	7E-40
OEC20	x	Go_EST_c7806	6,49	180	-	2	1,1	N	0.59							Contig45953.1	4E-07
OEC21	x	Go_EST_c5051	18,35	176		6	3,4	N	0.06							Contig6506.1	4E-23
OEC22	x	Go_EST_c7195	13,28	173	-	3	1,7	N	0.58								
OEC23	x	Go_EST_c6294	13,59	170	-	7	4,1	N	0.17	x							
OEC23a	x	Contig10334.1		157	-	7	4,5	N	0.18	2x							
OEC23b	x	Contig23615.1		173	-	7	4,0	N	0.11								
OEC24	x	Go_EST_c7190	11,15	167	-	2	1,2	N	0.54							Contig9661.1	3E-22
OEC25	x	Go_EST_c20364	1,61	165	-	7	4,2	N	0.05								
OEC25b	x	Contig19482.1		170	-	9	5,3	N	0.13	x							
OEC27	x	Go_EST_c6056	12,57	160		4	2,5	N	0.10		x						
OEC28	x	Go_EST_c268	305,33	154	CFEM domain	11	7,1	N									
OEC29	x	Go_EST_c2096	5,79	153	-	4	2,6	N	0.39		x						
OEC30	x	Go_EST_c11696	3,38	144	-	5	3,5	N	0.19		x						
OEC31	x	Go_EST_lrc6103	26,44	139	-	0	0,0	N	0.11					CSEP0441	9E-22	Contig3228.1	4E-30
OEC32		Go_EST_c8226	6,25	133	-	2	1,5	N		x						Contig5148.1	4E-11
OEC33		Go_EST_c599	632,14	175	-	0	0,0	Y	0.27							Contig7156.1	7E-07
OEC33.1		Go_EST_c3641	537,42	93		0	0,0	N	0.28							Contig7156.1	7E-07
OEC33.2	x	Go_EST_c997	666,32	171		0	0,0	N	0.42								
OEC35	x	Go_EST_c10045	4,82	126	-	0	0,0	N	0.06							Contig4677.1	9E-07
OEC37	x	Go_EST_c6918	14,09	121		6	5,0	N	0.26								
OEC38		Go_EST_c9349	5,38	121	-	5	4,1	N	0.29								
OEC39	x	Go_EST_c10702	6,28	120	-	3	2,5	N	0.03		x						
OEC40		Go_EST_c6800	10,86	235	-	8	3,4	Y 105	0.66		x			CSEP0078	3E-08	Contig1659.1	5E-27
OEC41	x	Go_EST_c9319	5,68	136	-	5	3,7	N	0.11	x							
OEC42	x	Go_EST_c1195	34,18	117	-	5	4,3	N	0.26								
OEC43	x	Go_EST_lrc4832	154,3	117	-	0	0,0	N	0.24					CSEP0307	3E-22	Contig10247.1	5E-19
OEC44	x	Go_EST_c16660	2,36	117	-	2	1,7	N	0.06	x							
OEC45	x	Go_EST_c5274	23,38	116		8	6,9	N	0.32	x							
OEC46		Go_EST_c348	64,44	113	-	0	0,0	N	0.46								
OEC47	x	Go_EST_c10191	6,35	95	-	10	10,5	N	0.32			cabog_capped_contig_000619	1e-07			Contig3311.1	8E-14
OEC48	x	Go_EST_c2438	925,47	108		0	0,0	N	0.21					CSEP0307	1E-21	Contig10247.1	9E-23
OEC49	x	Go_EST_lrc18129	2,17	107	-	2	1,9	N	0.11			cabog_capped_contig_001220	4e-10			Contig53707.1	3E-11
OEC5		Go_EST_c6401	9,06	334	-	9	2,7	N	0.59	x	x						
OEC50	x	Go_EST_c17250	1,74	104		1	1,0	N	0.33					CSEP0420	4E-09	Contig1756.1	3E-15
OEC51	x	Go_EST_c1572	10,79	101	-	9	8,9	N	0.16		x						
OEC51a	x	Contig32100.1		100		9	9,0	N	0.59	x	x						
OEC53		Go_EST_s30912	1	100	-	2	2,0	N	0.11							Contig7785.1	3E-18
OEC54	x	Go_EST_c1285	36,28	96		8	8,3	N	0.26		x						
OEC56	x	Go_EST_c253	78,49	86	Coiled-coil domain	0	0,0	Y 60	0.38								
OEC57	x	Go_EST_c7050	9,71	85	-	5	5,9	N	0.13								
OEC59	x	Go_EST_c21577	1,43	79	-	1	1,3	N	0.21							Contig2712.1	2E-13
OEC60	x	Go_EST_c4732	41,09	76		2	2,6	n	0.27							Contig4634.1	1E-06
OEC61	x	Go_EST_c19759	1,92	74	-	2	2,7	N	0.10								
OEC62		Go_EST_c13672	2,96	72	-	6	8,3	N	0.02								
OEC63	x	Go_EST_c5962	17,32	70		0	0,0	n	0.05							Contig18611.1	6E-06
OEC65	x	Go_EST_c21289	1,45	67		2	3,0	N	0.18								
OEC66	x	Go_EST_c13767	2,52	67	-	1	1,5	N	0.02								
OEC67	x	Go_EST_c27130	26,48	65	-	1	1,5	N	0.13								
OEC68	x	Go_EST_c13802	5,61	170	-	6	3,5	N	0.10							Contig13860.1	8E-18
OEC70	x	Go_EST_c2903	1462,99	102	-	1	1,0	N	0.09							Contig7785.1	3E-20
OEC71	x	Go_EST_c1028	268,99	91	-	1	1,1	N	0.31	x				CSEP0052	1E-13	Contig11968.1	2E-11
OEC73		Go_EST_c1080	48,28	79	-	1	1,3	N	0.02							Contig23415.1	4E-15
OEC74		Go_EST_c211174	1,84	62	-	3	4,8	N	0.32								
OEC75	x	Go_EST_c1950	11,14	63	-	2	3,2	N	0.01							Contig42089.1	4E-07
OEC76	x	Go_EST_c7942	5,98	63	-	3	4,8	N	0.17								
OEC77	x	Go_EST_c12422	3,05	63	-	0	0,0	N	0.09								
OEC78	x	Go_EST_c5198	20,07	64	-	4	6,3	N	0.17								

Supplemental Table 7 (continued from last page)

OEC	Cloned	Identified from	AverageCoverage	Length in AA	InterProScan results	# of cysteins	Cysteins/100AA	NLStradamus	NucPred	YxC motiv	FxC motiv	tBLASTn vs. *Bgh* genome	E-value	BLASTp vs. *Bgh* CSEPs	E-value	tBLASTn vs. *E. pisi* genome	E-value
OEC79		Go_EST_c6862	11,26	64	-	0	0,0	N	0.20							Contig14629.1	2E-08
OEC80		Go_EST_c11192	3,57	65	-	2	3,1	N	0.00								
OEC81	x	Go_EST_c22164	1,54	65	-	0	0,0	N	0.17								
OEC82		Go_EST_c10802	4,42	67	-	4	6,0	N	0.29								
OEC83	x	Go_EST_c29558	2,43	68	-	1	1,5	N	0.15								
OEC84	x	Go_EST_c16274	2,08	68	-	1	1,5	N	0.14								
OEC85	x	Go_EST_c17275	1,55	68	Prokaryotic membrane lipoprotein lipid attachment site	3	4,4	N	0.04								
OEC86		Go_EST_c6373	15,95	70	-	3	4,3	N	0.00								
OEC87		Go_EST_c23937	1,59	71	-	0	0,0	N	0.04							Contig1174.1	4E-26
OEC88	x	Go_EST_c5357	26,06	74	-	1	1,4	N	0.33								
OEC89	x	Go_EST_c6343	12,36	75	-	2	2,7	N	0.07								
OEC90	x	Go_EST_c5241	19,22	76	-	1	1,3	N	0.16								
OEC91		Go_EST_c89	87,38	77	-	4	5,2	N	0.33	x							
OEC92	x	Go_EST_c8726	7,37	80	-	5	6,3	N	0.14		x					Contig18377.1	1E-08
OEC93		Go_EST_c21126	1,61	80	-	1	1,3	N	0.22								
OEC94		Go_EST_c12241	3,25	81	-	1	1,2	N	0.06								
OEC95		Go_EST_c14422	2,77	81	-	2	2,5	N	0.04								
OEC96		Go_EST_c21648	1,85	81	-	0	0,0	Y	0.58								
OEC97	x	Go_EST_lrc29217	1,17	83	-	1	1,2	N	0.00			cabog_capped_contig_005138	6e-11			Contig25167.1	7E-22
OEC98		Go_EST_lrc9824	5,56	86	-	1	1,2	N	0.52								
OEC99	x	Go_EST_c353	70,19	87	-	7	8,0	N	0.16								
OEC13short	x	Go_EST_c808	33,41	136	-	2	1,5	N	0.17								

Supplemental Table 8: Protein sequences of predicted OECs.

OEC	ORF protein sequence
OEC10	MRSYTVALISTLLLSPISVLSTYHEADSDLSAHHENNADLDHSKSSTHLNALTVSIKILYDGDDTVKTCRVEKSDDEKDEDDDEEEEEKKEKRKRKRRGKILCHKVRRCKKKSKICHGGINPKDGFKCKKRFIKLKKVLSSAEDACNVLRSGSDRKMPKLYNASKFQAAPGPYLEWRVYNKYLNLGFKQRYRLVMTKRCAVVGVVVRNKDTSYTTCKFGPK
OEC100	MRFASGLLIPAFIGLSLALTESSVYIFKGERSHNKVAPVLSPEQARHFADRPLGLSKNSELADVSESTLSYINQFGKAQNSLFEPSD
OEC101	MTLLLLILTSFFTMISAVNIIVSSYAGQITSLSLRQTEDGEQTLTKLSVINSPMPQPSWLEKSGETIFLAKRKFRWSEWLFTSFKNK
OEC102	MFNLSSSLIILAILFATIFAAPLNINMGAYSPAMVVGDGAFSFSNSDTATKLINSLEGAAVDGSSANGANANGVADGANNPVQAGVVPA
OEC103	MSQRKLLATFYSAFLASLTSGNRKAGFRASGILHFDPNAVSFQYDFVLSSPSILGTWSAFEMGRNYNQSPGSSLVIVSTLYRMPMRLRIPVR
OEC104	MVTSYWLARVFLDRAATAFIPLFTWPSLFFHPWFGDEPCYVRQGGEAFAKNFPIPSSLLSCFVRSVITFYASMSRNLPYPYGDAHIFKILVLL
OEC105	MYMALRCLLTLSSTLIFIIPFVHSLPAWGEYKLNSQYPPWPSRPCADYGAYACFRPQQRKDSTQSKGLMVCDPGTEMWLPCLSCDILIGGALDC
OEC106	MWISSEMPVIVLLLFSVPCLAFNPTCLTIIWKSKNTDCSGCFVNHNMIARSLQNACPRESNRGRLTNKFRELQLYEGNGIEGAVPRAMWQSRGP
OEC107	MFVMECVVAVLGSLSGTYPIETLTLFKFNEETQRHFILASAIPSGHKCPRSVVSEFPSLAPYVKNAAIIKGTGNIFEICPVRVTMEDCERLYRVGKIRIR
OEC108	MSVPASIIATTLIQIYSVHAQHMIGRQLKRLIVYESDPDAKSNRAYSGPSSPAYRGIFQCLCTTMARYTVSRPDYTGQYMSRSETMCLYYEWREHLPNRCSE
OEC109	MCLLMRSRAVAVQSIGIAATVATCKYYSNLQPKSRHHYSAFRGEDWMKKLVYGPSDKRIEEVIGISQEGFISLCYNIEVMVGNRVRGTSDGGSPGRFCKRDTE
OEC11	MRHSATHLVVAFCTGMAVSAAPLSPLPPVSPAVLSPLPVHVPYAVIPRAESHEFENAYHVSDSEGIEERDTNSDDINDNGIEQSDAEFESAGNFDLDIDSGDDADHERRSTPSIFNRSPTPYPQNVKEEEAQDLNDPENDDDYASIASFPDFSDDEDDLSSPASDRVFSVASDKGDSGPENQPLDVLDNEKAEKRSVEIDGQSDRHGGRTYITKSEWKV
OEC110	MRFGAVGQVRFSVLLISLFILNVKGTDIRQTKFEDRVWCHNEKEFSPEDINALALKGCAMLKLEKHPPDRCLRLSKCSSDRPEKSTISRIIIMVFRVNQGRNLYLIK
OEC111	MRYSIFLLLALAAFSVAAEKPDAYNTPGTVIDKDSKNGSGKNKTEPASPSIAASYPKSSGSSSSGMKPNPYPLDSPLKSTASAILMIPLSQVGGLVSIAGLGIGFLIFM
OEC112	MQSFTLVTPFIILITTCSFVASTCWYPDGSTSEPGHVPCTQITQNPSACCASQDACSAGLCLSIHGTYRGTCTDQSWNSPNCPMKEYQTCINGNHNLCLSHVYDKFDIRYVN
OEC113	MRLFRYLSIWLYLTVSRLSLYHSIVALGSSSGSVGFKVKHQDSKVCWSSRPSLKWVQLVTGCVKLEDCRTSFPKLADIMDFGVKKEVICTALLYEDFHRHLPMRKPPISEKNR
OEC114	MGEGWGGVVVGALSPSVPCGQATSSVNTHHREKVRATSGYLSMLSPLYEYVIIARGCGWSCWIRTSSLLSQVGHVSKLPRLYLGERPRWHTTIPFDHDEVMMRNSTPIRMRLFLAIPNIQKYSEHT
OEC115	MRYFLTLFASSLLLSVPVHSHVVSKAVHPHDLDDTDKSLTPKYGVKIYVKVGSTIWDSEKGNVCHKDEAPCSGGDDKCHKHGSKCSNKTTNRYGFCRKKKFFNQEKVITAARKGCIRISKNDQKGKFPKAHRG
OEC116	MRISLFTVFGLCVAAAAYPEFVRRDDQPETNTTMSGPSSYTTTMSSMTMTSSGTAIGTGVETATAITSGVFSNSTSSSTGYASSPTSMAHKSSTTSMSETKTSSAGAAPTGVWENNNVKGAMAGAIGVLGLALAL
OEC117	MSSGQRNLPVFLAAFSGLLGSGGKLSSCFYEFVTSRYHHFTISRIIDIEMLGRAAKDYIPPPFKPDSHKALLLPRDQVRNGNFEELRRAGKSTKLNVDLKSYLNNLQTIQNKSPITDQTYKKKSNVKASCFKRTVN
OEC118	MFSILMILIALFSIVASAPAPPPVDSSNYEANGYYHKHHAPEPYKPKYPAPEPYKPNPYPQPSPAVPNYSNYGSYGSYDGYESHEGYKPYNSKPAPEYPHSTPPAGYGSYNHYDTYNPYESHGSQAENVDQPMDSKN
OEC119	MTTGDTARIFTLLLLCIFSLYQSAAYPLHFNEILNTHTLLRARSRGTDQPRRRTVGPIMGDIATTVFGNAIAGAIGPIFEEIGTSLSSGMSENSNGSRDQRHGDEFIEYQTIQEPHHEQTINEISRSKFKQDSEESYETPE
OEC120	MNTQQFSCLLVLIFTCHFAAVSALVTPNIIERMTALMQATTEAITKPHKKYTELESDEEENEEEDEDEEIEYTYTGSLIAGSVSEIVKLLKSGLNVPMTRQPYSRHGEYMNPRSTKCQKMRQHFESFIKASYIIMDNFDKKKWVLRPR
OEC121	MNTHQFSCLLVLILTCHFAAVSALVTPKTIRETTALMDISTRAITGSRKKYFNFDENKEEFYETIQPTLAKKYNDKNSKKCIVMREDFELFIKSSNKLIDAVENKQWVPKKLLTIGDLITEIKSRLSSRSSISKTEEKSMRAILSMIQKLWASRTPELSKSQFYRAATKAL
OEC122	MLSYTTLIIFLISTLSPATVISAQKGLCLTTRQDPDNCLATSPTTFTIHDFTTFSPADGNLTPASVSFRYSSNITLLVAHCSSKNDSVVDNDISALGENQQVSFTYNSNNLTIIEDYIICQTRTAAQVVGFLDVNTFCYPNYPPSPYGYGTKCITPSGSLSGSFSLKREN
OEC123	MRSIIITLISTLFSSVPTHSSTILSRDSGVNSDSVPGFQEVRISIVINGQRVDSYDHNSCPKEENKCSHEGNESTELKFKCGKKTFSNHKILRAAAAACPRIKKNSQKHIYPAAYAASRFEIDGPYWEWPISRNGHFWNRSSRSKYRIIMIKDCTVVGAVIRNKRDRSYEQCKAVSD
OEC124	MRSFLTVLASSLLLSVPVHSHVASSTVHPYGLSHTDDHSNQKPHIRIYVKIGSTIWDSEENNVCHKDEAPCAEEDDDCPKVHPTCPKKTTNRYGFRCKKKFFNQNRVMAAARKGCLSISKNNQKGKFPKAHLGKGYSKEGPYSEWPINKDGGFFNWCKFSRSLYAMDDTKELSSSKPQLSSRDDYGLHRRWRSN
OEC125	MRSFTVALISTLLLSPISVLSTYHEADSDLSTYHEADSDLSTHHEKNADLDHSKPSTRSKDLTVSIKFLYDGDDAVKTCRAEKSDDEKDEDDDDEEEEEEEEKN
OEC126	MRSVCDVIIGFATVLQITLASSVIPFHSESFGVLARNPSSSIKEKRFLPHNVFAKRQTIPLKTAQCTSSIHGNSKLQLSLQSNCLAKKKKLAELVKLGKPNKPPFPVFLGSNKFFSTEGPYFQIPAKSGFFPINSLKTYFLADSLP
OEC127	MKIACIIVALIGFAMAEMPFHYVCIKQSCKRLQILDGELSNGEISDVITLDDAYDCTNCLPKLEYNAYKNKENLFLSDCAEGDAMMTTGEKRYFCVGNVDYLSWISKRERKSVLNLKNQGQHPHRSG
OEC13	MFVQLMSSATLFSLAVATMSSSAYQQPTVLVTKNITMATAHTTKYATVSCSASAASCPTGQAFSSIPFIIKPEMNKTTGHRVPIGSLINNTTPFRSTPLRDASMTRFYKTNEPQLAPHTIVPVSSSNSLHVNASTMPRVFSSALVTHKSQTIEPAFSQANRTASTTKYSTIDSCDSSSSGGCPTNRVASTAVTESPKKPTYSTESLAPAANTATAPQGTVLATRTVSAKKPENSDANKNDHVTAAGRKIQRSTTLMVAGAILAALF
OEC14	MFCFISVFTLTLLIPPSLGISPVQGEQASEDDPLDSLDARKDLNFGPALHEFNAHDDMFVPAIDLGGFRLKRRHSQSDGYYCGKSPNHLEFTTQTTVKIAAKKACKELDRLKEEEEGDEDDEEDEDEVEEEEEGNKGKRRPDYPHPKNAFKYVKYPPYYESQIHKNGKKDKSVPSVIIDVDCHIVDVVARDEDKRYHQCVRV
OEC15	MRFLLVAVLISAFSQGYVGLRTHSYRTLERRWHENEKHTDQLIHKLPPKHVPDVDEEQPKEIVFRGLRCDKTLYEPANLKSAANEGCHRIRSGKKTWSFPRFPIPFPIDFTHLLDELSEIPGAQNLSGPFYLYPIQSDGKIFKFGFPGPHRVIVNRKCEPLGAVIQVKSKSKCEGIGCLNIFRKNHVAYRSCEEDHRK
OEC16	MRSFLTVLASSLLLSVPVHSHVASSTVHPYGLSHTDDHSNQKPHIRIYVKIGSTIWDSEENNVCHKDEAPCAEEDDDCPKVHPTCPKKTTNRYGFRCKKKFFNQNRVMAAARKGCLSISKNNQKGKFPKAHLGKGYSKEGPYSEWPINKDGGFFNWCKFSRSLYAMDDTKELSSSKPQLSSRDDYGLHRRWRSN
OEC16a	MRFFLAALSSSILLLSTHVHSHIVTRSVSPRSESKSISIYVRIINTSEKPGKGGECDGENKSCSDTDSPKDECDGENKSCSDTDSPKDEKFWKVNRCKDGESSCSRRPTYRYGFRCNKKFFNQDKVMKAAEAACTKIGKNSQRQVFPAPYTESEYEKPGPYVEWPILRNGRIWNRFFRRSKYRIVMTYDCTVVDAVIRHKNGESYTQCTVEPH
OEC17	MIYSFFLAAILAMLATALPLDTPIDAAEESKYTEYGSYGSYGTYDGYEISDKTVSPPLETPAVPRNFVAISTRSGDPDVHLRAVSASNQRFFIGKDTSTYCPLSDCSTYVNFTVFSARPNDANSNLGLFTATPGGQAAFVTEDGQLGYTQAHSGLQPTGSVNLPFQYTPETMPNSIGTFKFNSRWRGLHRPS
OEC20	MKCQTTLVLFAFSHVVLAVPQPWHQATSEHADRNSLLSARDHEHLPSSARSQAAEDLIRDEEIGFSTNENDPNENERKISINRRALSQSVTSGGLFRPASVDWDSSRSMNRKGNNSDDDDDEDDDDDDDDDENEDDKKKAKPGFFQRIKNFFKFRKSNSMSIQVKPANLMCKMLIVLSRG
OEC21	MFLKASLTVWALLAAEITLSLSTSIGRLANREVVDDINDNGIMIEWASCKGRHHDKEVIYETLKQACETKNSSTIFEKAVNLRPHIPSPSEKYHHEINPPYYAYSLPDTVFKDKLHPIDVIVMNDECKLAGVLMETTKISCNDDTCGSEPRYKDCEIRLSKTAPTPAETTPVEQLS
OEC22	MPSLGSIITVFATILQITRASSIIPSHSESINSKGSEYFGAPAKNPSSSIKRKRFSLGNMLSKRADEKLGQLCGKKFYGNEYVKTKVEKFCTKITKFKDNPQRGTPKLPVYQGNDELFKNQGALYQIPVKSFSKLRFMWNLLRKLCFLFLWSNHFLSYHLGRQSTFIGTFNNV
OEC23	MQFLTYFITLCLLGPLASVAVEPQTVDVPFSYTCENLIWIPRDVLRKEATEGCSNIMRAYECNGLNRCFGRRTKPIFSSSWAKEYRGFHFELGYEEKAYESYLYEREMKEFSSEIAGKDKFLVIIRFIPSFPYCILRGVVKRSGKRELECVETLFFDRGISSSSPRSRPI
OEC23a	MQFLTYFITLCLLGPLASVAVEPPTVPVFSSYRCPGNFEIPQDVLSKEATESCSKIREAYECNGLNRCFGFRTKPMISTPLATKYRGYNFELSPEEKIQNPSLYEWNMKKFSSETSERYKFLVIIKYIPRNEMCILRGVAMRSGKEEDECELKLPNR
OEC23b	MQFLTYFITLCLLGPLASVAVELYYGSPDAVSIPSSYECGETSIPKYSLRIEATKGCSRIKRQCEGLNTCFGRLKIPIVGSSRAKIYKGHHFQISSEENDFKFPVYEWNMREFSSKFMEKNEYLVIMRFNPSLKRCDFKGVVMRTATTEMECDEKPPKHNRVTRISSPRFAPI
OEC24	MHLIRVIFIALLCGAIAMPTRNVVSDPSKTTENPSQETTKEIFNSNTEFVGKIREHSISSSPLTNQTDTTTSETTTTIVSEFKQGAKIPNRASLSTNNLTRVFVLDSHNKKLAKRSFFGTSSVKRLLRCFRFTDKRSDHEDYNANRKQGIWQLGKEHRKGWIFRIFR
OEC25	MSLRSYIILCIFISVHVFARSRTEDSLIKFLPSFNDVKCTKPNSIPARQKFYQLKASDAVRVSFSKEKLDNAAKNVCLAVNRTQSCKGVKVCRVTNKFSEKPIPYLGGDFYNRDGSEFYLSHLFEKNALGGKYYAGVVRWNPTTKECEGVGAVKKTRAGNLKCNF
OEC25b	MRLTRYIHTIICCSVYIFACVKAANNPLNIYNAVFSAICESQDENADKTRVNGISGSRIPDITFTRKEINNAAIGVCITLNKILGCTGFRFCRIGKKSTGIPEAYKGKGFYKTNESQLYLSHISPLNQPDNKDYRVVVRWKTEARECGGAGVVKKTGEEYLKCPHRKPKT
OEC27	MRVSQFTIMVLTTFLGHQTTTALTQPFDAYGVTHRGFSCDSYKFMNHEIYAQANFACMGGKLNHSILFNEKVRPLSESAGDYINRKFGDAKSQIIIYFAPLFRSNVEEMQNTFINQKKDVGPYRLVLNNNCDIITAITYESNKNEKTLDSTENIHACEKF
OEC28	MQFTKLIVLAFVACVTATPSGLNFYVRRTDGGDDEAPLTCTEALQEIPKCALSCITQPPIDAGCKSAADFACSCEKKTQKQITKAETPCVLKACGLKEALAASRAGKDVCGACNTSPNEPSDGHGDDGDDDSYEKSVDAEKTPEIPNSMQNSDV
OEC29	MWIGAGDQVRFGVLLVLLTILSVKGEDRFFWSLKNRVQCGRKEKFEPAEVNEYARKGCRDIIAHEDSLSHVNSPQHRFPSRRKKRKLPKPYKGPHFTAINESLYVVKITRNNFINLTKYAVIFSWSRNSNFCKTRGVQYSPGLRGGNFLCVEL
OEC30	MWPLKFISLLWLLNSFVSGFPKRQQDNAVLLSGLGVNFFCAPSQRFTYYEINSRAYKGCQKLHKYFGSTKLLHLLSKIKPSIPSVFKYSGDNFDETSPGSILYKIRIPRGHSKKCPILHCFSYISKNLACYAKGVEMVEQKQNI
OEC31	MLLSNFVLLGLAAGVRTQILPVQVQNLADTTQAVSIATAAPSPDDIQHSLLSEASARVSSFSSVAASNIASITSSLGAEASQISSKLESVSSEMASKSSSYSSKYDPTNTPHDNLAAPVQTGAIAMGALLGLGAAVVNL
OEC32	MFRLKIITLLTLVIYSLLTSARTYDSIESRPVKRPKRKTEYVEEGDEYRCVKNVFKLDQVDDAVAACNYVNSGKKLGDSAGGPNLTGLKINPNSPSSVILFAYGLSWQMGKYLKDVSEVQEITSSLLMDHVN
OEC33	MKTYNTLYLVALLGVSIAAPLQENLASEYQAHIDALGPVQKNSLNTESSQPSNSILDIYNNYSVLEEDDGAEDQNDDDIENEIDSRDPLIRSAMRRNIAVLFRGQNSGVDQTKLLKRQRNGGGEGRGGGEGRGGGKGDLATSTHYFALISQLLSYKSQPQNYFDKPSANNQQHVI
OEC33.1	MKTYNTLYLVALLGVSIAAPLQENLASEYQAHIDALGPVQKNSLNTESSQPSNSILDIYNNYSVLEEDDGAEDQNDDDIENEIDSRDPLFDLL
OEC33.2	MKTYNTLYLVALLGVSIAAPLQENLASEYQAHIDALGPVQKNSLNTESSQPSNSILDIYNNYSVLEEDDGAEDQNDDDIENEIDSRDPLIRSAMRRNIAVLFRGQNSGVDQTKLLKRQRNGGGEGRGGGEGRGGGEGRGNGRGNGGGIGGGGRGEDNFDHDGTENEDDQN
OEC35	MRLHIFSLLLPVVVLGYDPQQITSTITTTTTTVTETVTVYIIPSAAPPLQTNGTLPYDKVHVTASASIPTPSQIYVNKNNTNVVDSPNPAAKPSTPIMRGNAAKYLINKKSILAVAGIITAVTAW
OEC37	MRLRVVGLICSGLLFASIIDYCVQAQTIQQIIKQIKLDFDMTCGGDNEIISSSTLNERAADGCKYLLGTPSRQAKRICNLLSCTFRSKDKVVELYGGPNYSSKNDILYSIKLDKKEDLSTFI
OEC38	MRFGAVDRVRFSVLLISLFILNVKGTQFSYAPLTYPVKCGDNKEFSTDEYNGFASRGCAMLSEKEDNPNQCSQHSNCNSYRPKKSAFPKPYDDGNIPDPRVKICIRSKSHTKSTSEELRTM
OEC39	MRVSQFTLMVLTTFLGHQTTTALTQPFDAYGVTHRGFSCGDHKFMNREIYAQVNFACMGGKLNSTITDNVNVRPQSTRVEVYVSDIMRDATSAGTIHFAPLFSSNVEEMQSMSYSHSFCL
OEC40	MRSFTVALISTLLLSPISVLSTYHEADSDLSTYHEADSDLSTHHEKNADLDHSKPSTRSKDLTVSIKFLYDGDDAVKTCRAEKSDDEKDEDDDDEEEEEEEEKKEKKKEKKKGKKLCYKVRRCKKKSKFCLGGIKPKDGFKCKKRFITMKKVLSRAEAACDYLRSNSDRKMPKLYTASDFKAAPGPYLEWRIYNKYLNFGFKQQYRLVMTKKCDVVVGAVIRNKDASYTQCKFGPK
OEC41	MQFLTYFITLCLLGPLASVAVEPPTVPVFSSYRCPGNFEIPQDVLSKEATESCSKISTPLATKYRGYNFELSPEEKIQNPSLYEWNMKKFSSETSERYKFLVIIKYIPRNEMCILRGVAMRSGKEEDECELKLPNR
OEC42	MKIACIIIALIGFAMARRSPKYVCNIYSSKDLQLSDGTEHNSLNEFRHCVPFRFRHRYRLKSQLVVTRCIIRETTKPPRENRFICIGHVPYDWIKDTIKFTPLLDLKNQGQHPHRSG
OEC43	MQISRITFISLFVALVAGHPTLYERQTITIPKIPEIPAVPEVPAVPEVHKRQSTITIPKIPDIPAVPEVPEVPGTKRQQTVTIPKIPTIPTVPDVPAVPSPHPRHTGIGPSKTQRLR
OEC44	MQLSILVIFFNILLVSSIAVNKPPTSTGINPPQIKGYQCTSQFIRLDLVNKAVDDCKSYLKKPGKKYKLINYYPSIWEKTEVGGTFFFLYPVANNFFRKLADMIRLEKIIPYRQSGL
OEC45	MRHSSFLMPIFALLVLFAMLSNTQPNPNAAQPHPNAADCPYEGRICDKKDIEPYRSVKYLRATCKKCGKITNNNVVGKKDYKLRYCLYCDMKYIHDLSLRKTKMLYKCPDCETELR
OEC46	MLLVSTSTIFILFASLTSTQAQLIEDHGSALVNRASTASVSTENLRRDPNMQSVSKIQVHSPPRNYRTIRHSDRTKDLTSRDVTQEQQAESSINFRALVQGRRGASRHTNGYH
OEC47	MKVSYLVLALLGFLGFCAAQRPRRSSDEEIRTAITLLPQCCLNCVLPLLNSMHCSLSNLTTFTDCFCTNQKVQRKISLCTGANCEFHKLKSECSK
OEC48	MQISRITFISLFVALVAGHPTLYERQTITIPKIPEIPAVPEVPAVPEVHKRQSTITIPKIPDIPAVPEVPEVPQVQKRQQTVTIPKIPTIPTVPDVPAVPSPHPKAHA
OEC49	MLQILILQLPLRSHVALSSPVSTFIREYPPRETLANPELSRNASTILHTIIHEKRGDGSAGFGPAIFRLKWGWCPGLADSNRETGPDGKTLHHPTRVVPFIHVGRCL

Supplemental Table 8 (continued from last page)

OEC	ORF protein sequence
OEC5	MLFFLALSVFLSTTLLQVVPVATTGPASNFEPGFKCEEDFISDAEITNVLIISKMVHPKFPSPNPYYGPHFREDRLLMYPVITHKRPEEIKSEVAKYFVVYQNPGHVVGVFALTQYNEHVPCSRNTFTPHTPPALHPTHSLLHMNVAIFGFQCGLDAID NEFISSKLLFTTRLLKRNSDRYVRFPEPFPGLEGPNLMWLLTNTHDPNSRKRRKARNPIYLITDKFGSFVQVNFMLKNGEHERCNVETIPNTIYPTLRTNQSGKIKMGYLCDVFFDDKDLSKCANAARIQDQVSFVYPKPEKLWSQNRKCFCLARFF LKINCHERFEMSIRLHSIK
OEC50	MRHSTAHLVVAFCSSMAVSAAPLSPLPPNSPALISPSLTPRSVETGEIENKDREAPVQKRSVGGFAYHRADSSTISKRTDDSAKSVMKTQNRPSGKYSDTEFRF
OEC51	MKCIPKKTSFLFCTLIILILFECASSEATSKATHICKLTPCYDKTVRKIFLNREIRVYKFCKNCKSYRGHRFTGKKLPALNEGERYCTDTRWIPYSDVRCF
OEC51a	MKCIPKKTSFLFCTLIILILFECASSKATSKATHICKMSTCYDEAVKKNLGPETSFYRFCKDCKSYYRYRLIGKKLPALYEGERYCTDTRWFRYSDVRCF
OEC53	MQFNIFAILALFVSPAIATETVTVSVCAPSASAYPSQGYAMPSVHPSAPSDPSSPAYPPSPSSGYSSPPPYQTPAPFTGAASINAAQGASAIIVAGFXRC
OEC54	MKIIPKKTSLLFCSLILLILFECVFSRYTHKCEISSCSRVVTTGLFGKNPELVEVCKRCKPYIIRQVLGFKIPNLNRGEKFCTDKRKLQLFGVRCG
OEC56	MLSLRGILRFALVAFFSMPLIVETLGAPTRESTTAQTTHLEPRGKKTKLALAGTAVYLVGKRRRKNNKIKKLKKDNKKLKNKLKGY
OEC57	MQFPSCIVALSVLVSIVSGAPLNVIQRIDAKSPANDVVCGGDVKFTDDKLKTLAIDVCQRLSDERNCSGSPSCLHTLKRRPSYST
OEC59	MLLSFAVISALAIAVSASLNNATVYVTEIHTAYTTVCPTSTQFVYNGVTYTATEVKFLNQRRRRIAINQLILVYNSNNH
OEC60	MKAKHLILTIALAAAARAEDLYDSSEGPRLKDQQLRAPFRIATAESTCSCATEYITYTGEGFRMLKILILILKRKF
OEC61	MEAKHLILTIALAAAARAEDLYDSSEGPRLKDQQLRAPFRIATAESTCSCAAEYITYTGEGFLYTADVSSVTKI
OEC62	MSIRIAVFALVFLAQVLSTLSKDVDQSQIKELPLCSYQCGALTRFKIIKNCPLSSSKCVCLIYGFVYALHCF
OEC63	MTMVEDPLLLLWLLSVLSPVSGANPVETALVRERLGERIGGAYEKLREILRRWQVLRSKLLSIRIVLELI
OEC65	MPSGLYAFKFWRILGTASSLGSISAEPLSLCRLRDRISRCWLNLVTVHSKTSVRPLQGKARQKIWQP
OEC66	MFNLELLTLLLIAATTVVRATRTYDTPGNVVELVNQAIQLKLCFGIVRKHLVAQKVELSTLLFKDAL
OEC67	MRSFLVWRLAIGVAFGMMVNRTYASGDAHDRKEESDMYLSTFYTRQEQKFYNLDCKNLDNTKRYL
OEC68	MNLTSFFIFSGLIFGAHALLNETQSVVWVTITTDIYTTFCPSITESSDGYMTSTASVPNFSISTDCPCTLAQTAYSSSTSIRAASQTIVDVDPLPSFNPKSLTRVWITVTEIVSELTTFCSSSTEFVHNLKTYTITEPTTLTISDCPCTISRIVPTTIQTTITSV FTTVW
OEC70	MQFNIFAILALFVSLAIATETVTVSVCAPSASAYPSQGYAMPSVHPSAPSDPSSPAYPPSPSGGYSSPPPYQTPAPFTGAASINAAQGASAIIVAGFVAMLI
OEC71	MQISSIALVFLGFFTSLVFSVPSPNTPWMPRRRQEGSGYGSPSPTDEYPSPEYPCPTGTGGYPAPTGTAGHPAPTDGYDEALKFKRYNFKN
OEC73	MTDTTTLIATISFFTLWAQCQARSMNMSNIVQLDGQLTYTIWASTMTAVFKSLKLHEVVIIGIKPLTGADDEEIKAHRG
OEC74	MEAAVETAKITLTLLLLCQDLCVVGIKFSRTTRCRKQWQQRERFAESNLVMLDVKAPMHAQK
OEC75	MVRCFGVVLLGLTKVQGCSEKEVGVLMNRSRLQETWVKEGNGHPVKFEKFSKKHESLYLLKIS
OEC76	MSCPARLALICAICLPRPQLPVLSHYRVLLEERSPISQTPSIIHNELVFSTRVDLTSLVDGGE
OEC77	MPMGIGTYPAGYKNRNHTKYTSKALTEIEPTMDYKYLDFSTPFLQVRPPDEHKPPIYPRLTAT
OEC78	MCYLKLLPLSLVCPCPAIESPLRADSYNRTMQVETKILRGPWPTVKSPQCADFYDIYDSRFTRI
OEC79	MPAPQNLALPIASAFSSASYTDITTPSASTSKDVKSDSPLISRPRPIAHNGTEKSFLLARYHLY
OEC80	MAPISLFVLVLILSFVPLSTCRSDIEKERSMPPVPEQILEGIEESILKVAADGSVCSFEDNSTYL
OEC81	MALISQSVHQLVYQLLFVLILQPALTSVLILKFQNLVLNQITQSSPASTQVILLHTYRLRPNLKP
OEC82	MSLTSLPLPKAKTFCIISSAISFTSCSQPASVLLLFSICHSRESERTKLPQGCDSGEFFGHDRRKGL
OEC83	MPFTHEMNTLSLGAFVPVSHAEPNQSGQDNTEVESGSPCANRKPRTSNSTEIDRNTIKTAARAGLSLK
OEC84	MPAASVVFVSAQLALTSSSRSYRRSFLDYAAKSYILKKKQPPLFCDNASSVNNPTPVEVLGVKGKVSP
OEC85	MSSVAKVGSIAVSDNAPPRTLFLYVGLLGGVASCRPKLRCDVEEALSSRVPSSCPSSPAWMMTVKVSK
OEC86	MPTYRCVTAGICLLKCLLMQHSIVAEIEEDPKEGYSFETEAFREAVQSAVLVSSIFNAESFSFLVSPPYL
OEC87	MKLISTLTALTLIMSVGLFTIGSRLQKPGLGLNRRSVLSSQKYKDLPNFTWRGWNAETRSPPTSSFRKGIG
OEC88	MSWHRLRQHSARTLILFPLHLTSQLYVLSFHVKAQKNLSIPTAEPQAFVHNDVRCSFQMLRYRASNMSSRDKGR
OEC89	MSIALFILFLDIATATFVVHANECLPNVRDKVAMRHQSAYCGRTRDEGTKIQELIKSALNIPKTASQNRVNGQNI
OEC90	MSINDVGSLFLQLLIFLTSLVNLSYAVSSLEPIVIVFLFGFSKVFTAPPESGIVAKCQLKDLYYGESLPTGGHLIF
OEC91	MRITCYATIFSILYALACGLGNTRWSRPKPTPFILDKISYDVKCFKDTMITQSTLNEFGKYACEQATINNIKNKDTE
OEC92	MTFCLWWSFIVLPFGSTFPLYNFRFEKDAAFKRRMLSFFLLIMPMRVDITEFDCTVIALSSTYCMEACKPHALFDCAITR
OEC93	MLAQRIPSSSFPSFMLWCSSYWSGIALPARYSGRSLFRIWWSVLRSQTFLDRNFNLTSRRENFSKLSTAIGEHVTMMTSD
OEC94	MITVPSLVTLVLGLHLIYTPIPILSRYQIIDQQERDDLKCIFLLRIVYSSYAVIVPVAVELLNHQDLFFSSTTLHLASIIL
OEC95	MLAAQCVIIVLGSFEAGLGIDKTSSLVWENPSDRPSVSVAEIAPSLADAKQILSEAGFIHEKIKGSGMSKYCYDGEPPFIR
OEC96	MALDELYVMKMGETQKLNFSTFLASKLTEAEVDIQSDRTKITMLLNAQNKSIRQALFENLPFTQRLLRAIGSNRQSNISTS
OEC97	MIDPLYLITSLVLLIPLIFLTLGRMVWWYAIWVVLPSRVWVAWTHAPLETGESWFESSTTNHNFSRCYVFVEWRMHTISEHFK
OEC98	MLKLIYLLYILGVLATSFSITNKILAQPWSLSGTLQSNQVVLILDIKRHQRNPQSLMTITRVKGLRCYGHPEKEDLSRAALDLGGE
OEC99	MAFSLRQGYHAANPATALRIILNLSFVMLCLTASMSNRKHFYSDSDSDNDNDIDIGNGNDDYCGDRCLNDSNCFGFCNKCKDGRCAP
OEC13short	MQPTVLVTKNITMATAHTTKYATVTSCSASAASCPTGQAFSSIPFIIKPEMNKTTGHRVPIGSLINNTTFPSTPLRDASMTRFPLAPHTIVPVSSSNSLHVNASTMPRVFSSALVTHKSQTIEPAFSQANRTASTT

Supplemental Table 9: Arabidopsis ORFs included in Space

AT1G01050	AT1G19540	AT1G53210	AT1G77330	AT2G29760	AT3G05460	AT3G27340	AT4G01070	AT4G27240	AT5G08570	AT5G41010
AT1G01070	AT1G19610	AT1G53520	AT1G77390	AT2G29820	AT3G05545	AT3G27520	AT4G01100	AT4G27360	AT5G08590	AT5G41330
AT1G01225	AT1G19690	AT1G53530	AT1G77410	AT2G29995	AT3G05560	AT3G27640	AT4G01130	AT4G27380	AT5G08630	AT5G41410
AT1G01290	AT1G19730	AT1G53540	AT1G77500	AT2G30000	AT3G05560	AT3G27880	AT4G01190	AT4G27390	AT5G08670	AT5G41650
AT1G01300	AT1G19850	AT1G53625	AT1G77510	AT2G30250	AT3G05700	AT3G27890	AT4G01280	AT4G27435	AT5G08750	AT5G41680
AT1G01310	AT1G19860	AT1G53840	AT1G77570	AT2G30280	AT3G05730	AT3G27940	AT4G01320	AT4G27520	AT5G08790	AT5G41920
AT1G01370	AT1G19910	AT1G53860	AT1G77720	AT2G30440	AT3G05810	AT3G28007	AT4G01560	AT4G27580	AT5G09225	AT5G41980
AT1G01450	AT1G19960	AT1G54000	AT1G77810	AT2G30700	AT3G05890	AT3G28100	AT4G01600	AT4G27620	AT5G09270	AT5G42020
AT1G01480	AT1G20070	AT1G54020	AT1G77855	AT2G30770	AT3G06060	AT3G28210	AT4G01650	AT4G27650	AT5G09390	AT5G42050
AT1G01560	AT1G20100	AT1G54020	AT1G77880	AT2G30810	AT3G06130	AT3G28450	AT4G01895	AT4G27652	AT5G09500	AT5G42070
AT1G01725	AT1G20220	AT1G54050	AT1G77890	AT2G30860	AT3G06230	AT3G28500	AT4G01990	AT4G27720	AT5G09600	AT5G42100
AT1G01730	AT1G20340	AT1G54080	AT1G77920	AT2G30910	AT3G06240	AT3G28710	AT4G01995	AT4G27750	AT5G09760	AT5G42110
AT1G01780	AT1G20340	AT1G54080	AT1G77930	AT2G30980	AT3G06260	AT3G28710	AT4G02075	AT4G27760	AT5G09820	AT5G42180
AT1G01820	AT1G20350	AT1G54100	AT1G77940	AT2G31010	AT3G06380	AT3G28857	AT4G02130	AT4G27880	AT5G09860	AT5G42290
AT1G01820	AT1G20460	AT1G54140	AT1G77940	AT2G31060	AT3G06390	AT3G28950	AT4G02200	AT4G27890	AT5G09920	AT5G42350
AT1G01830	AT1G20510	AT1G54200	AT1G78110	AT2G31090	AT3G06420	AT3G29100	AT4G02270	AT4G27920	AT5G09980	AT5G42440
AT1G01840	AT1G20520	AT1G54210	AT1G78120	AT2G31130	AT3G06435	AT3G29370	AT4G02370	AT4G28025	AT5G09990	AT5G42520
AT1G01860	AT1G20575	AT1G54250	AT1G78190	AT2G31140	AT3G06470	AT3G29430	AT4G02485	AT4G28070	AT5G10010	AT5G42560
AT1G02000	AT1G20610	AT1G54340	AT1G78290	AT2G31180	AT3G06620	AT3G29670	AT4G02520	AT4G28085	AT5G10040	AT5G42570
AT1G02130	AT1G20816	AT1G54500	AT1G78440	AT2G31210	AT3G06650	AT3G30430	AT4G02520	AT4G28220	AT5G10240	AT5G42590
AT1G02170	AT1G20930	AT1G54575	AT1G78510	AT2G31220	AT3G06660	AT3G32980	AT4G02550	AT4G28240	AT5G10300	AT5G42630
AT1G02280	AT1G21050	AT1G54650	AT1G78660	AT2G31270	AT3G06830	AT3G42150	AT4G02610	AT4G28260	AT5G10380	AT5G42660
AT1G02290	AT1G21070	AT1G54730	AT1G78770	AT2G31350	AT3G06850	AT3G42860	AT4G02640	AT4G28310	AT5G10390	AT5G42680
AT1G02360	AT1G21090	AT1G54850	AT1G78800	AT2G31560	AT3G06890	AT3G43110	AT4G02730	AT4G28360	AT5G10480	AT5G42760
AT1G02560	AT1G21100	AT1G54960	AT1G78870	AT2G31570	AT3G07080	AT3G43270	AT4G02770	AT4G28430	AT5G10610	AT5G42890
AT1G02700	AT1G21100	AT1G54990	AT1G78910	AT2G31610	AT3G07140	AT3G43440	AT4G02810	AT4G28550	AT5G10660	AT5G43020
AT1G02820	AT1G21120	AT1G55140	AT1G78970	AT2G31710	AT3G07300	AT3G43810	AT4G02850	AT4G28570	AT5G10760	AT5G43050
AT1G02850	AT1G21350	AT1G55170	AT1G79160	AT2G31720	AT3G07565	AT3G43980	AT4G02860	AT4G28630	AT5G10870	AT5G43070
AT1G02860	AT1G21360	AT1G55265	AT1G79230	AT2G31725	AT3G07590	AT3G44010	AT4G02880	AT4G28640	AT5G10990	AT5G43080
AT1G02950	AT1G21450	AT1G55280	AT1G79260	AT2G31880	AT3G07640	AT3G44160	AT4G02980	AT4G28690	AT5G11010	AT5G43170
AT1G02960	AT1G21540	AT1G55475	AT1G79510	AT2G31930	AT3G07650	AT3G44300	AT4G03180	AT4G28760	AT5G11060	AT5G43260
AT1G02970	AT1G21600	AT1G55480	AT1G79530	AT2G31945	AT3G07720	AT3G44330	AT4G03200	AT4G28770	AT5G11170	AT5G43270
AT1G03030	AT1G21610	AT1G55510	AT1G79550	AT2G31980	AT3G07740	AT3G44370	AT4G03250	AT4G28790	AT5G11300	AT5G43420
AT1G03130	AT1G21710	AT1G55580	AT1G79550	AT2G32030	AT3G07870	AT3G44380	AT4G03270	AT4G28950	AT5G11360	AT5G43450
AT1G03190	AT1G21720	AT1G55620	AT1G79580	AT2G32180	AT3G07880	AT3G44450	AT4G03330	AT4G29080	AT5G11460	AT5G43650
AT1G03210	AT1G21770	AT1G55630	AT1G79590	AT2G32210	AT3G07920	AT3G44630	AT4G04190	AT4G29260	AT5G11510	AT5G43710
AT1G03280	AT1G21910	AT1G55670	AT1G79700	AT2G32295	AT3G07990	AT3G45040	AT4G04210	AT4G29420	AT5G11560	AT5G43770
AT1G03310	AT1G22030	AT1G55675	AT1G79790	AT2G32460	AT3G08500	AT3G45080	AT4G04925	AT4G29430	AT5G11600	AT5G43890
AT1G03470	AT1G22070	AT1G55800	AT1G79820	AT2G32500	AT3G08550	AT3G45590	AT4G05000	AT4G29480	AT5G11670	AT5G43920
AT1G03475	AT1G22170	AT1G55920	AT1G79850	AT2G32510	AT3G08590	AT3G45740	AT4G05020	AT4G29530	AT5G11900	AT5G44000
AT1G03550	AT1G22220	AT1G56000	AT1G80080	AT2G32530	AT3G08760	AT3G45930	AT4G05070	AT4G29700	AT5G11910	AT5G44030
AT1G03760	AT1G22240	AT1G56020	AT1G80110	AT2G32600	AT3G08890	AT3G45940	AT4G05330	AT4G29735	AT5G12030	AT5G44080
AT1G03820	AT1G22250	AT1G56230	AT1G80245	AT2G32660	AT3G08930	AT3G46030	AT4G05370	AT4G29840	AT5G12050	AT5G44300
AT1G03850	AT1G22300	AT1G56240	AT1G80290	AT2G32670	AT3G08990	AT3G46090	AT4G05590	AT4G29910	AT5G12100	AT5G44320
AT1G03850	AT1G22370	AT1G56360	AT1G80310	AT2G32710	AT3G09000	AT3G46430	AT4G07410	AT4G29950	AT5G12240	AT5G44350
AT1G03870	AT1G22510	AT1G56440	AT1G80340	AT2G32760	AT3G09010	AT3G46530	AT4G07820	AT4G30200	AT5G12260	AT5G44370
AT1G03930	AT1G22730	AT1G56450	AT1G80370	AT2G32850	AT3G09162	AT3G46560	AT4G08160	AT4G30270	AT5G12410	AT5G44440
AT1G03930	AT1G22770	AT1G56600	AT1G80380	AT2G32950	AT3G09410	AT3G46790	AT4G08280	AT4G30360	AT5G12420	AT5G44580
AT1G03950	AT1G22780	AT1G56650	AT1G80440	AT2G32990	AT3G09470	AT3G46820	AT4G08320	AT4G30500	AT5G12470	AT5G44670
AT1G04020	AT1G22810	AT1G56700	AT1G80450	AT2G33180	AT3G09570	AT3G46830	AT4G08455	AT4G30630	AT5G12480	AT5G44710
AT1G04080	AT1G22930	AT1G57700	AT1G80510	AT2G33370	AT3G09580	AT3G46930	AT4G08470	AT4G30670	AT5G12840	AT5G44750
AT1G04090	AT1G22970	AT1G57870	AT1G80670	AT2G33380	AT3G09600	AT3G46980	AT4G08530	AT4G30820	AT5G12900	AT5G44785
AT1G04140	AT1G23040	AT1G58100	AT1G80690	AT2G33420	AT3G09680	AT3G47000	AT4G08602	AT4G30840	AT5G13030	AT5G44785
AT1G04200	AT1G23140	AT1G58360	AT1G80720	AT2G33560	AT3G09720	AT3G47180	AT4G08870	AT4G30880	AT5G13050	AT5G44820
AT1G04230	AT1G23220	AT1G59540	AT1G80940	AT2G33620	AT3G09800	AT3G47200	AT4G08960	AT4G31040	AT5G13070	AT5G45010
AT1G04270	AT1G23310	AT1G59580	AT2G01140	AT2G33820	AT3G09820	AT3G47520	AT4G09000	AT4G31050	AT5G13100	AT5G45190
AT1G04360	AT1G23330	AT1G59700	AT2G01180	AT2G33860	AT3G09830	AT3G47560	AT4G09030	AT4G31060	AT5G13370	AT5G45290
AT1G04370	AT1G23350	AT1G59730	AT2G01210	AT2G33980	AT3G09840	AT3G47690	AT4G09300	AT4G31080	AT5G13420	AT5G45350
AT1G04400	AT1G23410	AT1G59740	AT2G01270	AT2G34000	AT3G09850	AT3G47730	AT4G09420	AT4G31110	AT5G13630	AT5G45370
AT1G04440	AT1G23490	AT1G59860	AT2G01300	AT2G34140	AT3G09860	AT3G47800	AT4G09520	AT4G31140	AT5G13690	AT5G45410
AT1G04530	AT1G23490	AT1G59910	AT2G01400	AT2G34250	AT3G09880	AT3G47820	AT4G09550	AT4G31240	AT5G13770	AT5G45550
AT1G04550	AT1G23580	AT1G59940	AT2G01410	AT2G34330	AT3G09890	AT3G47833	AT4G09670	AT4G31270	AT5G13850	AT5G45590
AT1G04560	AT1G23790	AT1G60000	AT2G01470	AT2G34420	AT3G09900	AT3G47850	AT4G10030	AT4G31340	AT5G13880	AT5G45820
AT1G04570	AT1G23840	AT1G60170	AT2G01590	AT2G34420	AT3G09940	AT3G47910	AT4G10100	AT4G31370	AT5G13890	AT5G45880
AT1G04610	AT1G23860	AT1G60240	AT2G01640	AT2G34480	AT3G09950	AT3G47960	AT4G10150	AT4G31530	AT5G13910	AT5G46110
AT1G04645	AT1G23970	AT1G60690	AT2G01670	AT2G34500	AT3G10150	AT3G48000	AT4G10250	AT4G31560	AT5G13930	AT5G46150
AT1G04900	AT1G24120	AT1G60740	AT2G01830	AT2G34520	AT3G10160	AT3G48030	AT4G10330	AT4G31560	AT5G13990	AT5G46220
AT1G04920	AT1G24350	AT1G60790	AT2G01870	AT2G34590	AT3G10300	AT3G48070	AT4G10340	AT4G31620	AT5G14100	AT5G46300

Supplemental Table 9 (continued from last page)

AT1G05150	AT1G24580	AT1G60890	AT2G01930	AT2G34630	AT3G10320	AT3G48080	AT4G10350	AT4G31730	AT5G14380	AT5G46430
AT1G05180	AT1G24590	AT1G60950	AT2G02100	AT2G34655	AT3G10350	AT3G48185	AT4G10360	AT4G31750	AT5G14680	AT5G46620
AT1G05190	AT1G25141	AT1G61000	AT2G02120	AT2G34910	AT3G10460	AT3G48260	AT4G10550	AT4G31805	AT5G14710	AT5G46630
AT1G05205	AT1G25550	AT1G61040	AT2G02130	AT2G34930	AT3G10520	AT3G48270	AT4G10610	AT4G31950	AT5G14720	AT5G46640
AT1G05320	AT1G25580	AT1G61110	AT2G02160	AT2G34940	AT3G10525	AT3G48360	AT4G10620	AT4G32020	AT5G14730	AT5G46700
AT1G05380	AT1G26100	AT1G61215	AT2G02230	AT2G35010	AT3G10530	AT3G48420	AT4G10750	AT4G32040	AT5G14750	AT5G46860
AT1G05410	AT1G26210	AT1G61240	AT2G02400	AT2G35020	AT3G10540	AT3G48425	AT4G10920	AT4G32060	AT5G14780	AT5G46870
AT1G05430	AT1G26220	AT1G61410	AT2G02490	AT2G35100	AT3G10570	AT3G48450	AT4G10925	AT4G32080	AT5G14850	AT5G47110
AT1G05470	AT1G26340	AT1G61566	AT2G02500	AT2G35230	AT3G10610	AT3G48490	AT4G11140	AT4G32120	AT5G14900	AT5G47120
AT1G05610	AT1G26370	AT1G61620	AT2G02515	AT2G35290	AT3G10840	AT3G48510	AT4G11280	AT4G32250	AT5G14920	AT5G47140
AT1G05720	AT1G26380	AT1G61660	AT2G02540	AT2G35450	AT3G10850	AT3G48610	AT4G11300	AT4G32300	AT5G14960	AT5G47210
AT1G05730	AT1G26550	AT1G61820	AT2G02740	AT2G35510	AT3G11000	AT3G48740	AT4G11320	AT4G32320	AT5G14970	AT5G47220
AT1G05750	AT1G26580	AT1G61980	AT2G02880	AT2G35520	AT3G11120	AT3G48850	AT4G11330	AT4G32330	AT5G15120	AT5G47230
AT1G05805	AT1G26670	AT1G61990	AT2G03710	AT2G35550	AT3G11220	AT3G48990	AT4G11560	AT4G32410	AT5G15320	AT5G47240
AT1G05850	AT1G26770	AT1G62080	AT2G03740	AT2G35635	AT3G11230	AT3G49010	AT4G11570	AT4G32470	AT5G15340	AT5G47440
AT1G05900	AT1G26840	AT1G62120	AT2G03780	AT2G35650	AT3G11250	AT3G49050	AT4G11790	AT4G32540	AT5G15390	AT5G47530
AT1G05910	AT1G26945	AT1G62210	AT2G03880	AT2G35680	AT3G11280	AT3G49120	AT4G12000	AT4G32785	AT5G15430	AT5G47560
AT1G05940	AT1G27000	AT1G62240	AT2G04040	AT2G35760	AT3G11330	AT3G49270	AT4G12110	AT4G32830	AT5G15440	AT5G47600
AT1G05990	AT1G27140	AT1G62305	AT2G04305	AT2G35795	AT3G11410	AT3G49290	AT4G12250	AT4G32910	AT5G15460	AT5G47610
AT1G06100	AT1G27330	AT1G62390	AT2G04340	AT2G35800	AT3G11510	AT3G49360	AT4G12320	AT4G32940	AT5G15470	AT5G47630
AT1G06180	AT1G27340	AT1G62400	AT2G04400	AT2G35810	AT3G11540	AT3G49550	AT4G12420	AT4G33010	AT5G15500	AT5G47720
AT1G06210	AT1G27350	AT1G62510	AT2G04495	AT2G35910	AT3G11550	AT3G49650	AT4G12440	AT4G33010	AT5G15510	AT5G47800
AT1G06340	AT1G27440	AT1G62600	AT2G04520	AT2G35960	AT3G11600	AT3G49660	AT4G12480	AT4G33060	AT5G15530	AT5G47830
AT1G06400	AT1G27460	AT1G62640	AT2G04790	AT2G36170	AT3G11640	AT3G49670	AT4G12520	AT4G33080	AT5G15630	AT5G47870
AT1G06430	AT1G27590	AT1G62720	AT2G04830	AT2G36320	AT3G11660	AT3G49760	AT4G12530	AT4G33100	AT5G15710	AT5G47890
AT1G06430	AT1G27620	AT1G62730	AT2G04850	AT2G36480	AT3G11700	AT3G49780	AT4G12545	AT4G33110	AT5G15760	AT5G47970
AT1G06540	AT1G27640	AT1G62790	AT2G04890	AT2G36790	AT3G11890	AT3G49790	AT4G12550	AT4G33140	AT5G15980	AT5G47980
AT1G06550	AT1G27650	AT1G62820	AT2G05170	AT2G36885	AT3G11910	AT3G49850	AT4G12690	AT4G33220	AT5G16140	AT5G48140
AT1G06630	AT1G27695	AT1G62980	AT2G05220	AT2G36985	AT3G12100	AT3G49870	AT4G12710	AT4G33260	AT5G16160	AT5G48150
AT1G06680	AT1G27910	AT1G63010	AT2G05220	AT2G37080	AT3G12140	AT3G49890	AT4G12930	AT4G33430	AT5G16200	AT5G48300
AT1G06770	AT1G27960	AT1G63050	AT2G05270	AT2G37090	AT3G12203	AT3G50310	AT4G12940	AT4G33450	AT5G16220	AT5G48360
AT1G06780	AT1G27970	AT1G63090	AT2G05440	AT2G37120	AT3G12210	AT3G50340	AT4G13010	AT4G33460	AT5G16350	AT5G48370
AT1G06890	AT1G28060	AT1G63160	AT2G05510	AT2G37170	AT3G12340	AT3G50480	AT4G13050	AT4G33565	AT5G16380	AT5G48380
AT1G07070	AT1G28110	AT1G63180	AT2G05590	AT2G37300	AT3G12400	AT3G50500	AT4G13200	AT4G33720	AT5G16470	AT5G48480
AT1G07090	AT1G28200	AT1G63260	AT2G06025	AT2G37400	AT3G12670	AT3G50700	AT4G13290	AT4G33780	AT5G16620	AT5G48630
AT1G07150	AT1G28280	AT1G63290	AT2G06990	AT2G37460	AT3G12760	AT3G50740	AT4G13310	AT4G33865	AT5G16800	AT5G48870
AT1G07260	AT1G28370	AT1G63460	AT2G07180	AT2G37550	AT3G12780	AT3G50790	AT4G13480	AT4G33940	AT5G16810	AT5G48990
AT1G07270	AT1G28375	AT1G63640	AT2G07690	AT2G37600	AT3G12870	AT3G50800	AT4G13670	AT4G33980	AT5G16830	AT5G49020
AT1G07350	AT1G28395	AT1G63660	AT2G07771	AT2G37630	AT3G12880	AT3G50840	AT4G13710	AT4G33985	AT5G16870	AT5G49100
AT1G07370	AT1G28400	AT1G63690	AT2G10950	AT2G37690	AT3G12960	AT3G50940	AT4G13790	AT4G34050	AT5G16930	AT5G49220
AT1G07410	AT1G28410	AT1G63700	AT2G11910	AT2G37740	AT3G13050	AT3G51010	AT4G13940	AT4G34150	AT5G16970	AT5G49350
AT1G07470	AT1G28440	AT1G63770	AT2G12550	AT2G37820	AT3G13235	AT3G51030	AT4G13950	AT4G34555	AT5G16980	AT5G49410
AT1G07490	AT1G28530	AT1G63870	AT2G13820	AT2G37950	AT3G13275	AT3G51040	AT4G13990	AT4G34670	AT5G17160	AT5G49440
AT1G07600	AT1G28580	AT1G64105	AT2G14110	AT2G37970	AT3G13420	AT3G51050	AT4G14020	AT4G34770	AT5G17210	AT5G49460
AT1G07660	AT1G28600	AT1G64110	AT2G14120	AT2G38090	AT3G13450	AT3G51100	AT4G14040	AT4G34950	AT5G17220	AT5G49570
AT1G07750	AT1G28680	AT1G64190	AT2G14250	AT2G38130	AT3G13510	AT3G51130	AT4G14040	AT4G35020	AT5G17240	AT5G49610
AT1G07770	AT1G28960	AT1G64355	AT2G14460	AT2G38290	AT3G13570	AT3G51160	AT4G14100	AT4G35050	AT5G17330	AT5G49910
AT1G07790	AT1G29060	AT1G64380	AT2G14530	AT2G38780	AT3G13650	AT3G51325	AT4G14170	AT4G35070	AT5G17340	AT5G49920
AT1G07820	AT1G29070	AT1G64390	AT2G14540	AT2G38790	AT3G13660	AT3G51330	AT4G14210	AT4G35090	AT5G17440	AT5G50000
AT1G07880	AT1G29250	AT1G64440	AT2G14560	AT2G38810	AT3G13670	AT3G51330	AT4G14220	AT4G35190	AT5G17490	AT5G50090
AT1G07990	AT1G29260	AT1G64450	AT2G14610	AT2G38840	AT3G13674	AT3G51380	AT4G14310	AT4G35240	AT5G17560	AT5G50110
AT1G08010	AT1G29310	AT1G64470	AT2G15010	AT2G38920	AT3G13857	AT3G51400	AT4G14342	AT4G35335	AT5G17640	AT5G50200
AT1G08090	AT1G29340	AT1G64490	AT2G15020	AT2G38940	AT3G13880	AT3G51420	AT4G14350	AT4G35390	AT5G17660	AT5G50410
AT1G08110	AT1G29450	AT1G64660	AT2G15230	AT2G38960	AT3G14060	AT3G51500	AT4G14385	AT4G35480	AT5G17860	AT5G50430
AT1G08130	AT1G29490	AT1G64710	AT2G15345	AT2G39290	AT3G14067	AT3G51740	AT4G14400	AT4G35490	AT5G17900	AT5G50460
AT1G08150	AT1G29530	AT1G64770	AT2G15400	AT2G39400	AT3G14110	AT3G51750	AT4G14600	AT4G35590	AT5G18020	AT5G50480
AT1G08180	AT1G29660	AT1G64840	AT2G15560	AT2G39560	AT3G14150	AT3G51920	AT4G14615	AT4G35620	AT5G18120	AT5G50670
AT1G08180	AT1G29690	AT1G65180	AT2G15620	AT2G39570	AT3G14170	AT3G51940	AT4G14695	AT4G35650	AT5G18170	AT5G50820
AT1G08220	AT1G29770	AT1G65220	AT2G15695	AT2G39660	AT3G14200	AT3G52060	AT4G14713	AT4G35725	AT5G18250	AT5G51020
AT1G08270	AT1G29790	AT1G65260	AT2G15730	AT2G39800	AT3G14210	AT3G52060	AT4G14716	AT4G35750	AT5G18270	AT5G51210
AT1G08280	AT1G29970	AT1G65510	AT2G15760	AT2G39805	AT3G14210	AT3G52070	AT4G14716	AT4G35970	AT5G18380	AT5G51460
AT1G08350	AT1G30110	AT1G65520	AT2G15890	AT2G39820	AT3G14280	AT3G52090	AT4G14720	AT4G35980	AT5G18400	AT5G51600
AT1G08400	AT1G30130	AT1G65560	AT2G16005	AT2G39840	AT3G14310	AT3G52110	AT4G14780	AT4G36010	AT5G18430	AT5G51690
AT1G08510	AT1G30160	AT1G65730	AT2G16030	AT2G40095	AT3G14550	AT3G52210	AT4G14880	AT4G36030	AT5G18460	AT5G51810
AT1G08520	AT1G30220	AT1G65920	AT2G16660	AT2G40110	AT3G14560	AT3G52500	AT4G14960	AT4G36040	AT5G18540	AT5G51840
AT1G08630	AT1G30230	AT1G65970	AT2G16700	AT2G40130	AT3G14580	AT3G52530	AT4G15000	AT4G36090	AT5G18560	AT5G51940
AT1G08670	AT1G30490	AT1G65980	AT2G16760	AT2G40190	AT3G14680	AT3G52760	AT4G15210	AT4G36110	AT5G18630	AT5G51970
AT1G08700	AT1G30515	AT1G66090	AT2G16780	AT2G40290	AT3G14720	AT3G52780	AT4G15260	AT4G36250	AT5G18650	AT5G52030
AT1G08710	AT1G30520	AT1G66100	AT2G16940	AT2G40340	AT3G14740	AT3G52850	AT4G15290	AT4G36500	AT5G18670	AT5G52160
AT1G08760	AT1G30580	AT1G66120	AT2G16950	AT2G40460	AT3G14750	AT3G52860	AT4G15350	AT4G36640	AT5G19390	AT5G52220
AT1G08770	AT1G30630	AT1G66200	AT2G17030	AT2G40540	AT3G14790	AT3G52880	AT4G15410	AT4G36650	AT5G19500	AT5G52280
AT1G08820	AT1G30700	AT1G66210	AT2G17190	AT2G40550	AT3G14960	AT3G52890	AT4G15440	AT4G36830	AT5G19530	AT5G52360
AT1G09000	AT1G30757	AT1G66370	AT2G17220	AT2G40830	AT3G14990	AT3G52960	AT4G15475	AT4G36930	AT5G19690	AT5G52380
AT1G09030	AT1G30890	AT1G66410	AT2G17320	AT2G40860	AT3G15040	AT3G52990	AT4G15500	AT4G37000	AT5G19830	AT5G52390
AT1G09160	AT1G31020	AT1G66480	AT2G17390	AT2G41010	AT3G15080	AT3G53160	AT4G15540	AT4G37020	AT5G19870	AT5G52470
AT1G09240	AT1G31060	AT1G66500	AT2G17440	AT2G41050	AT3G15110	AT3G53190	AT4G15563	AT4G37070	AT5G19890	AT5G52500
AT1G09310	AT1G31170	AT1G66890	AT2G17500	AT2G41070	AT3G15150	AT3G53420	AT4G15610	AT4G37080	AT5G19930	AT5G52660
AT1G09370	AT1G31180	AT1G66940	AT2G17530	AT2G41230	AT3G15170	AT3G53530	AT4G15640	AT4G37090	AT5G19980	AT5G52760
AT1G09390	AT1G31220	AT1G67030	AT2G17705	AT2G41250	AT3G15240	AT3G53580	AT4G15660	AT4G37130	AT5G20020	AT5G52780
AT1G09420	AT1G31310	AT1G67070	AT2G17720	AT2G41390	AT3G15280	AT3G53620	AT4G15780	AT4G37295	AT5G20080	AT5G52810
AT1G09490	AT1G31330	AT1G67090	AT2G17950	AT2G41400	AT3G15351	AT3G53710	AT4G15790	AT4G37310	AT5G20110	AT5G52890
AT1G09590	AT1G31340	AT1G67110	AT2G17970	AT2G41430	AT3G15353	AT3G53720	AT4G15800	AT4G37410	AT5G20165	AT5G52900
AT1G09645	AT1G31500	AT1G67260	AT2G17990	AT2G41660	AT3G15470	AT3G53810	AT4G16030	AT4G37510	AT5G20290	AT5G53000
AT1G09795	AT1G31550	AT1G67290	AT2G18130	AT2G41710	AT3G15630	AT3G53990	AT4G16146	AT4G37550	AT5G20330	AT5G53045
AT1G09810	AT1G31660	AT1G67325	AT2G18170	AT2G41740	AT3G15650	AT3G54080	AT4G16265	AT4G37580	AT5G20520	AT5G53170
AT1G09815	AT1G31710	AT1G67330	AT2G18245	AT2G41750	AT3G15760	AT3G54140	AT4G16360	AT4G37610	AT5G20590	AT5G53190
AT1G09850	AT1G31720	AT1G67350	AT2G18280	AT2G41780	AT3G15880	AT3G54180	AT4G16430	AT4G37700	AT5G20600	AT5G53200
AT1G09950	AT1G31760	AT1G67410	AT2G18290	AT2G41810	AT3G15900	AT3G54200	AT4G16442	AT4G37710	AT5G20670	AT5G53290
AT1G09970	AT1G31800	AT1G67600	AT2G18410	AT2G41870	AT3G15920	AT3G54210	AT4G16444	AT4G37770	AT5G20820	AT5G53300
AT1G09995	AT1G31812	AT1G67630	AT2G18660	AT2G41945	AT3G16040	AT3G54250	AT4G16447	AT4G37830	AT5G20900	AT5G53300
AT1G10120	AT1G31812	AT1G67730	AT2G18840	AT2G42005	AT3G16080	AT3G54430	AT4G16500	AT4G37980	AT5G21090	AT5G53620
AT1G10150	AT1G31814	AT1G67785	AT2G18850	AT2G42040	AT3G16110	AT3G54460	AT4G16515	AT4G37980	AT5G21140	AT5G53770
AT1G10190	AT1G31850	AT1G67890	AT2G18860	AT2G42060	AT3G16140	AT3G54540	AT4G16695	AT4G38000	AT5G21170	AT5G53940
AT1G10210	AT1G31910	AT1G67990	AT2G18890	AT2G42190	AT3G16175	AT3G54600	AT4G16700	AT4G38020	AT5G21326	AT5G54070
AT1G10310	AT1G32050	AT1G68070	AT2G19270	AT2G42230	AT3G16270	AT3G54640	AT4G16720	AT4G38100	AT5G21430	AT5G54110
AT1G10350	AT1G32320	AT1G68100	AT2G19280	AT2G42240	AT3G16350	AT3G54710	AT4G16830	AT4G38160	AT5G21900	AT5G54130
AT1G10460	AT1G32360	AT1G68130	AT2G19470	AT2G42280	AT3G16400	AT3G54890	AT4G17060	AT4G38360	AT5G22000	AT5G54430
AT1G10480	AT1G32400	AT1G68160	AT2G19500	AT2G42300	AT3G16500	AT3G54890	AT4G17070	AT4G38440	AT5G22050	AT5G54490
AT1G10580	AT1G32470	AT1G68260	AT2G19560	AT2G42310	AT3G16560	AT3G54990	AT4G17350	AT4G38470	AT5G22090	AT5G54510
AT1G10585	AT1G32470	AT1G68310	AT2G19580	AT2G42540	AT3G16570	AT3G55000	AT4G17370	AT4G38495	AT5G22250	AT5G54530
AT1G10600	AT1G32530	AT1G68370	AT2G19720	AT2G42670	AT3G16650	AT3G55050	AT4G17390	AT4G38520	AT5G22270	AT5G54640
AT1G10630	AT1G32860	AT1G68660	AT2G19730	AT2G42840	AT3G16810	AT3G55070	AT4G17460	AT4G38580	AT5G22390	AT5G54740
AT1G10650	AT1G32940	AT1G68800	AT2G19740	AT2G42880	AT3G16830	AT3G55080	AT4G17530	AT4G38680	AT5G22450	AT5G54850
AT1G10750	AT1G33030	AT1G68810	AT2G19750	AT2G42900	AT3G16850	AT3G55120	AT4G17570	AT4G39210	AT5G22480	AT5G54880
AT1G10760	AT1G33055	AT1G68830	AT2G19860	AT2G42950	AT3G16890	AT3G55140	AT4G17730	AT4G39220	AT5G22790	AT5G54900
AT1G10770	AT1G33120	AT1G68840	AT2G20300	AT2G42975	AT3G17000	AT3G55230	AT4G17840	AT4G39235	AT5G22820	AT5G54930
AT1G11110	AT1G33140	AT1G68880	AT2G20350	AT2G43030	AT3G17040	AT3G55470	AT4G18060	AT4G39280	AT5G22875	AT5G55090
AT1G11320	AT1G33260	AT1G68945	AT2G20465	AT2G43080	AT3G17060	AT3G55560	AT4G18170	AT4G39300	AT5G22880	AT5G55140
AT1G11380	AT1G33330	AT1G69050	AT2G20495	AT2G43130	AT3G17090	AT3G55700	AT4G18230	AT4G39320	AT5G23040	AT5G55160
AT1G11475	AT1G33340	AT1G69060	AT2G20550	AT2G43260	AT3G17160	AT3G55740	AT4G18360	AT4G39510	AT5G23090	AT5G55170
AT1G11590	AT1G33360	AT1G69080	AT2G20590	AT2G43320	AT3G17210	AT3G55750	AT4G18375	AT4G39540	AT5G23100	AT5G55260
AT1G11700	AT1G33475	AT1G69220	AT2G20630	AT2G43330	AT3G17240	AT3G55830	AT4G18400	AT4G39570	AT5G23140	AT5G55280
AT1G11720	AT1G33520	AT1G69230	AT2G20700	AT2G43340	AT3G17330	AT3G55910	AT4G18550	AT4G39650	AT5G23420	AT5G55410
AT1G11870	AT1G33760	AT1G69400	AT2G20710	AT2G43350	AT3G17510	AT3G55920	AT4G18570	AT4G39670	AT5G23460	AT5G55530
AT1G11915	AT1G33770	AT1G69520	AT2G20750	AT2G43360	AT3G17530	AT3G56090	AT4G18580	AT4G39710	AT5G23570	AT5G55540
AT1G12050	AT1G33990	AT1G69620	AT2G20760	AT2G43430	AT3G17590	AT3G56200	AT4G18593	AT4G39770	AT5G23610	AT5G55550
AT1G12070	AT1G34020	AT1G69680	AT2G20770	AT2G43560	AT3G17650	AT3G56460	AT4G18730	AT4G39795	AT5G23690	AT5G55560
AT1G12090	AT1G34200	AT1G69740	AT2G20820	AT2G43680	AT3G17680	AT3G56650	AT4G18780	AT4G39830	AT5G23720	AT5G55600
AT1G12130	AT1G34380	AT1G69760	AT2G20825	AT2G43800	AT3G17750	AT3G56740	AT4G18830	AT4G39840	AT5G23730	AT5G55790
AT1G12200	AT1G34470	AT1G69800	AT2G20830	AT2G43850	AT3G17820	AT3G56820	AT4G18890	AT4G39930	AT5G23760	AT5G55900
AT1G12260	AT1G34510	AT1G69870	AT2G20840	AT2G43940	AT3G17840	AT3G56860	AT4G18960	AT4G40040	AT5G23920	AT5G56090
AT1G12420	AT1G34750	AT1G69900	AT2G20930	AT2G44240	AT3G17880	AT3G56860	AT4G18970	AT4G40070	AT5G23950	AT5G56140
AT1G12480	AT1G35180	AT1G69960	AT2G20940	AT2G44370	AT3G17910	AT3G56860	AT4G19110	AT5G01015	AT5G23980	AT5G56270
AT1G12570	AT1G35190	AT1G69980	AT2G20950	AT2G44590	AT3G18035	AT3G57000	AT4G19180	AT5G01020	AT5G24030	AT5G56280
AT1G12580	AT1G35260	AT1G70030	AT2G21045	AT2G44610	AT3G18040	AT3G57030	AT4G19190	AT5G01170	AT5G24060	AT5G56580

Supplemental Table 9 (continued from last page)

AT1G12710	AT1G35440	AT1G70160	AT2G21060	AT2G44680	AT3G18165	AT3G57120	AT4G19200	AT5G01220	AT5G24090	AT5G56710
AT1G12790	AT1G35510	AT1G70270	AT2G21070	AT2G44820	AT3G18260	AT3G57140	AT4G19400	AT5G01370	AT5G24170	AT5G56860
AT1G12880	AT1G35630	AT1G70510	AT2G21100	AT2G44940	AT3G18290	AT3G57150	AT4G19560	AT5G01450	AT5G24313	AT5G56900
AT1G13060	AT1G36060	AT1G70570	AT2G21120	AT2G45110	AT3G18350	AT3G57320	AT4G19570	AT5G01470	AT5G24340	AT5G56940
AT1G13195	AT1G36070	AT1G70670	AT2G21150	AT2G45130	AT3G18410	AT3G57360	AT4G19630	AT5G01520	AT5G24380	AT5G57000
AT1G13220	AT1G36340	AT1G70790	AT2G21200	AT2G45170	AT3G18420	AT3G57390	AT4G19640	AT5G01650	AT5G24430	AT5G57015
AT1G13245	AT1G36390	AT1G70830	AT2G21237	AT2G45210	AT3G18430	AT3G57450	AT4G19645	AT5G01670	AT5G24500	AT5G57040
AT1G13250	AT1G37130	AT1G70880	AT2G22740	AT2G45260	AT3G18550	AT3G57510	AT4G19830	AT5G01720	AT5G24520	AT5G57060
AT1G13340	AT1G43130	AT1G70920	AT2G22905	AT2G45310	AT3G18690	AT3G57580	AT4G20010	AT5G01740	AT5G24570	AT5G57090
AT1G13430	AT1G43170	AT1G70985	AT2G22910	AT2G45490	AT3G18750	AT3G57640	AT4G20020	AT5G01830	AT5G24655	AT5G57220
AT1G13510	AT1G43190	AT1G71040	AT2G22990	AT2G45520	AT3G18800	AT3G57650	AT4G20070	AT5G01920	AT5G24820	AT5G57270
AT1G13640	AT1G43640	AT1G71180	AT2G23170	AT2G45560	AT3G18850	AT3G57680	AT4G20280	AT5G01930	AT5G24840	AT5G57290
AT1G13670	AT1G43700	AT1G71210	AT2G23260	AT2G45600	AT3G18940	AT3G57730	AT4G20310	AT5G01940	AT5G24970	AT5G57450
AT1G13670	AT1G43790	AT1G71260	AT2G23270	AT2G45620	AT3G18950	AT3G57760	AT4G20360	AT5G02090	AT5G24980	AT5G57520
AT1G13700	AT1G43800	AT1G71270	AT2G23390	AT2G45680	AT3G19130	AT3G57800	AT4G20800	AT5G02110	AT5G25090	AT5G57560
AT1G13740	AT1G43860	AT1G71420	AT2G23560	AT2G45690	AT3G19150	AT3G57920	AT4G20870	AT5G02130	AT5G25160	AT5G57565
AT1G13780	AT1G44000	AT1G71520	AT2G23620	AT2G45700	AT3G19170	AT3G57930	AT4G20880	AT5G02280	AT5G25210	AT5G57670
AT1G13820	AT1G44100	AT1G71530	AT2G23760	AT2G45720	AT3G19350	AT3G57980	AT4G20890	AT5G02320	AT5G25240	AT5G57685
AT1G13910	AT1G44110	AT1G71690	AT2G23800	AT2G45740	AT3G19380	AT3G58030	AT4G20960	AT5G02380	AT5G25250	AT5G57760
AT1G14000	AT1G44790	AT1G71692	AT2G24260	AT2G45890	AT3G19440	AT3G58040	AT4G21010	AT5G02420	AT5G25280	AT5G57790
AT1G14030	AT1G44900	AT1G71695	AT2G24420	AT2G45970	AT3G19650	AT3G58130	AT4G21105	AT5G02450	AT5G25360	AT5G57815
AT1G14080	AT1G45050	AT1G71750	AT2G24640	AT2G45990	AT3G19790	AT3G58150	AT4G21250	AT5G02500	AT5G25380	AT5G57830
AT1G14160	AT1G45110	AT1G71830	AT2G24970	AT2G46110	AT3G19810	AT3G58470	AT4G21280	AT5G02550	AT5G25510	AT5G57890
AT1G14185	AT1G45150	AT1G71920	AT2G24990	AT2G46150	AT3G19820	AT3G58490	AT4G21450	AT5G02560	AT5G25590	AT5G57900
AT1G14250	AT1G45165	AT1G71930	AT2G25010	AT2G46225	AT3G19900	AT3G58570	AT4G21540	AT5G02620	AT5G25620	AT5G58020
AT1G14290	AT1G45170	AT1G71960	AT2G25090	AT2G46330	AT3G20015	AT3G58610	AT4G21610	AT5G02630	AT5G25760	AT5G58200
AT1G14300	AT1G45230	AT1G72130	AT2G25190	AT2G46370	AT3G20110	AT3G58640	AT4G21660	AT5G02710	AT5G25790	AT5G58375
AT1G14320	AT1G45976	AT1G72150	AT2G25210	AT2G46400	AT3G20170	AT3G58650	AT4G21800	AT5G02760	AT5G25810	AT5G58420
AT1G14320	AT1G45976	AT1G72210	AT2G25240	AT2G46490	AT3G20440	AT3G58690	AT4G21860	AT5G02870	AT5G25940	AT5G58590
AT1G14350	AT1G46768	AT1G72350	AT2G25250	AT2G46580	AT3G20560	AT3G58760	AT4G21870	AT5G03150	AT5G25980	AT5G58690
AT1G14370	AT1G47128	AT1G72430	AT2G25270	AT2G46620	AT3G20640	AT3G58840	AT4G21910	AT5G03200	AT5G26000	AT5G58700
AT1G14400	AT1G47230	AT1G72660	AT2G25310	AT2G46650	AT3G20650	AT3G58850	AT4G22000	AT5G03280	AT5G26210	AT5G58740
AT1G14410	AT1G47240	AT1G72670	AT2G25350	AT2G46735	AT3G20830	AT3G58970	AT4G22260	AT5G03340	AT5G26260	AT5G58760
AT1G14450	AT1G47280	AT1G72690	AT2G25420	AT2G46770	AT3G20870	AT3G59150	AT4G22320	AT5G03350	AT5G26280	AT5G58787
AT1G14490	AT1G47330	AT1G72790	AT2G25430	AT2G46830	AT3G20910	AT3G59280	AT4G22330	AT5G03415	AT5G26360	AT5G58960
AT1G14530	AT1G47380	AT1G72800	AT2G25500	AT2G47020	AT3G20920	AT3G59320	AT4G22360	AT5G03440	AT5G26740	AT5G59000
AT1G14570	AT1G47410	AT1G72970	AT2G25520	AT2G47270	AT3G21160	AT3G59330	AT4G22380	AT5G03460	AT5G26742	AT5G59030
AT1G14580	AT1G47420	AT1G73177	AT2G25560	AT2G47470	AT3G21190	AT3G59360	AT4G22550	AT5G03490	AT5G26780	AT5G59070
AT1G14685	AT1G47490	AT1G73380	AT2G25560	AT2G47560	AT3G21210	AT3G59370	AT4G22710	AT5G03530	AT5G26930	AT5G59120
AT1G14770	AT1G47670	AT1G73530	AT2G25620	AT2G47640	AT3G21330	AT3G59490	AT4G22820	AT5G03610	AT5G26940	AT5G59170
AT1G14840	AT1G47710	AT1G73630	AT2G25710	AT2G47910	AT3G21350	AT3G59540	AT4G22860	AT5G03730	AT5G26990	AT5G59220
AT1G14980	AT1G47820	AT1G73640	AT2G25720	AT2G47910	AT3G21390	AT3G59600	AT4G22940	AT5G03930	AT5G27420	AT5G59310
AT1G14990	AT1G47870	AT1G73690	AT2G25737	AT2G47950	AT3G21500	AT3G59630	AT4G22950	AT5G04130	AT5G27440	AT5G59350
AT1G15040	AT1G47970	AT1G73830	AT2G25740	AT2G47980	AT3G21550	AT3G59790	AT4G23130	AT5G04190	AT5G27470	AT5G59460
AT1G15140	AT1G48000	AT1G73850	AT2G25770	AT2G48090	AT3G21580	AT3G59845	AT4G23210	AT5G04250	AT5G27620	AT5G59510
AT1G15170	AT1G48040	AT1G73885	AT2G25880	AT3G01100	AT3G21740	AT3G59890	AT4G23410	AT5G04360	AT5G27700	AT5G59520
AT1G15230	AT1G48070	AT1G73980	AT2G26000	AT3G01120	AT3G21820	AT3G60030	AT4G23420	AT5G04420	AT5G27710	AT5G59550
AT1G15230	AT1G48130	AT1G74010	AT2G26100	AT3G01130	AT3G21870	AT3G60220	AT4G23500	AT5G04440	AT5G27720	AT5G59560
AT1G15270	AT1G48170	AT1G74230	AT2G26250	AT3G01250	AT3G21890	AT3G60245	AT4G23550	AT5G04600	AT5G27740	AT5G59730
AT1G15330	AT1G48175	AT1G74270	AT2G26280	AT3G01290	AT3G22060	AT3G60410	AT4G23590	AT5G04620	AT5G27770	AT5G59770
AT1G15400	AT1G48250	AT1G74300	AT2G26460	AT3G01325	AT3G22090	AT3G60450	AT4G23650	AT5G04720	AT5G27820	AT5G59780
AT1G15430	AT1G48300	AT1G74340	AT2G26470	AT3G01540	AT3G22410	AT3G60510	AT4G23720	AT5G04770	AT5G27920	AT5G59800
AT1G15440	AT1G48370	AT1G74370	AT2G26490	AT3G01590	AT3G22415	AT3G60530	AT4G23790	AT5G04830	AT5G27930	AT5G59840
AT1G15800	AT1G48480	AT1G74410	AT2G26510	AT3G01650	AT3G22420	AT3G60690	AT4G23810	AT5G04885	AT5G28290	AT5G59880
AT1G15880	AT1G48620	AT1G74470	AT2G26520	AT3G01830	AT3G22430	AT3G60850	AT4G23900	AT5G04900	AT5G28300	AT5G59960
AT1G15970	AT1G48635	AT1G74510	AT2G26640	AT3G01890	AT3G22435	AT3G60870	AT4G24015	AT5G05200	AT5G28460	AT5G60020
AT1G16290	AT1G48720	AT1G74640	AT2G26670	AT3G01950	AT3G22470	AT3G60880	AT4G24130	AT5G05280	AT5G28840	AT5G60050
AT1G16320	AT1G48750	AT1G74740	AT2G26670	AT3G01960	AT3G22480	AT3G60900	AT4G24140	AT5G05300	AT5G33300	AT5G60070
AT1G16330	AT1G48790	AT1G74860	AT2G26760	AT3G01970	AT3G22490	AT3G61060	AT4G24200	AT5G05360	AT5G34358	AT5G60230
AT1G16445	AT1G48920	AT1G74880	AT2G26780	AT3G01980	AT3G22540	AT3G61270	AT4G24230	AT5G05410	AT5G35100	AT5G60280
AT1G16460	AT1G49010	AT1G74890	AT2G26950	AT3G02000	AT3G22600	AT3G61460	AT4G24440	AT5G05470	AT5G35170	AT5G60400
AT1G16470	AT1G49050	AT1G74900	AT2G26980	AT3G02110	AT3G22630	AT3G61560	AT4G24450	AT5G05480	AT5G35320	AT5G60410
AT1G16510	AT1G49170	AT1G74920	AT2G27020	AT3G02290	AT3G22810	AT3G61570	AT4G24460	AT5G05510	AT5G35490	AT5G60580
AT1G16520	AT1G49230	AT1G75040	AT2G27040	AT3G02460	AT3G22820	AT3G61650	AT4G24620	AT5G05610	AT5G35630	AT5G60600
AT1G16530	AT1G49245	AT1G75090	AT2G27180	AT3G02555	AT3G22900	AT3G61770	AT4G24690	AT5G05630	AT5G35670	AT5G60620
AT1G16570	AT1G49320	AT1G75170	AT2G27290	AT3G02600	AT3G22942	AT3G61830	AT4G24740	AT5G05640	AT5G35740	AT5G60690
AT1G16640	AT1G49400	AT1G75180	AT2G27300	AT3G02670	AT3G22950	AT3G61970	AT4G24770	AT5G05710	AT5G36290	AT5G60750
AT1G16650	AT1G49500	AT1G75190	AT2G27330	AT3G02800	AT3G23090	AT3G62070	AT4G24780	AT5G05890	AT5G37050	AT5G60760
AT1G16705	AT1G49510	AT1G75250	AT2G27360	AT3G02830	AT3G23170	AT3G62160	AT4G24860	AT5G05930	AT5G37478	AT5G60790
AT1G16850	AT1G49520	AT1G75280	AT2G27370	AT3G02910	AT3G23200	AT3G62190	AT4G24960	AT5G05950	AT5G37530	AT5G60790
AT1G16960	AT1G49620	AT1G75350	AT2G27450	AT3G02920	AT3G23310	AT3G62220	AT4G25030	AT5G05987	AT5G37740	AT5G60950
AT1G17130	AT1G49720	AT1G75490	AT2G27530	AT3G02940	AT3G23410	AT3G62240	AT4G25100	AT5G06070	AT5G37770	AT5G60980
AT1G17140	AT1G49730	AT1G75560	AT2G27550	AT3G02950	AT3G23530	AT3G62560	AT4G25110	AT5G06140	AT5G37790	AT5G61030
AT1G17345	AT1G49780	AT1G75580	AT2G27740	AT3G03050	AT3G23530	AT3G62620	AT4G25220	AT5G06150	AT5G37840	AT5G61270
AT1G17450	AT1G50020	AT1G75760	AT2G27775	AT3G03070	AT3G23540	AT3G62720	AT4G25260	AT5G06310	AT5G37930	AT5G61310
AT1G17455	AT1G50250	AT1G75780	AT2G27790	AT3G03090	AT3G23580	AT3G62730	AT4G25300	AT5G06450	AT5G38130	AT5G61510
AT1G17460	AT1G50490	AT1G75820	AT2G27820	AT3G03130	AT3G23660	AT3G62810	AT4G25310	AT5G06480	AT5G38140	AT5G61590
AT1G17490	AT1G50570	AT1G76070	AT2G28000	AT3G03150	AT3G23690	AT3G62830	AT4G25380	AT5G06510	AT5G38160	AT5G61670
AT1G17590	AT1G50630	AT1G76080	AT2G28040	AT3G03210	AT3G23840	AT3G62910	AT4G25420	AT5G06560	AT5G38180	AT5G61670
AT1G17700	AT1G50640	AT1G76090	AT2G28100	AT3G03270	AT3G23920	AT3G62950	AT4G25480	AT5G06590	AT5G38195	AT5G61820
AT1G17710	AT1G50670	AT1G76100	AT2G28110	AT3G03280	AT3G24000	AT3G62960	AT4G25580	AT5G06680	AT5G38510	AT5G62020
AT1G17790	AT1G50710	AT1G76130	AT2G28130	AT3G03310	AT3G24070	AT3G63030	AT4G25600	AT5G06690	AT5G38630	AT5G62130
AT1G17860	AT1G50740	AT1G76200	AT2G28150	AT3G03380	AT3G24170	AT3G63040	AT4G25770	AT5G06830	AT5G38660	AT5G62150
AT1G17880	AT1G51070	AT1G76240	AT2G28160	AT3G03410	AT3G24230	AT3G63260	AT4G25870	AT5G06850	AT5G38700	AT5G62190
AT1G17890	AT1G51130	AT1G76320	AT2G28190	AT3G03420	AT3G24280	AT3G63330	AT4G25890	AT5G07030	AT5G38720	AT5G62380
AT1G18030	AT1G51200	AT1G76370	AT2G28330	AT3G03480	AT3G24350	AT3G63390	AT4G25910	AT5G07230	AT5G38780	AT5G62460
AT1G18090	AT1G51390	AT1G76420	AT2G28400	AT3G03530	AT3G24460	AT3G63400	AT4G26060	AT5G07240	AT5G38880	AT5G62490
AT1G18100	AT1G51650	AT1G76430	AT2G28430	AT3G03570	AT3G24506	AT3G63410	AT4G26150	AT5G07260	AT5G38990	AT5G62500
AT1G18170	AT1G51660	AT1G76440	AT2G28660	AT3G03580	AT3G24530	AT3G63420	AT4G26200	AT5G07310	AT5G39050	AT5G62575
AT1G18180	AT1G51670	AT1G76450	AT2G28670	AT3G03610	AT3G24550	AT3G63430	AT4G26230	AT5G07450	AT5G39090	AT5G62600
AT1G18350	AT1G51700	AT1G76460	AT2G28720	AT3G03760	AT3G24770	AT3G63450	AT4G26260	AT5G07500	AT5G39360	AT5G62610
AT1G18680	AT1G51930	AT1G76590	AT2G28740	AT3G03840	AT3G24820	AT3G63510	AT4G26510	AT5G07590	AT5G39590	AT5G62710
AT1G18730	AT1G52030	AT1G76670	AT2G28860	AT3G04300	AT3G24830	AT4G00050	AT4G26555	AT5G07690	AT5G39720	AT5G62790
AT1G18880	AT1G52190	AT1G76680	AT2G28870	AT3G04350	AT3G25100	AT4G00060	AT4G26630	AT5G07720	AT5G39865	AT5G62910
AT1G18890	AT1G52200	AT1G76690	AT2G29050	AT3G04520	AT3G25160	AT4G00080	AT4G26660	AT5G08100	AT5G40040	AT5G62940
AT1G19050	AT1G52270	AT1G76730	AT2G29090	AT3G04630	AT3G25165	AT4G00110	AT4G26690	AT5G08130	AT5G40080	AT5G63040
AT1G19070	AT1G52310	AT1G76800	AT2G29180	AT3G04640	AT3G25170	AT4G00170	AT4G26760	AT5G08160	AT5G40190	AT5G63080
AT1G19150	AT1G52320	AT1G76860	AT2G29290	AT3G04730	AT3G25230	AT4G00270	AT4G26780	AT5G08190	AT5G40370	AT5G63120
AT1G19210	AT1G52420	AT1G76890	AT2G29410	AT3G04830	AT3G25400	AT4G00330	AT4G26840	AT5G08200	AT5G40500	AT5G63150
AT1G19300	AT1G52550	AT1G76960	AT2G29540	AT3G04850	AT3G25530	AT4G00335	AT4G26890	AT5G08240	AT5G40530	AT5G63160
AT1G19320	AT1G52890	AT1G76990	AT2G29550	AT3G04910	AT3G25570	AT4G00490	AT4G26950	AT5G08290	AT5G40540	AT5G63400
AT1G19330	AT1G52910	AT1G77000	AT2G29570	AT3G05050	AT3G25600	AT4G00680	AT4G26965	AT5G08290	AT5G40650	AT5G63410
AT1G19360	AT1G52970	AT1G77090	AT2G29650	AT3G05070	AT3G25640	AT4G00752	AT4G27030	AT5G08370	AT5G40710	AT5G63450
AT1G19380	AT1G53035	AT1G77220	AT2G29670	AT3G05090	AT3G25717	AT4G00770	AT4G27070	AT5G08380	AT5G40780	AT5G63460
AT1G19400	AT1G53050	AT1G77250	AT2G29680	AT3G05230	AT3G25740	AT4G00830	AT4G27100	AT5G08400	AT5G40880	AT5G63840
AT1G19480	AT1G53100	AT1G77270	AT2G29700	AT3G05290	AT3G25760	AT4G00880	AT4G27160	AT5G08420	AT5G40950	AT5G63880
AT1G19510	AT1G53120	AT1G77290	AT2G29750	AT3G05350	AT3G25770	AT4G01050	AT4G27230	AT5G08480	AT5G40960	AT5G63980
AT5G64020	AT5G64060	AT5G64150	AT5G64180	AT5G64200	AT5G64300	AT5G64440	AT5G64460	AT5G64480	AT5G64490	AT5G64600
AT5G64650	AT5G64730	AT5G64740	AT5G64760	AT5G64830	AT5G64890	AT5G65090	AT5G65140	AT5G65160	AT5G65170	AT5G65180
AT5G65200	AT5G65207	AT5G65340	AT5G65350	AT5G65420	AT5G65640	AT5G65650	AT5G65670	AT5G65740	AT5G65830	AT5G65850
AT5G65910	AT5G66090	AT5G66130	AT5G66140	AT5G66160	AT5G66300	AT5G66330	AT5G66360	AT5G66380	AT5G66580	AT5G66675
AT5G66710	AT5G66930	AT5G67020	AT5G67080	AT5G67090	AT5G67190	AT5G67350	AT5G67360	AT5G67390	AT5G67430	AT5G67520
AT5G67590	AT5G67630	ATCG00720	ATCG00730							

Supplemental Table 10: Interactions of Arabidopsis proteins with OECs as determined by Y2H

AGI identifier	Space	Interacting OEC	AGI identifier	Space	Interacting OEC
AT1G12520	1	OEC45	AT3G48150	1	OEC67
AT1G21200	1	OEC45	AT3G51960	1	OEC112
AT1G22920	1	OEC21	AT3G51960	1	OEC25
AT1G22920	1	OEC25	AT3G51960	1	OEC45
AT1G22920	1	OEC61	AT3G61150	1	OEC25
AT1G22920	1	OEC67	AT4G00120	1	OEC45
AT1G22920	1	OEC70	AT4G01090	1	OEC45
AT1G22920	1	OEC71	AT4G02590	1	OEC78
AT1G22920	1	OEC78	AT4G04020	1	OEC78
AT1G22920	1	OEC85	AT4G08150	1	OEC45
AT1G22920	1	OEC89	AT4G15730	1	OEC45
AT1G25490	1	OEC119	AT4G17680	1	OEC61
AT1G25490	1	OEC70	AT4G22240	1	OEC78
AT1G25550	1	OEC67	AT4G24840	1	OEC25
AT1G25550	1	OEC78	AT4G25200	1	OEC117
AT1G31880	1	OEC78	AT4G25200	1	OEC76
AT1G54060	1	OEC70	AT4G25200	1	OEC78
AT1G55190	1	OEC65	AT4G25200	1	OEC88
AT1G63480	1	OEC45	AT4G26110	1	OEC56
AT1G69690	1	OEC21	AT4G28640	1	OEC115
AT1G69690	1	OEC39	AT4G30080	1	OEC78
AT1G69690	1	OEC67	AT5G11980	1	OEC25
AT1G69690	1	OEC78	AT5G24660	1	OEC25
AT1G71230	1	OEC21	AT5G42220	1	OEC70
AT1G71230	1	OEC25	AT1G04690	2	OEC55
AT1G71230	1	OEC36	AT1G17700	2	OEC65
AT1G71230	1	OEC49	AT1G23380	2	OEC84
AT1G71230	1	OEC67	AT1G55170	2	OEC118
AT1G71230	1	OEC70	AT1G77250	2	OEC45
AT1G71230	1	OEC71	AT2G02540	2	OEC21
AT1G71230	1	OEC77	AT2G02540	2	OEC45
AT1G71230	1	OEC78	AT2G02540	2	OEC78
AT1G71230	1	OEC85	AT2G45680	2	OEC27
AT2G05230	1	OEC118	AT2G45680	2	OEC39
AT2G23420	1	OEC123	AT2G45680	2	OEC49
AT2G23420	1	OEC16	AT2G45680	2	OEC67
AT2G23420	1	OEC25b	AT2G45680	2	OEC70
AT2G23420	1	OEC54	AT2G45680	2	OEC76
AT2G37020	1	OEC67	AT3G06940	2	OEC25
AT3G01670	1	OEC63	AT3G14750	2	OEC118
AT3G02150	1	OEC45	AT3G22420	2	OEC45
AT3G02150	1	OEC61	AT3G27010	2	OEC119
AT3G02150	1	OEC78	AT3G27010	2	OEC14
AT3G08530	1	OEC45	AT3G27010	2	OEC21
AT3G08530	1	OEC63	AT3G27010	2	OEC67
AT3G10480	1	OEC115	AT3G27010	2	OEC68
AT3G13720	1	OEC65	AT3G27010	2	OEC77
AT3G17860	1	OEC78	AT3G58030	2	OEC78
AT3G21215	1	OEC45	AT4G08320	2	OEC59
AT3G21490	1	OEC115	AT4G11790	2	OEC63
AT3G21490	1	OEC56	AT5G08130	2	OEC115
AT3G25800	1	OEC119	AT5G42480	2	OEC78
AT3G47620	1	OEC101	AT5G48370	2	OEC103
AT3G47620	1	OEC103	AT5G48370	2	OEC78
AT3G47620	1	OEC106	AT5G48370	2	OEC84
AT3G47620	1	OEC110	AT5G65180	2	OEC35
AT3G47620	1	OEC113	AT5G65180	2	OEC78
AT3G47620	1	OEC117			
AT3G47620	1	OEC119			
AT3G47620	1	OEC120			
AT3G47620	1	OEC123			
AT3G47620	1	OEC125			
AT3G47620	1	OEC16a			
AT3G47620	1	OEC21			
AT3G47620	1	OEC23a			
AT3G47620	1	OEC23b			
AT3G47620	1	OEC27			
AT3G47620	1	OEC35			
AT3G47620	1	OEC39			
AT3G47620	1	OEC45			
AT3G47620	1	OEC55			
AT3G47620	1	OEC60			
AT3G47620	1	OEC70			
AT3G47620	1	OEC88			
AT3G47620	1	OEC92			

Supplemental Table 11: T-DNA insertion lines used in this study. Lines were either obtained from NASC and screened for homozygous insertions with the primers listed or homozygous lines were provided by Jeff Dangl, University of North Caroline, Chapel Hill, USA as indicated.

AGI identifier	Name	T-DNA insertion line	Left Primer	Right Primer	TDNA Primer
AT1G04690		SALK_030039	GAGGGAATAGCTCCCTTGTTG	GATGTGAAAGAAGCGAAATCG	ATTTTGCCGATTTCGGAAC
AT1G21200		SALK_101859	TGTAGTGCTCTCGGCGATATC	ACTTATCCTCACATTGCTGCG	ATTTTGCCGATTTCGGAAC
AT1G23380		SALK_054482	AGCACACACAAAACAAAACCC	GTTTCCTTCCGATTACCAAGC	ATTTTGCCGATTTCGGAAC
AT1G55170		SALK_002678	GCAGGATGCTGAAATCAGAAG	GATGCATACCCACAAACAACC	ATTTTGCCGATTTCGGAAC
AT1G77250		SALK_012299	CGTAGTTCGGAAGCTGAACAC	AACCATTCTCCATTTGGAACC	ATTTTGCCGATTTCGGAAC
AT2G37020		SAIL_36	GGAGAAGTGAAACACAGGCAG	TCAAGTAGGATGCTAAGGGGG	TGAATTTCATAACCAATCTCGATACAC
AT3G01670		SALK_148614	CTGATGATCACCATGTTGCTG	TCTCCGAAACTTCCATAAACG	ATTTTGCCGATTTCGGAAC
AT3G06940		SALK_045336	TTCCGATCCTCATTTCTGATG	TTTGCATTTGACAGACACTCG	ATTTTGCCGATTTCGGAAC
AT3G10480		SALK_026244	TCCTAGCGTTTGTAAATCTTTGAAC	TTCATTTCCTGATCCACAAGC	ATTTTGCCGATTTCGGAAC
AT3G21215		SALK_055957	TTGAGATGGTTGCCTGGTTAC	AGGCTCCTCAATTCTTCTTCG	ATTTTGCCGATTTCGGAAC
AT3G22420		SALK_121042	CTCGTCTCATCTCATTCTCCG	TTGCGTTGGTACTTCAAAACC	ATTTTGCCGATTTCGGAAC
AT3G27010		SALK_016203	AAATTTCTTGAACCCACCACC	CCACCTGCAAGTTCAAACAAC	ATTTTGCCGATTTCGGAAC
AT3G61150		SALK_062171	CGACAAAGCTTAGGGCTTTTC	TTGAGATCTCACCGATAACGG	ATTTTGCCGATTTCGGAAC
AT4G08320		SAIL_731	GTTGGTTTGGCTTTTCAGTTG	GGAAAATATGCCGAGGCTATC	TGAATTTCATAACCAATCTCGATACAC
AT4G11790		SALK_043553	GTTTCGGGTTTCTTTGAAAGG	AAGAAGATTGGCACAACATTCTC	ATTTTGCCGATTTCGGAAC
AT4G15730		SALK_094600	AACTTTAAAGCGGCTCTGAGG	TGCCATAATTGATGAAGGTGG	ATTTTGCCGATTTCGGAAC
AT4G22240		SAIL_384	AGAGTTTTCAAAGTCCGAGCC	GGCCATAGACGAGATGTTCTG	TGAATTTCATAACCAATCTCGATACAC
AT4G30080		SAIL_272	TTATTTTCCGGGAAAATTTCG	TCGAGCATCTAATGCCTTGAC	TGAATTTCATAACCAATCTCGATACAC
AT5G08130		SALK_132178	TGTATTGTCCGAGATTCCACC	CACTCCTGAATTCTCCAATGC	ATTTTGCCGATTTCGGAAC
AT5G42220		SALK_151742	GCTTGACTTGTTGCAGGAAAC	TTGCCTAGGTTGTGAATGACC	ATTTTGCCGATTTCGGAAC
AT5G42480		SAIL_693	ATCAGCAACGGACATTTCAAC	TAAATGGTTTAAGCGGTGTGC	TGAATTTCATAACCAATCTCGATACAC
AT5G48370		SALK_122483	GCTGGCATGTCAGAGAAAATC	TCTTCACCCAACCATGAATTC	ATTTTGCCGATTTCGGAAC
AT5G65180		SALK_119527	TGCTCTCAGAAGAAGCTCCAC	AAGTTTGTGTAGCTTCGGCTG	ATTTTGCCGATTTCGGAAC
AT1G22920	*csn5a-1*	SALK_027705	homozygous lines below were provided by Jeff Dangl, University of North Carolina, USA		
At1g54060	*asil1-1*	SALK_124095C			
AT1G69690	*tcp15-1*	SALK_011491C			
AT3G02150	*tcp13-1*	SM_3_23151			
AT3G13720	*pra1.f3-1*	SALK_116960C			
AT3G13720	*pra1.f3-2*	SALK_079876			
AT3G17860	*jaz3-2*	SALK_067825C			
AT3G17860	*jaz3-1*	SALK_139337C			
AT3G47620	*tcp14-1*	SAIL_1145_H03			
AT3G48150	*apc8-1*	SALK_000028C			
AT4G02590	*une12-1*	SALK_010825C			
AT4G02590	*une12-1*	SALK_135303			
At4g04020	*fibrillin-1*	SALK_024528C			
At4g04020	*fibrillin-2*	SALK_130350			
AT4G17680	*sbp protein-1*	SAIL_71_D10			
AT4G17680	*sbp protein-2*	SAIL_420_E12			
At4g25200	*hsp23.6-1*	SAIL_373_B09			
At4g26110	*nap1.1-1*	SALK_144711			
AT4G28640	*iaa11-1*	SALK_033787C			
AT5G24660	*lsu2-1*	SALK_031648C			

Acknowledgements

An dieser Stelle möchte ich mich bei all Jenen bedanken die durch ihre Unterstützung zum Gelingen dieser Arbeit beigetragen haben, insbesondere bei:

Dir Ralph, für das Ersinnen des *G. orontii* Projekt nachdem aus den RNasen nichts wurde, es hat sich glaube ich gelohnt. Danke für deine Unterstützung während der gesamten Arbeit, besonders beim Schreiben der Paper. Zudem ein großer Dank für dein Blick für das Wesentliche und Machbare, ich habe viel gelernt.

Prof. Paul Schulze-Lefert für die Möglichkeit in seinem Department in einer wissenschaftlich inspirierenden Umgebung meine Doktorarbeit verfassen zu können. Danke auch für die wiederkehrenden Hinweise auf Nachteile der Effektorforschung, die Diskussionen mit dir regen zum Nachdenken an.

Dr. Pascal Braun für die anstrengende aber ertragreiche Zeit am CCSB in Boston, die nachfolgende Kooperation bei der Analyse der Y2H Daten und die „Netzwerksicht" der Dinge.

Prof. Martin Hülskamp für die Übernahme des Koreferats

Dr. Frank Takken for becoming my external examiner

Prof. Ulf Ingo Flügge für die Übernahme des Prüfungsvorsitz

Emiel ver Loren van Themaat, Takayuki Shindo und Amber Stephens für bioformatische Analysen bzw. die Klonierung der OECs.

Dem Team des CCSB, Dana-Farber Cancer Institut, Boston, USA für die Hilfe beim „High-troughput interactome mapping" und den damit verbundenen Problemchen.

Danken möchte ich auch der gesamten Panstruga-Gruppe. Ihr Alle habt viel zum Gelingen dieser Arbeit beigetragen, gerade auch durch die super Atmosphäre und das Gequatsche nebenbei. Besonders danken möchte ich Mark für die Einführung in die confocale Welt. Ein großer Dank auch an Justine, Johanna und Jens für das Abfedern des langsamen Braindrains der AG Panstruga. Jens – viel Glück als last (half) man standing ;). Eine große Umarmung aus Papier auch für dat Kölsche Mädchen Anja. Du hast ein soooo großes Herz, das passt gar nicht auf diese Seite (und immer nen guten fachlichen Rat).

Ein großer Dank an Matze und Anne für die Zeit in der Bib und die Einsicht das das doch alles gar nicht so schlimm ist. Es ist vorbei!

Mein vorletzter Dank gilt meine Eltern. Man sagt ja so schön „Zwei Dinge sollen Kinder von ihren Eltern bekommen: Wurzeln und Flügel." Ihr habt mir Beides gegeben, mich in die Welt geschickt und mich immer und ausnahmslos unterstützt, und das auch kritisch. Danke dafür.

Mein letzter aber größter Dank gilt dir, Lisa. Wie du mich antreibst, aufmunterst, beruhigst und mir den Spiegel vorhälst ist wunderbar. Danke für deine Unterstützung und Liebe, insbesondere während des Schreibens. Du hast in letzter Zeit viel alleine machen müssen. Und schließlich: Danke für Oskar. Dieses kleine Wunder ist das Beste was mir je passiert ist. Ich genieße jede Minute mit euch.

Erklärung

Ich versichere, dass ich die von mir vorgelegte Dissertation selbständig angefertigt, die benutzten Quellen und Hilfsmittel vollständig angegeben und die Stellen der Arbeit – einschließlich Tabellen, Karten und Abbildungen –, die anderen Werken im Wortlaut oder dem Sinn nach entnommen sind, in jedem Einzelfall als Entlehnung kenntlich gemacht habe; dass diese Dissertation noch keiner anderen Fakultät oder Universität zur Prüfung vorgelegen hat; dass sie – abgesehen von auf Seite I angegebenen Teilpublikationen – noch nicht veröffentlicht worden ist sowie, dass ich eine solche Veröffentlichung vor Abschluss des Promotionsverfahrens nicht vornehmen werde. Die Bestimmungen dieser Promotionsordnung sind mir bekannt. Die von mir vorgelegte Dissertation ist von Prof. Dr. Paul Schulze-Lefert betreut worden.

Köln, den 01.06.2013 _____

Ralf Weßling